ALFRED-WEGENER-INSTITUT
HELMHOLTZ-ZENTRUM FÜR POLAR- UND MEERESFORSCHUNG

788
2024

Berichte
zur Polar- und Meeresforschung

Reports on Polar and Marine Research

The Expedition PS138 of the Research Vessel POLARSTERN to the Arctic Ocean in 2023

Edited by

Antje Boetius and Christina Bienhold
with contributions of the participants

HELMHOLTZ

Die Berichte zur Polar- und Meeresforschung werden vom Alfred-Wegener-Institut, Helmholtz-Zentrum für Polar- und Meeresforschung (AWI) in Bremerhaven, Deutschland, in Fortsetzung der vormaligen Berichte zur Polarforschung herausgegeben. Sie erscheinen in unregelmäßiger Abfolge.

Die Berichte zur Polar- und Meeresforschung enthalten Darstellungen und Ergebnisse der vom AWI selbst oder mit seiner Unterstützung durchgeführten Forschungsarbeiten in den Polargebieten und in den Meeren.

Die Publikationen umfassen Expeditionsberichte der vom AWI betriebenen Schiffe, Flugzeuge und Stationen, Forschungsergebnisse (inkl. Dissertationen) des Instituts und des Archivs für deutsche Polarforschung, sowie Abstracts und Proceedings von nationalen und internationalen Tagungen und Workshops des AWI.

Die Beiträge geben nicht notwendigerweise die Auffassung des AWI wider.

Herausgeber
Dr. Horst Bornemann

Redaktionelle Bearbeitung und Layout
Susan Amir Sawadkuhi

Alfred-Wegener-Institut
Helmholtz-Zentrum für Polar- und Meeresforschung
Am Handelshafen 12
27570 Bremerhaven
Germany

www.awi.de
www.awi.de/reports

The Reports on Polar and Marine Research are issued by the Alfred Wegener Institute, Helmholtz Centre for Polar and Marine Research (AWI) in Bremerhaven, Germany, succeeding the former Reports on Polar Research. They are published at irregular intervals.

The Reports on Polar and Marine Research contain presentations and results of research activities in polar regions and in the seas either carried out by the AWI or with its support.

Publications comprise expedition reports of the ships, aircrafts, and stations operated by the AWI, research results (incl. dissertations) of the Institute and the Archiv für deutsche Polarforschung, as well as abstracts and proceedings of national and international conferences and workshops of the AWI.

The papers contained in the Reports do not necessarily reflect the opinion of the AWI.

Editor
Dr. Horst Bornemann

Editorial editing and layout
Susan Amir Sawadkuhi

Alfred-Wegener-Institut
Helmholtz-Zentrum für Polar- und Meeresforschung
Am Handelshafen 12
27570 Bremerhaven
Germany

www.awi.de
www.awi.de/en/reports

Titel: Ausbringen der Vorleine zum Eisanker der Polarstern
(Foto: Esther Horward, AWI)

Cover: Deploying the fore line to Polarstern's ice anchor
(Photo: Esther Horward, AWI)

The Expedition PS138 of the Research Vessel POLARSTERN to the Arctic Ocean in 2023

Edited by

Antje Boetius and Christina Bienhold
with contributions of the participants

Please cite or link this publication using the identifiers

https://epic.awi.de/id/eprint/59182/
https://doi.org/10.57738/BzPM_0788_2024

ISSN 1866-3192

PS138 / ArcWatch-1

03 August 2023 – 30 September 2023

Tromsø – Bremerhaven

Chief scientist
Antje Boetius

Co-Chief scientist
Christina Bienhold

Coordinator
Ingo Schewe

Contents

1.	**Überblick und Expeditionsverlauf**	**3**
	Summary and Itinerary	**12**
	Weather Conditions during PS138	**16**
2.	**Sea-Ice Physics**	**19**
	2.1 Routine sea-ice observations and remote sensing	**23**
	2.2 Transect measurements of physical properties of sea ice	**25**
	2.3 Airborne sea-ice surveys	**28**
	2.4 Remotely operated vehicle (ROV) operations	**33**
	2.5 Floe dynamics and numerical model work	**40**
3.	**Physical and Chemical Oceanography**	**44**
4.	**Biological Oceanography and Sea-Ice Biology**	**70**
5.	**Bathymetry, Benthic Biology and Biogeochemistry**	**102**
	5.1 Bathymetry	**103**
	5.2 Megabenthic ecology and high-resolution seafloor topography	**105**
	5.3 Macrofauna	**123**
	5.4 Meiofauna, microbial communities and biogeochemical parameters	**131**
	5.5 *In-situ* benthic fluxes	**137**
6.	**Autonomous Buoy Measurements**	**145**

APPENDIX **164**

A.1 Teilnehmende Institute / Participating Institutes **165**

A.2 Fahrtteilnehmer:innen / Cruise Participants **169**

A.3 Schiffsbesatzung / Ship‘s Crew **171**

A.4 Stationsliste / Station List PS138 **173**

A.5 ICE Station Maps **268**

A.6 Overview of Multicorer Cores retrieved during PS138 **272**

Tab. A.6.1: Overview of multicorer cores retrieved during PS138 and their distribution to scientists for different types of analyses **272**

1. ÜBERBLICK UND EXPEDITIONSVERLAUF

Antje Boetius, Christina Bienhold DE.AWI

Die schnelle Erwärmung der Arktis und der Rückgang des Meereises verändern nicht nur die Hydrographie des Arktischen Ozeans, sondern wirken sich auch in vielfältiger Weise auf biogeochemische und biologische Prozesse aus. Die Expedition PS138 (ArcWatch-1) hat die Biologie, Chemie und Physik des Meereises erkundet, sowie die Auswirkungen des Meereis-Rückgangs auf das gesamte Ozeansystem von der Oberfläche bis in die Tiefsee. Hierzu wurden die Dynamik des ein- und mehrjährigen Meereises, sowie die Rolle der sommerlichen Schmelze und herbstlichen Meereisbildung für die Nährstoffverteilung, Produktivität und Zusammensetzung der pelagischen und benthischen Lebensgemeinschaften untersucht, sowie auch der Export von organischem und inorganischem Material in die Tiefsee. Im Rahmen der Expedition PS80 (ARK27-3, IceArc) wurden während des bisher größten dokumentierten sommerlichen Meereisminimums in 2012 erhebliche Auswirkungen auf das gesamte Ökosystem des zentralen Arktischen Ozeans festgestellt (Boetius et al. 2013). Elf Jahre später diente die Expedition PS138 einer erneuten Zustandserfassung und vergleichenden Untersuchungen zu vorangegangenen Dekaden. Es wurden die gleichen Regionen wie in 2012 besucht (Abb. 1.1), um mittels interdisziplinärer Prozessstudien die Wechselwirkungen zwischen Eisphysik, Hydrographie, Biogeochemie und Biodiversität des arktischen Systems vom Meereis bis zum Meeresboden zu untersuchen. Zudem wurden auch Stationen der MOSAiC Expedition wiederholt. Dabei wurden vergleichende Untersuchungen in der Eisrandzone und solchen mit mehrjähriger Eisbedeckung in der zentralen Arktis durchgeführt. Für die Arbeiten wurden eine Reihe bewährter und neuer Technologien eingesetzt, wie z.B. Freifallgeräte, Schleppgeräte und ein Untereis ROV (remotely operated vehicle). Neben den wissenschaftlichen Einsätzen auf dem Eis und von Bord wurden Bojen und Verankerungen ausgebracht, welche die Physik, Chemie und Biologie des Arktischen Ozeans über verschiedene Zeiträume erfassen. Die Ergebnisse dieser Expedition im Sommer 2023, der von mehreren Anomalien in und um die Arktis herum geprägt war, stellen einen wichtigen Beitrag dar, um die Auswirkung des Rückgangs der Meereisbedeckung auf dem Arktischen Ozean und seinen Ökosystemen zu quantifizieren. Diese Expedition wird unterstützt vom Helmholtz Forschungsprogramm “Changing Earth – Sustaining our Future” Topic 2, Subtopic 1, 3 und 4 sowie Topic 6, Subtopic 1, 2 und 3, sowie verschiedenen nationalen und internationalen Programmen.

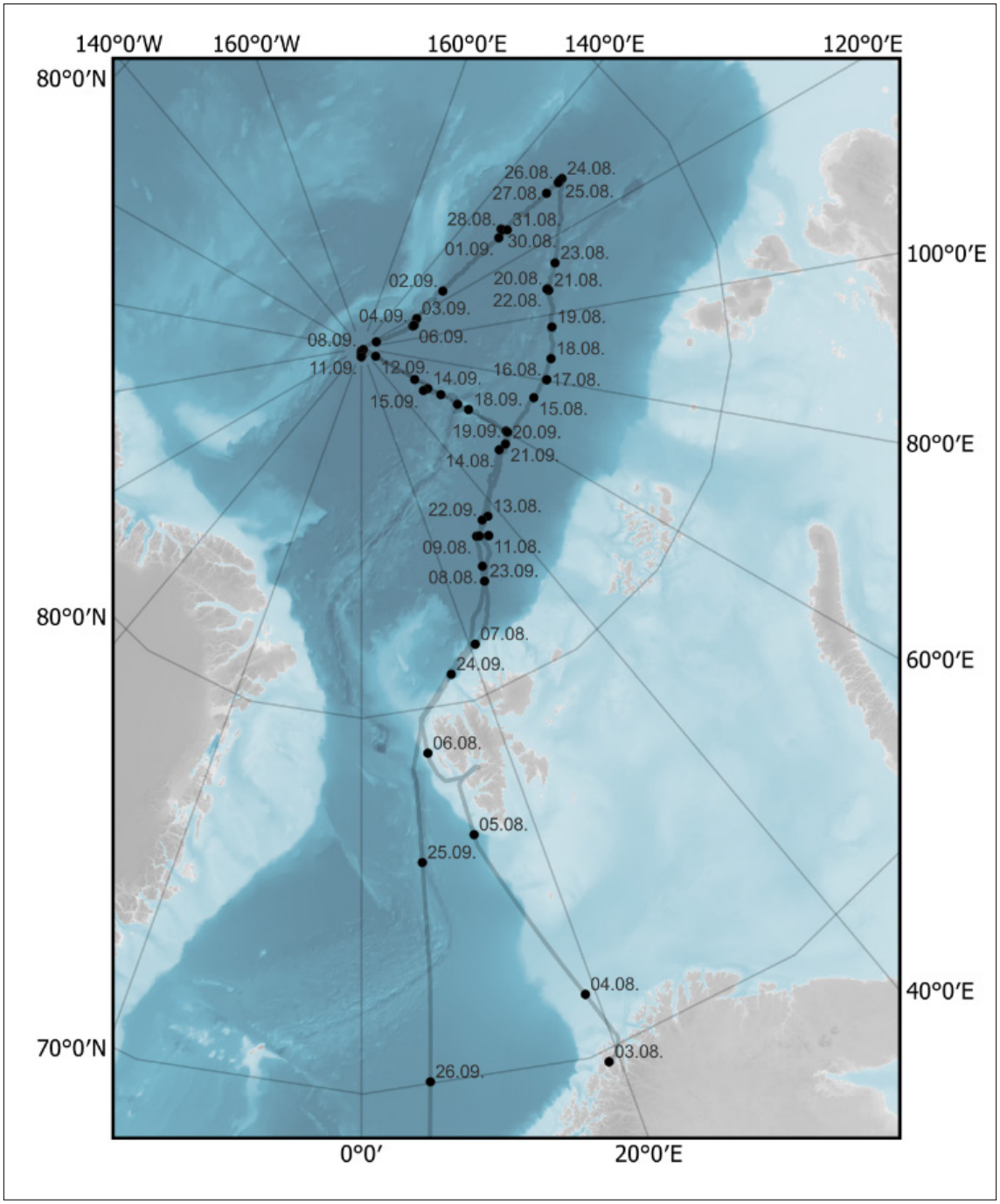

Abb. 1.1: Fahrtroute (grau) und Eis-Stationen (weiß) der Expedition PS138 (ArcWatch-1). Siehe https://doi.pangaea.de/10.1594/PANGAEA.963843 für eine Darstellung des Master tracks in Verbindung mit der Stationsliste für PS138. Die Reise begann am 3. August 2023 in Tromsø und endete am 30. September 2023 in Bremerhaven.

Fig. 1.1: Cruise track (grey) and ice stations (white) of the expedition PS138 (ArcWatch-1). See https://doi.pangaea.de/10.1594/PANGAEA.963843 to display the master track in conjunction with the station list for PS138. The expedition started on 3 August 2023 in Tromsø and ended on 30 September 2023 in Bremerhaven.

Die *Polarstern* Expedition PS138 (ArcWatch-1) begann am 03. August in Tromsø und führte durch norwegische Gewässer in Richtung Norden. Wir passierten am 05. August Spitzbergen westlich mit einem Zwischenstopp für die Abholung wissenschaftlichen Equipments sowie Proviants. Am 06. August 2023 wurden Bojen ausgesetzt und kurz vor dem Eisrand eine erste Teststation mit der CTD-Rosette durchgeführt, um Wasserproben aus verschiedenen Tiefen zu nehmen. Die Forschungsarbeiten begannen am 7. August mit Autonomen X-CTDs sowie den ersten Meereisdicken-Messungen mit dem Instrument “EM-Bird”: Die Messungen wurden von unserem Hubschrauber aus durchgeführt, während der EM-Bird unter dem Helikopter geschleppt wurde. Das AWI vermisste die Eisdicken im Arktischen Ozean seit 30 Jahren, diese Zeitreihe ist die einzige flugzeug- und hubschraubergestützte Messreihe, die über einen so langen Zeitraum in der Arktis durchgeführt wurde. Es ging zunächst in der Eisrandzone ostwärts bis 84°N und 30°E zur ersten Eisstation. Ziel der Reise war, zwischen 30 und 130°E und 84-90°N ausgewählte Eisstationen anzufahren, um eisphysikalische und ozeanographische Messungen durchzuführen und Proben für biogeochemische und biologische Analysen zu nehmen (Eis, Wasser, Meeresboden). Dabei wurde parallel gearbeitet: während die Eisforscher:innen die Vorgänge auf und unter dem Eis untersuchten, wurde die Wassersäule durch Wasserproben analysiert und der Meeresboden mit den benthischen Organismen untersucht. Der Hubschrauber wurde eingesetzt, um Personen oder Instrumente zwischen Schiff und Eisscholle zu transportieren. Wir verfolgten die Drift der Eisscholle mit Hilfe von GPS-Signalen, die von verschiedenen, auf dem Eis platzierten Bojen gesendet wurden. Für die Wasserproben kamen CTD-Wasserschöpfer und *In-situ* Pumpen zum Einsatz, für die Beprobung von Phyto- und Zooplankton verschiedene Netze (Handnetz, Bongo, Multinetz und Untereis-ROV-Netz). Auch mehrere benthische Probenahmegeräte wie der TV-MUC, Großkastengreifer, Epibenthischer Schlitten und Lander wurden an jeder Station eingesetzt. Für die beiden letzteren Geräte verließ *Polarstern* die Scholle, um in den Wasserlöchern zwischen den Schollen operieren zu können.

Abb.1.2: Erste Forschungsstation auf dem Eis © Esther Horvath

Fig. 1.2: First research station on the ice © Esther Horvath

Die erste Forschungsstation auf dem Eis fand bei 84°04.06 N 031°16.04 E vom 8.–12. August statt (Abb. 1.2). Das Eis hatte Schmelztümpel und einige Algenaggregate auf der stark abgeschmolzenen Unterseite. Der erste Tauchgang zur Ozeanbodenbeobachtung und Bathymetrie mit dem OFOBS (Ocean Floor Observation and Bathymetry System) zeigte in einer Tiefe von 4.000 m am Meeresboden reges Treiben und viele kleine abgesunkene Algenklumpen. Der Einsatz von 2 benthischen Landern stellte sich durch fehlenden Bugstrahler und defekte Posidonia-Navigationsanlage als eine große Herausforderung dar, eine Lander-Bergung musste aufgegeben werden, weil seine Ortung im Eis nicht möglich war.

Am 17. August begegneten wir dem LNG-betriebenen Kreuzfahrtschiff *Le Commandant Charcot*. Es gab einen Austausch zwischen beiden Schiffen für ein paar Stunden, Kapitän und Fahrtleitung wurden zu Vorträgen eingeladen. Die zweite Eisstation wurde am 14. August bei 85°N und 78°E erreicht und dauerte bis 18. August. Die Parallelarbeiten auf dem Eis wurden durch das Ausbringen von Eisankern gestützt, die Position des Schiffes an der Eisscholle wurde je nach Windrichtung angepasst, so dass der Wind das Schiff Backbord gegen die Scholle drückte und die Steuerbord-Seite an einem Wasserloch für die windengeführten Geräte genutzt wurde. Die meisten Geräte konnten so parallel zu den Eisarbeiten eingesetzt werden. Nur die Lander und der Epibenthos-Schlitten (EBS) wurden frei in Wasserkanälen zwischen Schollen eingesetzt. *Polarstern* schleppte den EBS direkt über den Meeresboden, so wurden Makrofauna und Megafauna in sehr gutem Zustand gesammelt für taxonomische Untersuchungen.

Am 18. August erreichten wir auf dem Weg zur dritten Eisstation einen Ausläufer des Gakkel-Rückens, einen kaum vermessenen Seeberg bei 84°46.3‘ N und 94°56.8‘ E. Er wurde mit einem Fächerecholot und einem Sedimentecholot kartiert.

Abb.1.3: Riesen-Seeanemonen in Gemeinschaft mit von Borstenwürmern besiedelten Schwämmen. © OFOBS

Fig. 1.3: Giant sea anemones together with sponges colonized by bristle worms. © OFOBS

Zudem tauchten wir mit OFOBS an die Spitze und den Hang des Seeberges. Der Seeberg ist von ausgedehnten Schwammgärten bedeckt, die Lebensgemeinschaft ist enorm vielfältig und erstreckt sich vom Gipfel bei 1.500 m Wassertiefe bis in über 2.000 m Wassertiefe (Abb. 1.3).

Am 19. August erreichen wir die dritte Eisstation bei 84°36' N und 108°30' E, die wir bis 22. August beprobten, einschließlich von zwei Lander Einsätzen. Zu den Eisstationen gehörte auch der Einsatz des ferngesteuerten Untereis-Roboters "Beast". Er ist mit einer CTD für Leitfähigkeit, Temperatur und Tiefe, einem Lichtsensor, einem pH-Sensor, Kameras, Hyperspektralkameras zur Untersuchung der Algenbiomasse und akustischem Multibeam zur Kartierung der Eistopographie ausgestattet. Auf dem Weg zur 4. Eisstation werden viele Eisbojen und XCTDs ausgesetzt. Die 4. Eisstation wurde bei 83°N und 130°E bei starkem Nebel durchgeführt, in der Zeit vom 24. bis 27. August. Aus dem westlichen Arbeitsgebiet ging es weiter in Richtung des Gebietes am dem die MOSAiC-Drift im Oktober 2019 startete. Die 5. Eisstation bei 85°N und 130°E dauerte vom 28. August bis 1. September. Zusätzlich zum Standardprogram brachten wir ein Netzwerk autonomer Systeme auf mehreren Schollen in der Region aus, das die Drift der MOSAiC Scholle wiederholen soll und – wenn alles gut geht – einen einmaligen Vergleichsdatensatz zum Bojen-Netzwerk von MOSAiC erzeugen wird.

Abb.1.4: Hydrographische Arbeiten auf dem Eis; hier Messungen mit dem Nitratsensor "Suna", der Stickstoff im Wasser misst. © Esther Horvath

Fig.1.4: Hydrographic work on the ice; here measurements with the "Suna" nitrate sensor, which measures nitrogen in water. © Esther Horvath

Am 1. September wurden zwei ozeanographische und biogeochemische Verankerungen ausgebracht (2 Parallelverankerungen, eine davon als Rohrverankerung direkt unter dem Eis; Abb. 1.5). Die Aufnahme dieser Verankerungen ist während der Expedition ArcWatch-2 in 2024 geplant. Die Eisschollen sind ungewöhnlich schneebedeckt, flach und zeigen immer noch keinen Bewuchs mit Untereisalgen. Auch in der Tiefsee finden sich kaum Algen-Aggregate, die Meeresbodenfauna weist erhebliche Unterschiede zu 2012 auf.

Abb.1.5: Die neue Rohr-Verankerung zur ganzjährigen hydrographischen Messung. © Esther Horvath

Fig. 1.5: The new pipe mooring for year-round hydrographic measurements. © Esther Horvath -

Am 2. September konnten wir zweimal an einem Seeberg des Lomonossow-Rückens tauchen. Dieser war nicht felsig wie der vorherige Seeberg am Gakkelrücken, sondern ganz mit Sedimenten bedeckt. Wir fanden wenige Schwämme auf dem Gipfel des Rückens und den stark sedimentierten Steilhängen südlich des Rückens, aber vor allem sehr viele Seegurken – Gemeinschaften bei der Paarung. Die 6. Eisstation fand bei 88°30‘N und 112°E statt, bei voller Eisbedeckung und dauerte vom 3. bis 5. September. Auch in dieser Region war das Eis von unten stark abgeschmolzen und kaum Export von Algen oder Partikeln sichtbar. Wir erreichten am 7. September den Nordpol für die siebte Eisstation, bei Temperaturen von -5° bis -8°C (Abb. 1.6). Es war das siebte Mal für die *Polarstern*.

Abb.1.6: Am Nordpol © Esther Horvath

Fig. 1.6: At the North Pole © Esther Horvath

Bis zum 11. September konnten wir bei guten Wetterverhältnissen und Minusgraden die gesamte Serie an Untersuchungen von Eis, Wasser und Meeresboden ausführen. In den Wasserkanälen bildete sich schon Neueis. Mit OFOBS konnten wir in rund 4220 Meter Tiefe den Meeresboden direkt am Nordpol erkunden – hier leben vor allem sehr große Igelwürmer und kleine, kriechende Seeanemonen. Während unseres Besuchs am Nordpol haben wir 200 kleine Holzboote neben einer autonomen Messboje auf dem Meereis ausgesetzt. Die Boote können auf ihrer Reise durch die Arktis mithilfe der Positionsdaten der Bojen verfolgt werden (https://data.meereisportal.de/relaunch/buoy.php?lang=en&active-tab1=method&active-tab2=buoy&singlemap&buoyname=2023P286). Wenn das Eis schmilzt, treiben die Boote weiter und werden hoffentlich an entfernten Küste gefunden und über die Website floatboat.org gemeldet. Float Your Boat ist ein Projekt des International Arctic Buoy Program.

Vom Nordpol ausgehend folgten wir einem Transekt bei 60°E mit CTD-Wasserschöpfer-Probennahmen im Wechsel mit XCTDs. Die 8. Eisstation wurde bei 88°N und 60°E vom 13. bis 15. September durchgeführt. Auch hier wurden erhebliche Veränderungen der Lebensgemeinschaften am Meeresboden festgestellt im Vergleich zu den Aufnahmen des Kameraschlitten OFOBS in 2012 (Abb. 1.7).

Abb.1.7: Ein Ausschnitt des Meeresbodens an der 8. Eisstation. Die weißlichen Flecken sind Überbleibsel der Eisalgen-Einträge vergangener Jahre © OFOBS

Fig. 1.7: A section of the seabed at the eighth ice station. The whitish patches are remnants of ice algae deposits from previous years © OFOBS

Nach der Station wurde der 60°E Transekt mit ozeanographischen Messungen fortgeführt. Alle ca. 10 Seemeilen wird die Wassersäule bis in 1.500 m Wassertiefe vermessen, davon alle 40 Seemeilen bis in ca. 4 km Wassertiefe zum Meeresboden. Dies dient der Untersuchung der Hydrographie des Eurasischen Beckens, welches das Amundsen und Nansen Becken sowie den Gakkelrücken umfasst. Es wird dabei auch untersucht, wie viel Kohlenstoff in der gelösten

organischen Fraktion des Meerwassers von den Küsten der Arktis und dem Permafrost stammt, und ob sich dieser Anteil regional verändert. Zudem werden Schadstoffe analysiert wie Per- und polyfluorierte Alkylverbindungen.

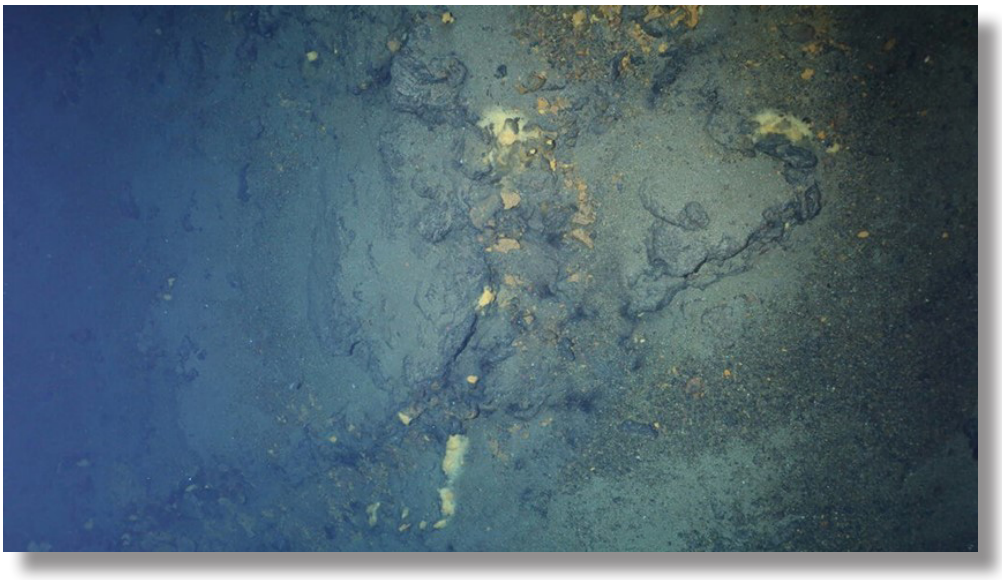

Abb.1.8: OFOBS-Tauchgang am Polaris Seeberg des Gakkel-Rückens © OFOBS

Fig. 1.8: OFOBS dive at the Polaris seamount of the Gakkel Ridge © OFOBS

Am 16. September erreichten wir die Ausläufer des Gakkel-Rückens bei 60° Ost und führten im nördlichen Bereich des Langseth-Rückens sowohl Bathymetrie-Transekte wie auch zwei OFOBS-Tauchgänge durch. Auch dieser Teil des Rückensystems ist von Kissenbasalten geprägt, zeigt aber deutlich mehr Sedimentation als die südliche Kette von Seebergen und keine deutliche Anreicherung des benthischen Lebens. Am 17. September setzten wir die Erkundung dieses Bereiches des Gakkelrückens fort mit einem Besuch des Polaris Seebergs. Hier fanden wir in 2016 Spuren aktiver hydrothermaler Prozesse in 3250 Metern Wassertiefe. Das geschleppte Kamerasystem OFOBS fuhr durch zwei dicke Partikelwolken, die vermutlich von hydrothermalen Quellen in 2.500 – 2.700 Metern Wassertiefe stammten. Der Meeresboden war eine Mischung aus Kissenlava-Feldern mit Glasschwämmen, steilen Terrassen mit unzähligen kleinen Fluidaustritten, bedeckt mit gelben und orangefarbenen Bakterienmatten auf geschwärzten Sedimenten und Felsen (Abb. 1.8). Haarsterne und Borstenwürmer schienen sich in diesen Bereichen besonders wohl zu fühlen.

Danach setzten wir den hydrographischen Transekt entlang 60°E fort. Er wurde beendet mit der 9. Eisstation bei 85°28’N. Ein Highlight der letzten Eisstation war ein kommentierter Livestream des Untereis-ROV Beast auf YouTube. Zum Ende der Fahrt konnten wir die erste Scholle für eine Wiederaufnahme von ausgebrachten Verankerungen auf dem Meereis und weiteren Messungen leider nicht erreichen. Sie war in die Russische Ausschließliche Wirtschaftszone gedriftet. Dem Anliegen in freier Passage ohne Forschung die Geräte nur abzubergen, wurde nicht entsprochen. Mit dem Aussetzen weiterer Bojen entlang unseres Transits durch das Eis beendeten wir das Forschungsprogramm der Expedition PS138. Wir verließen die Eiskante am 23. September und kehrten dann westlich von Spitzbergen Richtung Bremerhaven zurück. Die Ausläufer eines Hurrikans bekamen wir auf der Rückreise zu spüren mit gut 6 m hohen Wellen. Die Reise endete mit Einlaufen am 30. September in

Bremerhaven. Ein wichtiger Beitrag der Expedition zu internationalen Programmen ist die Ausbringung von 73 Bojen und Beobachtungssystemen auf dem Eis. Die Messungen werden den Jahresgang der Atmosphäre, des Schnees, des Meereises und des Ozeans aufzeichnen. Von der Hauptscholle an der MOSAiC Drift-Lokation werden regelmäßig Fotos gesendet, die die Veränderungen dokumentieren. Die Reise der Bojen kann im Meereisportal (www.meereisportal.de) verfolgt werden.

Abb.1.9: Polarstern-Besatzung am Nordpol. © Esther Horvath

Fig. 1.9: Polarstern Crew at the North Pole © Esther Horvath

Wir bedanken uns herzlich bei Kapitän Stefan Schwarze und der Crew der *Polarstern* Expedition PS138 (Abb. 1.9) für die tolle Zusammenarbeit und bei allen beteiligten Forschungsinstituten, Hochschulen und Forschungsförderern für die Unterstützung.

SUMMARY AND ITINERARY

The rapid warming of the Arctic and sea ice retreat affect not only the hydrography of the Arctic Ocean, but also biogeochemical and biological processes in various ways. The expedition PS138 (ArcWatch-1) investigated the biology, chemistry and physics of sea ice, as well as the impact of sea ice retreat on the entire ocean system from the surface to the deep sea. We studied the dynamics of first- and multiyear ice, as well as the role of summerly ice melt and re-growth in fall for the distribution of nutrients, productivity and the composition of pelagic and benthic communities, as well as the export of particulate matter to the deep sea. During the expedition PS80 (ARK27-3, IceArc) in 2012, which took place during the largest documented sea ice minimum to date, substantial impacts on the ecosystem were found (Boetius et al. 2013). Eleven years later, the expedition PS138 assessed the current ecosystem state and enables comparative studies with previous decades. We re-visited the same regions as in 2012 (Fig. 1.1), and used interdisciplinary process studies to examine interactions between ice physics and biology, hydrography, biogeochemistry and biodiversity of the Arctic ecosystem, from the sea ice to the seafloor. In addition, we repeated some studies at former MOSAiC sites. Our work included comparative studies between working areas in the marginal ice zone and areas covered by multiyear sea ice. During PS138 a range of established and novel technologies were deployed, such as moored lander systems, towed instruments and an under-ice ROV (remotely operated vehicle). In addition to scientific operations on the sea ice and from board, buoys, and short- and long-term moorings were deployed to assess the physics, chemistry and biology of the Arctic Ocean across different temporal scales. The results of this expedition in summer 2023, which was marked by several anomalies in and around the Arctic, are an important contribution toward quantifying the effects of changes in sea ice cover on the Arctic Ocean and its ecosystems. This expedition is supported by the Helmholtz research programme “Changing Earth – Sustaining our Future” Topic 2, Subtopics 1, 3 and 4, and Topic 6, Subtopics 1, 2 and 3, as well as various national and international programms.

Polarstern expedition PS138 (ArcWatch-1) began on 3 August in Tromsø and headed north through Norwegian waters. We passed Spitsbergen to the west on 5 August, with a stopover to pick up scientific equipment and provisions. On 6 August, buoys were deployed and a first test station with the CTD rosette was carried out before reaching the ice edge to take water samples from various depths. The research activities began on 7 August with autonomous XCTDs (eXpendable CTD) and the first sea ice thickness measurements with the “EM-Bird”: The measurements are carried out from our helicopter while the EM-Bird is towed under the helicopter. The AWI has been measuring ice thickness in the Arctic Ocean for 30 years, and this time series is the only airplane- and helicopter-based measurement series that has been carried out in the Arctic over such a long period of time.

The first part of the journey took us eastward along the ice margin to the first ice station at 84°N and 30°E. The aim of the expedition was to visit selected ice stations between 30°E and 130°E and 84 – 90°N, in order to carry out ice-physical and oceanographic measurements and take samples for biogeochemical and biological analyses (ice, water, seafloor). Work was carried out in parallel: while the sea ice researchers investigated the processes on and under the ice, the water column analyzed using water samples and the seabed with its benthic organisms

was studied. The helicopter was used to transport people or instruments between the ship and the ice floe. We tracked the drift of the ice floe with the help of GPS signals sent from various buoys placed on the ice. CTD rosettes with niskin bottles and *In-situ* pumps were used to retrieve water samples, and various nets (hand net, bongo, multi-net and under-ice ROV net) were used for sampling phytoplankton and zooplankton. Several benthic sampling devices such as the TV-MUC, giant box corer, epibenthic sledge and landers were also deployed at each station. For the latter two devices, *Polarstern* left the floe to operate in open water areas between the floes.

The first ice station took place at 84°04.06 N 031°16.04 E from 8 – 12 August (Fig 1.2). The ice had melt ponds and some algal aggregations on the heavily melted underside. The first dive for ocean floor observation and bathymetry with the OFOBS (Ocean Floor Observation and Bathymetry System) showed a lot of activity on the sea floor at a depth of 4,000 m and many small sunken algae clumps. The deployment and recovery of 2 benthic landers proved to be a major challenge due to the missing bow thruster and a defective Posidonia navigation system; the recovery of one lander had to be abandoned because it could not be located in the ice. On 17 August, we met the LNG-powered cruise ship *Le Commandant Charcot*. There was an exchange of people between the two ships for a few hours and the captain and chief scientist were invited to give talks. The second ice station was reached on 14 August at 85°N and 78°E and lasted until 18 August. The parallel work on the ice was supported by the placement of ice anchors; the position of the ship on the ice floe was adjusted depending on the wind direction, so that the wind pushed the ship's port side against the floe and the starboard side was used for the winch-guided equipment in open water holes. Most of the equipment could thus be used in parallel with the ice work. Only the landers and the epibenthic sledge (EBS) were deployed freely in open water areas between floes. *Polarstern* towed the EBS directly over the sea floor and collected macrofauna and megafauna in very good condition for taxonomic studies. On 18 August, on the way to the third ice station, we reached a spur of the Gakkel Ridge, a barely surveyed seamount at 84°46.3' N and 94°56.8' E. It is mapped with a multibeam echo sounder and a sediment echo sounder.

We also dived with OFOBS to the top and slope of the seamount. The seamount was covered by extensive sponge gardens, the biological community was enormously diverse and extended from the summit at 1,500 m water depth to over 2,000 m water depth (Abb. 1.3).

On 19 August we reached the third ice station at 84°36' N and 108°30' E, where we worked until 22 August, including two lander deployments. Ice stations also included the deployment of the remotely operated under-ice robot "Beast". It is equipped with a CTD for conductivity, temperature and depth measurements, a light sensor, a pH sensor, cameras, hyperspectral cameras for investigating algae biomass and an acoustic multibeam for mapping the ice topography. On our way to the fourth ice station, several ice buoys and XCTDs were deployed. The fourth ice station was carried out at 83°N and 130°E in heavy fog, from 24 – 27 August. From the western working area, we continued towards the area where the MOSAiC drift started in October 2019. The fifth ice station at 85°N and 130°E lasted from 28 August to 1 September. In addition to the standard programme, we deployed a network of autonomous systems on several floes in the region, which should repeat the drift of the MOSAiC floe and – if all goes well – will generate a unique data set to compare with the MOSAiC buoy network.

On 1 September, an oceanographic and a biogeochemical mooring was deployed (2 parallel moorings, one of them as a pipe mooring directly under the ice, Fig. 1.5). The recovery of these moorings is planned during the ArcWatch-2 expedition in 2024. The ice floes were unusually snow-covered, plane and still showed no growth of under-ice algae. There were also hardly any algae aggregates in the deep sea, and the seafloor fauna showed considerable differences compared to 2012.

On 2 September, we were able to perform two OFOBS dives at a seamount on the Lomonosov Ridge. This seamount was not rocky like the previous one on the Gakkel Ridge, but was completely covered with sediments. We found a few sponges on the summit of the ridge and on the heavily sedimented steep slopes to the south of the ridge, but above all many mating sea cucumbers. The sixth ice station took place at 88°30'N and 112°E, with full ice cover and lasted from 3 September to 5 September. In this region, the ice was also heavily melted from below and hardly any export of algae or particles was visible. On 7 September we reached the North Pole for the seventh ice station, at temperatures of -5° to -8°C (Abb. 1.6). For *Polarstern* it was the seventh time at the North Pole.

We were able to carry out the entire series of ice, water and seabed surveys in good weather conditions and sub-zero temperatures until 11 September. New ice was already forming in the water channels. With OFOBS, we were able to explore the seabed at a depth of around 4,220 meters directly at the North Pole, where very large spoon worms and small, crawling sea anemones live. During our visit to the North Pole, we deployed 200 small wooden boats next to an autonomous measuring buoy on the sea ice. The boats can be tracked on their journey through the Arctic using the position data from the buoys (https://data.meereisportal.de/relaunch/buoy.php?lang=en&active-tab1=method&active-tab2=buoy&singlemap&buoyname=2023P286). When the ice melts, the boats continue to drift and will hopefully be found on distant shores and reported via the floatboat.org website. Float Your Boat is a project of the International Arctic Buoy Programme.

Starting from the North Pole, we followed a transect at 60°E with CTDs including water sampling alternating with XCTDs. The eighth ice station was carried out at 88°N and 60°E from 13–15 September. Here, too, significant changes in the biotic communities on the sea floor were observed compared to the recordings from the OFOS camera sled in 2012 (Fig. 1.7).

After the station, the 60°E transect with oceanographic measurements was continued. Every approx. 10 nautical miles, the water column was measured down to a depth of 1,500 m, and every 40 nautical miles down to a depth of approx. 4 km to the sea floor. This serves to investigate the hydrography of the Eurasian Basin, which includes the Amundsen and Nansen Basins and the Gakkel Ridge. We will also investigate how much of the carbon in the dissolved fraction of the seawater comes from the Arctic coasts and the permafrost, and whether this proportion changes regionally. Pollutants such as perfluorinated and polyfluorinated alkyl compounds are also being analyzed.

On 16 September, we reached the foothills of the Gakkel Ridge at 60°E and conducted bathymetry transects as well as two OFOBS dives in the northern part of the Langseth Ridge. This part of the ridge system is also characterized by pillow basalts, but shows significantly more sedimentation than the southern chain of seamounts and no clear enrichment of benthic life. On 17 September, we continued our exploration of this area of the Gakkel Ridge with a visit to the Polaris seamount. Here, in 2016, we found traces of active hydrothermal processes at a water depth of 3,250 meters. The towed camera system OFOBS passed through two thick particle clouds that probably originated from hydrothermal vents at 2,500–2,700 meters water depth. The seafloor was a mixture of pillow lava fields with glass sponges, steep terraces with countless small fluid seeps, covered with yellow and orange bacterial mats on blackened sediments and rocks (Fig. 1.8). Brittle stars and bristle worms seemed to feel particularly comfortable in these areas.

We then continued the hydrographic transect along 60°E. It ended with the 9th ice station at 85°28'N. A highlight of the last ice station was a commented livestream of the under-ice ROV Beast on YouTube. At the end of the cruise, we were unfortunately unable to reach the first floe for a recovery of deployed instruments on the sea ice and further measurements. It had drifted into the Russian Exclusive Economic Zone. The request to recover the equipment in

free passage without research was not granted. With the deployment of further buoys along our transit through the ice, we ended the research programme of expedition PS138. We left the ice edge on 23 September and passed Spitsbergen on the West on our return to Bremerhaven. We felt the remnants of a hurricane on the return journey with wave heights of about 6 m. The expedition ended in Bremerhaven on 30 September. An important contribution of the expedition to international programms is the deployment of 73 buoys and observation systems on the ice. The measurements will record the seasonal changes in the atmosphere, snow, sea ice and the ocean. From the main floe at the MOSAiC drift location photos will be sent regularly to document changes. The journey of the buoys can be followed on meereisportal (www.meereisportal.de).

We would like to thank Captain Stefan Schwarze and the crew of *Polarstern* expedition PS138 (Fig. 1.9) for the great collaborative teamwork, and all participating research institutes, universities and funding agencies for their support.

References

Boetius A, Albrecht S, Bakker K, Bienhold C, Felden J, Fernández-Méndez M, Hendricks S, Katlein C, Lalande C, Krumpen T, Nicolaus M, Peeken I, Rabe B, Rogacheva A, Rybakova E, Somavilla R, Wenzhöfer F, and the RV Polarstern ARK27-3-Shipboard Science Party (2013) Export of Algal Biomass from the Melting Arctic Sea Ice. Science 339:1430–1432. https://doi.org/10.1126/science.1231346

WEATHER CONDITIONS DURING PS138

Julia Wenzel DE.DWD

On 3 August the *Polarstern* left the harbour near Tromsø with unusual warm conditions (25°C) starting its way to the Arctic with a short stop in Svalbard.

A low pressure system near the Lofoten Islands, whose warm sector had brought in the warm air from the south, moved to the northnorthwest in the following days while weakening. During the transit to Svalbard, a significant wave height of maximum 1.5 m occurred with mostly light to moderate winds, although at the height of the southern tip of Svalbard, the easterly wind temporarily increased to 6 Bft during the night to 5 August due to the wind increase caused by the corner effect.

On 5 August a secondary low formed over Svalbard at the occlusion point of the low previously mentioned low. This new low became the new controlling low and moved northeastward while temporary deepening. On this day *Polarstern* was in the fjord near Longyearbyen (Svalbard) with winds between 3 and 6 Bft from variable directions due to the orography of the surrounding mountains.

When *Polarstern* moved northeastwards following the low's centre, from 6 to 8 August a wind from southwest to west around 5 Bft dominated. The *Polarstern* reached the first ice station at 84°N 31°E on 8 August and was crossed by the cold front of the low in the morning. On the back side, there was a significant weather improvement, which was favourable to the work on the ice floe and helicopter flights.

On 8 August a new low formed at the northeast coast of Greenland and moved rapidly to the northeast deepening further. The *Polarstern* was crossed by its frontal system in the morning of 9 August, with the wind on the back side of the front shifting to northwest and increasing to 6 Bft.

A low south of Svalbard brought in a much more humid air mass from the south starting in the evening of 10 August, which led to dense fog formation from the night to 11 August onwards, lifting somewhat only for a few hours up to and including 12 August. With a newly deepening of the aforementioned low at that time lying between the North Pole and Severnaya Zemlya, the *Polarstern* was crossed by its southward moving occlusion on 13 August. This initiated a persistent fog phase with short interruptions, while the low moved eastward under weakening and a high north of Svalbard moved to Severnaya Zemlya under strengthening from 14 to 17 August causing an intensification of the inversion over the humid base layer. Meanwhile, the *Polarstern* continued eastward from 12 to 15 August to the second ice station at 85°N 80°E, where it stayed until 17 August.

A low pressure system moving from the Barents Sea (16 August) to the northeast and filling up between Franz-Josef-Land and the North Pole by 19 August brought in a moist air mass from the south again. In the night to 18 August, the wind in the frontal area briefly increased to 5 to 6 Bft. Between the high over the Laptev Sea and another high over the Norwegian Sea, a high-pressure bridge formed on 19 August, whose center of gravity shifted between the North

Pole and Franz Josef Land on 20 August and moved into the Laptev Sea until 22 August. During the work on the third investigated ice floe at 85°N 108°E (19 to 22 August) and the fourth floe at 83°N 130°E (24 to 26 August), the *Polarstern* was situated at the outer area of the high pressure system and was thus accompanied by dense fog, which at times lifted into deep stratus and persisted until 26 August.

From 26 August onwards the weather situation changed so that *Polarstern* was influenced by several low pressure systems. On 25 August, a strong low formed north of Greenland, deepened, crossed the North Pole on 27 August, and passed over *Polarstern* on 28 August. During the night to 27 August, *Polarstern* was crossed by its occlusion, with winds temporarily increasing to 6 Bft and reduced visibility due to snowfall. The weather continued to be characterized by low stratus and intermittent snowfall on the back side and in the area of the low centre. On 29 August, another low formed north of Greenland, which moved northward while deepening, crossing the North Pole and *Polarstern* (which just left the fifth floe at 85°N 130°E, where it had stayed from 28 to 31 August) on 1 September, and reaching the New Siberian Islands on 3 September, where it filled up. In the process, the wind temporarily increased to 6 Bft on 30 August. A third, weaker low developed just north of Greenland on 3 September, but this time taking a westerly path and quickly filling up.

From 3 to 6 September, *Polarstern* was anchored at the sixth floe at 88.5°N 112°E and was accompanied by continuous fog, which caused heavy ice accumulation on the ship. This at times very dense advection fog was caused by a storm low coming from the southwest and being situated over Svalbard on 5 and 6 September, which transported a warm, humid air mass north to the North Pole. Temperatures just above 0°C were recorded on 6 September. The low subsequently weakened and moved northwest, transporting a much cooler and drier air mass from Greenland to the North Pole from 7 September onwards. This led to one of the friendliest weather periods during the whole voyage, perfectly matching the North Pole visit of *Polarstern*, in whose immediate vicinity the seventh ice floe was scientifically investigated from 7 to 11 September. On 9 September, the low moved south over Ellesmere Island into the Baffin Bay (10 September) while weakening.

Starting in the night to 10 September, *Polarstern* was influenced by a deep low which moved from the Greenland Sea over Svalbard (8 September) and Franz-Josef-Land (9 September) to Severnaya Zemlya by 10 September. On this path, the deep low temporarily split into a low-pressure complex with several cores by forming secondary lows. On 11 September, the low moved towards the North Pole while weakening and on 12 September it changed direction towards Franz-Josef-Land, where it filled up until 18 September. Thereby, the low crossed *Polarstern* on 14 September, which was heading south along longitude 60°E from 12 September on including its eighth ice station at 88°N 60°E from 13 to 15 September. In the transported more humid and milder air mass, snowfall occurred regularly from 10 September in the evening until 15 September, and the wind temporarily increased to 5 Bft on 11 and 13 September. After passage of the low centre on the morning of 14 September, the wind even increased to 7 Bft on the back side.

On the back side, on 16 and 17 September, there was a significant weather improvement in the area of a high-pressure ridge extending from Greenland to the northeast and moving to the south.

From 18 to 23 September, *Polarstern* was influenced by a large-scale low-pressure system, which moved from the Beaufort Sea (16 September) over the North Pole (night to 20 September) to Svalbard (22 September) while weakening and then slowly filled up near Svalbard. Thereby, light snowfall often occurred and on 18 September a mean wind speed of 5 Bft from the northwest temporarily occurred. After the ninth and last floe had been investigated from 19 to 20 September at 85.5°N 60°E, *Polarstern* returned west to the position of the first floe. On

22 September, *Polarstern* started its way back to Bremerhaven and left the sea ice north of Svalbard during the night to 24 September.

The return voyage was characterized by several deep lows, which originated from former hurricanes. The first deep low moved from the northern tip of Norway (22 September) under further deepening across the Barents Sea until 24 September into the Kara Sea, while *Polarstern* travelled southward in a northerly air flow through the Fram Strait. Off the west coast of Svalbard, two small-scale depressions formed in the northerly flow on 24 September and were responsible for a momentary wind speed increase to 8 Bft and about 5 cm of new snow.

After a short period of intermediate high pressure, *Polarstern* was influenced by an even deeper low from 25 September onwards, which moved from the Faroe Islands to the northeast and crossed *Polarstern* over the Norwegian Sea in the night to 26 September. Thereby, the wind, which was still weak with 2 Bft in the morning of 25 September, shifted to the east by the night to 26 September and increased to 9 Bft, and the significant wave height rose to 6 m. The deep low moved into the Barents Sea while slow weakening until 27 September. In the meanwhile, *Polarstern* was accompanied by a wind from southwest of at first 8 to 9 Bft on 26 September, which decreased to 5 Bft by 27 September, while at the same time the sea slowly decreased to 2 m. However, it was followed by another deep low that formed just northeast of Iceland on 27 September and moved to the northnortheast, slowing down the decrease in wind and wave height.

A fourth low pressure system, which in the meantime had crossed the North Atlantic from the west and deepened into a deep low, moved northeast crossing Scotland in the night of 28 September and subsequently weakened. When entering the North Sea, by the morning of 28 September, wind and sea state therefore increased to 9 Bft from the southeast and 4 m. When the front of the deep low crossed *Polarstern* in the early morning of 28 September, isolated embedded showers and thunderstorms also occurred in the rain. Another deep low followed the previous one to the northeast and crossed the Faroe Islands on 29 September. On the remaining route to Bremerhaven occurred mostly wind of about 6 Bft from southwest to west and steadily decreasing significant wave heights, while a high pressure system was moving from the Bay of Biscay (29 September) to Germany (30 September). *Polarstern* finally arrived in Bremerhaven in the afternoon of 30 September.

2. SEA-ICE PHYSICS

Marcel Nicolaus[1], Emiliano Cimoli[2], Carolin Mehlmann[3], Ian Raphael[4], Julia Regnery[1], Thomas Richter[3], Jan Rohde[1]
not on board: Thomas Krumpen[1], Donald K. Perovich[4], Benjamin Allen Lange[5]

[1]DE.AWI
[2]AU.UTAS
[3]DE.OVGU
[4]EDU.DARTMOUTH
[5]NO.NGI

Grant-No. AWI_PS138_04 and AWI_PS138_09

Outline and objectives

Sea ice is an integrator between the atmosphere and the ocean. Studying the physical properties and key processes of sea ice and its snow cover was the main objective of our work during ArcWatch-1. This work was strongly linked to all other groups, in particular the ecosystem and biogeochemical properties and processes of sea ice. The overarching objectives of the ice physics work during ArcWatch-1 were to:

- Better understand the ongoing changes of the sea ice in the central Arctic. This work is embedded into various observational programmes and previous expeditions. In particular, the data will allow comparisons to sea-ice conditions of the IceArc 2012 (PS80, Boetius et al., 2013) and MOSAiC 2019/20 expeditions (Nicolaus et al., 2022)
- Better understand the seasonality of sea ice and snow processes. Here we focused on the transition from melt to freeze-up conditions. This work will closely link to the MOSAiC 2019/20 expedition (Nicolaus et al., 2022) and various *Polarstern* expeditions during the same time in previous years.
- Advance our process understanding of atmosphere-ice-ocean interactions, in particular with respect to thermodynamic processes, strongly linked to the role of sea ice as a habitat and as a barrier for atmosphere-ocean interaction.
- Advance observational capabilities, by gaining experience and new types of data sets from new instruments and measurement systems.
- Calibrate a hybrid sea-ice model in an optimal experimental design setup on board of *Polarstern*.

More specifically, our work at sea and the expected results can be grouped under 3 topics, each of them contributing to an improved understanding of the sea ice, snow and melt-ponds system and its linkages:

Sea ice mass balance and energy budgets

We studied the mass balance and thickness distributions on different spatial scales over the transition from melt to freeze-up conditions. ArcWatch-1 contributes to our Arctic sea-ice thickness monitoring program performed from vessels and aircrafts. During the expedition, we measured sea ice and snow distributions along the cruise track across the Arctic Ocean (for further information please see Section 2.1 and 2.3 of this chapter) and with higher spatial resolution during each ice station (floe-size distributions, see Section 2.2 and 2.4). Autonomous

instruments were deployed to cover snow and ice mass balance parameters over the annual cycle (Chapter 6) and numerical studies were performed linked to *in-situ* observations on floe dynamics (Section 2.5).

The main objective of the optical work during ArcWatch-1 was to quantify the horizontal and vertical distribution of short-wave radiation (hyperspectral and broadband), as it is reflected back to the atmosphere, absorbed in snow, melt ponds and sea ice, or transmitted into the uppermost ocean. These budgets were obtained on different spatial scales during all ice stations, ranging from point measurements and local transects to mapping of radiation conditions on floe-scales from above and below (Sections 2.2 and 2.4). This work continued studies from previous expeditions, in particular IceArc 2012 and MOSAiC 2019/20.

An important element connecting the mass and energy-budget studies is the fate of meltwater. The accumulation in melt ponds (surface) and in a meltwater layer right under the sea ice were targeted, but the ice conditions during the expeditions showed much less melt and melt water than expected. Hence this objective could not be followed as planned.

Bio-physical linkages

The role of sea ice as a habitat needs to be much better understood, while the extreme spatial and temporal variability adds most complexity. Key elements were optical mapping of sea ice from above and below and sampling of sea ice to derive its bio-physical properties. This allows creating budgets of biomass as well as improving process understanding and linkages. We performed ROV-based under-ice surveys (Section 2.4)

To provide a baseline for *in-situ* ROV optical data with sampled biogeochemical variables by other groups, we utilized a novel ice-core scanning system harnessing the full range VIS-SWIR (visible – short-range infrared) and sub-mm resolution to further link vertical biological, chemical and structural properties of the ice. While we will focus on the quantification of the physical environment, this work will strongly be linked to the work of the ecological group (Chapter 4).

Ice floe dynamics and numerical model improvements

It is important to directly connect field observations and numerical models to calibrate a hybrid sea-ice model in an optimal experimental design setup. The hybrid model explicitly describes the interactions between sea ice, ocean, and atmosphere at the floe scale using interacting particles (ice floes). To calibrate the hybrid sea-ice model, we gathered information on the drift of single sea-ice floes, characteristics of ice floes such as their size, shape, height, and environmental data, such as wind velocities (Section 2.5). The immediate connection of observations and on-board simulations allowed us to collect exactly and only those data that have a large impact on the model accuracy.

General ice conditions and ice station work

The expedition was conducted during the minimum sea-ice coverage in the Arctic in 2023. The minimum extent was reached on 15 September with an area of 4.33 Mio km^2 (for comparison: 2012: 3.48 Mio km^2, 2022: 5.03 Mio km^2). This was the 7th lowest extent of the area of satellite observations since 1979. Figure 2.1 shows the cruise track of the expedition, including the sea-ice concentration map of the minimum on 15 September 2023. Most of the sea ice that was sampled and measured during ArcWatch-1 originated from a central Arctic Ocean basin (e.g., 160°E/78°N). This is different to the origin of the main comparison years in 2012 and 2019/20, when the ice originated from the Laptev Sea shelves. This caused significant differences in ice and water-mass properties. Sea ice originating from the Laptev Sea, which would have

been important to relate to, could not be reached, because all this ice was drifting south of the expedition track in the Russian Exclusive Economic Zone (EEZ).

A major part of the sea-ice physics work was conducted during 9 ICE stations (Tab. 2.1 and Fig. 2.1), when the vessel was anchored to the ice for parts of the station time. Table 2.1 summarizes the main characteristics and statistics of each ICE station. Note that the term of ICE stations was used in two ways during the expedition: These were the stations where most on-ice work was performed, but also the main stations of most other groups, including deep-sea deployments (Chapter 5) and pelagic work (Chapters 3 and 4). Additional sea-ice physics work was performed continuously along the cruise track (Section 2.1) and during short stations, when the ice was accessed by mummy chair or zodiac. Details of these stations may be found in the other sub-chapters. Appendix A.5 contains maps of most ice stations (for some stations these maps are not available), providing an overview of relative locations of different activities on the sea ice.

It was part of the expedition plan to re-visit the ICE 1 floe at the end of the expedition again. This would have enabled a direct comparison of physical and biological sea-ice properties after 6 weeks of drift. Therefore, various autonomous stations were installed on, in, and under the sea ice (Chapter 6) and measurement sites were marked for repeat measurements. However, the floe drifted unexpectedly into the exclusive economic zone (EEZ) of Russia and was thus not accessible for a re-visit for political reasons. At the time of potential re-visit, the station was approx. 5 nmi into the EEZ (Fig. 2.1). The station continued drifting and sending positions and we hope to be able to recover it at a later time point.

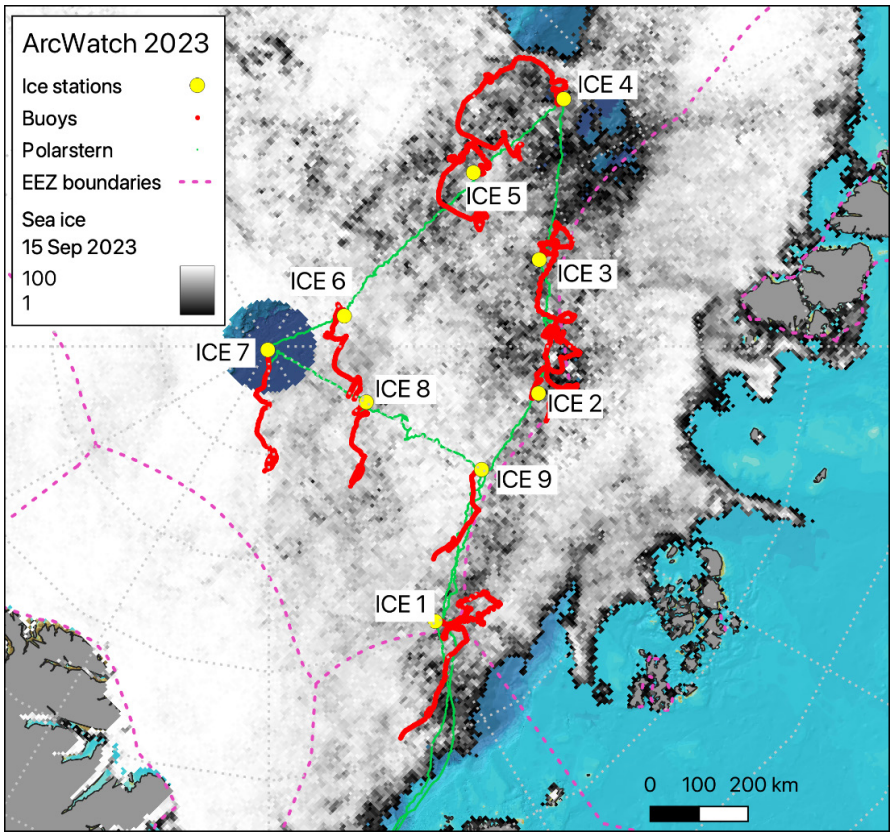

Fig. 2.1: Cruise map of ArcWatch-1. The map shows all ICE stations (yellow dots), the cruise track of Polarstern (green line), the drift of the ICE stations based on buoy data (red lines, Chapter 6) until 17 October 2023, and sea-ice concentration on the day of minimum extent on 15 September 2023 (from meereisportal.de).

Tab. 2.1: Basic information of all ICE stations during ArcWatch-1. Selected buoys are included as markers of the respective station. They are identified through their name (e.g., 2023O17, see meereisportal.de) and their International Mobile Equipment Identity (IMEI) number.

Station	**ICE 1**	**ICE 2**	**ICE 3**
Event	PS138_9-1	PS138_31-1	PS138_52-1
Date Time (Start)	08.08.2023 10:40	15.08.2023 06:08	19.08.2023 12:00
Longitude (°E, Start)	31.212	80.140	107.792
Latitude (°N, Start)	84.074	84.950	84.761
Date Time (End)	12.08.2023 02:05	17.08.2023 10:17	21.08.2023 20:02
Longitude (°E, End)	34.102	80.111	107.713
Latitude (°N, End)	83.848	84.956	84.684
Floe size (in nmi)	1.5 x 2.5	0.9 x 0.6	1.0 x 0.7
CTD buoy	2023O17 (300234068166760)	none	none
Snow Buoy	2023S103 (300234066896250)	none	none
Thermistor buoy	2023T104 (300234068527600)	none	none
Position buoys	2023P273 (300534064261600)	2023P268 (300534063489680)	2023P264 (300534063486700)
	2023P278 (300534064264600)		
	2023P280 (300534064264620)		
Station	**ICE 4**	**ICE 5**	**ICE 6**
Event	PS138_75-1	PS138_101-1	PS138_129-1
Date Time (Start)	24.08.2023 06:32	28.08.2023 09:25	03.09.2023 06:39
Longitude (°E, Start)	129.993	130.350	112.038
Latitude (°N, Start)	82.902	85.045	88.496
Date Time (End)	26.08.2023 18:26	31.08.2023 20:36	06.09.2023 09:49
Longitude (°E, End)	129.872	129.408	114.508
Latitude (°N, End)	82.958	84.940	88.459
Floe size (in nmi)	--	0.5 x 0.3	--
CTD buoy	2023O18 (300234068514740)	2023O20 (300534060151880)	2023O23 (300534064368480)
Snow Buoy	2023S123 (300234060543140)	2023S126 (300234060729780)	none
Thermistor buoy	2023T99 (300534061345540)	2023T106 (300534063056460)	2023T102 (300234068701300)
Position buoys	none	none	none
Station	**ICE 7**	**ICE 8**	**ICE 9**
Event	PS138_152-1	PS138_178-1	PS138_213-1
Date Time (Start)	07.09.2023 19:56	13.09.2023 08:30	19.09.2023 19:50
Longitude (°E, Start)	-15.223	60.323	59.97

Station	ICE 1	ICE 2	ICE 3
Latitude (°N, Start)	89.936	87.928	85.464
Date Time (End)	11.09.2023 15:01	15.09.2023 15:46	20.09.2023 12:28
Longitude (°E, End)	3.779	56.911	59.983
Latitude (°N, End)	89.689	87.882	85.472
Floe size (in nmi)	--	--	0.8 x 0.4
CTD buoy	none	none	none
Snow Buoy	2023S100 (300234066088170)	2023S101 (300234066797650)	none
Thermistor buoy	2023T110 (300534061780910)	2023T100 (300534061348580)	none
Position buoys	2023P286 (300534063804280)	none	2023P272 (300534064260620)

2.1 Routine sea-ice observations and remote sensing

Work at sea

We operated a panorama camera (type Panomax, PS138_0_Underway-33) above the crow's nest during the entire expedition, taking regular photographs of the sea ice and weather conditions in 5 min intervals. The first photo was taken on 5 August 2023 19:30 UTC and the last photo on 24 September 2023 10:40 UTC (total 13,211 photos). The photos were available in the intranet on board. Note a time offset of the original photos of 48 min (photo time = UTC + 48 min).

In addition, a surveillance camera (type Reolink, PS138_0_Underway-54) was operated on A-Deck looking over starboard side from 08 August 21:05 UTC in 5 min intervals until 21 September 13:45 UTC (total 12,593 photos).

Spectral solar irradiance was recorded with a Ramses spectral radiometer (type Trios Ramses VIS ACC, Sensor ID SAM8333, PS138_0_Underway-53) in 10 min intervals during the entire expedition. The first spectrum was recorded on 4 August 2023 12:20 UTC and the last spectrum on 24 September 2023 10:10 UTC (total 7,330 spectra).

Sea-ice observations were conducted from the bridge of *Polarstern* while the vessel was moving through ice and not on station. The observations describe the conditions within a radius of 1.5 nmi around the vessel, including sea-ice concentration, floe size, fraction of ridged ice and melt ponds, sea-ice thickness, and weather conditions. The vessel crossed the sea-ice edge on 6 August 2023 around 20:00 UTC and left the ice again on 24 September 2023 08:00. The first ice observation was performed on 6 August 2023 21:30 UTC and the last observation on 23 September 2023 18:00 UTC (PS138_0_Underway-55). In total 181 observations were recorded.

Various satellite images were received on board during the expedition. These data were automatically imported into the on-board Mapviewer software to support navigation and station planning. In addition, the images will be used for further analyses of sea-ice conditions in connection with the other sea-ice and surface observations. High resolution versions of different data products are available once back on shore. Main data products were: AMSR-2 sea-ice concentration (provided by University of Bremen), ESA Radarsat Constellation Mission radar images (RCM, provided by Drift & Noise Polar Services), TerraSAR-X radar images in

ScanSAR and StripMap modi (TSX, provided by DLR), Sentinel 1 radar images (provided by Drift & Noise Polar Services). While most data products were retrieved automatically, the high resolution TSX images were ordered manually through direct communication with DLR. Daily orders were placed defining the target regions and modus. In addition, sea-ice drift forecast data were received through the Polar Prediction Network programme SIDFEX (provided by Valentin Ludwig, AWI).

Preliminary (expected) results

These routine observations will mostly be used as supplemental material of the other data sets. They allow creating a timeline of events and changing conditions as travelling through space and time during the expedition. Examples of the panorama photos are shown in Figure 2.2. The photos of 10 August and 22 September were taken at approx. the same location, but 6 weeks apart. This illustrates the effects of freeze-up at the surface, freezing all melt ponds and new ice formation in open water. The photograph of ICE 7 shows the conditions at the North Pole with remarkably little melt ponds and a thick snow cover at the time. The regular photographs can be rectified and geo-referenced to e.g., derive sea-ice concentration along track with high temporal resolution. The measurements of solar irradiance support the other optical measurements during the different ice stations and can be compared to identical measurements on previous or later expeditions.

The satellite images will be used to derive sea-ice conditions along track after the expedition. In connection with the buoy deployments, they will be combined with the direct measurements of the buoys to support further analyses and discussion of observed changes, both ways from the buoys to satellite images and the other way around. Examples of buoy data are shown in Chapter 6. The satellite data will support improvements of satellite algorithms to derive sea-ice surface properties.

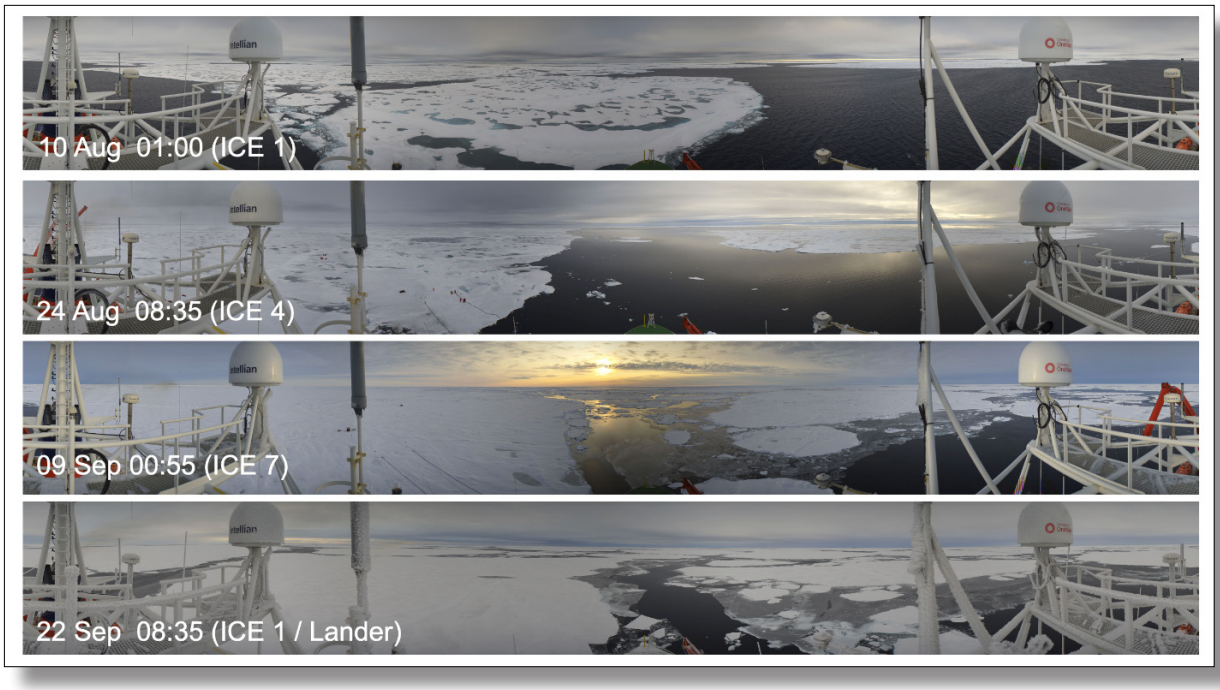

Fig. 2.2: Sea-ice conditions on four selected days, as recorded from the 360° panorama camera mounted on the crow's nest.

2.2 Transect measurements of physical properties of sea ice

Work at sea

Sea ice and snow thickness were measured along transects across the floe on each ICE station. Table 2.2 summarizes all existing data sets. The total transect length depended on snow, sea ice and weather conditions, as well as the floe size. The aim was always retrieving as long and as representative transects as possible from each floe. All transects were performed by walking and pulling a pulka with the GEM device and probing the snow with a Magna Probe.

Incident and reflected irradiance were measured at each station with a hyperspectral radiometer (type ASD Fieldspec) and a Kipp/Zonen broadband pyranometer (Tab. 2.3). Here we use the short name ASD for the hyperspectral radiometer. The measurements were co-located with the work using the remotely operated vehicle (ROV, Section 2.4) along a 100 m long transect every 5 m (Fig. 2.3). The lines were chosen to follow one of the survey area gridlines. Under-ice surveys were conducted using the ROV that included transmission measurements directly below the surface optics transects.

Sea-ice temperature and salinity were measured from ice cores on each ice station. The work and results are described in Chapter 4. Additional cores were drilled, packed and shipped to Bremerhaven for later texture analyses and as archive cores. Sea-ice cores for further optical properties are described in Section 2.4.

Tab. 2.2: Transect measurements for sea-ice thickness (GEM) and snow depth (Magna Probe)

Label	Date	Time	Device short name	Latitude	Longitude
PS138_9_GEM_001	09.08.2023	09:39	gem2-512	84.067	31.217
PS138_31_GEM_001	15.08.2023	10:50	gem2-512	84.950	80.133
PS138_52_GEM_001	19.08.2023	16:46	gem2-512	84.767	107.783
PS138_52_Magna_001	19.08.2023	16:48	magnaprobe-steffi	84.767	107.783
PS138_75_GEM_001	25.08.2023	14:31	gem2-512	82.902	129.993
PS138_101_GEM_001	30.08.2023	13:26	gem2-512	85.045	130.350
PS138_101_Magna_001	30.08.2023	13:32	magnaprobe-steffi	85.045	130.350
PS138_129_GEM_001	04.09.2023	14:55	gem2-512	88.496	112.038
PS138_129_Magna_001	04.09.2023	15:00	magnaprobe-steffi	88.496	112.038
PS138_152_GEM_001	10.09.2023	06:52	gem2-512	89.936	-15.223
PS138_152_Magna_001	10.09.2023	06:57	magnaprobe-steffi	89.936	-15.223
PS138_178_GEM_001	14.09.2023	08:55	gem2-512	87.928	60.232
PS138_178_Magna_001	14.09.2023	09:02	magnaprobe-steffi	87.928	60.232
PS138_213_GEM_001	19.09.2023	17:06	gem2-512	85.464	59.970
PS138_213_Magna_001	19.09.2023	17:08	gem2-512	85.464	59.970

Tab. 2.3: Transect measurements for optical properties using the ASD (spectral) and Kipp/Zonen (broadband) instruments. Abbreviation: K/Z: Kipp/Zonen

Station and devices	**Survey date, time (dd.mm.yyyy, hh:mm) Device Operation**	**Solar noon (hh:mm)**	**Sky conditions**	**Solar disk visible**	**Surface conditions**
ICE 1 ASD Kipps	09.08.2023, 11:00 PS138_9_ASD_001 N/A	10:00	Partly cloudy	yes	SSL >3 cm, <1 cm snow in places; melt ponds
ICE 2 ASD Kipps	16.08.2023, 07:30 PS138_31_ASD_001 PS138_31_Kipps_001	06:44	High clouds	Yes	SSL, snow (3-4 cm), refrozen (~2 cm) melt ponds
ICE 3 ASD Kipps	20.08.2023, 06:13 PS138_52_ASD_001 PS138_52_Kipps_001	04:52	Foggy, overcast	Yes	SSL, snow in some places, refrozen (4-8 cm) melt ponds
ICE 4 ASD Kipps	25.08.2023, 03:30 PS138_75_ASD_001 PS138_75_Kipps_001	03:21	Foggy, overcast	No	Snow in ridges; refrozen melt ponds
ICE 5 ASD Kipps	29.08.2023, 05:40 PS138_101_ASD_001 PS138_101_Kipps_001	03:19	High clouds	No	Fresh snow 2-3 cm
ICE 6 ASD Kipps	04.09.2023, 04:15 PS138_129_ASD_001 PS138_129_Kipps_001	04:31	Foggy, low clouds	Yes	10 cm cold, new snow
ICE 7 ASD Kipps	10.09.2023, 06:45 PS138_154_ASD_001 PS138_154_Kipps_001	12:58	Overcast, light precipitation, on the edge of rain	No	2-3 cm new, wet snow; no old snow; well developed SSL and glazed surface in some places, crust ~2cm thick.
ICE 8 ASD Kipps	13.09.2023, 07:15 PS138_178_ASD_001 PS138_178_Kipps_001	07:54	Overcast	No	Fresh snow >5 cm
ICE 9 ASD Kipps	20.09.2023, 08:30 PS138_213_ASD_001 PS138_213_Kipps_001	07:53	Partly cloudy, lightly snowing	Yes	New 5-8 cm snow cover on all surfaces

Fig. 2.3: Measuring spectral albedo using the ASD spectral radiometer at ArcWatch-1 station ICE 9.

Preliminary (expected) results

At all ICE stations, the total thickness of snow and ice was measured using the GEM2 electromagnetic sounding instrument. Additionally at all stations with snow, the snow thickness was measured using the Magna Probe. An exception was station ICE 2, here the Magna Probe data was lost due to a corrupt memory stick. The thickness of snow and ice can be compared to EM-Bird measurements and the ROV under-ice measurements.

The spectral and broadband albedo surveys were performed at all ICE stations and contribute to the long-term record of albedo measurements in the central Arctic. These observations will help fill observation gaps from the MOSAiC expedition and will help us continue characterizing and understanding the variability in surface albedo during the transition from the melt season to the winter. For technical reasons, broadband albedo measurements were not made at ICE 1. Figure 2.4 shows the broadband albedo for each ICE station. ICE 4 had the lowest mean albedo of 0.60, while all other stations ranged between 0.73 and 0.87. Later analyses will merge these survey data with the surface photography from the drone (Section 2.3) and the ROV (Section 2.4). This will provide a 2-dimensional view on albedo and transmission properties during the melt season and into freeze-up and improve our understanding of spatial variability of these properties.

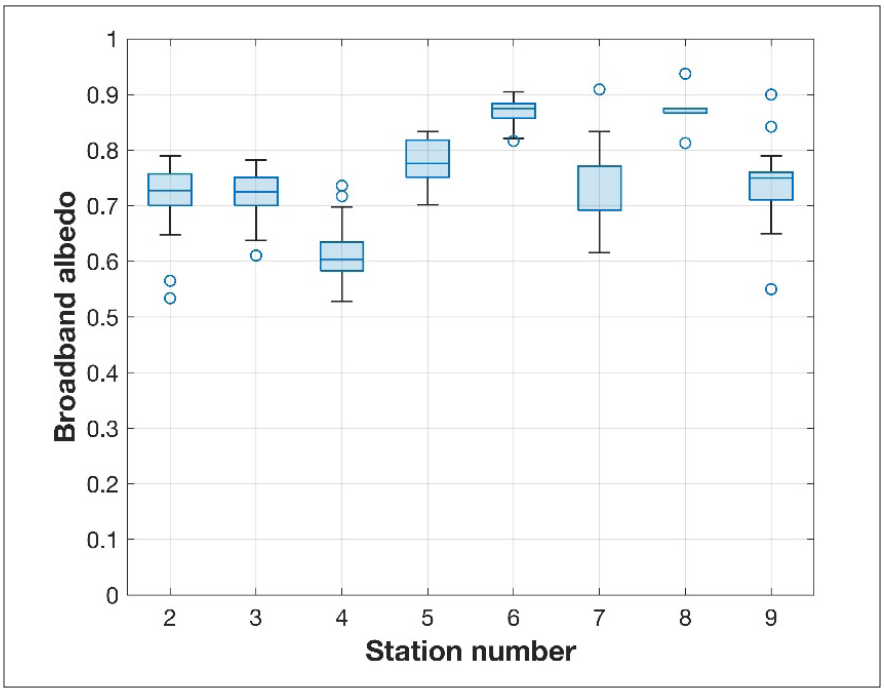

Fig. 2.4: Broadband albedo measurements at ArcWatch-1 stations ICE 2 to ICE 9 (broadband albedo measurements were not made at ICE 1). Boxes represent the upper and lower quartiles of the measurements at each station. The bar inside each box represents the sample median. The whiskers represent the minimum and maximum non-outlier values; outliers are shown as circles.

2.3 Airborne sea-ice surveys

Work at sea

Total (sea ice plus snow) sea-ice thickness was measured using airborne electromagnetic induction sounding. For the first time, we operated the newly developed EM-bird system built at AWI. In total, we conducted 16 flights with a total distance of about 900 km. Figure 2.5 shows a map with all flight tracks and Table 2.4 gives additional information for each survey. With these flights, we were able to derive sea-ice thickness distribution functions representative for up to 60 nmi around the cruise track. Flight operations were mostly limited by weather conditions (fog, low ceiling, visibility). In addition to the scientific results, operating the new system will help to further develop the system and gain more experience in different ice conditions.

We conducted drone-based (type: DJI Mavic 3) photo surveys of each floe, and a few underway ice conditions, to map the sea-ice surface conditions with high-resolution visual photographs. These photographs were stitched afterwards and allow surface descriptions, classifications, and the quantification of surface properties, such as surface albedo. In total, we performed 18 surveys as summarized in Table 2.5. Most surveys targeted the ROV area, while often a lower survey was performed to retrieve higher surface resolution and a higher survey for a larger area coverage. The drone was mostly operated from the ice. Operations from *Polarstern*, e.g. for the underway flights, were performed from the helicopter deck.

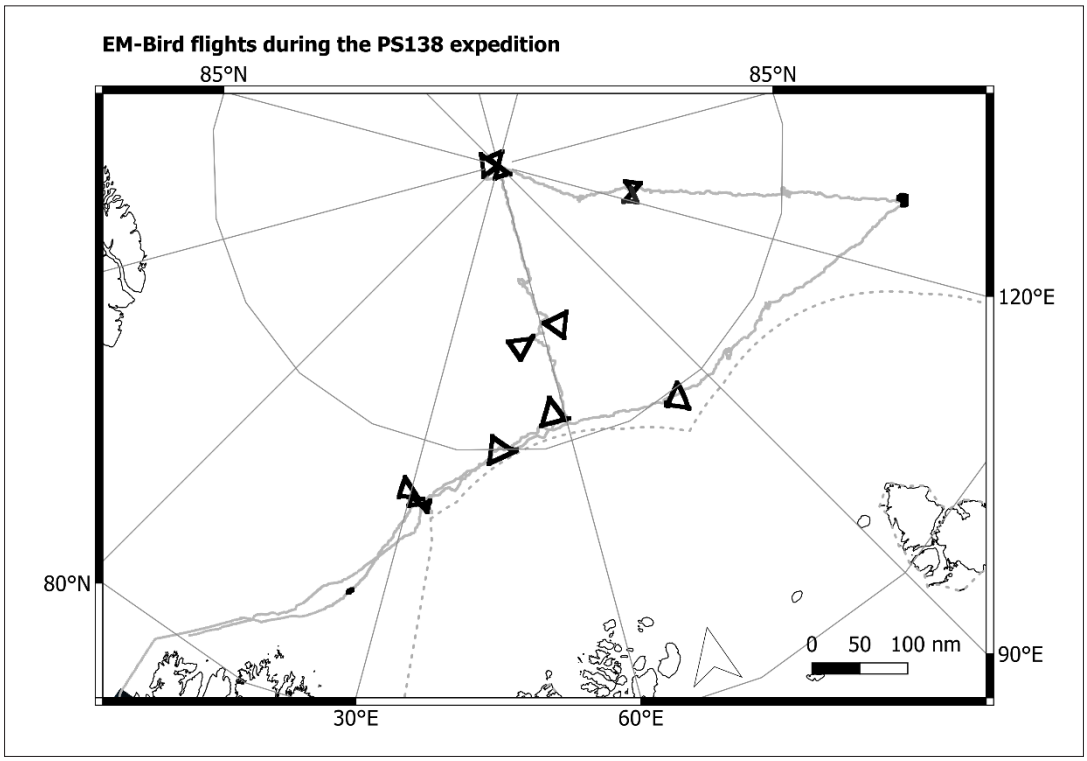

Fig. 2.5: Map with all EM-bird flights during ArcWatch-1. Black lines show the EM-bird tracks and the grey line shows the Polarstern track. The dashed line marks the exclusive economic zone (EEZ) of Russia.

Tab. 2.4: List of all surveys with the EM-bird during ArcWatch-1.

Label	Date, time	Latitude	Longitude	File names	Comment
PS138_Heli_ EM-Bird_001	2023-08-07 07:33 to 07:49	82.15242	25.6765	20230807092931.tdms 20230807093336.tdms	Flight aborted due to weather.
PS138_Heli_ EM-Bird_002	2023-08-08	84.06541	31.0061	20230808152614.tdms 20230808153018.tdms 20230808155701.tdms 20230808161830.tdms	Flight near first ice station.
PS138_Heli_ EM-Bird_003	2023-08-16 11:13 to 12:39	84.90896	80.223	20230816131350.tdms 20230816132048.tdms 20230816134038.tdms 20230816141006.tdms 20230816143009.tdms	Flight near second ice station. no wind, sunshine, a lot of open water.
PS138_Heli_ EM-Bird_004	2023-08-16 13:09 to 13:37	84.9328	80.2200	20230816150957.tdms 20230816151122.tdms	Second flight near second ice station. A short flight over the ice station.

Label	Date, time	Latitude	Longitude	File names	Comment
PS138_Heli_ EM-Bird_005	2023-08-20 07:50 to 07:51			20230820095030.tdms laser-offset-measurement.JPG	The difference between laser height and coil plane is measured.
PS138_Heli_ EM-Bird_006	2023-08-24 09:31 to 10:47	82.9117	130.0705	20230824113111.tdms 20230824113401.tdms 20230824115743.tdms 20230824122109.tdms 20230824124216.tdms	Flight near the fourth ice station.
PS138_Heli_ EM-Bird_007	2023-08-27 11:48 to 12:39	84.5956	130.1629	20230827134805.tdms 20230827135052.tdms 20230827141422.tdms	Short flight during Transit that had to be aborted due to bad weather.
PS138_Heli_ EM-Bird_008	2023-09-02 07:26 to 08:43	87.6256	124.4385	20230902092653.tdms 20230902092924.tdms 20230902095350.tdms 20230902101459.tdms	Flight during transit.
PS138_Heli_ EM-Bird_009	2023-09-07 13:05 to 14:16	89.9912	-32.1852	20230907150505.tdms 20230907150734.tdms 20230907150750.tdms 20230907151506.tdms 20230907153431.tdms 20230907155244.tdms	Flight at the North Pole
PS138_Heli_ EM-Bird_010	2023-09-08 07:11 to 08:59	89.9238	32.5704	20230908091116.tdms 20230908091430.tdms 20230908093606.tdms 20230908095209.tdms 20230908101434.tdms 20230908103115.tdms 20230908104824.tdms	Second flight at the North Pole and flight over the ice station.
PS138_Heli_ EM-Bird_011	2023-09-16 10:43 to 11:52	87.1022	61.9356	20230916124333.tdms 20230916124657.tdms 20230916130813.tdms 20230916133014.tdms 20230916135217.tdms	Flight during transit. Experiment for new calibration.
PS138_Heli_ EM-Bird_012	2023-09-17 08:08 to 09:16	86.9588	55.7967	20230917100847.tdms 20230917101135.tdms 20230917103229.tdms 20230917105110.tdms	Flight during transit.
PS138_Heli_ EM-Bird_013	2023-09-19 07:37 to 08:54	85.4537	60.0418	20230919093731.tdms 20230919094004.tdms 20230919100504.tdms 20230919100521.tdms 20230919102944.tdms	Flight near Ice station 9.

Label	Date, time	Latitude	Longitude	File names	Comment
PS138_Heli_EM-Bird_014	2023-09-19 13:58 to 14:36	85.4549	59.8929	20230919155909.tdms 20230919160707.tdms	Second flight near ice station 9, survey of the ice floe.
PS138_Heli_EM-Bird_015	2023-09-21 08:05 to 09:22	85.0287	48.5201	20230921100549.tdms 20230921100804.tdms 20230921103352.tdms 20230921105740.tdms	Transit back to area of ice station 1.
PS138_Heli_EM-Bird_016	2023-09-22 08:36 to 09:43	83.9567	32.0423	20230922103704.tdms 20230922103957.tdms 20230922105904.tdms 20230922111801.tdms	Back at area of ice station 1.

Tab. 2.5: Drone surveys during ArcWatch-1.

Event Label	Date (dd. mm.yyyy)	Time (hh:mm:ss)	Height (m)	Number images	Comment
PS138_9_DRONE_001	10.08.2023	19:29:46	36	113	ICE 1 floe grid
PS138_9_DRONE_002	10.08.2023	19:37:14	43	52	ICE 1 ROV grid
PS138_31_DRONE_001	15.08.2023	16:12:44	15	120	ICE 2 ROV grid
PS138_31_DRONE_002	16.08.2023	10:22:02	25	14	ICE 2 floe grid
PS138_52_DRONE_001	19.08.2023	16:24:28	133	56	ICE 3 floe grid
PS138_52_DRONE_002	20.08.2023	16:27:38	265	134	ICE 3 ROV grid
PS138_75_DRONE_001	24.08.2023	11:40:48	96	148	ICE 4 floe grid
PS138_101_DRONE_001	28.08.2023	14:02:42	274	119	ICE 5 floe grid
PS138_101_DRONE_002	29.08.2023	05:11:14	219	20	ICE 5 ROV grid
PS138_129_DRONE_001	03.09.2023	14:16:54	196	71	ICE 6 ROV grid
PS138_152_DRONE_001	09.09.2023	16:02:28	150	153	ICE 7 floe grid
PS138_178_DRONE_001	13.09.2023	11:50:08	422	103	ICE 8 floe grid
PS138_198_DRONE_001	16.09.2023	12:44:06	181	235	On transit
PS138_202_DRONE_001	17.09.2023	09:42:26	147	262	On transit
PS138_202_DRONE_002	17.09.2023	09:52:38	49	104	On transit
PS138_206_DRONE_001	18.09.2023	10:28:00	150	215	On transit
PS138_213_DRONE_001	19.09.2023	15:04:48	340	50	ICE 9 floe grid
PS138_213_DRONE_002	19.09.2023	15:19:06	200	98	ICE 9 ROV grid

Preliminary (expected) results

The AWI-developed EM-Bird performed very well. The instrument worked very reliably, which was also noticed positively by the helicopter team. Data analysis on board showed a resolution of ±5 cm. It should be mentioned that this accuracy was sometimes only in the range ±10 cm when there were strong flight movements or strongly changing weather. The exact reason for the changing accuracy still has to be determined. Overall, the data quality and resolution of the system is significantly better than the equipment previously used at AWI and the development of the new instrument can be considered as a success. To be improved in the future is the

performance of the operator software, which consumed a lot of computing and battery power, as well as the stability of the WiFi link, which failed twice during the expedition for 10 to 30 seconds. The new altimeter display was considered well suitable for the EM-Bird operation by the helicopter pilots.

The modal ice thickness of all surveys was 1.2 m with a mean thickness of 1.37 m without open water and 1.17 m including open water (Fig. 2.6). The modal thickness of 1.2 m was less than measured in the last years and also less than measured during the two IceBird campaigns in 2023. At the same time, the sea ice was extremely flat during ArcWatch-1 and had a very low sail frequency, compared to previous years (data not shown). The approximately 900 km of ice-thickness data was a typical result compared to past EM-Bird missions.

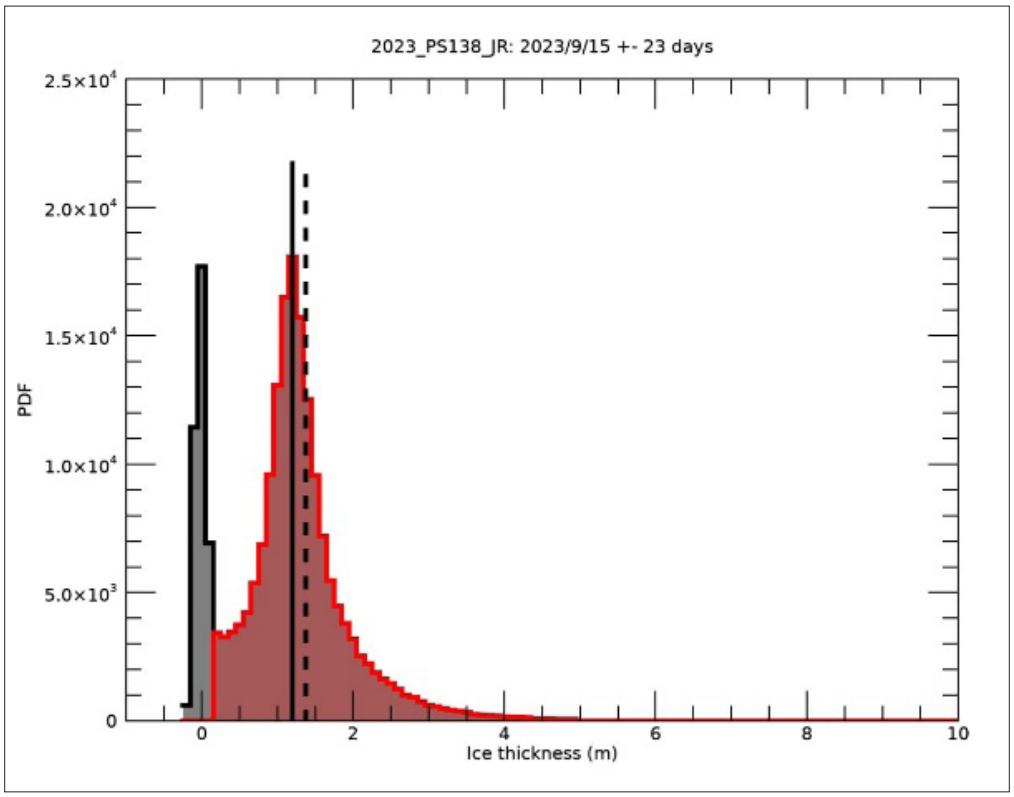

Fig. 2.6: Sea-ice thickness distribution of all EM-bird flights during ArcWatch-1 (map in Fig. 2.5). The black line marks the modal thickness of 1.2 m and the dashed line the mean thickness of 1.37 m (without open water).

Figure 2.7 shows an example for one of the photogrammetry grids, taken on station ICE 7 at the North Pole on 9 September 2023. The photo was cropped to a rectangular image from originally 153 individual photos taken from a height of 150 m. It shows the ROV grid with the deployment hole in the bottom centre of the photo. The main axis of the ROV grid (Section 2.4) heads towards the ice edge and 90° anti-clockwise from there into the floe. A few old melt ponds are visible mostly towards the floe edge, while new ice is forming in the open water.

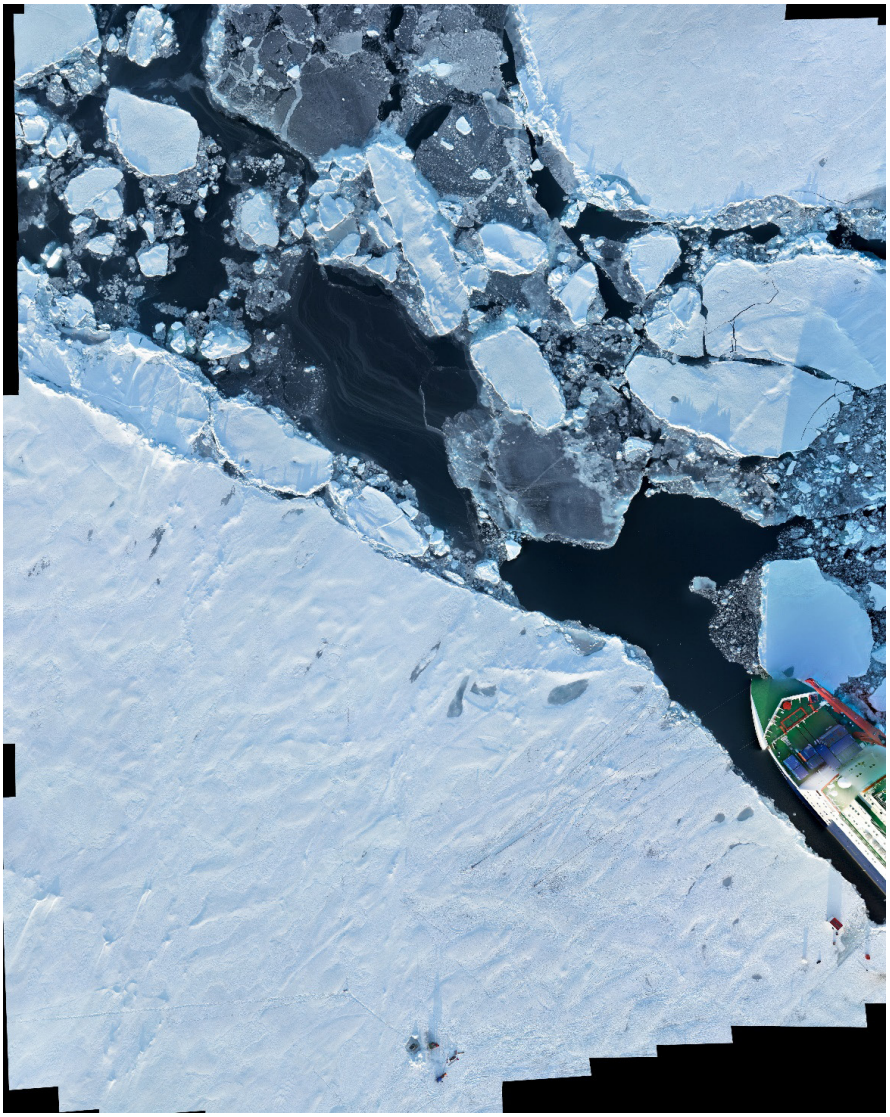

Fig. 2.7: Photomosaic of the drone survey of ICE 7 on 9 September 2023.
The photo shows the ROV area with the hole (centre bottom), the floe edge with Polarstern alongside, and the ROV hut (red roof) on the ice next to Polarstern. The photo covers approx. 250 x 400 m.

2.4 Remotely operated vehicle (ROV) operations

Work at sea

We operated the AWI ROV system “Beast” (Fig. 2.8) with its interdisciplinary sensor suite, as described in Katlein et al. (2017) with an additional Underwater Hyperspectral Imaging (UHI, Figs 2.8B and 2.12) system and additional GoPro cameras for still photos looking up to the ice bottom. The ROV was launched through the sea ice during each ICE station and operated in a radius of 300 m around the access hole. We tested a new configuration where the ROV control hut was setup next to *Polarstern* and thus directly at the ice edge (Fig. 2.8).

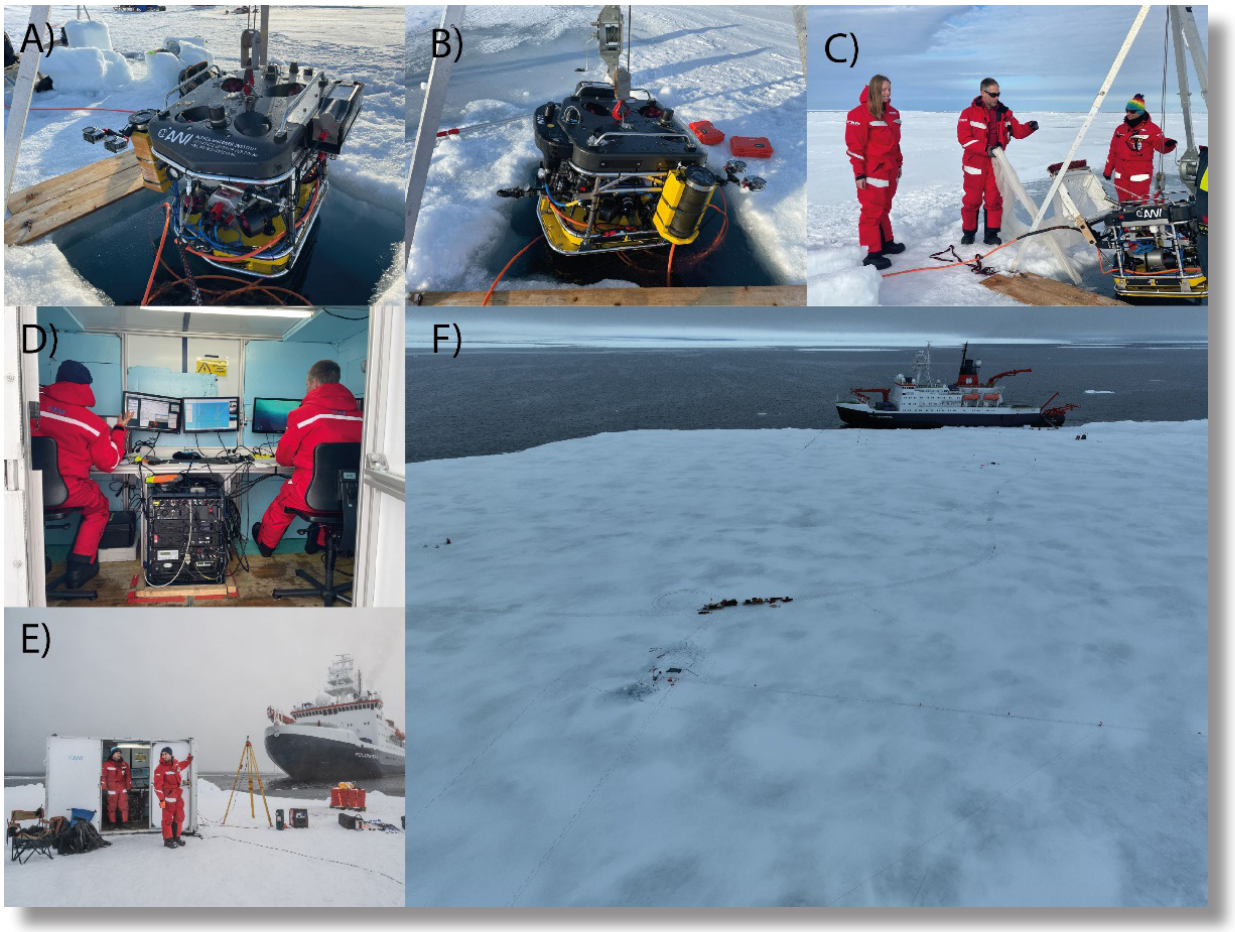

Fig. 2.8: Remotely operated vehicle operations during ArcWatch-1. (A+B) The ROV Beast at the ROV hole during deployment with the Underwater Hyperspectral Imaging (UHI) system and additional GoPro cameras mounted on the side, (C) The ROV-net setup at the ROV hole, (D) inside the ROV control hut, (E) ROV hut from the outside at the ice edge, (F) aerial view of the ROV site during station ICE 3. The main grid can be seen as the perpendicular 100 m long lines towards the front. The ROV hut is set up at the ice edge next to Polarstern.

This eased and accelerated deployment, because transportation of the hut across the ice was avoided. The system was, for the first time, powered with a combination of battery and generator power. Most ROV operations were performed in absence of *Polarstern* from the floe. In two occasions, when *Polarstern* was present during stations ICE 8 and 9 (needed for the internet link), live streams from the ROV dives to land were realized, demonstrating capabilities of remote interaction and live participation. The ROV setup enabled access to all different ice types present at that station and the open ocean / new sea ice. Figure 2.9 shows the navigation map, as used during ROV operations by the pilot(s), including the (uncorrected) track, and attention points. The background image helps orientation and navigation. These images were taken for each station, by drone, at the beginning of each ICE station.

We performed a total of 23 ROV dives (Tab. 2.6) with a total dive time of 74:41 hours. The dives consisted of different amounts of surveys and were of different complexity, mostly depending on time constrains within the overall station plan. We realized the following dive missions:

- 15 optical surveys to measure under-ice radiance (7° opening) and irradiance (cosine receptor) in horizontal (in 2 m depth) and vertical (down to 100 m depth). These

measurements included dedicated measurements along two lines, which were marked with marker poles (below the ice) and flags (above the ice) (Fig. 2.8F).

- 9 optical surveys with the upward looking UHI system to map the microscale under-ice habitat (Tab. 2.9) in very high spectral (<6 nm) and spatial (<10 mm2) resolution. The sites were selected to be representative for every ice floe station coupled with upward looking GoPro 11 imagery (Tab. 2.7).
- 8 surveys for mapping of sea-ice draft (for later estimates of sea ice thickness) using the multi-beam sensor.
- 8 surveys towing a plankton net. Mostly two dives were performed per survey, one in a depth of 10 m and one scratching the sea-ice bottom.
- 4 ocean surveys to map the oceanographic conditions from the open ocean across the floe edge into the ice floe. Focus were temperature, salinity and depth for the horizontal microstructure, but also all other sensors were recording.
- 5 surveys for different purposes, mostly video surveys to document ice conditions and the installation of under-ice instrumentation.

Through emerging ice core scanning technologies, we also imaged 1 to 2 ice cores per station using coupled VNIR and SWIR hyperspectral imaging cameras to evaluate the presence and distribution of algal biomass within the brine channels (using VNIR imagery), and to explore the possibility to detect crystal formation (e.g., gypsum) within the ice non-invasively (using SWIR imagery).

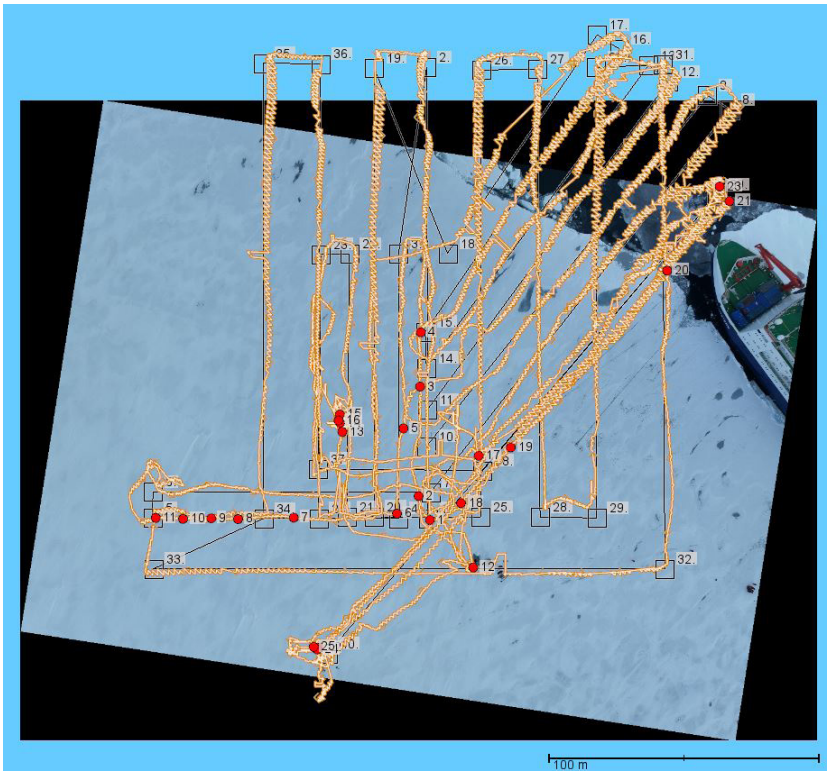

Fig. 2.9: Screenshot of the pilot's view of a dive map during ROV operations on station ICE 7. The background image is a photo mosaic from the actual station, as shown in Figure 2.7. The yellow line shows the (uncorrected) ROV track under the ice. Red dots show attention points, which are used to support dive documentation. Additional black lines help orientation and guidance of the pilot.

Tab. 2.6: ROV surveys during ArcWatch-1. Survey names refer to the folder names of the ROV data work flow.

Station	Event Label	Survey Name	Date	Start Time	Dive Mission
ICE 1	PS138_009_ROV_001	20230810_1	10.08.2023	19:54	Short dive along marker lines
ICE 1	PS138_009_ROV_002	20230811_1	11.08.2023	17:24	Dive along marker lines and to buoys
ICE 1	PS138_009_ROV_003	20230811_2	11.08.2023	19:22	Optics survey
ICE 2	PS138_031_ROV_001	20230815_1	15.08.2023	15:22	Multibeam survey
ICE 2	PS138_031_ROV_002	20230816_1	16.08.2023	08:38	ROV-net
ICE 2	PS138_031_ROV_003	20230816_2	16.08.2023	10:41	Optics survey
ICE 2	PS138_031_ROV_004	20230816_3	16.08.2023	14:51	Video dive
ICE 3	PS138_052_ROV_001	20230820_1	20.08.2023	08:19	Multibeam + optics surveys
ICE 3	PS138_052_ROV_002	20230820_2	20.08.2023	15:41	ROV-net
ICE 3	PS138_052_ROV_003	20230821_1	21.08.2023	08:19	CTD transects
ICE 4	PS138_075_ROV_001	20230824_1	24.08.2023	16:26	ROV-net
ICE 4	PS138_075_ROV_002	20230825_1	25.08.2023	07:51	Multibeam + optics + CTD surveys
ICE 5	PS138_101_ROV_001	20230828_1	28.08.2023	14:30	Optics along markers, ROV-net
ICE 5	PS138_101_ROV_002	20230829_1	29.08.2023	07:26	Optics survey, part 1
ICE 5	PS138_101_ROV_003	20230830_1	30.08.2023	08:00	Optics survey, part 2, multibeam survey, media dive
ICE 6	PS138_129_ROV_001	20230903_1	03.09.2023	14:32	Optics along markers, ROV-net
ICE 6	PS138_129_ROV_002	20230904_1	04.09.2023	08:16	Optics + multibeam survey, video dives
ICE 7	PS138_152_ROV_001	20230909_1	09.09.2023	09:01	Multibeam + optics + CTD surveys
ICE 7	PS138_152_ROV_002	20230910_1	10.09.2023	07:25	ROV-net
ICE 8	PS138_178_ROV_001	20230913_1	13.09.2023	13:37	Optics along markers, ROV-net, multibeam survey, ROV-net
ICE 8	PS138_178_ROV_002	20230914_1	14.09.2023	07:58	Optics survey
ICE 9	PS138_213_ROV_001	20230919_1	19.09.2023	17:50	Multibeam + ocean surveys
ICE 9	PS138_213_ROV_002	20230920_1	20.09.2023	06:43	Optics survey, ROV-net

Tab. 2.7: ROV UHI

Station	Date	UHI	GoPro imagery	Active lights session	Sky conditions	Surface conditions
ICE 1	09.08.2023	Yes	No	No	Partly cloudy	SSL >3 cm, <1 cm snow in places; melt ponds
ICE 2	16.08.2023	Yes	Yes	Yes	High clouds	SSL, snow (3-4 cm), refrozen (~2 cm) melt ponds
ICE 3	2023.08.20	Yes	Yes	Yes	Foggy, overcast	SSL, snow in some places, refrozen (4-8 cm) melt ponds
ICE 4	2023.08.25	Yes	Yes	Yes	Foggy, overcast	Snow in ridges; refrozen melt ponds
ICE 5	2023.08.29	Yes	Yes	Yes	High clouds	Fresh snow 2-3 cm
ICE 6	2023.09.04	Yes	Yes	Yes	Foggy, low clouds	10 cm cold, new snow
ICE 7	2023.09.10	Yes	Yes	Yes	Overcast	2-3 cm new, wet snow. No old snow; well-developed SSL and glazed surface in some places, crust ~2cm thick
ICE 8	2023.09.13	Yes	Yes	Yes	Overcast	Fresh snow >5 cm
ICE 9	2023.09.20	Yes	Yes	Yes	Partly cloudy	New 5-8 cm snow cover on all surfaces

Preliminary (expected) results

Figure 2.10 shows the light transmittance for each ICE station. Data are not yet corrected for depth, while transmittance decreases with depth. Overlays of different light conditions at the same point along individual tracks result often from different dive depths. ICE 1 had the highest transmittance of all stations. Values as high as ICE 1 were only reached by parts of the grids that cover open water or new ice (stations ICE 2, 5, 6, 7, 8). The result of ICE 7 may be well compared to the surface conditions and the dive track in Figure 2.9, while dive tracks of surveys with different depth (multibeam, CTD, nets) are not included in Figure 2.10.

Figure 2.11 gives an example of the sea-ice draft map and distribution function of station ICE 7 on 9 September 2023. The data result from the single beam sonar, because data processing of the much more complex multibeam data will only be done later. Modal draft was 0.85 m, which represents the ice that survived summer melt. The result also includes draft values of the new ice region, as it may also be seen in Figure 2.7. Draft values in this region were mostly between 0.00 and 0.30 m. The thickest ice was found along the ice edge of the floe and in ice blocks floating in the new ice / open water. This ice reaches daft values up to 2.3 m.

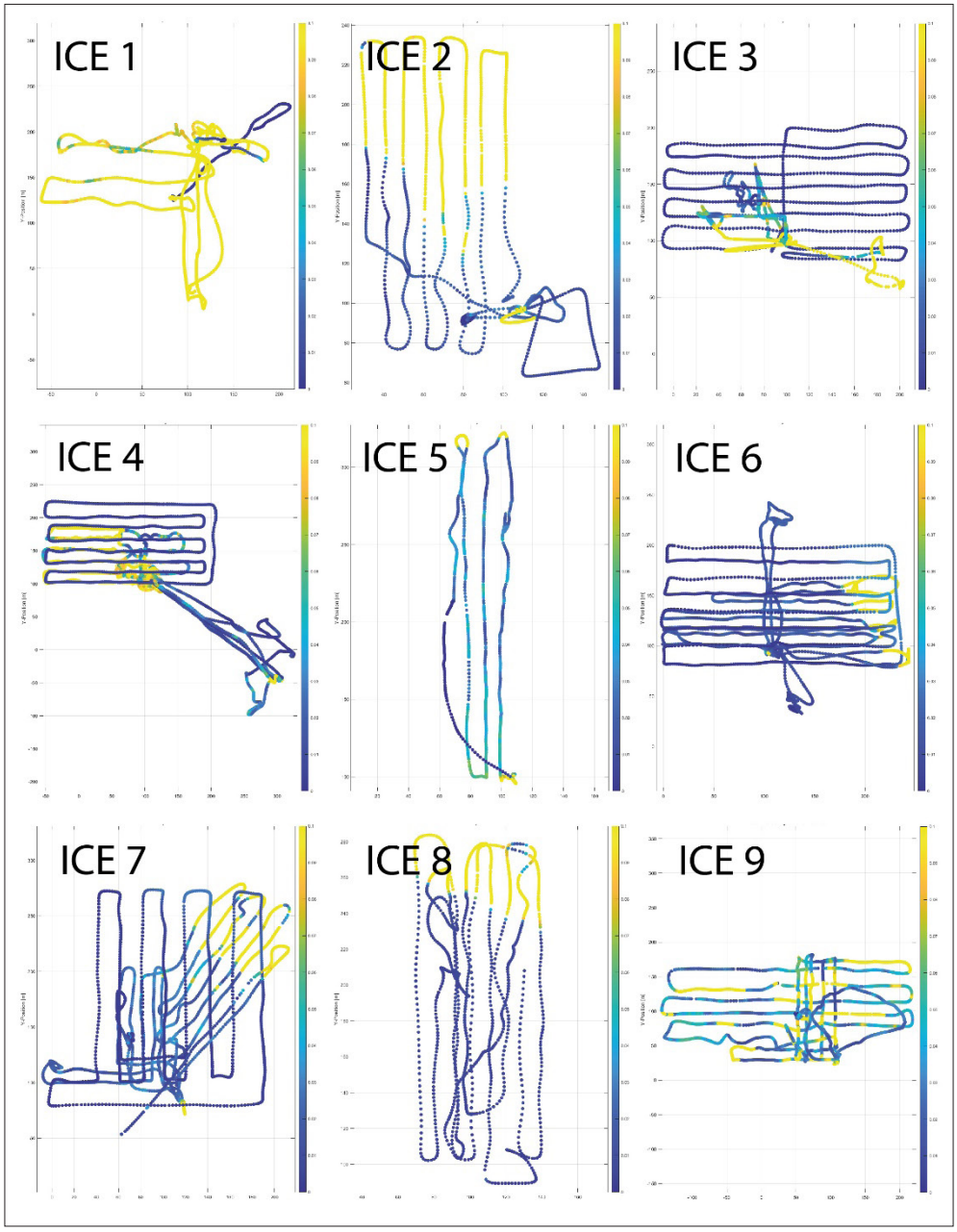

Fig. 2.10: Light transmittance through sea ice for each ICE station based on the radiance measurements on the ROV. Station details may be found in Table 1. Note the different horizontal scales, while the colour scale is identical for each station from 0 to 0.1.

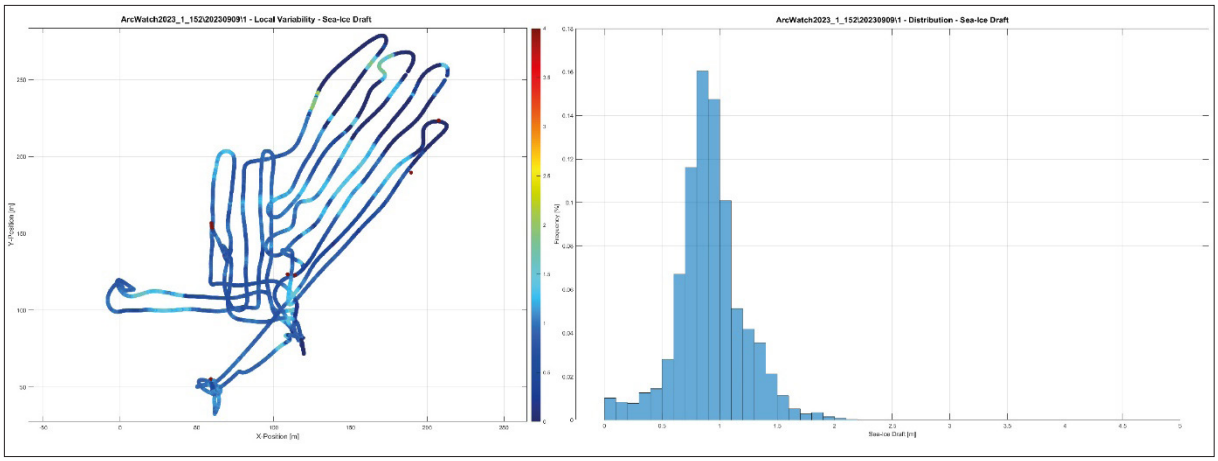

Fig. 2.11: Exemplary results of the sea-ice draft measured by the ROV (single beam data) on station ICE 7 on 9 September 2023. Left: horizontal distribution of sea-ice draft. Right: histogram of sea-ice draft. Surface conditions (with dive tracks) are shown in Figure 2.9.

As shown in a data sample from station ICE 1 (Fig. 2.12), the UHI is expected to be able to track fine and medium scale patterns of sea ice biophysical properties such as algal biomass, and photo physiology proxies through transmitted radiance within 400-720 nm. The goal for this data is to be correlated to biogeochemical and ecological processes being monitored by other groups (e.g., grazing, and sediment traps and biogeochemistry) and understand their spatial drivers and relationship with other sea-ice properties (e.g., ice floe history to thickness and snow depth). Figure 2.13 shows representative UHI data "chunks" acquired and algal distribution patterns observed for every station. In some stations we utilized active light sources in areas to test imaging capability under very low conditions (e.g., thick under ridges, overcast conditions), stations that included such tests are indicated in station action list and Table 2.7.

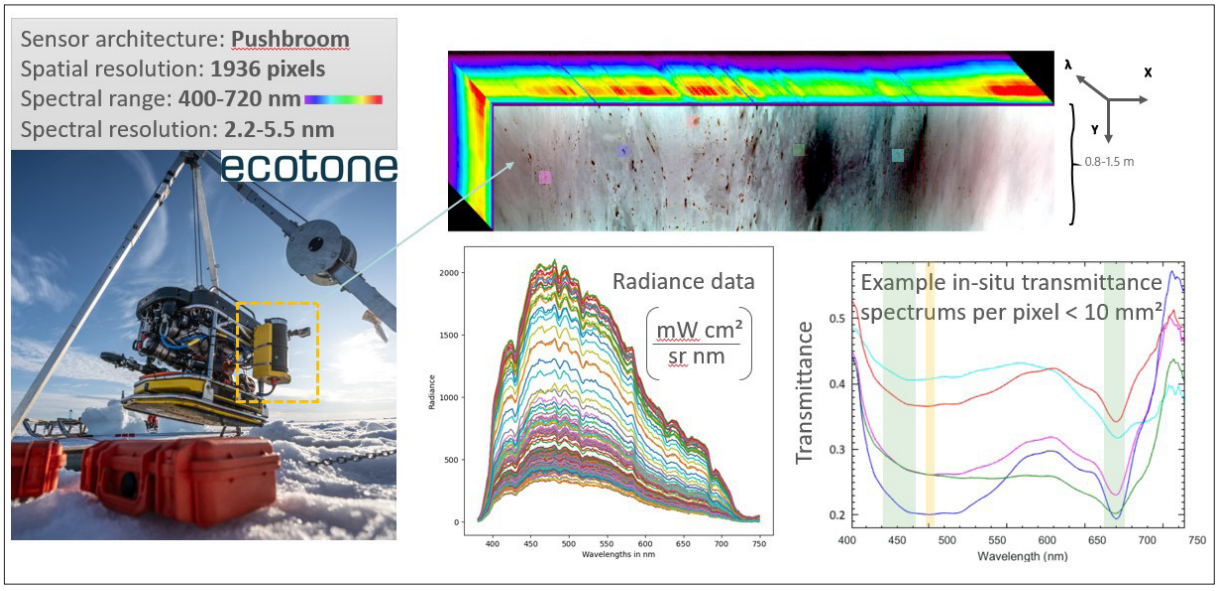

Fig. 2.12: Underwater Hyperspectral Imaging (UHI) measurements. Left: The UHI system (yellow box) mounted on the ROV Beast. Top right: Sample data set composed of the visible image (x-y-plane), and the spectral information with wavelength in the 3rd dimension. Bottom middle: Sample spectra of (under-ice incoming) radiance. Bottom right: Transmittance spectra for selected spectra, also highlighting ecological absorption bands.

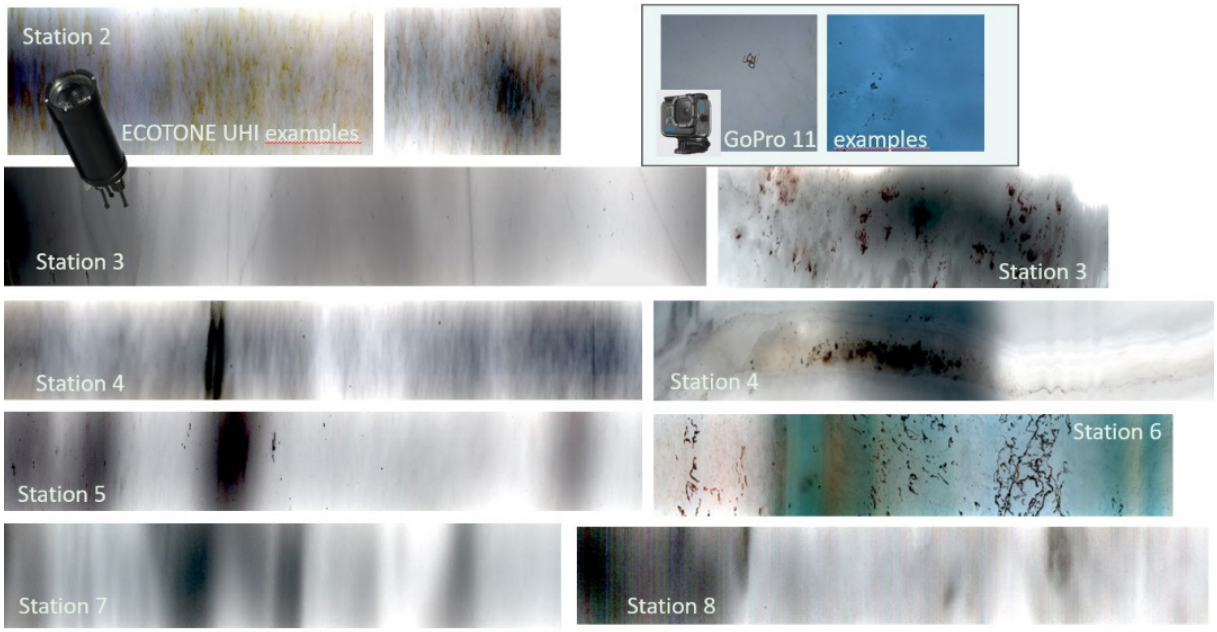

Fig. 2.13: Exemplary results from the Underwater Hyperspectral Imaging (UHI) for the different ICE stations. For comparison, 2 photographs of an additional GoPro 11, mounted on the ROV, are shown.

All other data from the bio-physical sensors on the ROV need further processing and analyses. The work with the ROV net is described in Section 2.4. The photo and video material will mostly be used to support analyses.

2.5 Floe dynamics and numerical model work

Work at sea

We collected data with a camera system (GoPro, PS 138_0_Underway-52 GoPro_PS) installed in the crow's nest facing the bow (Tab. 2.8). In particular during ice stations, when the ship was anchored at the station floe, time lapse photography (10 s) of surrounding floes was recorded. This data was processed onboard with Python scripts to generate a bird's eye view of the surrounding (Fig. 2.14).

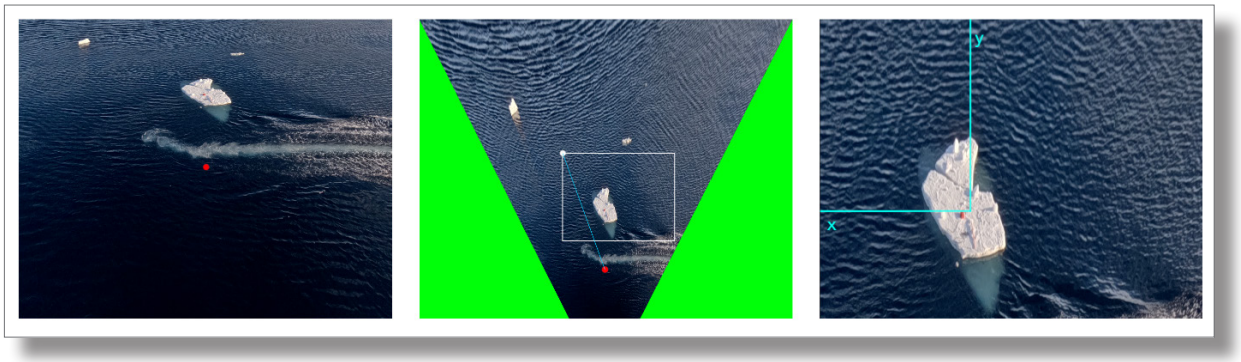

Fig. 2.14: Image processing of floe movement photos. From left to right: raw image, transformed to bird's eye view and selecting area of interest, object tracking in local coordinate system

Finally, object recognition and tracking algorithms were employed to detect floes and follow their position. The resulting floe position was then merged with DSHIP's data on the ship's position and drift and transformed to a fixed local coordinate system that has the ship position at initial floe-time as origin.

To minimize the ship's influence on the drift of the floes we have mainly collected data with the camera facing forward to reduce the impact of the stern thruster (the bow thruster was not operational). Furthermore, configurations in which the floe was in the lee of the ship have been excluded. For a calibration of the camera system and the geometric transformation of the identified coordinates and floe drift, single floes were visited with a Zodiac in two occasions during station ICE 5 (PS 138_106-1) and station ICE 7 (PS 138_170-1). Here, GPS trackers were deposited on 3 floes each. In addition, thickness of the floes and floe sizes were measured. At the same time the camera system tracked the floes. After this calibration and fine tuning of the image processing system the error of the floe drift detection algorithm has been decreased to around 2% in the position.

For calibration of a small-floe drift model the collected floe data is merged with the wind velocity taken from the ship's meteorological system.

Tab. 2.8: Station list of time lapse photographs for floe drift detection.

Files in directory	Date	Device short name	Station
13_08_23_18_43_multiple_floes_strong_winds	13.08.2023	GoPro_PS	ICE 1
19_08_23_15_21	19.08.2023	GoPro_PS	ICE 2
19_08_23_17_37	19.08.2023	GoPro_PS	ICE 2
19_08_23_23_40	19.08.2023	GoPro_PS	ICE 2
20_08_23_19_23_floes_in_distance	20.08.2023	GoPro_PS	ICE 2
20_08_23_3_10_EINE_SCHOLLE	20.08.2023	GoPro_PS	ICE 2
24_08_23_14_08_part4	24.08.2023	GoPro_PS	ICE 4
24_08_23_14_part1	24.08.2023	GoPro_PS	ICE 4
24_08_23_14_part2	24.08.2023	GoPro_PS	ICE 4
24_08_23_part3	24.08.2023	GoPro_PS	ICE 4
28_08_23_14_49	28.08.2023	GoPro_PS	ICE 5
03_09_23_Drift_new_formed_ice	03.09.2023	GoPro_PS	ICE 6
12_09_23_13_08_thin_single_floe_strong_wind	12.09.2023	GoPro_PS	ICE 7
12_09_23_9_multiple_thin_floes_strong_wind	12.09.2023	GoPro_PS	ICE 7
13_09_23_01)1_einzelne_Schollle	13.09.2023	GoPro_PS	ICE 8
13_09_23_14_03_single_floe_strong_winds	13.09.2023	GoPro_PS	ICE 8
13_09_23_18_43_strong_wind_new_cie	13.09.2023	GoPro_PS	ICE 8
19_09_23_14_00	19.09.2023	GoPro_PS	ICE 9
No files	29.08.2023	Zodiac	ICE 5
No files	11.09.2023	Zodiac	ICE 7

Preliminary (expected) results

In a first simple statistical analysis we measured the relative velocity and turning angle of the floes with respect to the wind. For example, at station 3 the measured average velocity was 2.2 % of the wind velocity while the floe drifted with a 53-degree angle to the right of the wind direction. The next step was the calibration of a standard drift model with the goal to estimate wind and ocean drag coefficients and turning angles. For this purpose, we added ocean data obtained by ADCP measurements of the ocean team.

As previously mentioned, in literature the drift of small floes only partially follows the usual rule of thumb, yielding approximately 2 % of the wind velocity, deflected by 20 – 40 degrees (Fig. 2.15). While the velocity of the floes was in good agreement, deflections can be significantly larger (reaching 90 degrees). To follow the hypothesis that small floes are strongly affected by the surrounding, in particular if the floes are located in direct proximity of large ice-covered areas a detailed Navier-Stokes simulation is set up. Here, specific configurations including ice edge, ship location, wind and ocean current (top 50 m) are modeled to identify the effect of the ice-covered region on the free water where the drift of the small floes is observed. Using such detailed finite element simulations, we are able to explain the effects of the surrounding on the current in the surface and the resulting motion of the small floes. The problem of the Navier-Stokes simulations is found in the extreme effort that makes their use in large scale simulations not feasible. Hence, our future work will be on embedding the findings in an efficient tool.

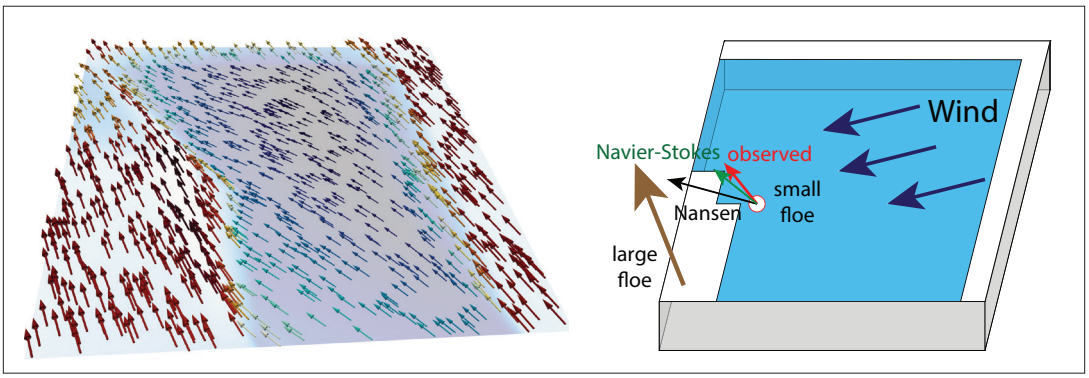

Fig. 2.15: Left: Navier-Stokes simulation of the upper ocean layer. The large floes have a dominant effect on the open water and little floes. Right: Sketch of the configuration and resulting motion prediction (in green) which is very close to the observation (in red)

Data management

Environmental data will be archived, published and disseminated according to international standards by the World Data Center PANGAEA Data Publisher for Earth & Environmental Science (https://www.pangaea.de) within two years after the end of the expedition at the latest. By default, the CC-BY license will be applied. Any other data will be submitted to an appropriate long-term archive that provides unique and stable identifiers for the datasets and allows open online access to the data.

Along with the data we will also publish documented versions of all computer scripts that are required for the evaluation. The hybrid sea-ice model which is developed in a parallel DFG project by C. Mehlmann will be put under an open license and maintained in an open GitLab repository.

This part of the expedition is supported by the Helmholtz Research Programme “Changing Earth – Sustaining our Future” Topic 2, Subtopic 1.

In all publications based on this expedition with co-authorship by any participant listed above, the **Grant No. AWI_PS138_04** or **AWI_PS138_09** (Mehlmann, Richter) or, in case of multidisciplinary work, **AWI_PS138_00** will be quoted and the following publication will be cited:

Alfred-Wegener-Institut Helmholtz-Zentrum für Polar- und Meeresforschung (2017) Polar Research and Supply Vessel POLARSTERN Operated by the Alfred-Wegener-Institute. Journal of large-scale research facilities, 3, A119. http://doi.org/10.17815/jlsrf-3-163.

References

Boetius A, Albrecht S, Bakker K, Bienhold C, Felden J, Fernández-Méndez M et al. (2013) Export of Algal Biomass from the Melting Arctic Sea Ice. Science 339:1430–1432. https://doi.org/10.1126/science.1231346

Katlein C, Schiller M, Belter HJ, Coppolaro V, Wenslandt D, Nicolaus M (2017) A New Remotely Operated Sensor Platform for Interdisciplinary Observations under Sea Ice. Frontiers in Marine Science 4. https://doi.org/10.3389/fmars.2017.00281

Nicolaus M, Perovich DK, Spreen G, Granskog MA et al. (2022) Overview of the MOSAiC expedition: Snow and sea ice. Elementa: Science of the Anthropocene 10. https://doi.org/10.1525/elementa.2021.000046

3. PHYSICAL AND CHEMICAL OCEANOGRAPHY

Jacob Allerholt[1], Frederik Bussmann[1], Rebecca Gorniak[1], [1]DE.AWI
Mario Hoppmann[1], Yusuke Kawaguchi[2]; Boris Koch[1], Ivan [2]JP.UTOKYO
Kuznetsov[1], Alejandra Quintanilla-Zurita[1], Benjamin Rabe[1], [3]DE.BSH
Daniel Scholz[1], Sinhué Torres-Valdés[1]
not on board: Walter Geibert[1], Birgit Klein[3], Sandra
Tippenhauer[1]

Grant-No. AWI_PS138_03

Objectives

The central Arctic Ocean is an important part of the global climate system, yet, notoriously under-observed. Decades of repeat surveys using icebreakers and autonomous instrumentation and, to some extent, remote sensing, have allowed identifying variability on interannual to decadal time scales, covering most of the Eurasian and Amerasian basins (e.g. Behrendt et al. 2018). Large-scale changes have been identified by temperature and salinity profile data, e.g. liquid freshwater content (e.g. Rabe et al. 2014). Water sample analysis has led to further insight into water mass pathways by using various tracers (e.g. Bauch et al. 2011) and macronutrients (e.g. Alkire et al. 2017), or into carbon storage (Ulfsbo et al. 2018). *In-situ* sensor data of some of these properties had recently been available and were analysed (e.g. Stedmon et al. 2021). To identify further development of the variability, in particular, in the light of the “new Arctic” (e.g. Weingartner et al. 2022, and references therein) requires repeat hydrographic surveys and deployment of autonomous instrumentation. Further attention has been paid to local process studies on the scale of one ice floe and the surrounding region, e.g. MOSAiC (Rabe et al. 2022; Nicolaus et al. 2022; Shupe et al. 2022; Kawaguchi et al. 2022) and N-ICE (Granskog et al. 2018). However, further research and *in-situ* observation is needed to shed light on these processes and, ultimately, improve model parameterisation and our understanding of the Arctic and global climate system. The team aims to both improve the temporal and spatial data coverage on the basin scale as well as use the extensive ice stations to study local processes, such as leads, shallow ocean stratification and feedback with the ice, snow and atmosphere, considering the physical and chemical environment and the ecosystem. The study is part of the ArcWatch series of *Polarstern* expeditions and embedded in wider frameworks, such as the International Arctic Buoy Programme (IABP; https://iabp.apl.uw.edu/) and GEOTRACES (e.g. Charette et al. 2020).

Work at sea

Lowered Conductivity Temperature Depth (CTD) rosette and mounted sensors

As part of the physical oceanography work we measured various seawater properties from the ship. The ship-based Conductivity Temperature Depth system (Seabird, SBE911+) mounted on a rosette for water sampling (CTD/rosette) with 24 x 12 l OTE bottles was deployed along sections and during the ice stations to record water column profiles of temperature, salinity, dissolved oxygen, optical beam transmission, chlorophyll a (chl-a) and Coloured Dissolved Organic Matter (CDOM) fluorescence and photosynthetically active radiation (PAR). An

altimeter provided distance to the seafloor within about 30-80 m. Images of the setup are given in Figure 3.1, and sensor types and serial numbers are listed in Table 3.1. Note the duplicate sensor setup for temperature, conductivity and oxygen.

A SUNA nitrate sensor (SN1472) was installed on the CTD/rosette during casts shallower than 2,000 m. The instrument was deployed on 21 casts to obtain high-resolution nitrate profiles down to max. 1,973 m (Table 3.2) and recorded the data internally as soon as power was supplied by the SBE911+.

An Underwater Vision Profiler (UVP) was attached to the rosette to continuously record Plankton and particle images during the CTD downcast, recording data internally. The instrument was operated by the Biological Oceanography group with the help of the Physical and Chemical Oceanography group.

The initial configuration (*conf1*) of the SBE911+ CTD on the rosette remained unchanged throughout the cruise.

The altimeter performed overall well, giving reliable values from about 50 m above the seafloor on most casts, apart from the crossing of the Gakkel Ridge around 60 E, where intermittent readings only showed about 20-30 m from the seafloor; during those casts, the downcast finished about 20 m from the seafloor. Otherwise, we tried to approach the seafloor to about 5 m.

The CDOM sensor on the CTD/rosette did not work properly, exhibiting excessive noise and a superimposed regular oscillation. This phenomenon was observed with the same sensor during PS131. Raw CTD files were sent to SeaBird for evaluation, but no reply was received so far. Troubleshooting was done by reconfiguring the analogue range to AR2, and by using a different split (y-) cable. However, the issue remained, and further inspection is required at home. The sensor will also be sent to service.

A summary of all casts obtained during PS138 is provided in Table 3.3.

Water samples were taken throughout and analysed for the correction of temporal drift and pressure effects of the conductivity and oxygen sensors. For the salinity samples the respective bottles were closed after at least a 60 s wait at the sampling depth. The samples will be used to finalise the data sets after the expedition using those bottle sample data as well as the manufacturer's calibration pre- and post-expedition. Additional samples for chemical and biological variables, such as nitrate and Chl a, will be used to correct the Chl a fluorescence and nitrate sensors after the expedition.

We obtained high-precision salinity measurements with an Optimare Precision Salinometer (OPS, SN 006) for a more accurate calibration of the CTD's conductivity sensors. The samples from the CTD/rosette were measured in 5 batches of 12, 18, 22, 24 and 28 bottles, 104 samples in total. The day before each session, the salinity bottles were heated in a water bath to approximately 30° C, and then cooled down at room temperature for about 20 h. The pressure within the bottles was released with an injection needle directly after the warm bath. Before using the OPS, the samples were shaken thoroughly to overcome any stratification in the bottle. While sampled by the OPS, the opening of the bottles was sealed with parafilm to inhibit evaporation. Overall the difference between the salinity of duplicate samples of each rosette bottle agree well, to within 10^{-3} (Fig. 3.2). A preliminary comparison of the salinometer results and the CTD sensor salinity reveal a small positive drift for the initial 8 casts during August and early September, with a jump in differences thereafter. However, the difference between the salinities from the duplicate CT and the depth sensors shows only a small negative drift, with values changing by less than 10^{-3}.

The oxygen sampling and titration is detailed under Chemical oceanography and sampling.

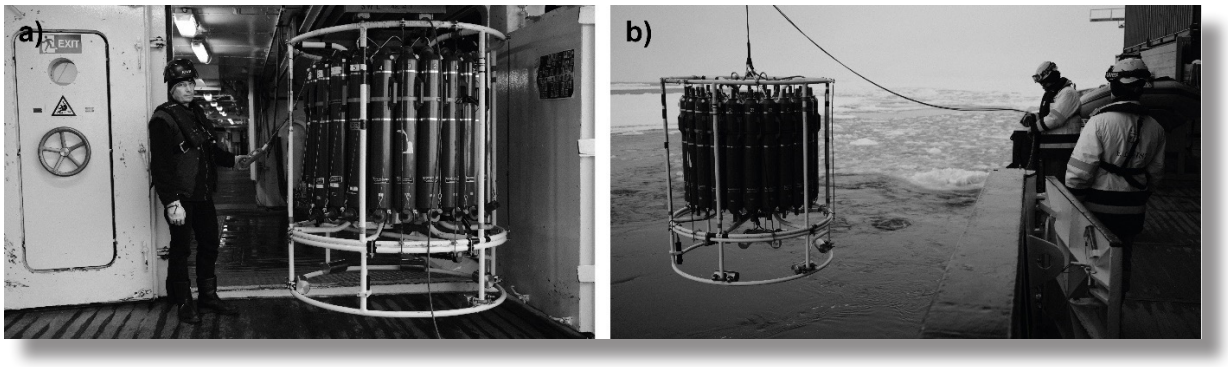

Fig. 3.1: Photos of ship-based CTD rosette during deployment

Tab. 3.1: Sensor configuration for the ship-based CTD rosette used during PS138

Parameter	SN	Calibration Date	Channel	Sensor type
	457	--	-	Deckunit Seabird11plus
Temperature 1	4127	23-Nov-22	F0	Seabird SBE3plus
Conductivity 1	2618	24-Nov-22	F1	Seabird SBE4c
Pressure	0937	14-Nov-17	F2	Seabird SBE9plus
Temperature 2	5115	23-Nov-22	F3	Seabird SBE3plus
Conductivity 2	3290	24-Nov-22	F4	Seabird SBE4c
Oxygen 1	4019	10-Dec-22	V0	Seabird SBE43
Oxygen 2	1605	02-Aug-22	V1	Seabird SBE43
Altimeter	46611	--	V2	Teledyne Benthos PSA916
CDOM fluorescence	7239	12-Sep-21	V3	WETlabs ECO CDOM
Chl-a fluorescence	1853	16-Nov-21	V4	WETlabs ECO Chl-a
Beam Transmission	1220	07-Sep-22	V5	WETlabs C-Star
PAR	2197	30-Nov-21	V6	Seabird PAR-LOG
Nitrate	1472		V7	Satlantics Deep SUNA V2

Tab. 3.2: Meta-data of all PS138 ship-based nitrate profiles. “Station” refers to the final part of the respective event label, starting with “PS138_”.

Station	Date	Time	Latitude	Longitude	Profile depth	Cal file	SN
2-1	06.08.2023	15:38:56	80.9481	15.3507	1973	SNA1472D	1472
19-1	10.08.2023	16:38:39	83.8683	33.2088	100	SNA1472D	1472
22-1	10.08.2023	18:11:50	83.8771	33.1696	100	SNA1472D	1472
43-1	17.08.2023	09:32:10	84.9524	80.1189	101	SNA1472D	1472
47-1	17.08.2023	12:08:11	84.9563	80.038	250	SNA1472D	1472
47-2	17.08.2023	12:56:21	84.9567	80.0283	200	SNA1472D	1472
63-1	21.08.2023	16:57:34	84.6917	107.5329	151	SNA1166G	1166

Station	Date	Time	Latitude	Longitude	Profile depth	Cal file	SN
66-1	21.08.2023	18:48:37	84.6874	107.6594	200	SNA1166G	1166
88-1	25.08.2023	17:35:02	83.0083	129.8858	250	SNA1472D	1472
109-1	29.08.2023	17:25:16	85.0335	130.0132	101	SNA1472D	1472
113-1	29.08.2023	19:20:40	85.0387	129.9677	200	SNA1472D	1472
139-1	04.09.2023	18:02:40	88.4353	114.185	100	SNA1472D	1472
143-1	04.09.2023	19:21:24	88.4335	114.0151	250	SNA1472D	1472
162-1	10.09.2023	21:13:40	89.772	-1.9406	115	SNA1472D	1472
166-1	10.09.2023	22:50:33	89.7646	-2.1952	200	SNA1472D	1472
173-1	12.09.2023	03:07:51	89.3394	59.1993	1502	SNA1472D	1472
175-1	12.09.2023	15:44:18	88.6707	60.1893	1501	SNA1472D	1472
186-1	14.09.2023	12:29:24	87.944	57.1231	101	SNA1472D	1472
190-1	14.09.2023	14:10:15	87.9601	56.8507	200	SNA1472D	1472
204-1	17.09.2023	23:33:45	86.6605	60.0617	1853	SNA1472D	1472
206-1	18.09.2023	10:24:00	86.0026	60.4171	1502	SNA1472D	1472

Tab. 3.3: Metadata of all CTD stations. “Station” refers to the final part of the respective event label, starting with “PS138_”.

Station	Date	Time	Latitude	Longitude	Water depth [m]	
2-1	06.08.2023	15:38:56	80.9481	15.3507	2028	
19-1	10.08.2023	16:38:39	83.8683	33.2088	3976	
22-1	10.08.2023	18:11:50	83.8771	33.1696	3976	
26-1	11.08.2023	01:55:47	83.8561	34.1177	3970	
40-1	17.08.2023	02:37:23	84.9155	80.2544	3736	
43-1	17.08.2023	09:32:10	84.9524	80.1189	3732	
47-1	17.08.2023	12:08:11	84.9563	80.038	3737	
47-2	17.08.2023	12:56:21	84.9567	80.0283	3738	
63-1	21.08.2023	16:57:34	84.6917	107.5329	3528	
66-1	21.08.2023	18:48:37	84.6874	107.6594	3751	
69-1	21.08.2023	23:02:45	84.7331	107.5728	3977	
85-1	25.08.2023	16:29:37	83.0047	129.9682	4164	
88-1	25.08.2023	17:35:02	83.0083	129.8858	4163	
90-1	25.08.2023	18:09:35	83.0123	129.8486	4168	
109-1	29.08.2023	17:25:16	85.0335	130.0132	4301	
113-1	29.08.2023	19:20:40	85.0387	129.9677	4302	
115-1	29.08.2023	22:46:06	85.0324	129.9476	4303	
139-1	04.09.2023	18:02:40	88.4353	114.185	4315	
143-1	04.09.2023	19:21:24	88.4335	114.0151	4315	
145-1	04.09.2023	23:16:59	88.4404	113.844	4320	
162-1	10.09.2023	21:13:40	89.772	-1.9406	4242	

Station	Date	Time	Latitude	Longitude	Water depth [m]
166-1	10.09.2023	22:50:33	89.7646	-2.1952	4244
168-1	11.09.2023	02:08:19	89.7518	-2.1939	4242
172-1	11.09.2023	21:18:13	89.6476	57.3322	4283
173-1	12.09.2023	03:07:51	89.3394	59.1993	4325
174-1	12.09.2023	09:24:10	88.9953	59.6113	4356
175-1	12.09.2023	15:44:18	88.6707	60.1893	4372
176-1	12.09.2023	21:57:21	88.334	59.6152	4372
186-1	14.09.2023	12:29:24	87.944	57.1231	4376
190-1	14.09.2023	14:10:15	87.9601	56.8507	4376
193-1	14.09.2023	20:28:36	87.9712	56.3694	4374
195-1	15.09.2023	20:45:51	87.6616	59.7725	4067
196-1	16.09.2023	03:31:33	87.3387	59.9224	3505
201-1	17.09.2023	02:01:40	86.9777	60.021	4207
204-1	17.09.2023	23:33:45	86.6605	60.0617	1854
205-1	18.09.2023	05:02:56	86.3302	60.0618	2764
206-1	18.09.2023	11:06:42	85.9992	60.4357	3868
207-1	18.09.2023	16:30:36	85.6577	60.1123	3885
218-1	20.09.2023	03:01:38	85.4327	60.0704	3881
222-1	20.09.2023	08:57:11	85.4368	59.9856	3884

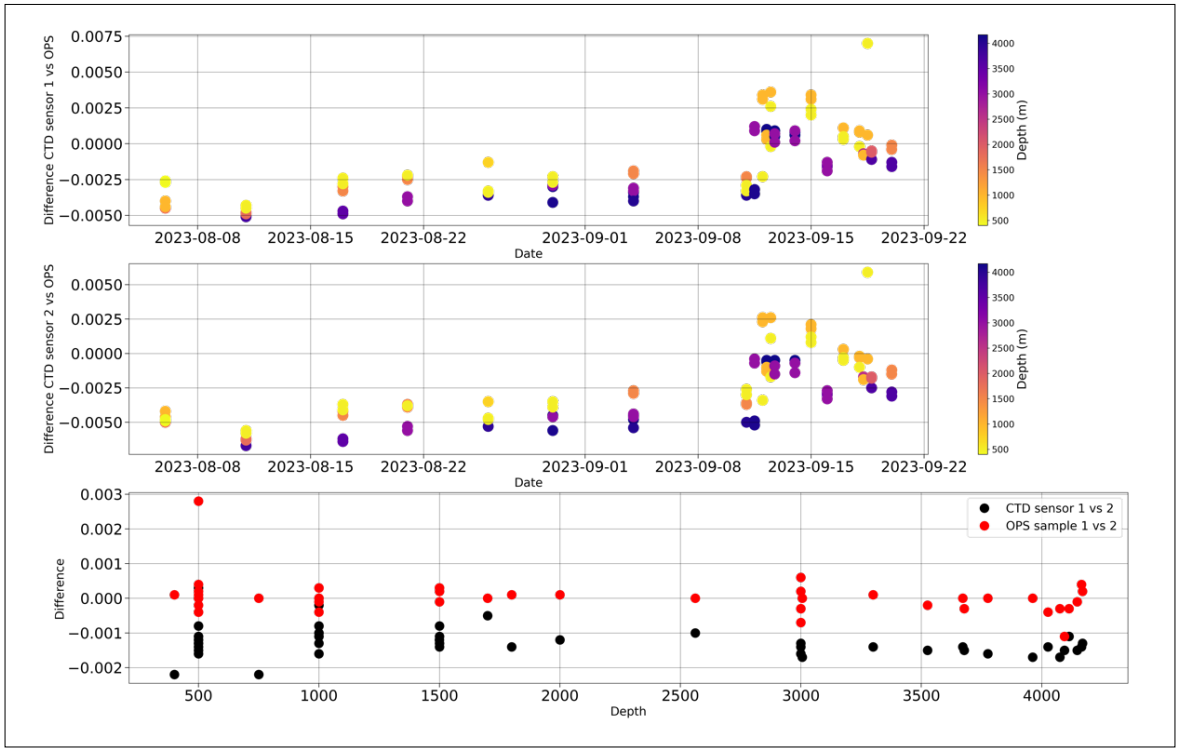

Fig. 3.2: Comparison of the results from OPS and CTD sensor 1 and 2

Chemical oceanography and sampling

The chemical oceanography programme aims to constrain the links between biogeochemical property exchange in Fram Strait and the central Arctic Ocean (CAO) and to investigate temporal changes of biogeochemical properties in the CAO. As part of a collaboration with researchers from the University of Edinburgh, we collected samples for the measurement of stable N and O isotopes in dissolved nitrate. These data, in conjunction with other environmental data (e.g., nutrients, temperature, salinity) will be used to investigate N-cycling processes determining the availability of N (e.g., Tuerena et al. 2021a,b; Francis et al. 2022; Santos-Garcia et al. 2022). In the central Arctic Ocean, these types of measurements are sparse and thus, new measurements are needed to fill in gaps in knowledge. We also carried out SUNA-Nitrate profiles from the ice floe during ice stations. These data will be combined with micro-structure profiles to compute nitrate upward fluxes. Data will also allow us to improve our observations of the finer vertical structure of nutrient fields. Finally, we measured nutrients in snow samples in order to test the hypothesis that some nitrogen inorganic species may be derived from atmospheric deposition, which is not well constrained in the Arctic marine environment.

We also addressed the role of Dissolved Organic Matter (DOM) and dissolved contaminants in the Arctic marine organic carbon cycle. As a follow-up of the efforts carried out during the MOSAiC expedition, we took samples for chemical characterization of DOM to better constrain the quantity of terrestrial dissolved organic carbon (DOC) in the Arctic Ocean that ultimately is exported to the deep Atlantic via Fram Strait. In addition, we sampled DOM in sea ice, snow and the melt water to track organic matter that is derived by ice related primary production and transferred into the ocean surface. An on-board experiment was carried out to track the chemical changes that ice derived DOM experiences when it is incubated with the surface water microbial communities. The experiment aims at tracking DOC from sea ice into the ocean and at acquiring kinetics for the microbial turnover.

One of the main mechanisms that couples the surface ocean to deeper layers, especially with respect to the carbon cycle, is the sinking of organic particles. However, the separation between suspended, non-sinking organic matter, sinking organic matter and matter with active movement is not always possible by direct measurements in the ocean. The elements thorium and polonium, both natural radionuclides represented with several isotopes in the natural uranium and thorium decay series, strongly bind to particles. They are produced at a well-known rate, and deviations between the observed (measured) inventory and their expected production can therefore be used to infer integrated carbon export rates. While thorium-234 (^{234}Th, half-life 24 days) is a widely used proxy for carbon export, polonium-210 (^{210}Po) is analytically more demanding but has the advantage of being more specific for organic carbon and of integrating a longer period due to its longer half-life (138 days). Both isotope systems have been used in the past in studies of the Central Arctic Ocean and beyond (Roca-Martí et al. 2018; Roca-Martí et al. 2016). During PS138, both isotope systems will be monitored, the ^{238}U/^{234}Th disequilibrium and the ^{210}Pb/^{210}Po disequilibrium. After the cruise, both sample types require a re-counting to determine the background from other isotopes/the parent. Methods largely followed Roca-Martí et al. (2016).

A total of ~650 different samples were acquired from water, snow, ice, experiment samples, and quality controls (Tab. 3.4 and Fig. 3.3). Samples were analysed onboard for inorganic nutrients (nitrate, nitrite, ammonium, silicate, phosphate concentration), dissolved organic nitrogen (DON), dissolved organic phosphorus (DOP), dissolved oxygen (DO). Analyses were carried out following GO-SHIP best practice recommendations as described in Hydes et al. (2010), Becker et al. (2020) and Langdon (2010), using a Seal Analytical AA-500 continuous segmented flow nutrient analyser and a Ti-Touch Metrohm titration unit set up with the Winkler titration method. All variables were measured within 24 h after sampling and random

duplicates from the CTD samples were analysed for quality control. Other parameters such as nitrate isotope ratios, dissolved organic carbon (DOC), total dissolved nitrogen (TDN), CDOM fluorescence and absorption, a suite of anthropogenic contaminants (EU project ONE-BLUE), and dissolved organic matter (DOM) characterization by ultrahigh-resolution mass spectrometry will be carried out after the cruise. At all ice CTD stations and selected 60°E transect stations (total of 15 stations) a profile with 8-9 water depths was sampled for particulate and total thorium (^{234}Th) concentration and for total polonium (^{210}Po). Both elements allow to quantify export production and were quantified using a beta counter on board. A 2-months microbial incubation experiment was carried out at 0°C with ice algal biomass as substrate and ocean surface water as inoculum to simulate organo-chemical changes occurring during the decay of fresh ice-derived biomass. Bacterial diversity (BD), cell counts (DAPI), and total dissolved amino acid concentrations (AA) will be determined after the cruise.

Apart from the CTD, bottom water was sampled from bottles mounted to the Lander and OFOBS systems and were and will be analysed for the parameters mentioned above. One OFOBS sample was acquired from a hydrothermal plume at the Gakkel Ridge.

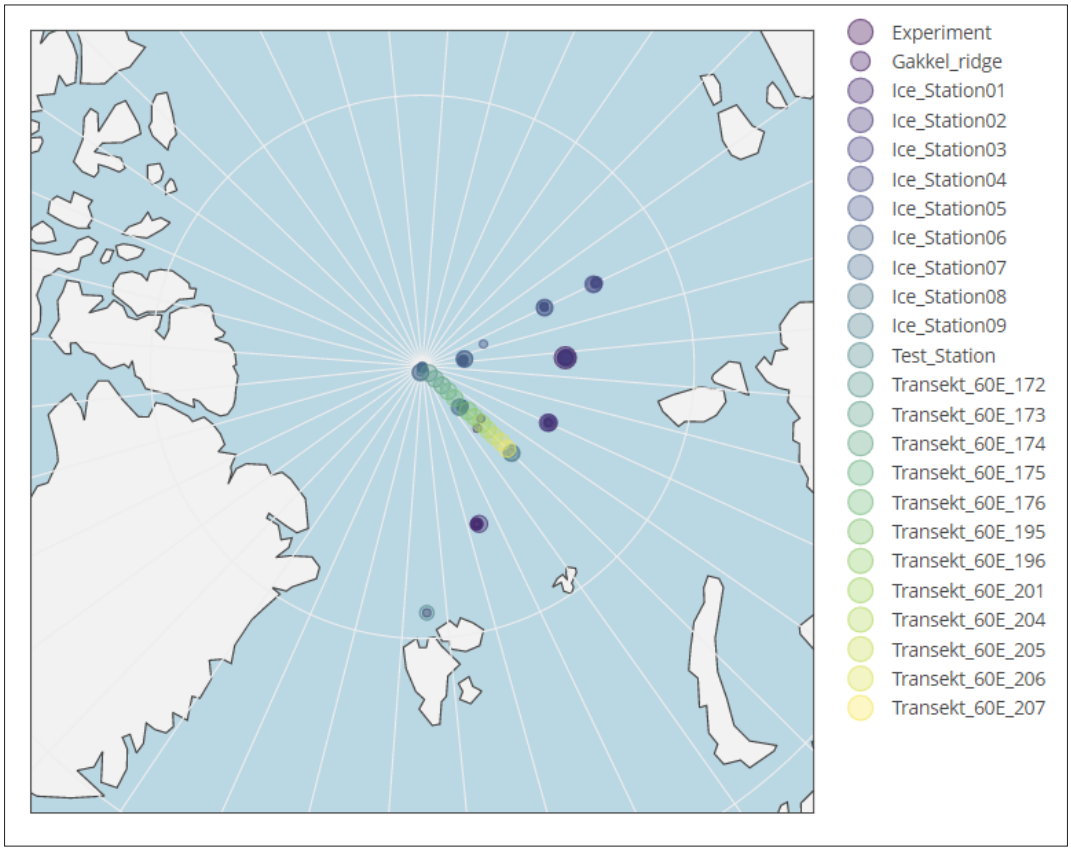

Fig. 3.3. Sampling locations of chemical oceanography; dot size indicates number of samples.

For all DOC and fluorescence samples, at least 1 L of water was filtered using pre-combusted (450° C, 5 h) glass fibre filters (Whatman, GFF, 42 mm diameter) and a glass filtration unit that was rinsed three times with ultrapure water at the beginning of CTD bottle processing. Before filtration of a sample, the filtration unit was rinsed three times the respective sample. Samples were filled into pre-cleaned and thoroughly rinsed high-density polyethylene HDPE bottles (50 mL). All samples were stored at -20° C until further analyses. For quality control,

some unfiltered samples were stored frozen to determine total organic carbon (TOC) for quality control.

Solid phase extraction was carried out onboard for DOM and contaminant analyses. 500 mL of filtered seawater were acidified with 550 µL concentrated HCl (30 %, suprapur), filled into pre-cleaned HDPE reservoirs, and loaded on the pre-cleaned (2 fillings methanol and water, respectively) SPE cartridges (PPL, Agilent, 200 mg) using the HDPE reservoirs (500 mL) connected by Luer adaptors at a flow rate of ~3 mL per min (gravity). After loading with samples, cartridges were rinsed with 2 x 3 mL of pH 2 water. The cartridges were completely dried with nitrogen gas, stored frozen at -20 °C and will be eluted with 2 mL of methanol back in the AWI lab. For selected samples, the permeate of the extraction was also collected for DOC analysis and DOM characterization.

For thorium and polonium analyses, approximately 16 L (12+4L) of water was collected each water depth. Sample depths were 1,000 m, 500 m, 400 m, 250 m, 200 m, 150 m, 100 m, 50 m, Chl_{max}, and surface. The sample volume of the initial canister was separated into additional canisters for particulate and total thorium (4 L each) and polonium (5 L). Polonium samples were filtered using a peristaltic pump and processed as described in the Rio5 Cookbook (RiO5 METHOD (15)). Thorium samples were filtered in a plastic filtration unit into a 10 L glass vacuum bottle and subsequently processed according to RiO5 METHOD (45). Radioactive decay of total and particulate Th was counted onboard for 2,000 minutes (33.3 h) using a beta counter. A technetium standard and blanks were also measured for quantification and quality control.

The hydrothermal plume water was sampled from the Niskin water bottle (stainless steel spring) that was mounted at the bottom of the OFOBS. Water was sampled for dissolved oxygen, inorganic nutrients, 3D fluorescence, and dissolved organic carbon, nitrogen, and phosphorus. 0.5 L of filtered (pre-combusted GF/F, Whatman) water was acidified to pH2 (HCl suprapur) and dissolved organic matter was solid-phase extracted (PPL, 0.2 mg) for subsequent dissolved organic matter characterization using ultrahigh-resolution mass spectrometry. 2.627 L of water was filtered (qpore, MCE membrane filter, 0.22 µm pore size, 25 mm diameter) in a pre-rinsed plastic filtration unit in the *Polarstern* chemistry lab. The filter was stored frozen in a pre-combusted glass petri dish and wrapped in aluminium foil. The filtrate was collected in a glass vacuum bottle and transferred into a 5 L PE canister (rinsed with ultrapure water), acidified to pH2 using 2.6 mL hydrochloric acid (30 %, Merck, ultrapure) and stored at 0°C.

To aid identifying water masses with respect to ice formation and melt, and continental runoff, we took samples for oxygen isotopes (d18O), primarily from the CTD/rosette. These samples were taken by twice rinsing 20 ml glass bottles and filling them to the top with sample water, then closing them using a plastic lid with a soft inlay to ensure the bottles were sealed. The samples have been stored at 4 °C before being processed on land.

Tab. 3.4: Number of chemical oceanography samples taken for the different sample types and parameters

Sample type	# samples
Sea ice	18
Melt ponds / gap layers	8
Hydrothermal vents	1
Ocean, bottom	12
Ocean	353
Sea ice lead	7
Snow	37
Experiments	100
Quality control	40

Parameter	# samples
Dissolved organic carbon (DOC)	547
Inorganic nutrients, DON, and DOP	650
Total organic carbon (TOC)	78
Dissolved organic matter (DOM)	536
DOM solid phase extraction (SPE)	485
SPE Permeate	49
Fluorescence	488
Fe/Mn ratio	2
Particulate thorium (Th_part)	127
Total thorium (Th_tot)	127
Polonium (Po)	120
Bacterial diversity (BD)	15
Amino acids (AA)	60
Cell counts (DAPI)	60

Underway observations

The ship-based 150 kHz Acoustic Doppler Current Profiler (ADCP; RDI-Teledyne Ocean Surveyor) was continuously operated outside Norwegian territorial waters to measure the velocity field of the upper ocean. The instrument had been erroneously mounted with 2 beams aligned along the ship, as opposed to be offset by 45 degrees. Vertical bin size was set to 4 m, narrowband mode. Problems to resolve velocities potentially occurred due to low backscatter (low particle concentration in the water), shallow water depth, and/or sea ice in front of the beams. The multibeam echosounder HYDROSWEEP (15.5 kHz), the Parasound and the 18 kHz channel of the EK80 were operated almost continuously during the expedition. These and the acoustic signal from the POSIDONIA system for locating and releasing moorings might also affected the velocity data. Most of the ship's echosounders, including the VMADCP, were intermittently switched off during some of the POSIDONIA operations. Further data gaps resulted from the system acquisition software (VMDAS) stalling in combination with the software channelling data to DSHIP. However, overall data quality was good with the usual, intermittent interference by lowered instruments. Full processing will be carried out after the expedition.

A duplicate SBE21 thermosalinograph (Seabird) was continuously recording surface temperature and salinity along the cruise track; the system also included two auxiliary SBE38 temperature sensors (Seabird). The SBE21 was installed in an underway seawater pumped throughflow system to obtain salinity measurements while the auxiliary sensor was used to measure the actual temperature at the throughflow inlet at about 11 m depth in the *Polarstern* keel.

During transits through ice-covered seas we used eXpendable CTDs (XCTD; deck unit MK150 by TSK, probes TSK/Lokheed-Martin Sippican XCTD 1) to increase the spatial resolution of the regular CTD sections in the upper water column. A total of 49 XCTD-1 probes were deployed during PS138 (Tab. 3.5) to collect profiles of temperature and salinity along the cruise track as a complement to the regular CTD stations. The probes were launched from the aft of the

ship using a standard hand-held launcher connected to a MK150 deck unit (Fig. 3.4). The majority of profiles achieved a full depth of 1,100 m. Three probes were defect or did not reach critical depth before ceasing to respond. The obtained data has been combined with the DSHIP extract and saved in ODV format.

Tab. 3.5: Overview of XCTD deployments

XCTD Station	Date	Time	Latitude	Longitude	Max. Depth [m]	SN
PS138_7-1	07.08.2023	03:27	81.81	24.09	963	21117949
PS138_7-2	07.08.2023	05:54	81.99	25.15	1085	21117947
PS138_7-3	07.08.2023	08:10	82.15	25.61	1085	16103093
PS138_7-4	07.08.2023	11:01	82.33	26.45	1085	21117945
PS138_7-5	07.08.2023	13:41	82.5	27.1	1085	21117948
PS138_7-6	07.08.2023	15:34	82.66	27.33	1085	21117944
PS138_7-7	07.08.2023	20:28	82.97	28	1085	21117946
PS138_7-8	08.08.2023	00:48	83.32	29.17	1085	21117942
PS138_7-9	08.08.2023	04:46	83.65	30.2	1085	21117941
PS138_29-1	12.08.2023	21:43	84.31	35.85	1085	21117943
PS138_29-2	13.08.2023	07:47	84.59	39.52	1085	16103038
PS138_29-3	13.08.2023	18:59	85.16	48.66	1085	21117939
PS138_29-4	14.08.2023	00:46	85.39	54.19	1085	21117940
PS138_29-5	14.08.2023	13:38	85.35	60.61	1085	22031227
PS138_29-7	14.08.2023	18:04	85.29	67.32	1085	16103048
PS138_29-8	14.08.2023	23:04	85.18	72.48	1085	22031226
PS138_49-1	17.08.2023	21:28	84.92	84.2	1085	16103040
PS138_49-2	18.08.2023	03:54	84.81	91.15	1085	22031229
PS138_49-3	18.08.2023	13:18	84.79	95.3	1085	22031225
PS138_49-4	19.08.2023	03:40	84.73	100.34	1085	22031228
PS138_49-5	19.08.2023	08:35	84.74	105.41	1085	22031231
PS138_72-1	22.08.2023	22:00	84.4	112.11	1085	22031235
PS138_72-2	23.08.2023	02:42	84.11	116.18	1085	22031234
PS138_72-3	23.08.2023	07:49	83.84	120.28	1085	22031236
PS138_72-4	23.08.2023	18:50	83.22	127.22	1085	22031230
PS138_94-1	26.08.2023	23:13	83.4	129.94	1085	22031233
PS138_94-2	27.08.2023	04:15	83.89	129.72	1085	22031232
PS138_94-3	27.08.2023	08:54	84.37	130.03	1085	22031213
PS138_121-2	01.09.2023	02:49	85.44	128.65	1085	22031219
PS138_121-3	01.09.2023	08:05	85.95	128.18	1085	22031222
PS138_121-5	01.09.2023	14:39	86.45	127.15	1085	22031214
PS138_121-6	01.09.2023	19:15	86.94	126.57	1085	22031220
PS138_121-7	02.09.2023	02:03	87.42	125.47	1085	22031223
PS138_121-8	02.09.2023	20:23	88	121.69	1085	22031224

XCTD Station	Date	Time	Latitude	Longitude	Max. Depth [m]	SN
PS138_149-1	06.09.2023	16:44	88.99	112.77	1085	22031221
PS138_149-2	06.09.2023	22:39	89.48	110.98	1085	22031216
PS138_171-1	11.09.2023	17:27	89.82	57.63	1085	22031218
PS138_171-2	12.09.2023	00:39	89.5	60.05	1085	22031217
PS138_171-3	12.09.2023	05:32	89.16	60.26	1085	22031215
PS138_171-4	12.09.2023	13:04	88.83	59.47	1085	22031241
PS138_171-5	12.09.2023	18:07	88.51	60.36	1085	22031238
PS138_171-6	13.09.2023	01:38	88.17	59.74	1085	22031240
PS138_171-7	15.09.2023	17:20	87.76	58.2	1085	22031243
PS138_171-8	16.09.2023	00:03	87.51	59.55	1085	22031246
PS138_171-9	16.09.2023	21:53	87.17	59.99	1085	22031237
PS138_171-10	17.09.2023	20:16	86.83	58.84	1085	22031239
PS138_171-11	18.09.2023	01:56	86.5	59.97	495	22031245
PS138_171-12	18.09.2023	08:24	86.17	60.07	1085	22031242
PS138_171-13	18.09.2023	13:50	85.83	60.09	1085	22031248

Fig. 3.4: XCTD deployment using a hand-held launcher

Additional CTD observations

The data collected with the XCTD were supplemented with measurements by a light-weight, self-recording CTD sensor package (SST 48M; by Sea&Sun Technology, SST; SN 1459) with a motorised fishing rod at a few sites on the ice reachable by helicopter (Fig. 3.5 and Tab. 3.6)

Fig. 3.5: Helicopter flight with "Fishing rod CTD" during the transect.

Tab. 3.6: Overview of "Fishing rod CTD" deployments.

Event	Date	Time	Latitude	Longitude	Max. Depth [m]	SN
PS138_HELI_FishingRod_1	13.08.2023	12:08	84.87	43.58	303	1459
PS138_HELI_FishingRod_2	23.08.2023	13:50	83.52	123.79	256	1459

We did not use the Underway CTD (UCTD; no longer manufactured) system due to high ship speed in open water (> approximately 9 kts), which would have risked the CTD probes to be lost.

Under-ice profiling for Microstructure Turbulence (MSS), nitrate and temperature / salinity in the ice-ocean boundary layer

During ice stations, a microstructure profiler (MSS 90 by SST) was deployed through holes in the ice to measure temperature, salinity, oxygen, chl-a fluorescence, as well as shear to study turbulent exchange processes at different ice stations. The two probes, MSS SN 075 and 097, were configured with the same sensors: two airfoil probes aligned parallel to each other (shear probes type PNS6), a fast-tip thermistor (FP07, with a small sensor guard), an acceleration sensor (for body vibration measurements), conventional CTD sensors (SST) for precision measurements, a Turner Design Cyclops-7 in Vivo Chlorophyll/Blue sensor for Chl-a fluorescence, and a fast optical dissolved oxygen sensor (SST); serial numbers of the sensors can be found in Table 3.6. The profiling was carried out with the probe in free-fall by paying out slack cable ("loops") before being winched back to the surface by a SWM400 electrical winch system. The setup on the ice was powered by a Honda EU22 generator. The protective cage around the MSS sensor array was removed for most of the profiles to reduce noise and, thus, facilitate higher sensitivity to low-level turbulence (see preliminary results). All channels sampled at 512 Hz.

We also note that the sensor guard of the FP07 likely limited the size of the eddies resolved by this sensor. The instrument was ballasted for a typical fall speed of ~ 0.5 m s^{-1}, although several profiles had different fall speeds, between 0.4 and 1 m s^{-1}. All sensors pointed downward during profiling. Data were transmitted in real-time to a field laptop on the ice. A typical MSS deployment was done using a mobile setup mounted to a Nansen sledge, and through a hole opened by joining 4 – 5 augered holes, usually located approximately 200 – 300 m away from the ship. A pop-up tent was erected over the hole as a shelter (Fig. 3.6). We collected profiles down to 280 – 420 m, depending on the ice drift that caused the probe to displace laterally relative to our ice hole. During an ice station, the MSS profiler was left in the water between casts by securing it to a separate strap, leaving the MSS data cable slack. Different series of consecutive profiles were carried out during several days of ice station work (Tab. 3.7).

We deployed an additional SUNA nitrate sensor (SN 1166) during ice station work, that was manually lowered to a depth of up to 100 m using a tripod setup (Fig. 3.7 and Tab. 3.8). In order to obtain additional data for further processing we co-deployed an SST 75M (SN CTM689) multiparameter sensor package during the first 21 SUNA casts. The following 59 casts were accompanied by one of our SST48M CTD (SN 1459) because the SST75M malfunctioned and produced erroneous pressure and salinity data. The SUNA data is processed following Sakamoto et al. (2009), using the CTD's temperature and salinity data. Further quality control was conducted by comparison to the CTD's OTD bottle nitrate data. For this purpose, we also deployed the SUNA sensor used during ice station work alongside one ship based CTD cast (see Tab. 3.2).

The nitrate and turbulence profiles will be used to determine the turbulent exchange of nutrients.

A particular focus of our ice work had been to investigate the spatio-temporal variability of the thin melt water layer beneath the sea ice. We tested new methods and measurement protocols, as the ice-ocean boundary is typically difficult to sample. We did not use a small boat to obtain CTD and MSS profiles in open leads, and to deploy and recover a floating ADCP, due to environmental conditions (fog, freezing) and lack of time. Shallow stratification, close to the ice, was observed by a custom-made uprising system, consisting of a robust, stand-alone CTD (RBR s/n 2010909; inductive conductivity) attached to a rope with a length of 15 – 30 meters.

To assess horizontal variability and study submesoscale dynamics beneath the ice on the scale of individual ice floes, we conducted transect measurements from the edge of the ice floe towards its center (Tab. 3.9 and Fig. 3.8). We used the SST 48M CTD (SN 1459) with the fishing rod and the uprising RBR CTD (SN 2010909) to carry out upper water-column CTD transects across parts of the ice floes at ice stations. A total of 3 transects were completed. One transect was interrupted due to the thickness of the ice on one side of the ice floe (exceeding 2 meters) and an abrupt halt in ice operations. Initial measurements were taken at the ice floe's edge, progressing towards the centre with measurements at distances ranging from 50 to 150 meters. For each profile, a single borehole was drilled, followed by the use of a "fishing rod" and then the upriser. The maximum depth of the fishing rod profile was 250 meters, while the upriser ranged from 15 to 30 meters for different transects. For each profile, geographical coordinates were recorded using a smartphone. Subsequently, the coordinates were transformed into a rectangular coordinate system relative to the ice floe with the center at the position of one of the ROV GPS sensors.

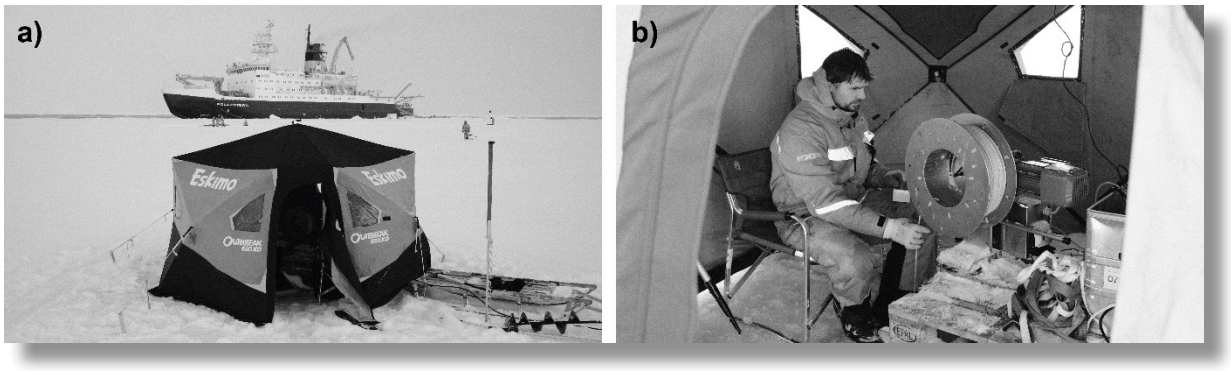

Fig. 3.6: Microstructure profiler measurements on the sea ice. a) Tent used as a shelter from weather; b) Setup of the SWM400 winch operated through a hole in the ice.

Tab. 3.6: Overview of MSS measurements during ice stations

MSS SN	Sensor	Sensor SN	Time of operation	Comment
097	Shear 1	6121	Before 11.08 2023	
	Shear 2	6204	Whole expedition	
	Shear 1	6185	11. – 17.08.2023	
	Shear 1	6121	From 18.08.2023	Repaired snagged cable of sensor
075	Shear 1	6104	Whole expedition	
	Shear 2	6103	Whole expedition	

Tab. 3.7: Overview of MSS measurements during ice stations. All profiles were run with the protective cage detached from the profiler, unless noted otherwise. Start / end times and geographic positions of each time series of profiles are given for each day and station.

(Ice) Station Event	MSS SN	Date	Time	Long. (°N)	Lat. (°E)	Number of profiles	Comment
PS138_9_MSS_1	097	08.08.2023	14:17 15:20	31.3554 31.3497	84.0407 84.0311	7	1-4 with cage
PS138_9_MSS_2	097	09.08.2023	09:13 16:37	32.2485 32.0951	84.0448 83.9610	3	
PS138_9_MSS_3	075	10.08.2023	12:32 20:49	33.4613 33.6544	83.878 83.8779	14	With Cage
PS138_9_MSS_4	075	11.08.2023	17:09 22:26	33.9591 34.0703	83.8493 83.8735	14	With Cage
PS138_31_MSS_1	075	15.08.2023	10:36 18:23	80.1918 80.127	84.941 84.9272	17	With Cage
PS138_31_MSS_2	075	16.08.2023	08:59 16:05	80.2944 80.2948	84.9068 84.9045	18	With Cage. 1 failed profile

(Ice) Station Event	MSS SN	Date	Time	Long. (°N)	Lat. (°E)	Number of profiles	Comment
PS138_52_MSS_1	097	19.08.2023	15:51 18:36	107.7147 107.7033	84.7484 84.7408	6	1-3 with cage
PS138_52_MSS_2	075	20.08.2023	06:30 13:40	107.6454 107.3805	84.693 84.6874	17	
PS138_52_MSS_3	075	21.08.2023	07:04 14:33	107.2584 107.3914	84.6902 84.6916	16	
PS138_75_MSS_1	075	24.08.2023	16:08 17:04	130.1602 130.1268	82.9144 82.9184	4	
PS138_75_MSS_2	075	25.08.2023	07:09 15:43	129.9939 130.057	82.9894 83.0044	14	
PS138_101_MSS_1	075	28.08.2023	16:52 19:00	130.2151	85.0382	1	Only one profile, one position
PS138_101_MSS_2	075	29.08.2023	06:55 12:50	130.2151 130.3105	85.0382 85.035	11	
PS138_129_MSS_1	075	03.09.2023	14:15 16:26	112.0177 112.1683	88.4923 88.4891	5	
PS138_152_MSS_1	075	09.09.2023	13:16 16:26	6.0793 0.5403	89.9025 89.9034	7	Ship position
PS138_152_MSS_2	075	10.09.2023	07:25 10:09	-1.7687 -1.4391	89.8242 89.8132	7	Ship position
PS138_178_MSS_1	075	13.09.2023	10:42 16:58	59.9451 59.226	87.9241 87.9173	16	
PS138_178_MSS_2	075	14.09.2023	12:42 15:43	57.0214 56.6555	87.9461 87.9706	10	
PS138_213_MSS_1	075	19.09.2023	14:24 18:20	60.0375 59.9873	85.457 85.443	18	
PS138_213_MSS_2	075	20.09.2023	04:32 10:27	60.078 60.046	85.4307 85.4394	12	

Fig. 3.7: Photo of ice-based SUNA nitrate profiling setup.

Tab. 3.8: Meta-data of all PS138 ice-based nitrate profiles

Event Label	Date	Time	Latitude	Longitude	Cal file
PS138_009_SUNAprofil_001	10.08.2023	15:38:56	83.8763	33.4784	SNA1166G
PS138_031_SUNAprofil_002	15.08.2023	11:16:00	84.9476	80.1528	SNA1166G
PS138_052_SUNAprofil_003	19.08.2023	16:26:00	84.7469	107.7075	SNA1166G
PS138_075_SUNAprofil_004	25.08.2023	07:09:00	83.0156	130.1196	SNA1166G
PS138_101_SUNAprofil_005	28.08.2023	17:03:00	85.0382	130.3066	SNA1166G
PS138_129_SUNAprofil_006	03.09.2023	15:11:19	88.4897	112.1261	SNA1166G
PS138_152_SUNAprofil_007	09.09.2023	12:45:54	89.9144	0.6322	SNA1166G
PS138_178_SUNAprofil_008	13.09.2023	11:28:00	87.9239	59.8558	SNA1166G
PS138_213_SUNAprofil_009	19.09.2023	15:03:23	85.4456	60.0143	SNA1166G

Tab. 3.9: The coordinates of the start and end points of the transects with Fishing rod CTD and Upriser CTD.

Event	Date	Time	Latitude start	Longitude start
PS138_31_UpperOceanIceFloeTransect_1	16.08.2023	7:30 – 9:30	84.91	80.23
PS138_52_UpperOceanIceFloeTransect_1	20.08.2023	8:30 – 11:30	84.69	107.57

Event	Date	Time	Latitude start	Longitude start
PS138_101_UpperOceanIceFloeTransect_1	30.08.2023	14:50 – 16:20	89.82	2.08
PS138_152_UpperOceanIceFloeTransect_1	10.09.2023	7:00 – 10:30	84.95	129.04

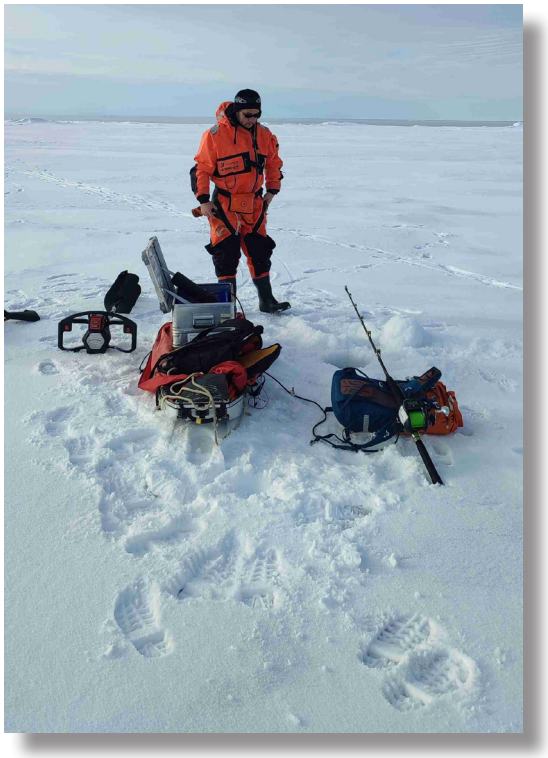

Fig. 3.8: Fishing rod and Uprising CTD ice floe transect.

Additional CTD transects were carried out by the ROV (see Chapter 2).

Under-ice continuous observations

Apart from shallow stratification and melt water layers we focused on the dynamics and thermodynamics related to turbulent fluxes in the ice-ocean boundary layer (IOBL). When sea ice is forced to move by winds, the vertical shear of flow between ice and ocean may produce turbulent motions in water, resulting in diapycnal fluxes of momentum, heat and salt. They subsequently affect the heat budget near the ice bottom, and hence the thermodynamic growth and decay. Using an eddy-covariance system (ECS = Nortek Vector + JFE RINKO-EC) and a high-resolving ADCP (Nortek Signature 1000) we aimed to obtain direct observations of the fluxes for each variable at all ice stations (Tabs. 3.10 and 3.11, please see the end of the chapter). Additionally, temperature and conductivity were continuously measured in the IOBL and the upper halocline using autonomous thermistor- and salinity-chains.

During all stations, an RDI WH-300 kHz ADCP (SN 12667) was suspended through another hole, typically 10 to 20 m away from the microstructure profiling hole, sampling continuously through the ice station, at 3-s intervals, and with a 2-m vertical bin size. The output was set to give velocity in instrument coordinates with additional compass heading. The data will later be averaged to larger time intervals after analysing compass performance during our expedition close to the magnetic north pole. This ADCP was deployed at all ice stations (Tab. 3.12).

Various GPS receivers and buoys recorded the floe position continuously, even *Polarstern* was not moored to the floe due to parallel work elsewhere. These data will subsequently be used to obtain floe translation and rotation to obtain geographically referenced velocity from and / or check the performance of the compass of the under-ice ADCP.

Tab. 3.10: Overview of under-ice measurements during ice stations with the 1M Hz ADCP (Nortek Signature 1000), collecting mean and burst current velocities at 30 min and 10 min intervals respectively. Longitude and latitude are referenced to those corresponding to MSS.

(Ice) Station Event	Label	Date	Time	Longitude (°N)	Latitude (°E)	File name
PS138_9_1	PS138-9_Nortek_s1000_102149-001	08.09.2023 08.10.2023	00:00 20:23	31.355 31.350	84.041 84.031	S102149A026_PS1381.ad2cp
PS138_31_1	PS138-31_Nortek_s1000_102149-001	15.08.2023 16.08.2023	12:00 19:00	80.192 80.295	84.941 84.905	S102149A027_PS1382.ad2cp
PS138_52_1	PS138-52_Nortek_s1000_102149-001	19.08.2023 21.08.2023	16:00 18:33	84.748 84.741	107.715 107.703	S102149A028_PS1384.ad2cp
PS138_75_1	PS138-75_Nortek_s1000_102149-001	24.08.2023 25.08.2023	10:00 18:43	130.160 130.127	82.914 82.918	S102149A029_PS1383.ad2cp
PS138_10_11	PS138-101_Nortek_s1000_102149-001	28.08.2023 31.08.2023	10:10 06:29	130.215	85.038	S102149A031_PS1385.ad2cp
PS138_129_1	PS138-129_Nortek_s1000_102149-001	03.09.2023 04.09.2023	12:00 17:05	112.018 112.168	88.492 88.489	S102149A032_PS1386.ad2cp”
PS138_152_1	PS138-152_Nortek_s1000_102149-001	08.09.2023 11.09.2023	10:00 08:30	6.079 0.540	89.903 89.903	S102149A033_PS1387.ad2cp
PS138_178_1	PS138-178_Nortek_s1000_102149-001	13.09.2023 14.09.2023	14:00 17:42	57.021 56.656	87.946 87.971	S102149A035_PS1388.ad2cp
PS138_213_1	PS138-213_Nortek_s1000_102149-001	19.09.2023 20.09.2023	15:00 11:22	60.038 59.987	85.457 85.443	S102149A036_PS1389.ad2cp

Tab. 3.11: Overview of eddy covariance measurement during ice stations with Nortek vector and JFE Advantech RINKO-EC, collecting 8-Hz sequential velocities at 10 min burst interval. Longitude and latitude are referenced to those corresponding to MSS.

(Ice) Station Event	Label	**Date**	**Time**	**Long. (°N)**	**Lat. (°E)**	**Number of samples**	**File Name**
PS138_9_1	PS138-9_ Vector_5418-001	08.09.2023 08.10.2023	00:00 20:32	31.355 31.350	84.041 84.031	547724	PS138113.VEC
PS138_31_1	PS138-31_ Vector_5418-001	15.08.2023 16.08.2023	12:00 19:00	80.192 80.295	84.941 84.905	381245	PS138214.VEC
PS138_52_1	PS138-52_1_ Vector_5418-001	19.08.2023 21.08.2023	16:00 18:33	84.748 84.741	107.715 107.703	622077	PS138315.VEC
PS138_75_1	PS138-75_ Vector_5418-001	24.08.2023 25.08.2023	10:08 17:28	130.160 130.127	82.914 82.918	387072	PS138416.VEC
PS138_101_1	PS138-101_ Vector_5418-001	28.08.2023 31.08.2023	10:00 06:37	130.215	85.038	843835	PS138517.VEC
PS138_129_1	PS138-129_ Vector_5418-001	03.09.2023 04.09.2023	12:00 17:22	112.018 112.168	88.492 88.489	361615	PS138618.VEC
PS138_152_1	PS138-152_ Vector_5418-001	08.09.2023 11.09.2023	10:00 08:30	6.079 0.540	89.903 89.903	726712	PS138719.VEC
PS138_178_1	PS138-178_ Vector_5418-001	13.09.2023 14.09.2023	14:00 17:21	57.021 56.656	87.9461 87.9706	336581	PS138820.VEC
PS138_213_1	PS138-213_ Vector_5418-001	19.09.2023 20.09.2023	15:00 11:22	60.038 59.987	85.457 85.443	250741	PS138922.VEC

Tab. 3.12: Overview of under-ice measurements during ice stations with the 300 kHz ADCP. The start and end times / dates (UTC) are shown together with the respective geographic positions. Note the first part of the event label denotes the ice station (e.g. “PS138_9”) and the latter part the specific event action of the device.

Event label	**Date**	**Time**	**Lon. (°E)**	**Lat. (°N)**
PS138_9_ ICEADCP300_1	08.08.2023 11.08.2023	14:17 22:26	31.3554 34.0703	84.0407 83.8735
PS138_31_ ICEADCP_1	15.08.2023 16.08.2023	10:36 16:05	80.1918 80.2948	84.941 84.9045
PS138_52_ ICEADCP_1	19.08.2023 21.08.2023	15:51 14:33	107.7147 107.3914	84.7484 84.6916
PS138_75_ ICEADCP_1	24.08.2023 25.08.2023	16:08 15:43	130.1602 130.057	82.9144 83.0044
PS138_101_ ICEADCP_1	28.08.2023 29.08.2023	16:52 12:50	130.2151 130.3105	85.0382 85.035
PS138_129_ ICEADCP_1	03.09.2023	14:15 16:26	112.0177 112.1683	88.4923 88.4891

Event label	Date	Time	Lon. (°E)	Lat. (°N)
PS138_152_ ICEADCP_1	09.09.2023 10.09.2023	13:16 10:09	6.0793 -1.4391	89.9025 89.8132
PS138_178_ ICEADCP_1	13.09.2023 14.09.2023	10:42 15:43	59.9451 56.6555	87.9241 87.9706
PS138_213_ ICEADCP_1	19.09.2023 20.09.2023	14:24 10:27	60.0375 60.046	85.457 85.4394

Autonomous ice-tethered buoys

We also deployed various autonomous ice-tethered buoys. Details are given in Chapter 6.

Instrument calibration casts

Inter-calibration of the SST 48M CTD sensors was performed using the onboard CTD. Instruments with serial numbers s/n 1459 and s/n 1495 were attached to the rosette frame during the PS138_206_1 cast. Resulted files are H9181253_1.SRD and H9181303_4.SRD. The sensor test with s/n 1495 in the previous days revealed a defect in the pressure data. This sensor needs to be repaired on the ground before the next expedition departure. The inter-calibration of this sensor is only possible by comparing time, not depth. The uprising RBR CTD instrument with s/n 2010909 was used in parallel with SST 48M CTD s/n 1459 during ice floe transects (see Tab. 3.9).

Mooring deployments

We co-deployed two seafloor-mounted moorings, CAO1 and CAO2, in the eastern Amundsen Basin (Tab. 3.13) on 31 August 2023, close to the ICE5 ice station (see Fig. 3.9).

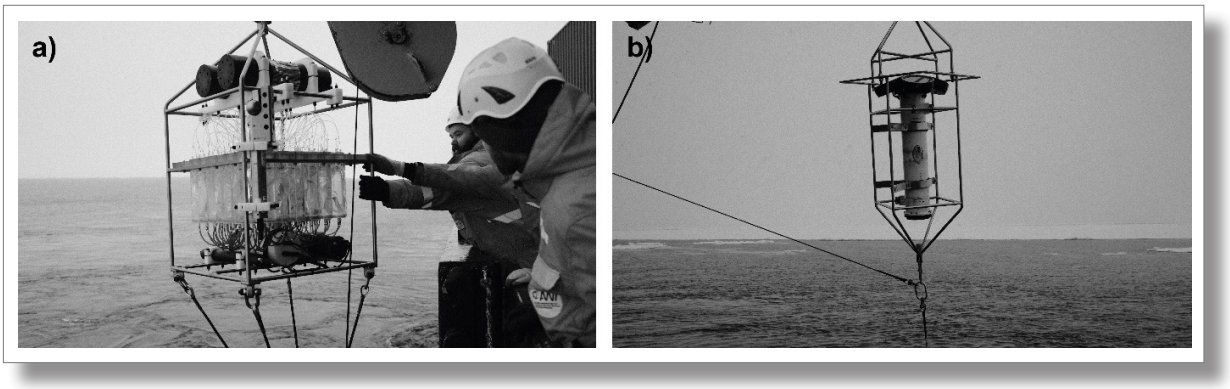

Fig. 3.9: Exemplary photos of mooring deployments.
a) Lower Remote Access Sampler (RAS); b) 75 kHz ADCP.

They were placed approximately 2 nm apart from each other. Mooring CAO1 (see Fig. 3.10 at the end of the chapter) was equipped with 7 Seabird SBE56 temperature loggers, 9 Seabird SBE37 MicroCats, one RDI Longranger 75 kHz ADCP, one Develogic Sonovault and one Nortek S500 ADCP. The upper 27 m of the mooring were equipped with several interconnected segments of a solid plastic pipe, to protect the comparably shallow mooring against sea ice keels and icebergs. Mooring CAO2 (Fig. 3.11 at the end of the chapter) was equipped

with 3 SBE37 Microcats, 2 Aanderaa RCM11 current meters, one RDI 300kHz Workhorse ADCP, one ASL Acoustic Zooplankton Fish Recorder (AZFP), one AURAL Acoustic Recorder, 2 Sediment Traps, one BoP trap, and 2 Remote Access Samplers (RAS) including sets of SBE37 Microcats, Satlantics SUNA nitrate sensors, Sunburst SAMI pH and CO2 sensors, and additional Wetlabs ECO PAR & ECO Triplet sensors on the upper RAS. The RAS were programmed to collect seawater samples at weekly intervals for the measurement of dissolved nutrients in seawater and SUNA calibration (D. Scholz and S. Torres-Valdés), and for genetic analyses (K. Metfies, M. Wietz, C. BIenhold).

Tab. 3.13: Overview of mooring deployments

Mooring ID	Time (UTC)	Latitude	Longitude	Device operation	CTD profile	Water depth [m]
CAO1-01	31.08.2023 12:35	84° 54.462’ N	129° 15.291’ E	PS138_118-1	PS138_115-1	4304
CAO2-01	31.08.2023 18:24	84° 53.230’ N	129° 37.807’ E	PS138_119-1	PS138_115-1	4301

Argo Floats

In collaboration with the German Hydrographic Office (BSH) we deployed two ARGO floats in the Nansen Basin near Svalbard and in the eastern Amundsen Basin, north of the Laptev Sea, to further improve the use of this technology in the (partly) ice-covered Arctic Ocean (see Tab. 3.14). The floats were started using a BSH standard procedure, and thrown overboard from 3 m height in the aft of the ship (Fig. 3.11 at the end of the chapter).

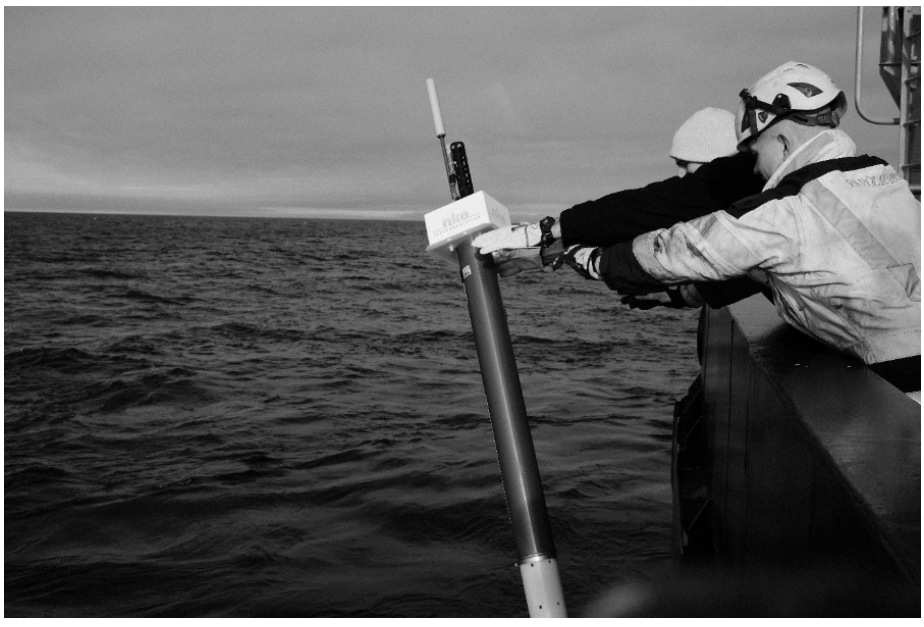

Fig. 3.12: Deployment of ArgoFloat AI2600-23DE011.

Tab. 3.14: Overview of ArgoFloat deployments

Float ID	WMO ID	Time (UTC)	Latitude	Longitude	Device operation	CTD profile	Water depth [m]
AI2600-23DE011	4903667	06 Aug 2023 16:25	80° 56,849' N	015° 20,890' E	PS138_3-1	PS138_2-1	2031
AI2600-23DE010	1902597	26 Aug 2023 19:10	83° 01,921' N	129° 57,471' E	PS138_93-1	PS138_90-1	4163

Preliminary results

Preliminary results from thorium measurements indicated a pronounced particle export particularly in the first three ice stations (Fig. 3.12). We do not present further preliminary results as further processing on land is needed for in-depth analysis.

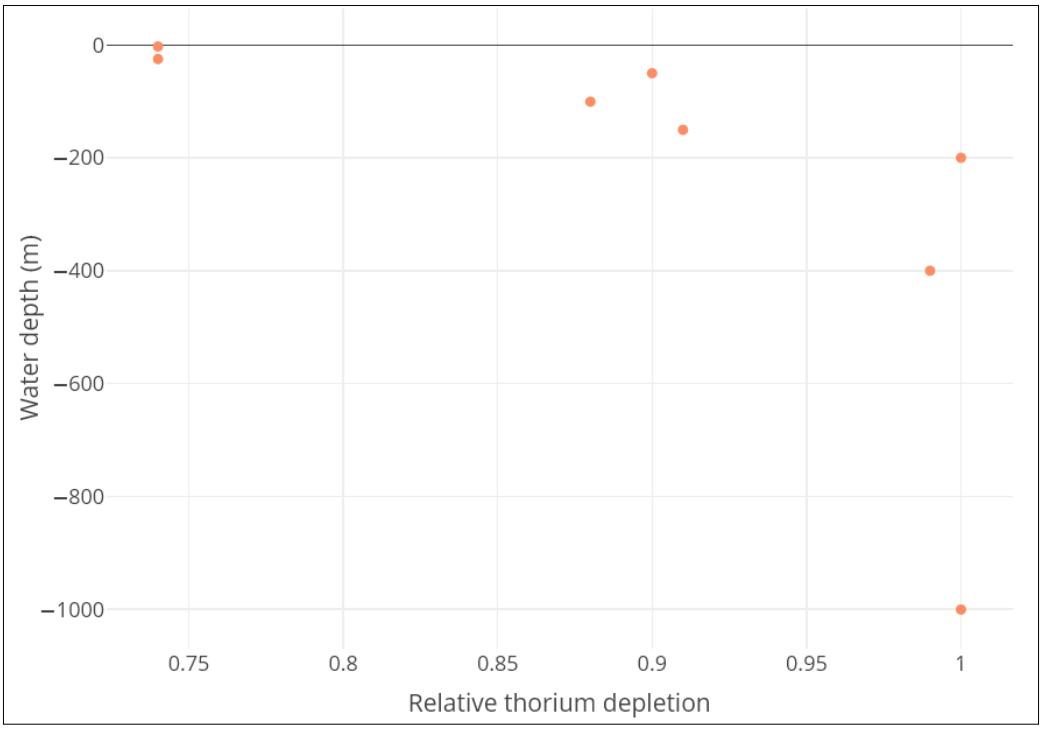

Fig. 3.13: Ice station 3: Relative depletion of total ^{234}Th compared to the total ^{234}Th concentration at 1,000 m water depth. The deficiency in the upper 200 m of the water column reflects particle export.

Data management

The preliminary thermosalinograph data are available from the DAVIS SHIP data base (https://dship.awi.de) at a resolution of 1 s. All data described herein will be archived, and published after final processing according to the FAIR principles by the World Data Center PANGAEA Data Publisher for Earth & Environmental Science (https://www.pangaea.de) within two years after the end of the expedition. By default, the CC-BY license will be applied.

The iridium buoy data will be stored on the server infrastructure of the respective manufacturer, and in the database of the International Arctic Buoy Programme. Selected buoys also report their data directly to the WMO's Global Telecommunication System (GTS) in near-real time, thereby contributing to improved global numerical weather predictions.

This part of the expedition is supported by the Helmholtz Research Programme "Changing Earth – Sustaining our Future" Topic 2, Subtopics 1, 3 and 4, and Topic 6, Subtopics 1, 2 and 3.

In all publications based on this expedition with co-authorship by any participant listed above, the **Grant No. AWI_PS138_03** or, in case of multidisciplinary work, **AWI_PS138_00** will be quoted and the following publication will be cited:

Alfred-Wegener-Institut Helmholtz-Zentrum für Polar- und Meeresforschung (2017) Polar Research and Supply Vessel POLARSTERN Operated by the Alfred-Wegener-Institute. Journal of large-scale research facilities, 3, A119. http://doi.org/10.17815/jlsrf-3-163.

References

Alkire MB, Morison J, Schweiger A, et al (2017) A Meteoric Water Budget for the Arctic Ocean. Journal of Geophysical Research-Oceans 122:10020–10041. https://doi.org/10.1002/2017JC012807

Bauch D, van der Loeff MR, Andersen N, et al. (2011) Origin of freshwater and polynya water in the Arctic Ocean halocline in summer 2007. Prog Oceanogr 91:482–495. https://doi.org/10.1016/j.pocean.2011.07.017

Becker S, Aoyama M, Woodward EMS, et al. (2020) GO-SHIP Repeat Hydrography Nutrient Manual: The Precise and Accurate Determination of Dissolved Inorganic Nutrients in Seawater, Using Continuous Flow Analysis Methods. Front Mar Sci 7:581790. https://doi.org/10.3389/fmars.2020.581790

Behrendt A, Sumata H, Rabe B, Schauer U (2018) UDASH – Unified Database for Arctic and Subarctic Hydrography. Earth Syst Sci Data 10:1119–1138. https://doi.org/10.5194/essd-10-1119-2018

Charette MA, Kipp LE, Jensen LT, et al (2020) The Transpolar Drift as a Source of Riverine and Shelf-Derived Trace Elements to the Central Arctic Ocean. JGR Oceans 125. https://doi.org/10.1029/2019JC015920

Francis A and Ganeshram RS and Tuerena RE and Spencer RGM and Holmes RM and Rogers J A and Mahaffey C (2023) Permafrost degradation and nitrogen cycling in Arctic rivers: insights from stable nitrogen isotope studies.Biogeosciences, 20 (2): 365-382, https://doi.org/10.5194/bg-20-365-202

Granskog MA, Fer I, Rinke A, Steen H (2018) Atmosphere-Ice-Ocean-Ecosystem Processes in a Thinner Arctic Sea Ice Regime: The Norwegian Young Sea ICE (N-ICE2015) Expedition. J Geophys Res Oceans 123:1586–1594. https://doi.org/10.1002/2017JC013328

Hydes DJ, Aoyama M, Aminot A, et al. (2010) The GO-SHIP Repeat Hydrography Manual: A Collection of Expert Reports and Guidelines. Version 1.Determination of Dissolved Nutrients (N, P, SI) in Seawater With High Precision and Inter-Comparability Using Gas-Segmented Continuous Flow Analysers. [SUPERSEDED by http://dx.doi.org/10.25607/OBP-555]. https://doi.org/10.25607/OBP-15

Kawaguchi Y, Koenig Z, Hoppmann M, et al. (2022) Turbulent mixing during late summer in the ice-ocean boundary layer in the central Arctic Ocean, J Geophys Res Oceans, 127(8), e2021JC017975, https://doi.org/10.1029/2021JC017975?af=R

Langdon C (2010) Determination of Dissolved Oxygen in Seaweater By Winkler Titration using Amperometric Technique. In, The GO-SHIP Repeat Hydrography Manual: A Collection of Expert Reports and Guidelines. Version 1, GO-SHIP.

Nicolaus M, Perovich DK, Spreen G, et al. (2022) Overview of the MOSAiC expedition: Snow and sea ice. Elementa: Science of the Anthropocene 10:000046. https://doi.org/10.1525/elementa.2021.000046

Rabe B, Heuzé C, Regnery J, et al. (2022) Overview of the MOSAiC expedition: Physical oceanography. Elementa: Science of the Anthropocene 10. https://doi.org/10.1525/elementa.2021.00062

Rabe B, Karcher M, Kauker F, et al (2014) Arctic Ocean basin liquid freshwater storage trend 1992-2012. Geophys Res Lett 41:961–968. https://doi.org/10.1002/2013GL058121

Roca-Martí M, Puigcorbé V, Friedrich J, et al. (2018) Distribution of 210Pb and 210Po in the Arctic water column during the 2007 sea-ice minimum: Particle export in the ice-covered basins. Deep Sea Research Part I: Oceanographic Research Papers 142:94–106. https://doi.org/10.1016/j.dsr.2018.09.011

Roca-Martí M, Puigcorbé V, Rutgers Van Der Loeff MM, et al. (2016) Carbon export fluxes and export efficiency in the central Arctic during the record sea-ice minimum in 2012: a joint 234 Th/ 238 U and 210 Po/ 210 Pb study. J Geophys Res Oceans 121:5030–5049. https://doi.org/10.1002/2016JC011816

Sakamoto, CM, Johnson, KS, Coletti, LJ (2009) Improved Algorithm for the Computation of Nitrate Concentrations in Seawater using an in situ Ultraviolet Spectrophotometer. Limnology and Oceanography: Methods, 7, 132-143

Santos-Garcia M, Ganeshram RS, Tuerena RE, et al. (2022) Nitrate isotope investigations reveal future impacts of climate change on nitrogen inputs and cycling in Arctic fjords: Kongsfjorden and Rijpfjorden (Svalbard). Biogeochemistry: Stable Isotopes & Other Tracers

Shupe MD, Rex M, Blomquist B, et al (2022) Overview of the MOSAiC expedition: Atmosphere. Elementa: Science of the Anthropocene 10:00060. https://doi.org/10.1525/elementa.2021.00060

Stedmon CA, Amon RMW, Bauch D, et al. (2021) Insights Into Water Mass Origins in the Central Arctic Ocean From In-Situ Dissolved Organic Matter Fluorescence. Journal of Geophysical Research-Oceans 126. https://doi.org/10.1029/2021JC017407

Tuerena RE, Hopkins J, Buchanan PJ, et al. (2021a) An Arctic Strait of Two Halves: The Changing Dynamics of Nutrient Uptake and Limitation Across the Fram Strait. Global Biogeochemical Cycles 35:. https://doi.org/10.1029/2021GB006961

Tuerena RE, Hopkins J, Ganeshram RS, et al. (2021b) Nitrate assimilation and regeneration in the Barents Sea: insights from nitrate isotopes. Biogeosciences 18:637–653. https://doi.org/10.5194/bg-18-637-2021

Ulfsbo A, Jones EM, Casacuberta N, et al. (2018) Rapid Changes in Anthropogenic Carbon Storage and Ocean Acidification in the Intermediate Layers of the Eurasian Arctic Ocean: 1996-2015. Global Biogeochem Cycles 32:1254–1275. https://doi.org/10.1029/2017GB005738

University of Alaska Fairbanks, Weingartner T, Ashjian C, et al. (2022) Introduction to the Special Issue on the New Arctic Ocean. Oceanog. https://doi.org/10.5670/oceanog.2022.132

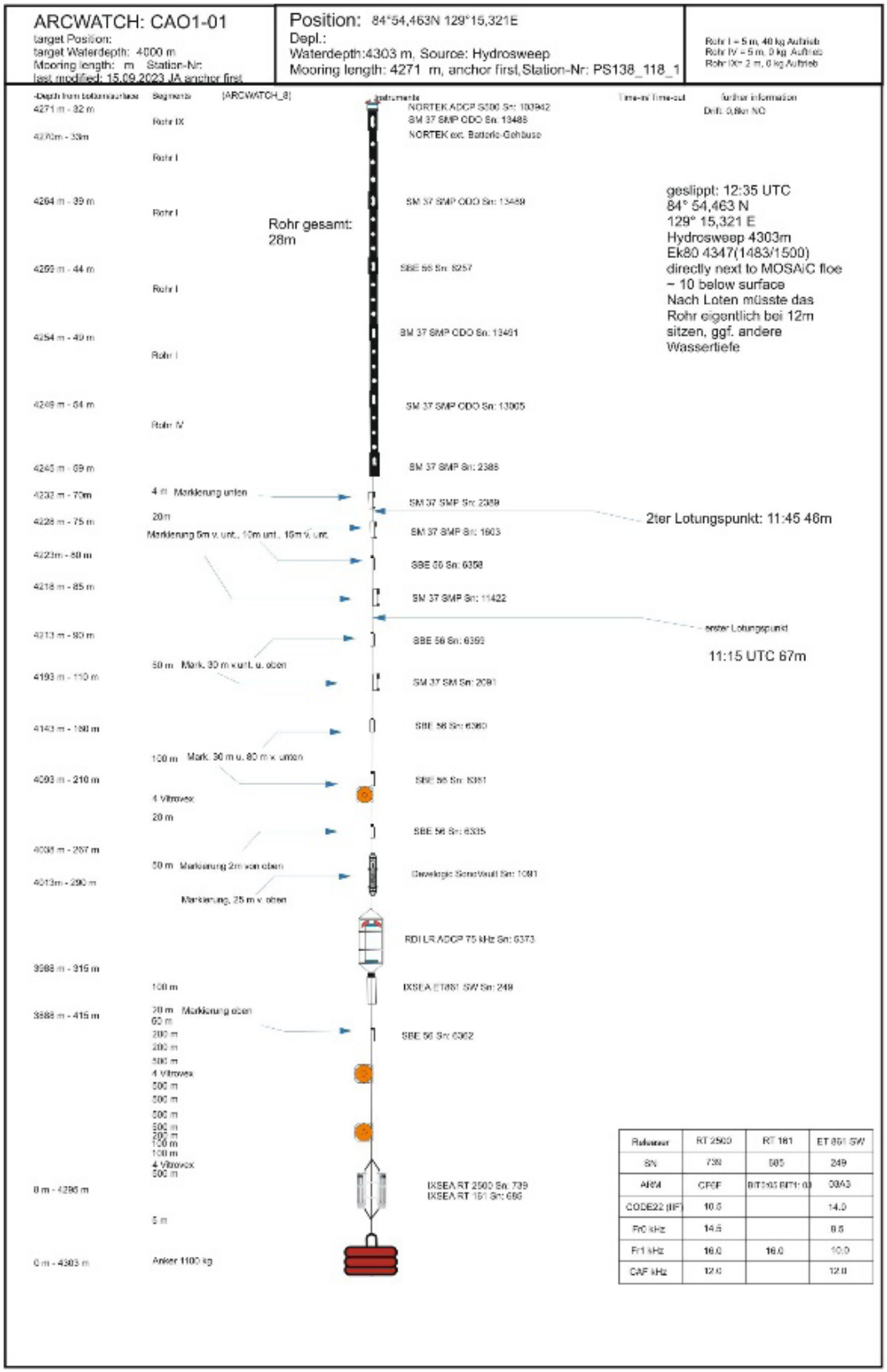

Fig. 3.10: Schematic of mooring CAO1-01

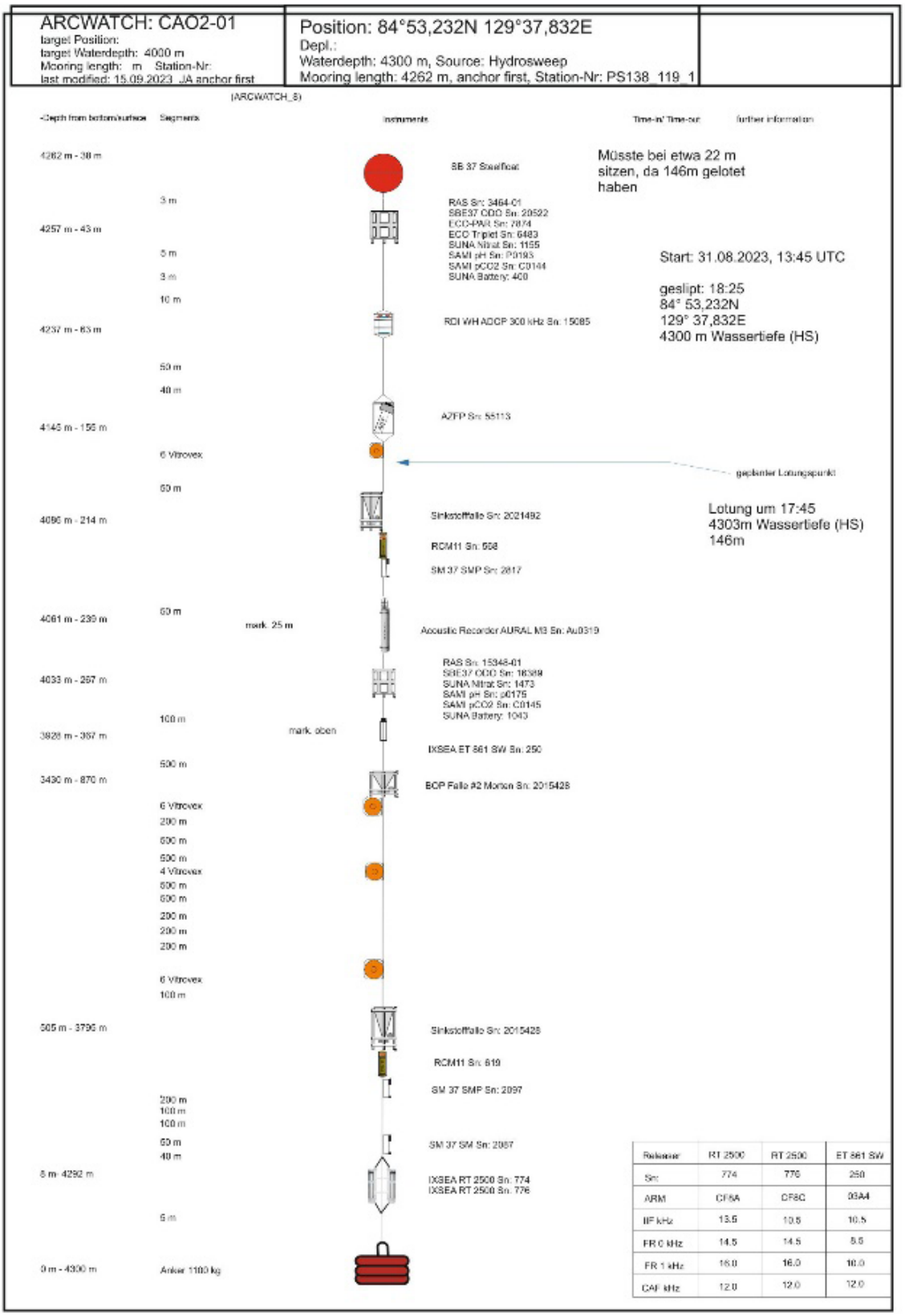

Fig. 3.11: Schematic of mooring CAO2-01

4. BIOLOGICAL OCEANOGRAPHY AND SEA-ICE BIOLOGY

Morten Iversen[1,2], Erika Allhusen[1], Natasha Anne Bryan[1], Kathryn Cook[3], Sarah Lena Eggers[1], Tim Kalvelage[4], Laurent Oziel[1], Ruben Lennart Schulte-Hillen[5], Antonia Thielecke[1], Kim Vane[1], Matthias Wietz[1]
not on board: Mar Fernandez-Mendez[1], Daniel Mayor[3]

[1]DE.AWI
[2]DE.MARUM
[3]UX.UE
[4]DE.K*
[5]DE.UNI-FREIBURG

Grant-No. AWI_PS138_02

Outline

Due to the rapidly advancing climate warming, the Arctic Ocean is experiencing unprecedented changes. The decline in summer sea-ice coverage by ~13 % per decade compared to the mean extent for 1981–2010 (Serreze and Meier 2019), coupled with increasing temperatures and declining ice thickness and loss of multiyear ice (Kwok 2018), is already altering the composition of primary producers in the Arctic Ocean (Wassmann and Reigstad 2011). It is still unclear which consequences these changes will have for the food web, pelagic-benthic coupling, and biogeochemical cycling in the Arctic Ocean (Wiedmann et al. 2020). Hence, during ArcWatch-1, we studied how different ice- and nutrient-regimes impacted productivity, community composition, trophic interactions, remineralization and carbon sequestration. These parameters will be compared to previous expeditions in the central Arctic Ocean in order to improve our ability to predict future changes in ecosystem dynamics and carbon storage.

Objectives

The Arctic sea-ice cover is a critical component of the Earth's climate system where it directly reflects sunlight back into space, hosts a unique diversity of life, and plays a crucial role in regulating heat exchange and ocean circulation. The recent record-lows in sea-ice extent in 2012 and 2020 with less than 4 million km^2 of ice-cover are accompanied by a shift from thicker multi-year ice to thinner first-year ice in the central Arctic. Shifts from multi-year to first-year ice have large implications for the cryo-benthic and cryo-pelagic coupling, ultimately affecting the entire Arctic Ocean ecosystem. A reduction in sea-ice thickness may result in a higher primary production of sea-ice algae, which may impact sea-ice associated metazoans. During ArcWatch-1, we identified and studied different ice-associated ecosystems by sampling for biogeochemical parameters, phyto- and zooplankton community composition, measured primary productivity, microbial remineralization rates of passively sinking aggregates, the vertical distribution of zooplankton and particles in the water column, as well as vertical export of organic matter.

Our research was based on the following hypotheses:

- Declining silicic acid availability in the marginal ice-zone will decrease primary production.
- Low silicic acid availability will cause a shift from diatoms to non-silicified phytoplankton and ice-algae.

- *Cal*anus *hyperboreus* that migrate to depths of 1,500 meters have assimilated more sea-ice algal basal resources than those at the surface.
- Zooplankton metabolic activity decreases with increasing depth, thereby decreasing conversion of lipid to carbon dioxide at depth during diapause.
- The meltwater-layer below sea ice retains settling aggregates allowing efficient grazing on the aggregates by zooplankton, and the establishment of specific heterotrophic microbiomes.
- Carbon export is high at marginal ice-zones where cryo-minerals are efficiently released from first-year ice as sea-ice melts.
- Microbial diversity and functional ecology show distinct signatures relating to sea-ice cover, showcasing adaptations to central Arctic habitats.
- Bacterial chemotaxis is enriched in sea-ice associated habitats, foremost melt ponds, in comparison to pelagic seawater.
- Seasonality in the central Arctic Ocean is weaker in relation to boundary regions, such as the Fram Strait.

Work at sea

Ice sampling for biogeochemical parameters (coring, melt ponds, under-ice water)

We sampled for biogeochemical parameters at all nine ice stations by collecting sea ice cores (Biocores 1-9; Fig. 4.1), seawater directly under the ice (UIW), and meltpond water (MPW) if present. Additionally, three sea-ice cores were taken, for physical parameters, including salinity (SAL, from station 3 onwards), texture (TEX), and for archiving (ARC) for further analyses in the home laboratory. Prior to coring, three snow samples were collected from the coring sites 1-3 and temperatures in the air, snow and snow-ice interface were determined. SAL cores were cut into 10 cm sections on site. Within each section the temperature was determined immediately by drilling a hole in the center of each section and inserting a thermometer. The sections were melted on board at room temperature and volume and salinity of the melt-water were determined. UIW was sampled using a manual pump through the first ice core hole from ~10 cm below the underside of the ice. MPW was sampled with the same pump. Salinity measurements were used to determine if the melt pond was open, i.e. melted through to the ocean below the ice, or closed prior to sampling and to check for salinity gradients within the melt pond.

Nine cores for biogeochemical parameters, phytoplankton and microbial diversity were sectioned into a bottom part (lower 13 cm) and top part (remaining). On board, the top parts of the nine cores were carefully broken apart to accelerate melting, which was done at 4°C. The pieces from the nine top parts of the cores were pooled together to ensure enough melt-water for the biogeochemical analyses. The bottom parts of the nine cores were melted whole and individually at 4°C and pooled afterwards. From all melted ice core sections, the volume and the salinity of the melt-water were determined. The pooled samples of top and bottom sections, as well as UIW and MPW were divided for analysis of the following particulate parameters: phytoplankton cell counts, pigments (HPLC), particulate biogenic silicate (PbSi), particulate organic carbon and nitrogen (POC/PON), particulate inorganic carbon (PIC), particulate organic phosphate (POP), net primary productivity (NPP), and microbial diversity via environmental DNA (eDNA).

Fig. 4.1: Images of sampling procedure; handnet deployment off the side of the ship (left); drilling ice cores (top right) and assessing core length and structure on site (bottom right)

Particulate biogeochemical parameters in the water column

At each of the nine ice-stations and during a 60°E transect, we sampled the vertical distribution of particulate organic and inorganic matter using the CTD rosette to collect seawater from five different depths in the upper 200 m of the water column. Aliquots were filtered for biogeochemical parameters using gentle vacuum filtration (< 300 mBar): pigments (HPLC; GFF), particulate biogenic silica (PbSi; 0.8 µm CA filter), particulate organic carbon and nitrogen (POC/PON; pre-combusted GFF), particulate inorganic carbon (PIC; pre-combusted GFF), and particulate organic phosphate (POP; pre-combusted GFF). Furthermore, unfiltered water samples were fixed with formaldehyde (final concentration 2%) for later quantitative assessment of the phytoplankton community through inverted microscopy. At six of the stations (ice stations 2-7) additional POC samples were collected from depths below 200 m and down to the seafloor. At two stations (ice stations 6 and 7) aggregates were turned into a homogenous solution through thorough shaking, diluted, and then measured according to the water samples procedure. When aggregates were present (stations 1, 5, 6, and 7) in the ROV net, subsamples were filtered into different size-fractions, >10 µm, 10-3 µm, and 3-0.4 µm using Millipore polycarbonate filters for eDNA analysis.

Phytoplankton community composition

At all nine ice stations, oblique phytoplankton net hauls (20 µm mesh size) in the upper 20 m of the water column were deployed from the ship simultaneously with the CTD deployment (Fig. 4.1 and 4.2). Onboard microscopy was done to determine a semi-quantitative composition of phytoplankton and to identify the dominant species at each station. Further subsamples were fixed with 2% formaldehyde for quantitative analyses in the home laboratory.

Fig. 4.2: Image of handnet sample at station 1: Calanus hyperboreus copepods are visible with their large red antennas.

Net primary production and nutrient uptake rates

Net primary production (NPP) was analysed using the 14C uptake method (Steemann Nielsen, 1952) at a total of 21 stations (9 ice stations + 12 stations during the 60°E CTD transect). During all ice stations, we determined NPP from the melt-water from both the top and bottom part of the ice cores, from seawater samples collected using the CTD-Rosette (10 m and Chl max), and from under-ice water and melt-ponds. At two stations (ice stations 1 and 6), we measured NPP from aggregates that were turned into a homogenous solution through thorough shaking, diluted and then measured according to the methodology used for the water samples. For each sample, subsamples (triplicates) were taken for dissolved inorganic carbon (DIC) analysis. Then 200 ml of sample was spiked with 0.1 µCi mL^{-1} of 14C-labelled sodium bicarbonate and distributed in 10 clear bottles (20 mL each). Subsequently, the samples were incubated for 8h at 0°C under different scalar irradiances (0–430 µmol photons m^{-2} s^{-1}) which were measured with a spherical sensor (Spherical Micro Quantum Sensor USSQS/L, Heinz Walz, Effeltrich, Germany). At the end of the incubations, samples were filtered onto 0.2 µm nitrocellulose filters and the particulate radioactive carbon uptake was determined by liquid scintillation counting using filter count scintillation cocktail (Perkin Elmer, Waltham, USA). The carbon uptake values in the dark were subtracted from the carbon uptake values measured in the light incubations.

At ice station 3, where aggregates accumulated in the ice edge and in the sediment trap holes, intact aggregates were carefully sampled from the sediment trap hole to obtain an NPP to aggregate volume relationship. Aggregate size was assessed using scaled images. Individual aggregates (triplicates + 1 dark incubation) were then placed in 100 ml of filtered under-ice water, spiked with 0.1 µCi mL^{-1} and incubated for 12h *in situ* in the sediment trap hole. Afterwards the sample was treated as described above.

At five stations (ice stations 1, 2, 5, 7, 8) additional incubations were conducted for nutrient uptake rates and diatom shell thickness. Two different incubations were performed at each of these stations using a silicic acid gradient (0, 2, 5, 10, 20 µM) and different light levels (0, 10, 40, 80, 320 µE): 24h incubations were performed to investigate carbon, nitrate, and silicic acid

uptake rates and 48h incubations were performed to investigate silica incorporation. Initial samples were taken for HPLC, POC/PON, BSi, POP, PIC, DIC, nutrient analysis and cell counts. Nutrients (nitrate, nitrite, phosphate, silicic acid) were added using F/2 medium stock solution to create a silicic acid gradient and avoid nutrient limitation during the incubations. To measure nutrient uptake rates, stable isotopes (^{13}C, ^{15}N, ^{30}Si) were added to each 2 L bottle. Subsequently the bottles were incubated for 24h at 4°C and under stable light conditions. After the incubation the water was filtered for subsequent POC/PON and BSi analysis allowing for changes in productivity and uptake rates to be assessed. At stations 6, 7 and 8, reverse filtration and hand net samples were used to concentrate the natural phytoplankton community due to very low biomass and to create an inoculum which was added to each of the bottles in order to obtain a signal.

To investigate silica incorporation, the phytoplankton community was first up-concentrated using reverse filtration and then incubated for 48h in cell culture bottles with the silica stain PDMPO under the same silicic acid gradient. Incubations were also performed at all light levels with 5 µM added silica. Afterwards, the samples were fixed with formalin (final concentration 2%) to subsequently assess differences in silica incorporation with an Imaging Flow Cytometer (Amnis ImageStreamX Mk II Imaging Flow Cytometer). Additional 17 samples were taken to develop automated phytoplankton species recognition using the Amnis Imaging Flow Cytometer by concentrating water from the CTD (2-50 m, 20-50 L) using reverse filtration (3 µm polycarbonate filter) and fixing the concentrated sample with 2% formaldehyde until further analyses at AWI.

Taxonomic and functional diversity of microbial communities via eDNA

To characterise the composition and function of bacteria, archaea and microbial eukaryotes, water was sampled from the CTD rosette, resulting in a total of ~250 samples from 12 depths (Tab. 4.1). This included the entire 60° E transect with 12 CTDs (interchanging shallow and deep) for assessing diversity gradients across the Transpolar Drift. The 60° E transect was bordered by ice stations 7 (North Pole) and 9, with station 8 in the middle. Furthermore, a Niskin bottle mounted on the OFOBS provided 5 water-samples that were collected directly above the seafloor, plus a sample from the plume of the Polaris hydrothermal vent field. Sea-ice, meltpond and under-ice water resulted in ~30 samples.

Tab. 4.1: CTD types and sampling depths

CTD type	**Depths sampled**
Ice stations (one shallow, one deep cast)	5 m from bottom, 20 m from bottom, 3,000 m, 2,000 m, 1,500 m, 1,000 m, 500 m, 200 m, 100 m, 50 m, Chl-max, 10 m, and 2 m
60°E Transect (shallow or deep cast)	3,000 m, 1,000 m, 500 m, 200 m, 100 m, 50 m, Chl-max, and 10 m

All water and melted ice-samples were filtered onto 0.22 µm Sterivex cartridges using peristaltic pumps within a few hours after sampling/melting while kept cool. Filters were directly frozen at -20°C to preserve eDNA, to be extracted in the home lab. Subsequent amplicon and metagenome sequencing will inform about taxonomic and functional diversity of microbial communities across the Central Arctic, in relation to environmental conditions. This evidence will be placed in the larger biogeographic context by additional DNA samples obtained from the AUTOFIM system (Fig. 4.3), programmed to automatically sample in intervals of 4-12h (depending on transiting between stations, or being at ice stations). The cruise tracks to and

from the North Pole were largely congruent, providing samples from more or less the same location but weeks apart – illustrating microbial dynamics at the same location during different stages of ice-melt and ice-reformation. AUTOFIM continued sampling until ~65°N, additionally providing a high-resolution microbial inventory across the northern Atlantic Ocean.

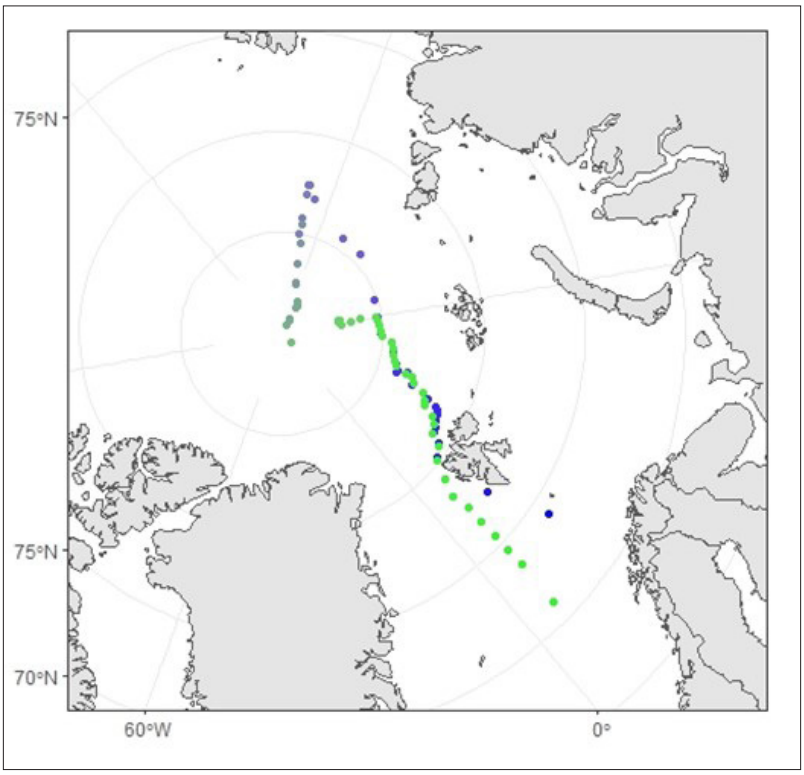

Fig. 4.3: AUTOFIM sample locations. The AUTOFIM device collected DNA samples continuously throughout the expedition, providing an additional high resolution microbial profile. The colour gradient illustrates sampling days (blue early, green late).

Microbial in situ gene expression

At all nine ice stations, a CTD was deployed to collect water samples through the entire water column. In addition to providing eDNA samples (see above), four *in-situ* pumps were attached to the CTD wire at four depths per cast: 20 m above the CTD (i.e. bottom layer), 2,000 m, 250 m (Atlantic water), and 30 m (surface/chl-max). The pumps were programmed to start pumping once they had reached their target depths. Each pump was actively pumping for 2h, with sequential filtration through pore-sizes of 10 µm and 0.2 µm (142 mm diameter, polycarbonate) to separate larger organisms (diatoms, zooplankton, particles and associated microbes) from smaller aggregates and free-living microbes. Some deployments failed due to unknown instrument errors, likely due to heavy load on the batteries at cold temperatures (despite carefully checking the pump's control system before each cast, with careful cleaning after and before each deployment). To limit failures, we kept the pumps at relatively warm temperatures inside the working alley. Furthermore, to prevent ice formation in filter towers prior to deployment, these were not prepared with MilliQ but sterile artificial seawater. In total, we obtained the following samples (Tab. 4.2), with pumps filtering on average between 200-800 L of water. Filters were flash-frozen in liquid nitrogen directly after recovery, and stored at -80°C. From these, DNA and RNA will be extracted to obtain metagenome and metatranscriptome data – elucidating microbial diversity, metabolic potential and gene expression respectively, for

the first time across the Central Arctic. *In-situ* plus deep CTD samples link to benthic work, and contribute to better understanding of microbial activities associated with cryo-bentho-pelagic coupling.

Tab. 4.2: *In-situ* pump deployments at the nine ice stations. Successful = more than 50L pumped.

Event	Ice station	Date	Depth [m]	Successful?
PS138_26-1_1	1	2023-08-11	3969	yes
PS138_26-1_2	1	2023-08-11	2000	yes
PS138_26-1_3	1	2023-08-11	250	yes
PS138_26-1_4	1	2023-08-11	30	no
PS138_40-1_1	2	2023-08-17	3660	yes
PS138_40-1_2	2	2023-08-17	2000	yes
PS138_40-1_3	2	2023-08-17	250	yes
PS138_40-1_4	2	2023-08-17	30	no
PS138_69-1_1	3	2023-08-21	3900	yes
PS138_69-1_2	3	2023-08-21	2000	yes
PS138_69-1_3	3	2023-08-21	250	yes
PS138_69-1_4	3	2023-08-21	30	no
PS138_90-1_1	4	2023-08-25	3700	yes
PS138_90-1_2	4	2023-08-25	2000	yes
PS138_90-1_3	4	2023-08-25	250	no
PS138_90-1_4	4	2023-08-25	30	no
PS138_115-1_1	5	2023-08-29	4230	yes
PS138_115-1_2	5	2023-08-29	2000	yes
PS138_115-1_3	5	2023-08-29	250	no
PS138_115-1_4	5	2023-08-29	30	yes
PS138_145-1_1	6	2023-09-04	4300	yes
PS138_145-1_2	6	2023-09-04	2000	yes
PS138_145-1_3	6	2023-09-04	250	yes
PS138_145-1_4	6	2023-09-04	30	yes
PS138_168-1_1	7	2023-09-11	4220	yes
PS138_168-1_2	7	2023-09-11	2000	yes
PS138_168-1_3	7	2023-09-11	250	yes
PS138_168-1_4	7	2023-09-11	30	no
PS138_193-1_1	8	2023-09-14	4376	yes
PS138_193-1_2	8	2023-09-14	2000	yes
PS138_193-1_3	8	2023-09-14	250	yes
PS138_193-1_4	8	2023-09-14	30	yes
PS138_218-1_1	9	2023-09-20	3880	yes
PS138_218-1_2	9	2023-09-20	2000	yes
PS138_218-1_3	9	2023-09-20	250	yes
PS138_218-1_4	9	2023-09-20	30	yes

Bacterial chemotaxis

Microbial motility and chemotaxis (the ability to move in response to a chemical gradient) are substantial advantages to acquire resources. These traits are especially relevant in view of particle fluxes and aggregates, which can carry a “plume” of chemical compounds that bacteria can sense and respond to. However, current techniques restrict chemotaxis research to the laboratory. On ArcWatch-1, we used a newly developed *in situ* chemotaxis assay (ISCA) to detect microbial chemotaxis *in situ*. For this, close exchange with the developer JB Raina provided considerable support in the experimental design, with subsequent collaboration in sample processing and data analyses. The ISCA is a microfluidic device consisting of a 20-well array, in which chemicals of interest can be loaded and diffuse out of the wells (Fig. 4.4), creating concentration gradients that microbes sense and respond to by swimming into the wells. We performed different experiments; firstly with methanolic extracts of the phytoplankton species *Fragilariopsis* sp. (isolated from Arctic sea-ice) and *Thalassiosira* sp. (isolated from temperate seawater), reconstituted onboard in sterile seawater. Extracts originate from a collaboration with Tilmann Harder (University of Bremen), who previously performed physiological experiments with those phytoplankton. This knowledge facilitates subsequent interpretation of the results, since e.g. the growth state of the phytoplankton species has been characterised and chemistry can be analyzed with e.g. NMR. *Fragilariopsis* and *Thalassiosira* extracts were incubated in two different dilutions (1:5, 1:10) in sterile-filtered meltpond water, always from the same site where ISCA were deployed to omit passive movement into the wells via salinity gradients. Not all stations were sampled, due to absence of meltponds. For those meltponds sampled, we observed a variety of “morphologies”, from a classic blue meltpond at station 1 (Fig. 4.4) to completely refrozen and snow-covered at station 2 (Fig. 4.4).

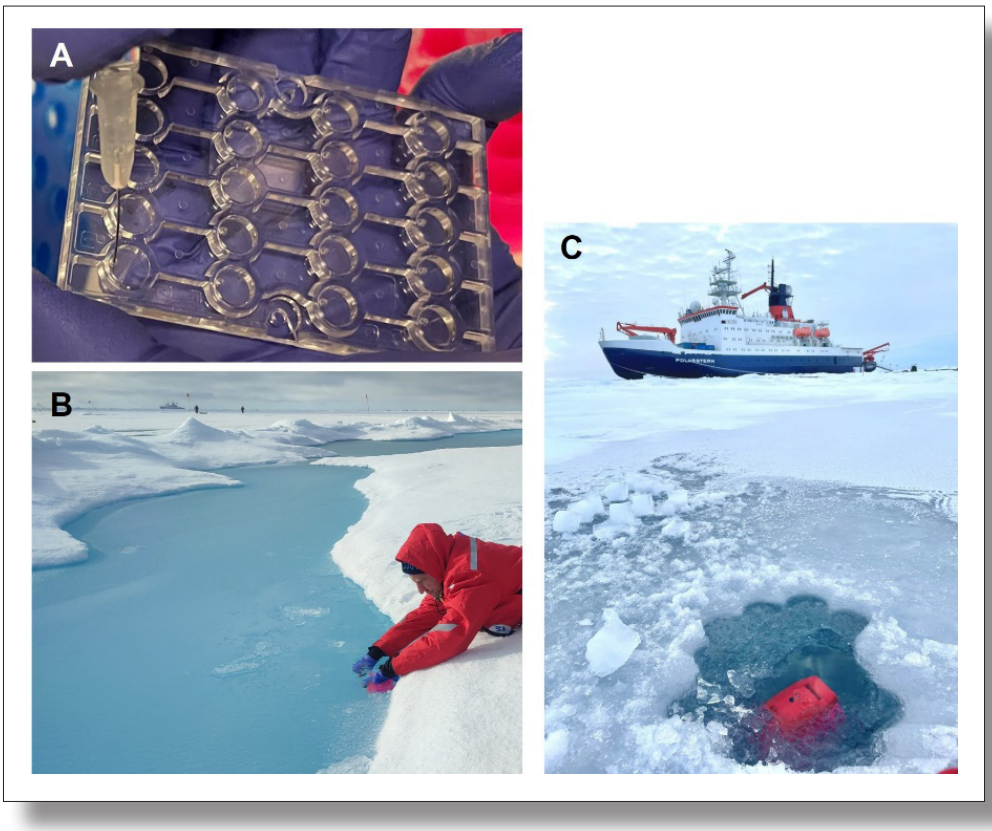

Fig. 4.4: In situ chemotaxis assay. ISCA multiwell plates were loaded with chemoattractants (A) and deployed in the field, including blue (B) and refrozen (C) meltponds.

Secondly, we prepared an extract of algal aggregates sampled at ice station 3. At the edge of this ice floe, aggregates (containing largely *Melosira* and also *Fragilariopsis* cells; Fig. 4.5) were sampled directly from the water surface. We applied threefold ultrasonication, freeze-thawing in liquid nitrogen, and vortexing to break up algal cells and release their contents, resulting in a greenish extract which hence likely contained chlorophyll and algal metabolites. This extract was not incubated in meltponds, but shipboard embedded in under-ice water sampled 1.5 m below the sea-ice – a habitat where bacteria likely encounter such metabolites.

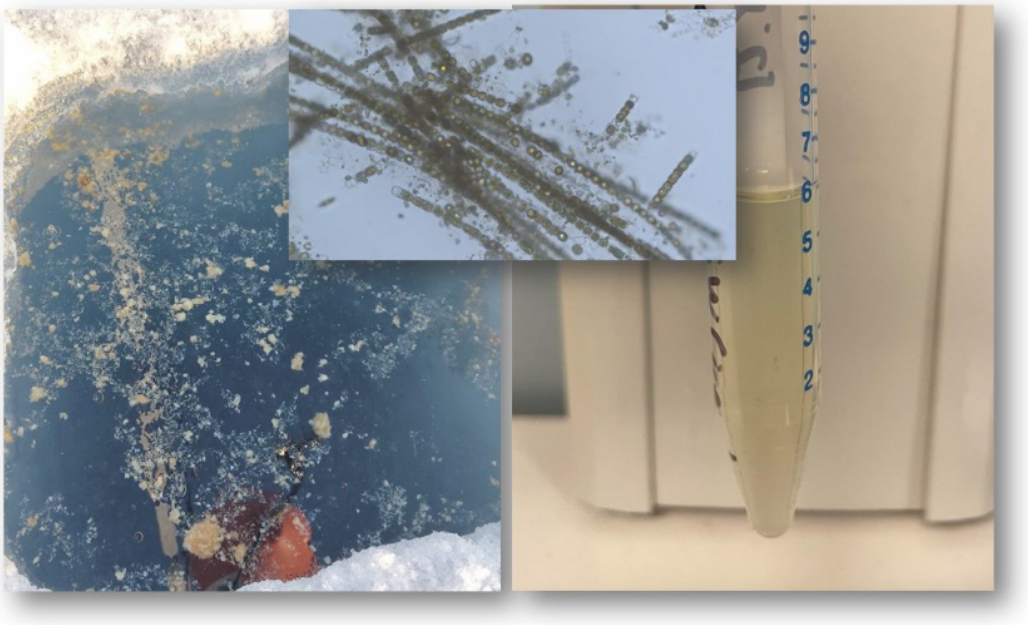

Fig. 4.5: ISCA with natural aggregates. Algal aggregates floating in core hole at station 3 (left), containing Melosira and other algal cells (middle) resulting in a crude extract (right) used in ISCA with under-ice water.

DMSP, a known chemoattractant with relevance in ice-associated ecosystems, served as positive control; in parallel providing ecologically relevant information about responses to a metabolite abundant in sea-ice and phytoplankton blooms. A negative control (only seawater) was applied as well. All ISCAs were set-up in five replicates (i.e. wells) per treatment, subsequently pooled and sampled for (i) flow cytometry (fixing each 100 µL in 2% glutaraldehyde v/v) and (ii) snap-freezing the remainder in liquid nitrogen for later DNA extraction and sequencing. For 21 selected samples, each 10 µL were spread-plated on agar medium, and/or added to artificial seawater plus 0.2% (w/v) glucose in enrichment cultures. From agar plates, forming colonies were pure-cultured, aiming at supporting sequencing results with physiological evidence (e.g. chemotactic abilities, degradation of algal metabolites). Assessing the role of algal chemoattractants in bacterial chemotaxis helps identifying major players in bacteria-algae interactions in sea-ice habitats, an important factor for biogeochemical cycling in meltponds and under-ice water. Overall, we performed the following experiments, resulting in ~200 samples for later analyses (Ta. 4.3).

Tab. 4.3: ISCA deployments. UIW: under-ice water; AGG: algal aggregates

Label	Meltpond characteristics	Incubation type
PS138_9_ISCA-001	size 10x2 m, ~30 cm depth, blue water, deployed at pond edge	insitu in melt pond
PS138_31_ISCA-001	size 3x2 m, ~30 cm depth, refrozen	insitu in melt pond
PS138_31_ISCA-002		shipboard with ice-edge water
PS138_52_ISCA-001	no meltpond	shipboard with UIW
PS138_75_ISCA-001	size 3x2 m, ~30 cm depth, refrozen	insitu in melt pond
PS138_75_ISCA-002		shipboard with UIW
PS138_101_ISCA-001	refrozen pond (ca 20 cm ice); covered with ca 5 cm snow	insitu in melt pond
PS138_101_ISCA-002		shipboard with UIW
PS138_129_ISCA-001	no meltpond	shipboard with UIW
PS138_129_ISCA-002		shipboard with AGG
PS138_152_ISCA-001	covered with snow, near public walking track	insitu in melt pond
PS138_152_ISCA-002		shipboard with UIW
PS138_152_ISCA-003		shipboard with AGG
PS138_178_ISCA-001	20 cm snow cover, 40 cm deep, re-covered with ice and snow after ISCA deployment	insitu in melt pond
PS138_178_ISCA-002		shipboard with UIW
PS138_178_ISCA-003		shipboard with AGG
PS138_213_ISCA-001	no meltpond	shipboard with UIW
PS138_213_ISCA-002		shipboard with AGG

Microbial seasonality

Two Remote Access Samplers (RAS) were deployed on mooring CAO-1 (PS138_118-1), at depths of 250 and 30 m respectively. These devices have been programmed to sample water in weekly intervals over the coming year, and will be recovered during ArcWatch-2 in 2025. The samples will subsequently provide a year-round inventory of microbial diversity and functionality based on eDNA extraction and sequencing. These data are relevant to compare with year-round studies in the Fram Strait time-series, allowing to assess seasonality in “true” Arctic vs. Arctic-Atlantic boundary conditions.

Mesozooplankton

The Hydro-Bios Midi Multinet (Fig 4.6A) was deployed twice at each ice-station. The Multinet was fitted with 5 x 150 µm nets that open and close sequentially at specific depths. These opening/closing depths were consistent across all deployments and divided the sampled water column into intervals: 1500-1000, 1000-500, 500-200, 200-50, 50-0 m. The Multinet was deployed using winch EL30 at a speed of 0.5 m/s. The Multinet was run in real-time mode using the Deck Command Unit to communicate with the Multinet in order to open the nets manually at depth according to the integrated pressure sensor. Flowmeter readings were recorded, but the flowmeter did not function correctly on all deployments so should be used with caution. Samples from the first Multinet deployment were transferred to 200 mL Kautex bottles and preserved at 4% hexamethylenetetramine buffered formaldehyde for later abundance and biomass analysis at AWI. Samples from the second deployment were used to pick and preserve specimens at -20°C and -80°C for later biochemical analyses at AWI and the University of Exeter. A Bongo net (300 µm mesh, non-filtering cod-ends, Fig. 4.6B) [CK4] was deployed to 50 m to collect additional specimens for biochemical analyses. For under-ice mesozooplankton observations and biochemical sampling, a 150 µm mesh net was attached to the Remote Operated Vehicle (Fig. 4.6C) and trawled separately directly underneath the ice and at 10 meters depth. Mesozooplankton for biochemical analysis were removed and the remainder was preserved in 4% hexamethylenetetramine buffered formaldehyde for later abundance and biomass analysis at AWI. From all nets individual *Calanus hyperboreus* and C. *glacialis* with full stomachs were preserved in 99% ethanol and stored at -20°C for DNA analysis. Other mesozooplankton, such as jellyfish *Atolla* sp. and *Botrynema brucei*, amphipods; *Themisto* sp., *Cyclocaris guilelmi*, *Onisimus* sp., shrimp; *Hymenodora glacialis*, krill; *Thysanoessa* sp., sea snails; *Limacina helicina*, *Clione limacina* were also collected and stored at -20°C.

Calanus spp. copepodite stage 5 (C5) and adult females (C6F) were frozen at -80°C for carbon and nitrogen (CN) biomass, lipid content, metabolic rate estimation using enzyme rate measurements (Electron Transport System (ETS) activity as a measure of respiration rate; Amino-Acyl-t-RNA-Synthetases (AARS) activity as a measure of growth), and molecular species identification at the University of Exeter.

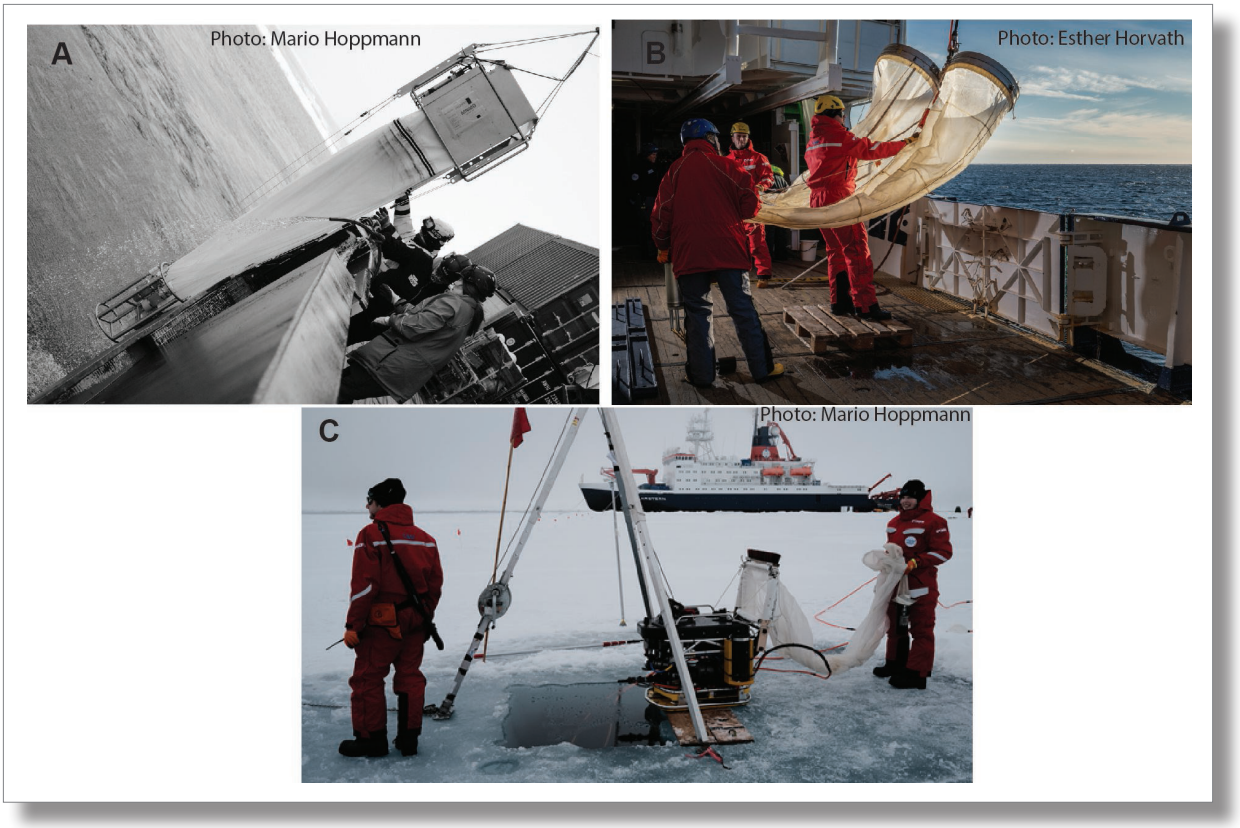

Fig. 4.6: A) The Hydrobios Midi multi-net with 5 nets with 150 µm mesh size, B) Bongo net with 300 µm mesh size, C) A 5 meter long net with 150 µm mesh size attached to the Remote Operated Vehicle (ROV).

High vertical resolution of zooplankton and particles

Underwater Vision Profiler (UVP)

The Underwater Vision Profiler (UVP) (version 5HD, SN204) was integrated as part of the CTD-Rosette frame (Fig. 4.7) in order to capture vertical abundance and size-distribution of particles and zooplankton during every CTD cast (except the deep CTD cast at ice-station #1 where we had a technical issue with the UVP). The UVP is an *in situ* optical tool that images particles and zooplankton within a size-range between 100 µm and ~5 cm. In total, we deployed the UVP at 37 CTD-Profiles, including the test station. The data were semi-processed during the cruise and we made "vignettes" (or crops) of zooplankton, as well as histograms of particle size-distributions. This partial processing provided 5 size-classes of particle types. However, to have a full resolution distribution and recognition of zooplankton species, the dataset must be uploaded and finally processed by the artificial intelligence algorithms: eco-part (https://ecopart.obs-vlfr.fr/) and eco-taxa (https://ecotaxa.obs-vlfr.fr/) respectively.

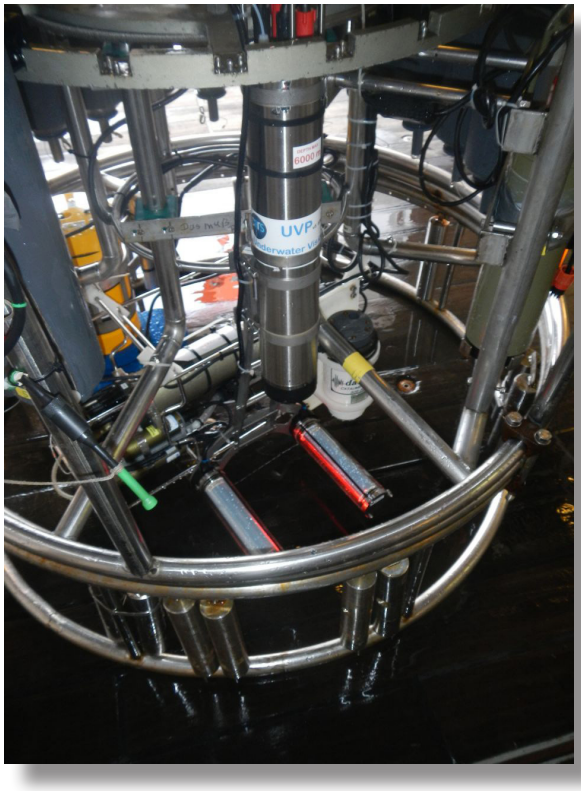

Fig. 4.7: The Underwater Vision Profiler (UVP)

ROSINA and JellyCam

The modular *in situ* imaging system ROSINA was deployed at each of the nine ice-stations. The ROSINA system consisted of two different camera systems that combined measured vertical profiles of particle and zooplankton abundance and size-distribution through the water column. The ROSINA system (Fig. 4.8) included the JellyCam and the ROSINA camera system (Remotely ObServing INsitu camera for Aggregates), and a CTD (OceanSeven 310, Idronaut S.r.l). The whole system was deployed via a coaxial winch cable and continuously sent data and images to the winch control room via a telemetry unit, which allowed the user to control the camera and light setting during deployment.

Fig. 4.8: ROSINA frame with the ROSINA camera system, Jelly camera and the Idronaut CTD

ROSINA (Remotely ObServing INsitu camera for Aggregates)

The profiling particle camera ROSINA is a highly flexible and modular system that consists of a measurement unit and a control unit. The measurement unit contains the optical system (camera, lenses and light sources), computing unit, standalone CTD, battery and telemetry. The optical system consists of a 24 MPixel camera and macro-lens, which allows to image particles with either reflected light or as shadow images. The size-range of captured particles is between 20 µm and 5 cm. Since the system is equipped with telemetry, the operator is able to observe the measurement and make changes via the control unit during deployment. The control unit consists of the telemetry, which provides the communication interface and power for the measurement unit, and an operator workstation.

Jelly Camera (JellyCam)

The JellyCam consisted of an industrial camera with backend electronics for timing, image acquisition and storage of data. The camera is equipped with variable focal length lens, which can be adjusted from the ship while the camera is deployed. Custom made light-sources were encapsulated with resin and triggered via the electronics. The system was controlled online by the operator via the ROSINA telemetry unit. With that configuration the operator can change various parameters, including exposure time, flash trigger, gain, zoom, focus, and lights. The captured images were saved on the deployed system but a screen-shot was monitored online in the winch control room during the deployments.

OceanSeven 310 CTD (Idronaut S.r.l.)

The ROSINA platform was equipped with an OceanSeven 310 CTD that measured pressure, temperature, conductivity, oxygen, turbidity, and chlorophyll a (Chla). The system was deployed in an unattended with a sampling rate of 2 Hz.

Under-Ice Sediment Traps

We deployed two sediment trap arrays in parallel under the ice at each of the nine ice stations (Fig. 4.9). One trap array was equipped with viscous gels at each collection depth. The gels preserved the size and structure of the settling aggregates, allowing to quantify the export of different particles types under the sea ice. The additional sediment trap array was used to collect biogeochemical samples, this array had a larger collection area, in order to collect enough material for flux determinations of HPLC measurements of pigments, particulate organic carbon and nitrogen, particulate inorganic carbon, particulate organic phosphorus, and biogenic silica. We collected particle flux from four different depths below the ice: 5 m, 20 m, 40 m, and 90 m. After recovery of the under-ice traps, the samples were split into subsamples and filtered for biogeochemical parameters on board. The particles collected in the gel traps were photographed with a digital camera on board and frozen for further detailed investigations in the home laboratory. The image analyses of the gel traps will be used to determine the composition, abundance and size distribution of the sinking particles.

Fig. 4.9: Deployment of under-ice sediment traps. The traps depicted here have one collection tube per depth for biogeochemical fluxes and one trap tube equipped with a gel trap, which preserved the size and structure of individual settling aggregates.

Under Ice Cameras

At ICE 5, ICE 6, ICE 7, ICE 8, and ICE 9 we deployed under ice cameras for time-lapse recordings. The ice cameras were Raspberry Pi cameras that were deployed in glass pressure houses which had integrated light. We captured two images every two seconds and aimed to have the capture sequence throughout 24 hours. This was at times shorter due to logistical or technical issues.

Marine Snow Catcher

A large volume water sampler, the Marine Snow Catcher (MSC), was used to collect *in situ* formed marine snow and other particles. The MSC consists of a 100 L cylindrical water sampler with a particle collection tray at the bottom and was deployed to a target depth using the ship's winch system. Once at the target depth, a messenger weight and a release system were used to close the MSC. The closed MSC was placed on deck for a few hours to allow the collected particles to sink to the collection tray. After gently draining the water from the 100 L cylinder, the collection tray that contained the settling particles was removed and brought to the laboratory where the size, type, composition, settling velocity, microbial respiration, and carbon content was measured as a function of size for each collected aggregate type.

The size-specific settling velocities and microbial respiration of each of the collected aggregates was measured on board in a vertical flow chamber at *in situ* temperatures. Individual aggregates were placed in the flow chamber, whereby the upward flow was increased until the aggregate remained suspended. The sinking velocity of each aggregate was calculated from the flow rate divided by the cross-sectional area of the flow chamber. Microbial respiration was measured using oxygen microsensors to determine the oxygen gradients through the aggregate-water interface.

Bio-Optical Platform (BOP)

We deployed the BioOptical Platform (BOP) as part of the Central Arctic mooring array, CAO2, that we deployed near station ICE 5 on 31 August 2023 (see Chapter 3 under Mooring deployments). The BOP system measures aggregate dynamics at high temporal resolution

throughout a whole year (Fig. 4.10). BOP uses an *in situ* camera system to determine daily size-distribution, abundance, and size-specific sinking velocities of settling particles at one particular depth throughout one year (on the CAO2 mooring, BOP was deployed at 870 m depth). Settling velocities are measured in a settling cylinder to which we have attached a perpendicular camera system that records image sequences daily. At the bottom of the settling cylinder, two rotation tables are mounted and contain a total of 40 collection cups that are equipped with a viscous gel to preserve the aggregate size and structure. By rotating each cup under the settling column for a pre-determined collection period, we are able to determine the seasonal composition of the individual aggregate types and relate this to their size-specific settling velocities.

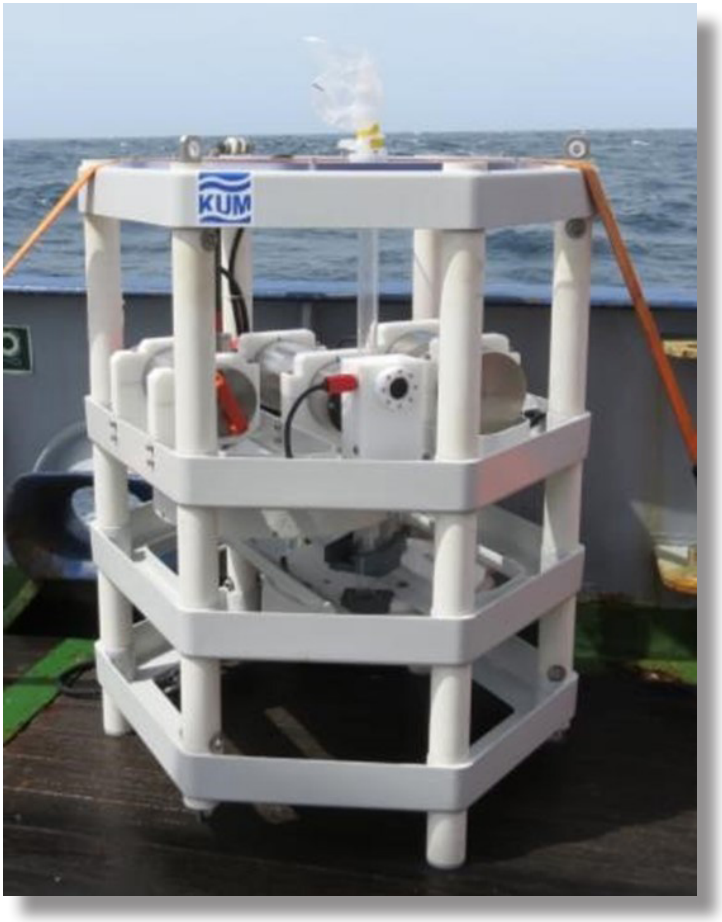

Fig. 4.10 The Bio-Optical Platform was developed by the SeaPump group at AWI and MARUM and measures size-specific settling velocities of organic aggregates two times daily during a one-year deployment. Additionally, it collects intact and individual aggregates in 40 gel traps, which each is open between three and seven days.

Long-term sediment traps

We deployed two sediment traps on long-term moorings to determine the sedimentation of particulate organic and inorganic matter throughout one year in the central Arctic. The sediment traps were KUM K/MT 234 traps that were deployed at 214 m and 3,795 m depth on the mooring CAO2 (see Chapter 3) near the ICE 5 ice station. The sediment traps have a

collection area of 0.5 m^2 and are equipped with 20 collection cups that were timed to capture the seasonal differences in particulate sedimentation and carbon flux.

Preliminary (expected) results

The majority of samples obtained during this cruise were frozen and stored until later processing and analysis in the home lab, thus few preliminary results are available yet.

We expect to observe a strong impact of ice-regimes on the pelagic and ice-associated plankton communities, which will directly influence the efficiency and magnitude of carbon export to deeper water depths. Furthermore, release of cryominerals will ballast organic aggregates and potentially enable them to cross the salinity gradients at the base of the meltwater layer. This will result in sporadic export events, where a large fraction of the organic matter that was retained in the meltwater layer is exported to the deep sea and seafloor. We expect this mechanism to be a driving factor for the biological carbon pump in the central Arctic Ocean. During periods with little to low ballasting from cryo-minerals, we expect the meltwater-layer to be a region of high biological activity and efficient grazing on organic aggregates. The aggregates are porous and will be retained at the salinity gradient, allowing extended time for microbial degradation and zooplankton grazing on the aggregates. This means that strongly stratified regions below Arctic sea ice are characterized by retention and only little export takes place without ballasting from cryo-minerals or production of compact and dense zooplankton fecal pellets. These points will directly translate to patterns among microbial communities, which are expected to show distinct taxonomic and metabolic signatures during high-ice conditions. Furthermore, we expect an enriched potential for microbial chemotaxis and carbon cycling in ephemeral, productive habitats like melt ponds.

Phytoplankton community composition

As expected for a cruise during late Arctic summer, the phytoplankton abundance was very low overall and largely dominated by mixotrophic groups. Preliminary on-board microscopy of handnet samples showed that apart from ice station 1, which was diatom-dominated, all stations with loose sea-ice coverage and strong melting (stations 2 to 4, as well as 8), were characterised by non-existent to very low diatom-abundance typical for a heterotrophic post-bloom community (Fig. 4.11 and Tab. 4.4 for species list). The community was instead composed of diverse ciliate and dinoflagellate populations as well as silicoflagellates. As the ship moved into areas with dense ice cover and more recent lead formation the phytoplankton community shifted towards diatom dominance. The diatoms were able to capitalize the available nutrients and the recently increased light intensity thus outcompeting the heterotrophic grazer community. Diatoms were present in high biodiversity albeit low overall abundances (station 5). Ice stations 6, 7 and 9 were dominated mostly by different species of *Chaetoceros*.

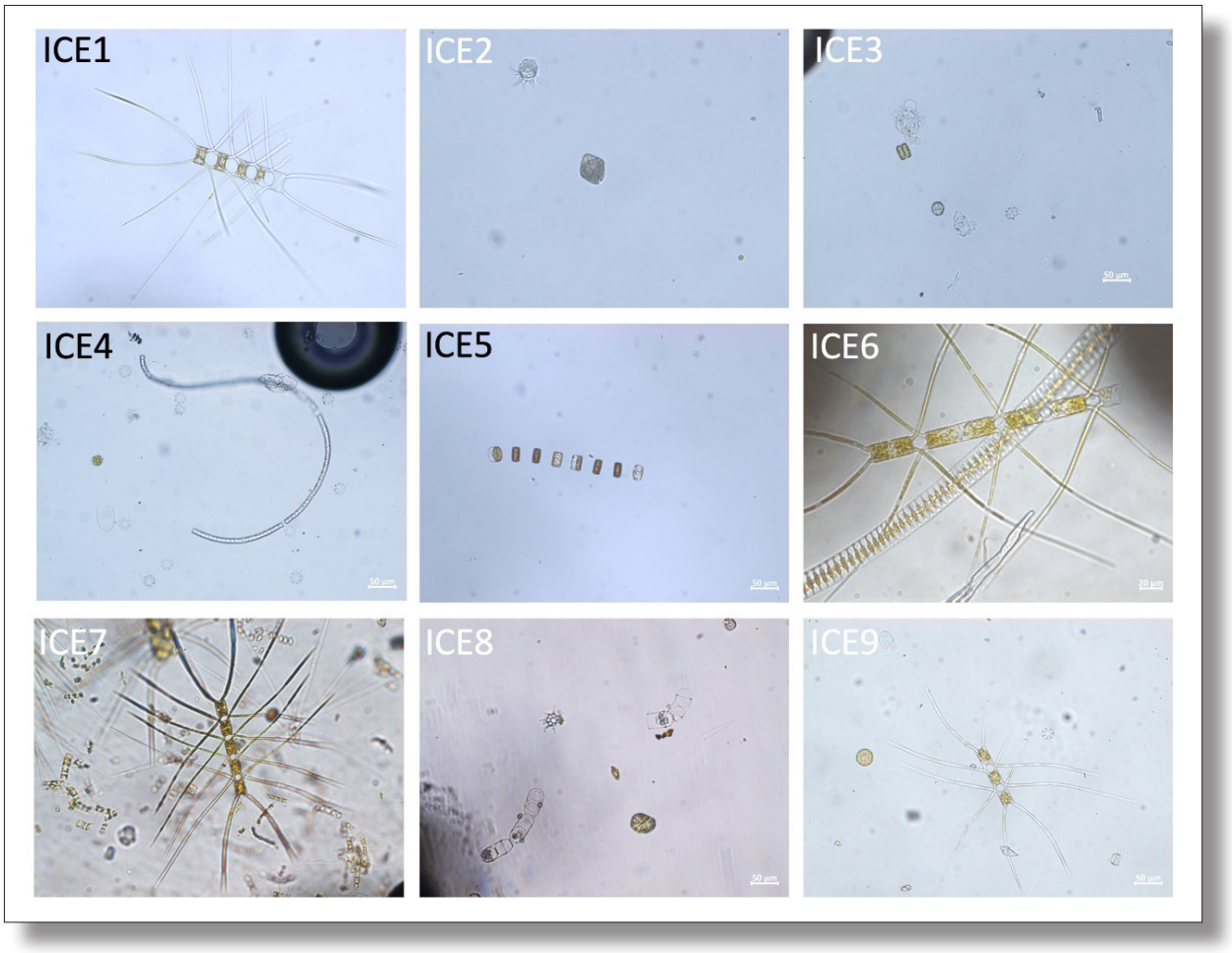

Fig. 4.11: Representative images of handnet samples taken at each ice station (ICE 1-9).

In addition to the handnet samples, we used microscopy to assess aggregate community composition (Fig. 4.12). Contrasting the cruise in 2012 only few aggregates were found at each station (except station 1 and 3). While aggregates of *Melosira arctica* were found at each ice station in 2012, we only found *Melosira* aggregates at ice stations 4 and 5. At ice station 1, 2 and 3 the aggregates consisted of mostly dead pennate diatoms as they are commonly found within the sea ice (such as *Nitzschia sp., Pseudonitzschia sp., Cylindrotheca sp.,* and *Navicula sp.*). Those sea-ice algae are characterised by high production of transparent exopolymers (TEP), which form a mucus layer that is used by the cells to move around the brine channels. Aggregate formation of sea-ice algae has been previously described as an effect of rapid sea ice melting thus ejecting the algae from the sea-ice and resulting in aggregate formation underneath the sea-ice due to the stickiness of the TEP (Fernández-Méndez et al. 2014). As this mucus is positively buoyant the aggregates remain underneath the sea-ice accumulating in hollows underneath the ice floe.

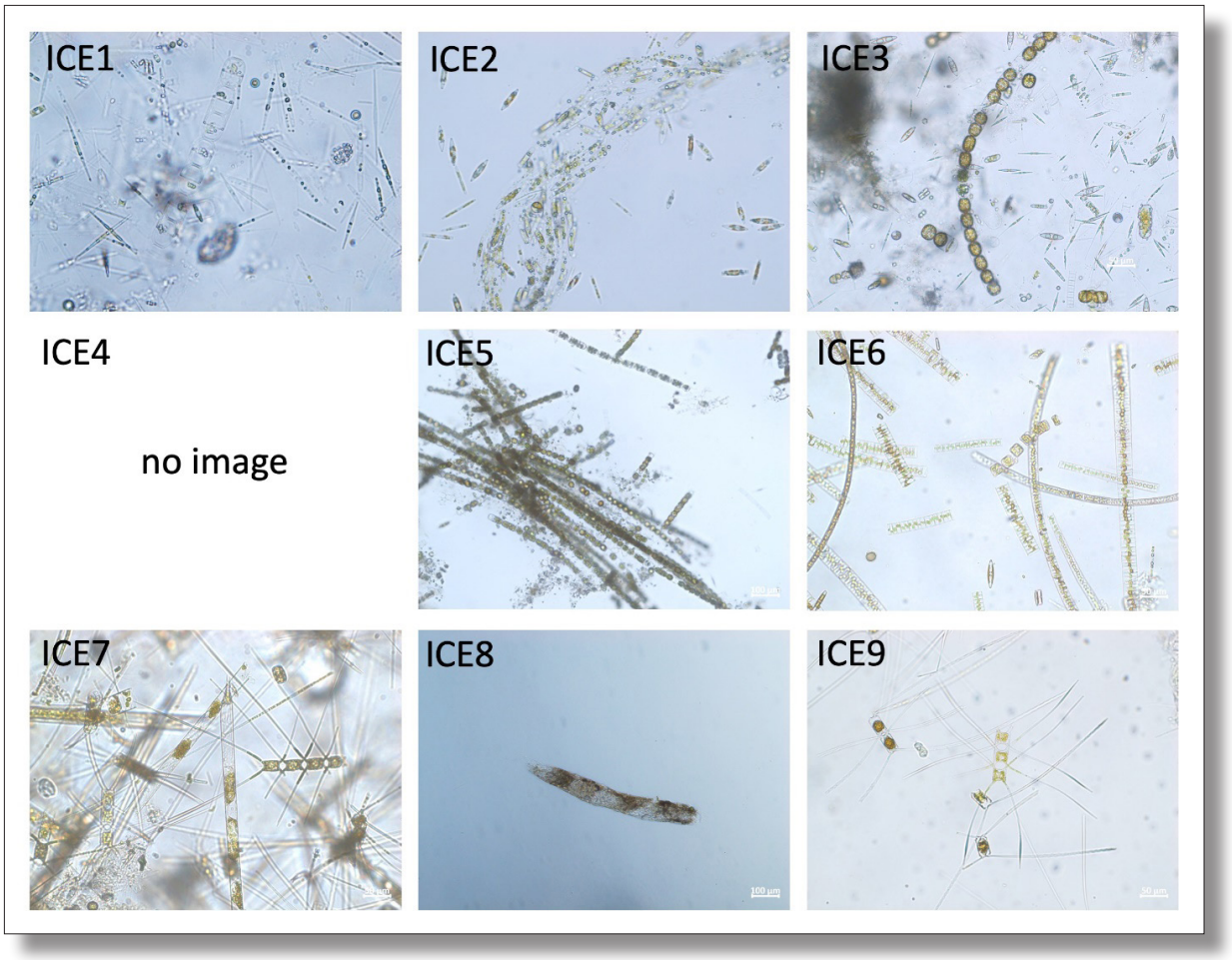

Fig. 4.12: Representative images of ROV net samples / aggregates from the ROV hole sampled at each ice station (ICE 1-9)

The brine channels within the bottom part of the sea-ice are generally inhabited by small, pennate diatoms. Microscopy analysis of the ice cores showed a consistent community composition across all ice stations consisting of *Navicula sp*. and *Nitzschia frigida*. Unexpectedly cells of equal quantities were found in the bottom and the top sections of the ice cores. Unusual for the season we only found open melt ponds at the first stations. At subsequent stations the melt ponds were frozen over and eventually on the last stations (stations 8 and 9) covered additionally by a thick snow cover. As such ice-cores at most stations (except stations 1, 8 and 9) contained layers of refrozen slushy melt ponds. As the ice is melting and melt ponds are developing diatoms are known to migrate upwards through the brine channels into the melt ponds where they grow rapidly due to the high light availability (Fernández-Méndez et al. 2014). Although we did not observe distinct aggregates within the meltponds filters were stained (although greyish not brown, as is common for abundant primary producers) even with low volumes indicating high biomass. As such the sea-ice algae were likely more equally distributed across the ice core than usual due to the loose structure of the ice resulting from previous intense melting.

Tab. 4.4: Overview of dominant phytoplankton group, overall abundances and species composition at each ice station as obtained from plankton net hauls, aggregates from the ROV hole and ice cores.

Station	Sample Origin	Dominant group and abundance	Community composition
1	Handnet	diatoms, high abundance	many different *Chaetoceros, Thalassiosira, Rhizosolenia*
2	Handnet	mixotrophs/heterotrophs, low abundance	Dinoflagellates, Silicoflagellates, Ciliates, no Diatoms
3	Handnet	mixotrophs/heterotrophs, low abundance	Dinoflagellates (Dinophysis, Protoperidinium), Silicoflagellates, Ciliates, almost no diatoms (few T*halassiosira, Navicula* shells)
4	Handnet	mixed, low abundance	Dinoflagellates, Silicoflagellates, Ciliates, div. Diatoms (*Thalassiosira, Nitzschia frigida, Fragilariopsis, Melosira* shells)
5	Handnet	diatoms, low abundance	low abundance, but diverse diatom community (*Nitzschia frigida, Thalassiosira, Fragilariopsis, Chaetoceros*), silicoflagellates
6	Handnet	diatoms	Diatoms (many different *Fragilariopsis*, different Chaetoceros, Nitzschia, *Thalassiosira, Pseudonitzschia, Navicula, Cylindrotheka*), Silicoflagellates, Dinoflagellates, Ciliates
7	Handnet	diatoms, high abundance	Diatoms (many different *Chaetoceros, Thalassiosira, Rhizosolenia*)
8	Handnet	mixed, low abundance	Dinoflagellates, Ciliates, Silicoflagellates, Diatoms (*Thalassiosira, Melosira* shells)
9	Handnet	diatoms	Diatoms (different *Chaetoceros, Thalassiosira*), Dinoflagellates, Silicoflagellates, Ciliates
1	ROV net / Aggregates from ROV hole	diatoms	empty diatoms (*Melosira, Nitzschia, Fragilariopsis*), Ciliates, Dinoflagellates
2	ROV net / Aggregates from ROV hole	diatoms	*Navicula, Nitzschia, Fragilariopsis*
3	ROV net / Aggregates from ROV hole	diatoms	*Melosira, Navicula, Cylindrotheka, Nitzschia, Fragilariopsis*

Station	Sample Origin	Dominant group and abundance	Community composition
4	ROV net / Aggregates from ROV hole	diatoms (Melosira)	Melosira
5	ROV net / Aggregates from ROV hole	diatoms (Melosira)	Melosira, Nitzschia, Navicula, Cylindrotheka, Fragilariopsis
6	ROV net / Aggregates from ROV hole	diatoms (Fragilariopsis)	many different Fragilariopsis, Thalassiosira, Navicula, Nitzschia, Melosira
7	ROV net / Aggregates from ROV hole	diatoms (Chaetoceros)	many different Chaetoceros, Rhizosolenia, Thalassiosira, Navicula, Fragilariopsis
8	ROV net / Aggregates from ROV hole	no phytoplankton	only fecal pellets
9	ROV net/ Aggregates from ROV hole	diatoms (Chaetoceros)	Chaetoceros
1-9	Ice cores	diatoms	Nitzschia frigida, Navicula

Net primary productivity

Photosynthesis vs. irradiance (PI) curves are preliminary as calculations are based on assumed DIC values for all sample types (Fig. 4.13). Overall NPP ranged between 2 and 25 µmol C L^{-1} d^{-1}. Generally, NPP measurements matched the abundance estimates as obtained from hand net microscopy. Thus stations 1 and 8 were the most productive. At station 7 there was a strong discrepancy between NPP measurements and abundance, as NPP was very low whereas the handnet sample identified station 7 as one of the most productive due to high abundances of *Chaetoceros sp*. NPP was declining across the cruise track with highest measurements obtained at stations 1 and 2 (Fig. 4.14). Except for ice station 6, NPP was lowest in the bottom parts of the ice cores across all stations. Where available NPP in melt ponds was within the same range or higher than the NPP measured for the ice core top samples, supporting the hypothesis of diatoms migrating from the bottom of the sea-ice into the melt ponds, which refroze and were then being sampled as part of the ice cores. Within the water column samples NPP declined with depth across all stations (except stations 1 and 3, when NPP was highest at 2 m), with highest measurements in the under-ice water and lowest in the Chl max sample (15-20 m), indicating that light availability was more important than nutrients in determining differences in NPP.

Almost all samples showed photoinhibition above light intensities of 150 µE. Intensity of photoinhibition varied according to light intensity, generally increasing with depth. In addition, ice samples from stations 8 and 9, which had strong snow cover, showed strong photoinhibition for light intensities > 50 µE.

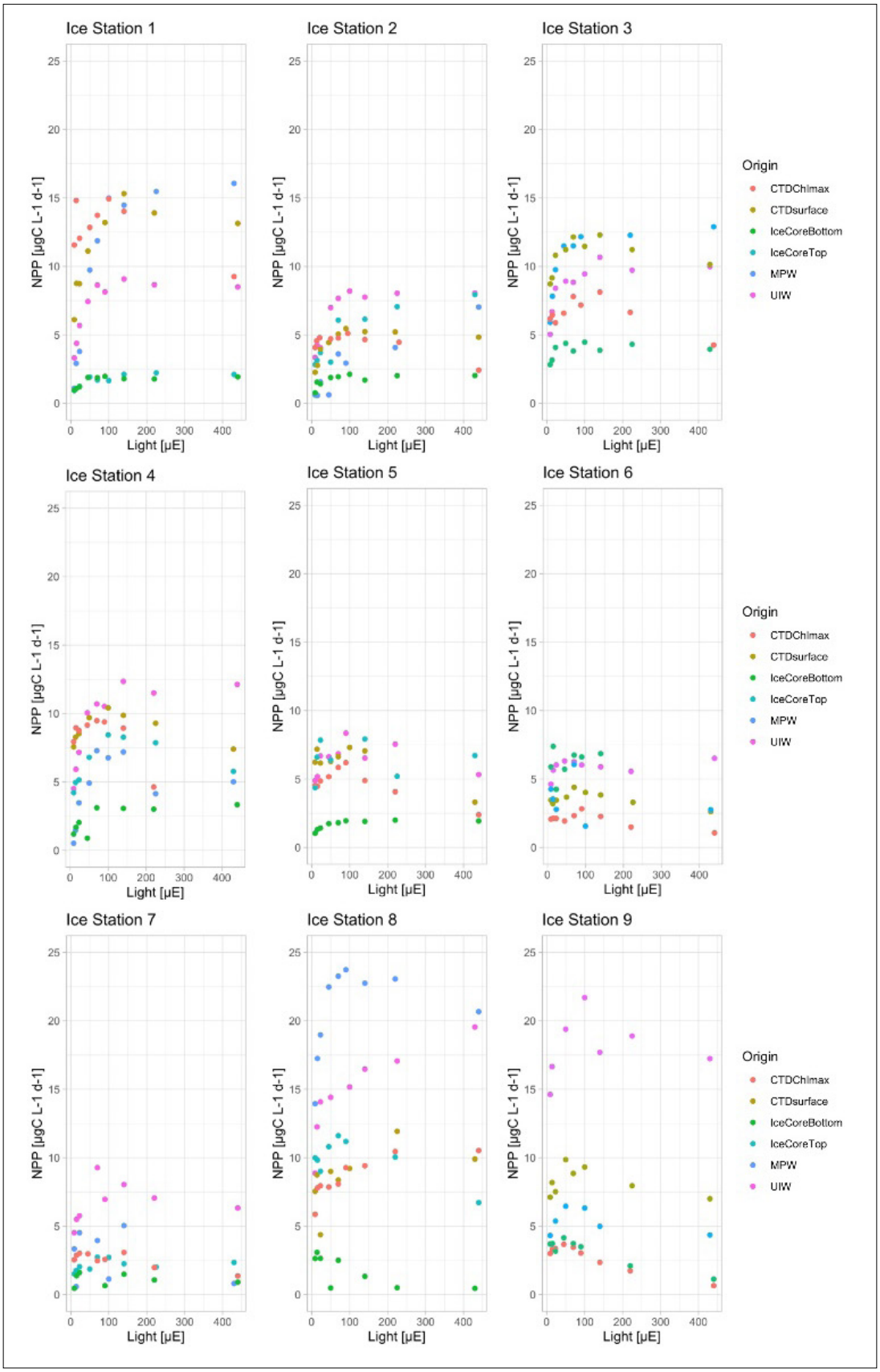

Fig. 4.13: Preliminary photosynthesis vs. irradiance curves for all ice stations coloured by sample type.

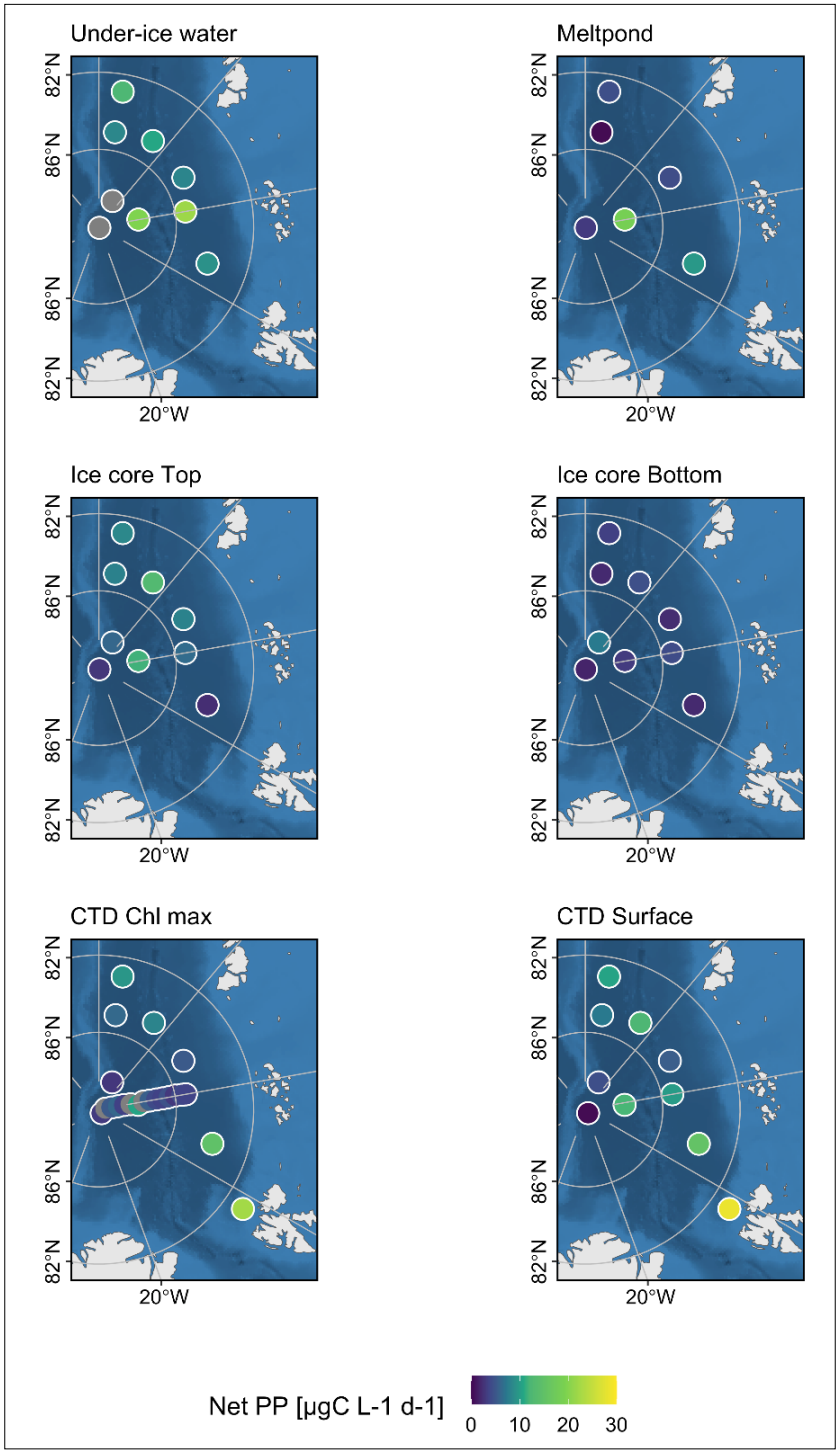

Fig. 4.14: Figures of estimated Pmax (maximum measured NPP value of each PI curve) for each sample type and ice station. Grey=no data.

Bacterial communities

Most samples are frozen and need detailed procedures in the home lab (DNA extraction and sequencing), which cannot be done on board. Isolation of bacterial strains from ISCA deployments indicated that bacteria were swimming into the wells, hence being chemotactic (Fig. 4.15).

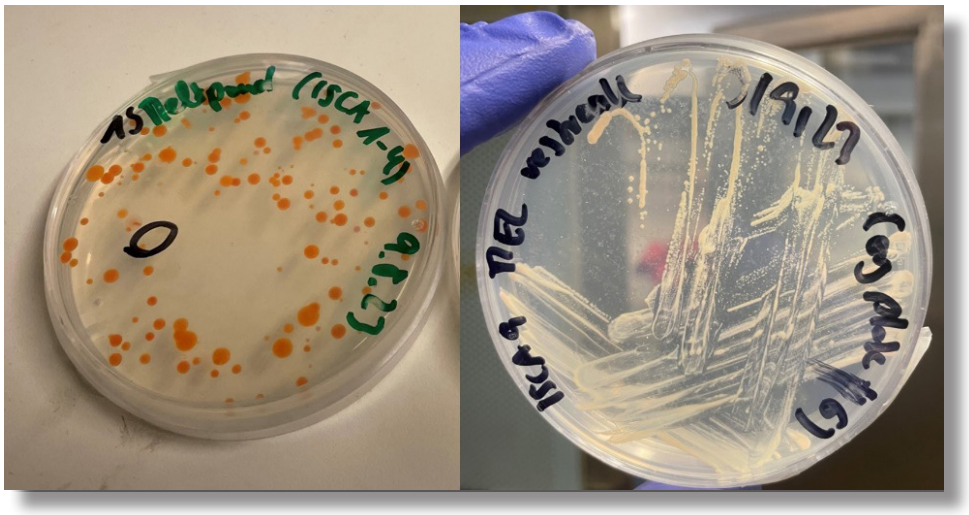

Fig. 4.15: Bacteria isolated from melt pond water (left) and Melosira aggregates (right).

Mesozooplankton

Table 4.5 gives a full list of Multinet and Bongo net deployments and Table 4.6 gives a list of samples taken from the nets for analysis at the University of Exeter. Initial discrimination of *Calanus glacialis and finmarchicus* was done only on relative size. The smallest C5s and females were assumed to be *C. finmarchicus*. *C. hyperboreus* stage C5s were found at all depths at all stations. *C. hyperboreus* females were only found in the top 200 m at ice stations 1 and 2, but at all depths at the remaining stations. *C. glacialis* and *C. finmarchicus* were generally only found in the top 500 m, except for ice station 4 when *C. glacialis* C5s and females and *C. finmarchicus* females were found at 1,500 m. *C. glacialis* C5s were also found deeper than 500 m at ice stations 1 and 2. *C. finmarchicus* C5s were only found at ice station 9. Additionally, a list of ROV trawls under-ice and at 10 meters depth can be found in Table 4.7 with some of the most dominant mesozooplankton species found and phytoplankton species captured.

Tab. 4.5: Multinet (MN) and Bongo net (BN) deployments.

Date	Ice stn	Station	Sampler	Lat	Long	Net depth [m]	Time start [UTC]	Time end [UTC]	Analysis
09/08/23	IS1	PS138_12-1	MN1	84.02	31.52	1500	02:54	04:25	Biomass
09/08/23	IS1	PS138_13-1	MN2	84.02	31.52	1500	04:40	06:20	Biochemistry
10/08/23	IS1	PS138_20-1	BN1	83.87	33.20	50	17:07	17:17	Biochemistry
15/08/23	IS2	PS138_32-1	MN3	84.95	80.13	1500	08:22	10:06	Biomass
17/08/23	IS2	PS138_41-1	MN4	84.94	80.15	1500	07:21	09:02	Biochemistry
17/08/23	IS2	PS138_46-1	BN2	84.96	80.04	50	11:19	11:30	Biochemistry
20/08/23	IS3	PS138_55-1	MN5	84.70	107.65	1500	01:56	03:34	Biomass
20/08/23	IS3	PS138_56-1	MN6	84.70	107.63	1500	03:43	05:21	Biochemistry
21/08/23	IS3	PS138_65-1	BN3	84.69	107.58	50	17:35	17:41	Biochemistry

Date	Ice stn	Station	Sampler	Lat	Long	Net depth [m]	Time start [UTC]	Time end [UTC]	Analysis
25/08/23	IS4	PS138_81-1	MN7	82.97	130.21	1500	01:38	03:13	Biomass
25/08/23	IS4	PS138_82-1	MN8	82.97	130.14	1500	03:21	04:58	Biochemistry
25/08/23	IS4	PS138_89-1	BN4	83.01	129.86	1500	18:01	18:07	Biochemistry
28/08/23	IS5	PS138_103-1	MN9	85.04	130.34	1500	20:18	22:08	Biomass
28/08/23	IS5	PS138_104-1	MN10	85.04	130.40	1500	22:15	23:56	Biochemistry
29/08/23	IS5	PS138_114-1	BN5	85.04	129.97	50	19:52	19:59	Biochemistry
03/09/23	IS6	PS138_133-1	MN11	88.49	112.76	1500	21:47	23:32	Biomass
04/09/23	IS6	PS138_138-1	MN12	88.44	114.41	1500	15:56	17:29	Biochemistry
04/09/23	IS6	PS138_144-1	BN6	88.43	113.94	50	19:58	20:06	Biochemistry
09/09/23	IS7	PS138_158-1	MN13	89.94	41.49	1500	00:51	02:32	Biomass
09/09/23	IS7	PS138_159-1	MN14	89.94	35.28	1500	02:37	04:20	Biochemistry
11/09/23	IS7	PS138_167-1	BN7	89.76	-2.27	50	23:18	23:26	Biochemistry
14/09/23	IS8	PS138_183-1	MN15	87.90	58.19	1500	03:31	05:06	Biomass
14/09/23	IS8	PS138_184-1	MN16	87.91	58.14	1500	05:12	06:57	Biochemistry
14/09/23	IS8	PS138_191-1	BN8	87.96	56.79	50	14:39	14:48	Biochemistry
19/09/23	IS9	PS138_214-1	MN17	85.46	59.99	1500	13:33	15:17	Biomass
19/09/23	IS9	PS138_215-1	MN18	85.45	60.01	50	15:24	17:00	Biochemistry
20/09/23	1S9	PS138_221-1	BN9	85.43	59.98	50	08:01	08:06	Biochemistry

Tab. 4.6: *Calanus* spp. samples (C. hyper = *C. hyperboreus*, C .glac = *C. glacialis*, C. fin = *C. finmarchicus*, C5 = copepodite stage 5, F = adult female) taken from the Multinet (MN) and Bongo net (BN) deployments for analysis at the University of Exeter. LM = Lipid/metabolic rate, CN = Carbon and Nitrogen biomass, M = Molecular confirmation of species.

Date	Ice stn	Station	Sampler	Net	Net depth [m]	C. hyper		C. glac		C. fin		Cal spp.
						C5	F	C5	F	C5	F	Mixed
09/08/23	IS1	PS138_13-1	MN2	1	1500	LM		LM				
09/08/23	IS1	PS138_13-1	MN2	2	1000	LM		LM				
09/08/23	IS1	PS138_13-1	MN2	3	500	LM		LM				
09/08/23	IS1	PS138_13-1	MN2	4	200		LM	LM CN	LM		LM	M
09/08/23	IS1	PS138_13-1	MN2	5	50	LM	LM	LM CN	LM		LM	M
10/08/23	IS1	PS138_20-1	BN1	1	50	LM	LM	LM CN	LM		LM	M
17/08/23	IS2	PS138_41-1	MN4	5	50	LM	LM	LM CN	LM		LM	M
17/08/23	IS2	PS138_41-1	MN4	4	200		LM CN	LM CN	LM CN		LM CN	M
17/08/23	IS2	PS138_41-1	MN4	3	500			LM				
17/08/23	IS2	PS138_41-1	MN4	2	1000	LM		LM				
17/08/23	IS2	PS138_41-1	MN4	1	1500	LM						
17/08/23	IS2	PS138_46-1	BN2	1	50	LM	LM	LM				
20/08/23	IS3	PS138_56-1	MN6	5	50	LM	LM	LM	LM CN			
20/08/23	IS3	PS138_56-1	MN6	4	200	LM		LM	LM CN			
20/08/23	IS3	PS138_56-1	MN6	3	500	LM	LM	LM	LM			
20/08/23	IS3	PS138_56-1	MN6	2	1000	LM	LM					M
20/08/23	IS3	PS138_56-1	MN6	1	1500	LM	LM					
21/08/23	IS3	PS138_65-1	BN3	1	50	LM	LM	LM	LM			
25/08/23	IS4	PS138_82-1	MN8	5	50	LM	LM	LM	LM CN		LMM	
25/08/23	IS4	PS138_82-1	MN8	4	200	LM		LM	LM CN		LMM	
25/08/23	IS4	PS138_82_1	MN8	1	1500	LM	LM					
25/08/23	IS4	PS138_89_1	BN4	1	1500	LM	LM	LM	LM		LMM	
28/08/23	IS5	PS138_104-1	MN10	5	50	LM		LM	LM CN			
28/08/23	IS5	PS138_104-1	MN10	4	200	LM	LM	LM	LM CN		LMM	
28/08/23	IS5	PS138_104-1	MN10	3	500	LM	LM	LM	LM		LMM	
28/08/23	IS5	PS138_104-1	MN10	2	1000	LM	LM					
28/08/23	IS5	PS138_104-1	MN10	1	1500	LM	LM					
29/08/23	IS5	PS138_114-1	BN5	1	50	LM		LM	LM		LM	M
04/09/23	IS6	PS138_138-1	MN12	5	50	LM		LM CN	LM CN		CN	

Date	Ice stn	Station	Sampler	Net	Net depth [m]	C. hyper		C. glac		C. fin		Cal spp.
						C5	F	C5	F	C5	F	Mixed
04/09/23	IS6	PS138_138-1	MN12	4	200	LM	LM		LM CN			M
04/09/23	IS6	PS138_138-1	MN12	3	500		LM					
04/09/23	IS6	PS138_138-1	MN12	2	1000	LM	LM					
04/09/23	IS6	PS138_138-1	MN12	1	1500	LM CN	LM					
04/09/23	IS6	PS138_144-1	BN6	1	50				LM			
09/09/23	IS7	PS138_159-1	MN14	1	1500	LM CN	LM					
09/09/23	IS7	PS138_159-1	MN14	2	1000	LM CN	LM					
09/09/23	IS7	PS138_159-1	MN14	3	500	LM CN	LM					
09/09/23	IS7	PS138_159-1	MN14	4	200	LM	LM	LM	LM CN		LMM	
09/09/23	IS7	PS138_159-1	MN14	5	50	LM		LM	LM CN			
11/09/23	IS7	PS138_167-1	BN7	1	50	LM	LM	LM	LMCN			M
14/09/23	IS8	PS138_184-1	MN16	5	50	LM		LM	LM CN			
14/09/23	IS8	PS138_184-1	MN16	4	200	LM	LM		LMCN			
14/09/23	IS8	PS138_184-1	MN16	3	500	LM	LM					
14/09/23	IS8	PS138_184-1	MN16	2	1000	LM CN	LM					
14/09/23	IS8	PS138_184-1	MN16	1	1500	LM CN						
14/09/23	IS8	PS138_191-1	BN8	1	50	LM CN	LM	LM	LM			M
19/09/23	IS9	PS138_215-1	MN18	5	50	LM			LM	LM CN	LM	
19/09/23	IS9	PS138_215_1	MN18	4	200	LM	LM	CN	LM CN	LM CN	LM	
19/09/23	IS9	PS138_215-1	MN18	3	500	LM	LM			LM	LM	
19/09/23	IS9	PS138_215-1	MN18	2	1000	LM	LM					
19/09/23	IS9	PS138_215-1	MN18	1	1500	LM						
20/09/23	IS9	PS138_221-1	BN9	1	50	LM	LM		LM	LM CN	LM	

Tab. 4.7: Preliminary observations on mesozooplankton and under-ice algae in the ROV net deployed directly under the ice and at 10 meters underneath the ice.

Event	Date	Under-ice mesozooplankton	Under-ice algae	Mesozooplankton at 10 meters
PS138_031_ROV_002	16-08-23	*Apherusa glacialis*, *Beroe* sp., *C. glacialis*	*Navicula*, *Nitzschia*, *Fragilariopsis*	-
PS138_052_ROV_002	20-08-23	*A. glacialis*	*Melosira*, *Navicula*, *Cylindrotheka*, *Nitzschia*, *Fragilariopsis*	*C. glacialis*, *C. hyperboreus*, *Thysanoessa* sp.
PS138_075_ROV_001	24-08-23	*A. glacialis*	*Melosira*	*C. hyperboreus*, *C. glacialis* (very high Calanus abundance), *Thysanoessa* sp., *Beroe* sp., *Mertensia ovum*
PS138_101_ROV_001	28-08-23	*A. glacialis*	*Melosira*, *Navicula*, *Cylindrotheka*, *Nitzschia*, *Fragilariopsis*	*C. glacialis*, *C. hyperboreus*
PS138_129_ROV_001	03-09-23	*A. glacialis*	*Fragilariopsis*	*C. hyperboreus*, *Clione limacina*
PS138_152_ROV_002	10-09-23	*A. glacialis*	*Chaetoceros*	*C. hyperboreus*, *C. glacialis*, *Limacina helicina*, *Mertensia ovum*
PS138_178_ROV_001	13-09-23	*A. glacialis*, *Onisimus* sp.	No phytoplankton	*C. glacialis*, *C. hyperboreus*
PS138_213_ROV_002	20-09-23	*A. glacialis*, *Onisimus* sp., *Gammarus wiltzkitzkii*	*Chaetoceros*	*C. hyperboreus*, *C. glacialis*, *Themisto* sp., *Mertensia ovum*

Imaging systems for aggregates and zooplankton

The (Underwater Vision Profiler) UVP (version 5HD, SN204) was set up on the CTD-rosette frame and was recording data at every CTD cast (except the deep CTD cast of ice station #1 due to malfunction). The UVP is an imaging system that captures and counts particles of zooplankton within the size-range between 100 µm and ~5 cm. In total, there were 37 casts, including the test station. The data were semi-processed before the end of the cruise, providing "vignettes" (or crops) of zooplankton images and histograms of particle size distributions. This partial processing provides 5 size classes of particles (Fig. 4.16). However, to have a full resolution distribution and recognition of zooplankton species, the dataset must be uploaded and finally processed by the artificial intelligence algorithms: eco-part (https://ecopart.obs-vlfr.fr/) and eco-taxa (https://ecotaxa.obs-vlfr.fr/) respectively. In general, compared with lower latitude sampling, the profiles indicated very (particulate and zooplankton) poor environments. For instance, in the southern stations, influenced by Atlantic waters (Fig. 4.16A), the UVP

recorded several thousands of images (2,479 for ice station #1) whereas at the North Pole station #7 it only recorded 192 pictures (Fig. 4.16B). This number even dropped to 35 pictures for the shallow cast. Overall, the visual inspection of images mostly showed aggregates, with very rare zooplankton. The vertical distribution of particles was usually concentrated at the very surface within the top 10 m and was rapidly attenuated at depth. The maximum was either situated at the surface or very shallow sub-surface (5-10 m). The concentration of particles did fall to almost zero below the mixed layer (~20 m), indicating very weak meso-pelagic carbon fluxes, and an accumulation of particles in the upper layer formed from fresh sea-ice melt-water. For the ice stations, the distribution of particles was generally dominated by the small or medium size classes, with radius < 500 µm. Interestingly, in some cases such as last ice station #9 (Fig. 4.16C), the concentration of particles increased again in the bathy-pelagic layer (in our case deeper than 3,000 m and until the bottom at ~3,900 m). The data set will need to be further investigated after full processing, and combined with other complementary imaging systems (JellyCam, ROSINA), sediment traps, sinking velocity of aggregates to give a full overview of the vertical carbon fluxes during the expedition ArcWatch-1.

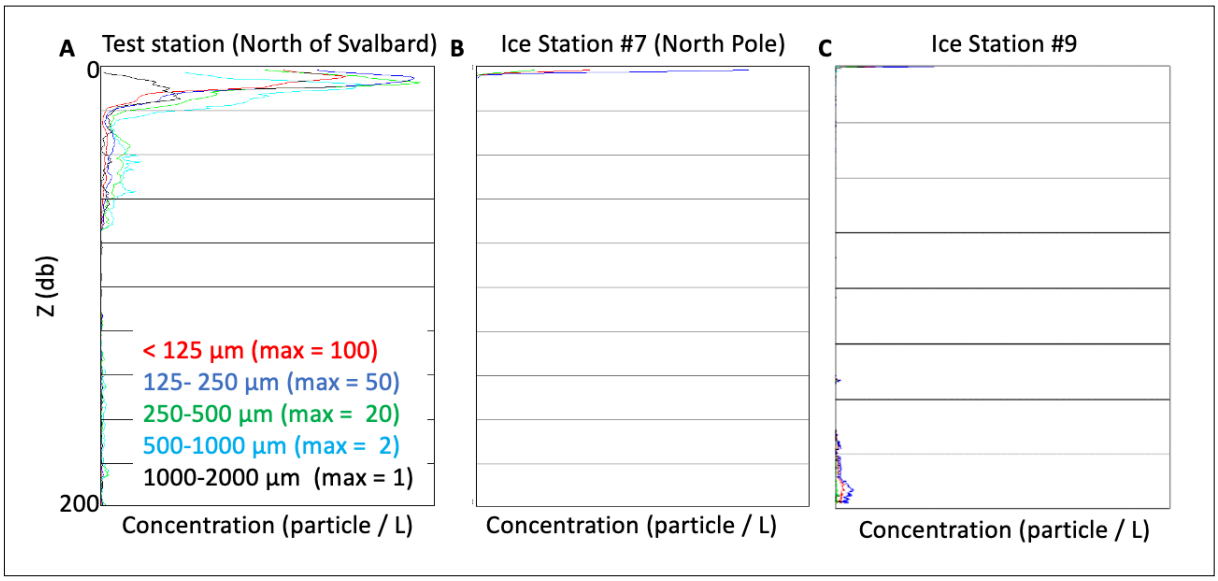

Fig. 4.16: Examples of preliminary particle profiles from the UVP comparing two contrasting stations; the colour lines indicate different particle size classes.

Settling aggregates

The majority of the aggregates that sank out of the upper mixed layer consisted of zooplankton fecal pellets. Most of the stations had very low export flux and the settling particles and aggregates were heavily degraded at 90 m. This suggested that there was intense zooplankton grazing and microbial degradation of the settling particles in the upper 90 m of the water column.

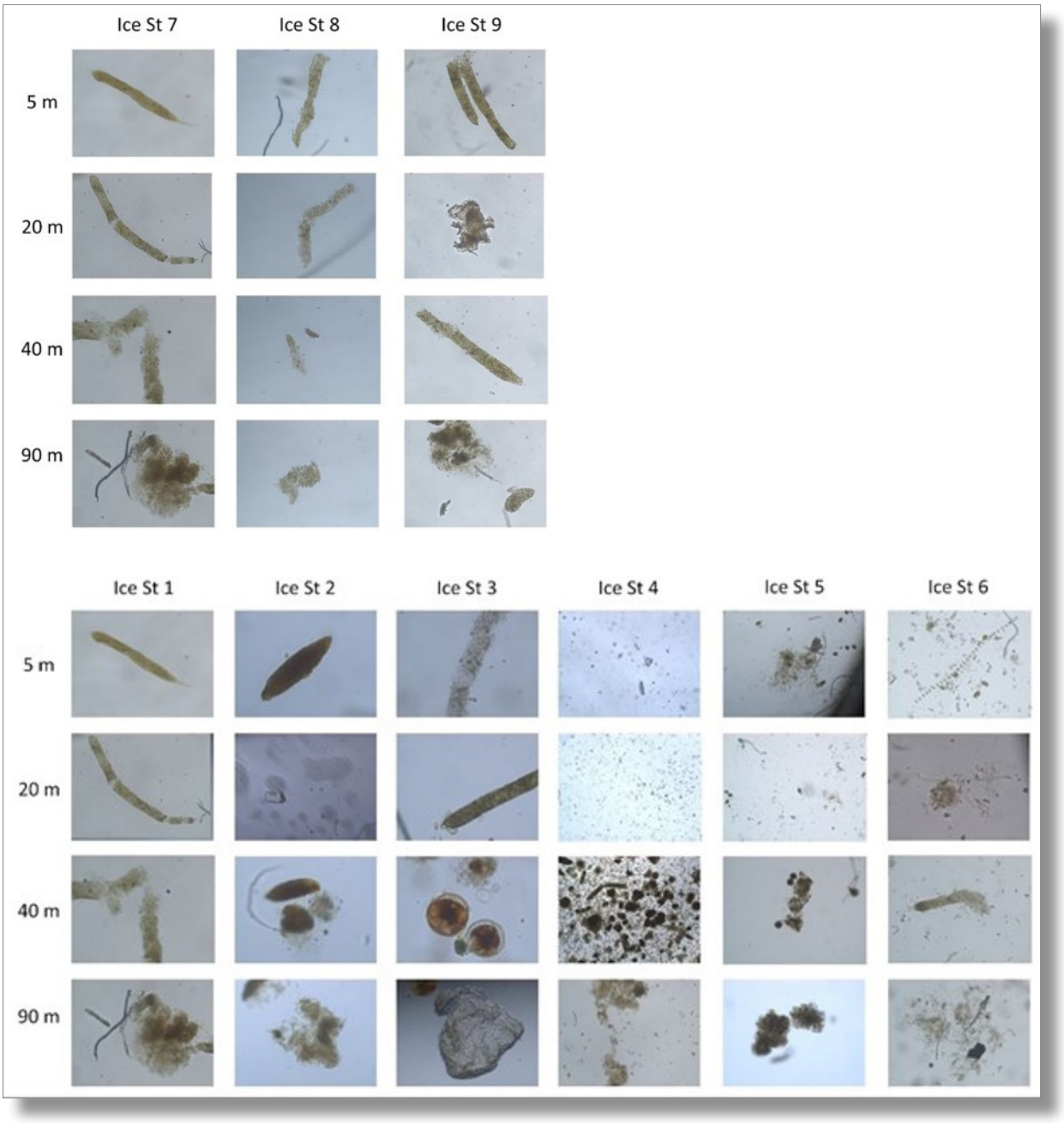

Fig. 4.17: Examples of settling aggregates collected in the under-ice sediment traps for each ice station from 1 to 9 and each collection depth; 5 m, 20 m, 40 m, and 90 m.

The gel traps that were deployed under the ice also preserved cryominerals well and in most of the traps we observed vast amounts of cryominerals, including gypsum (Fig. 4.18). We plan to conduct careful investigations of the settling aggregates to study the ballasting effects from cryominerals at the different ice stations.

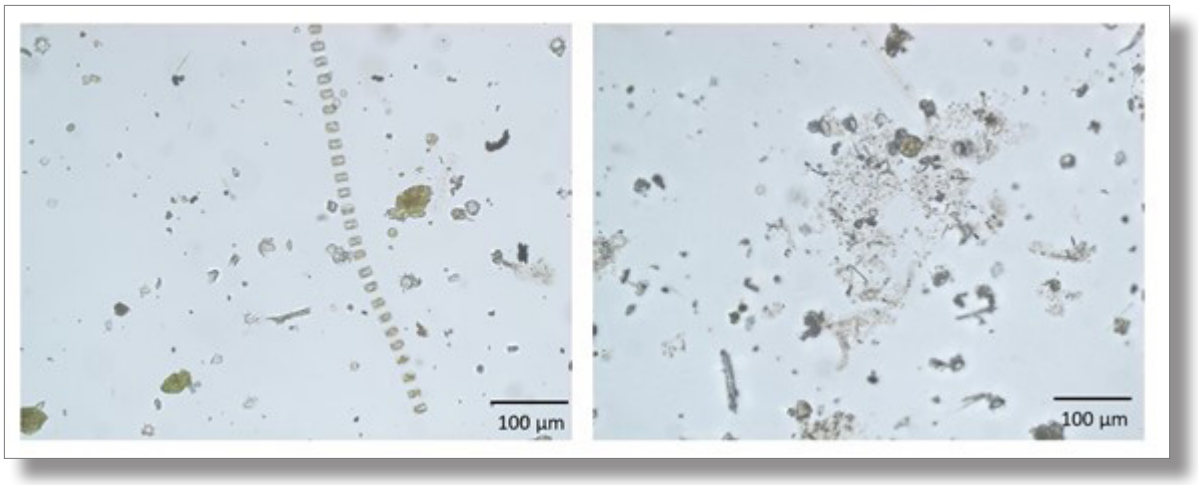

Fig. 4.18: Two example images from the gel traps collected at 5 m below the ice at ice station 6. Several cryominerals with different sizes are observed together with a few diatoms.

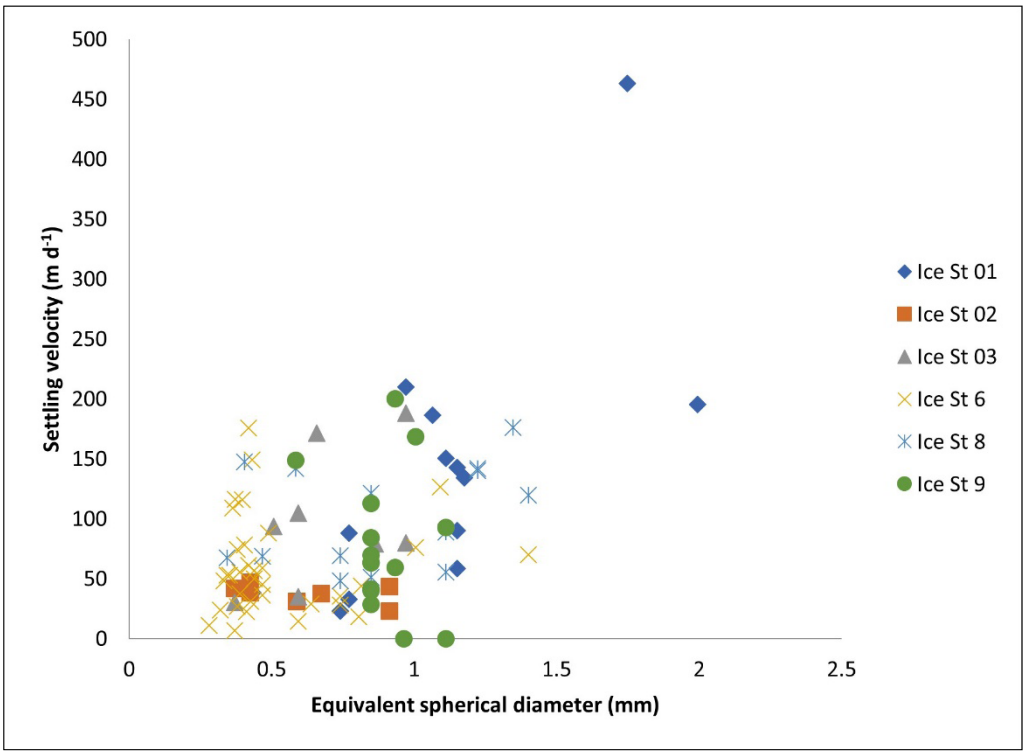

Fig. 4.19: Size-specific settling velocities for individual aggregates collected using the marine snow catcher at the different ice stations.

Data management

Environmental data will be archived, published and disseminated according to international standards by the World Data Center PANGAEA Data Publisher for Earth & Environmental Science (https://www.pangaea.de) within two years after the end of the expedition at the latest.

By default, the CC-BY license will be applied.

Molecular data (DNA and RNA data) will be archived, published and disseminated within one of the repositories of the International Nucleotide Sequence Data Collaboration (INSDC, www.insdc.org) comprising of EMBL-EBI/ENA, GenBank and DDBJ.

Any other data will be submitted to an appropriate long-term archive that provides unique and stable identifiers for the datasets and allows open online access to the data.

This part of the expedition is supported by the Helmholtz Research Programme “Changing Earth – Sustaining our Future” Topic 6, Subtopics 1, 2 and 3.

In all publications based on this expedition, the **Grant No. AWI_PS138_02** or, in case of multidisciplinary work, **AWI_PS138_00** will be quoted and the following publication will be cited:

Alfred-Wegener-Institut Helmholtz-Zentrum für Polar- und Meeresforschung (2017) Polar Research and Supply Vessel POLARSTERN Operated by the Alfred-Wegener-Institute. Journal of large-scale research facilities, 3, A119. http://dx.doi.org/10.17815/jlsrf-3-163.

References

Boetius A, et al. (2013) Export of algal biomass from the melting Arctic sea ice. Science 339:1430–1432. https://doi.org/10.1126/science.1231346

Fernández-Méndez M, Wenzhöfer F, Peeken I, et al (2014) Composition, Buoyancy Regulation and Fate of Ice Algal Aggregates in the Central Arctic Ocean. PLoS ONE 9:e107452. https://doi.org/10.1371/journal.pone.0107452

Henson S, Le Moigne F, Giering S (2019) Drivers of carbon export efficiency in the global ocean. Glob. Biogeochem. Cycles 33:891–903. https://doi.org/10.1029/2018GB006158

Kwok R (2018) Arctic sea ice thickness, volume, and multiyear ice coverage: losses and coupled variability (1958–2018). Environ. Res. Lett. 13:105005. https://doi.org/10.1088/1748-9326/aae3ec

Lambert B et al. (2017) A microfluidics-based in situ chemotaxis assay to study the behaviour of aquatic microbial communities. Nat. Microbiol. 2:1344–1349. https://doi.org/10.1038/s41564-017-0010-9

Leu E, et al. (2015) Arctic spring awakening—steering principles behind the phenology of vernal ice algal blooms. Prog. Oceanogr. 139, 151–170. https://doi.org/10.1016/j.pocean.2015.07.012

Lewis K M, van Dijken G L, Arrigo K R (2020) Changes in phytoplankton concentration now drive increased Arctic Ocean primary production. Science 369:198–202. https://doi.org/10.1126/science.aay8380

Perrette M, Yool A, Quartly G D, Popova E E (2011) Near-ubiquity of ice-edge blooms in the Arctic. Biogeosciences 8:515–524. https://doi.org/10.5194/bg-8-515-2011

Serreze M C, Meier W N (2019) The Arctic’s sea ice cover: trends, variability, predictability, and comparisons to the Antarctic. Ann. N. Y. Acad. Sci. 1436:36–53. https://doi.org/10.1111/nyas.13856

Wassmann P, Reigstad M (2011) Future Arctic Ocean seasonal ice zones and implications for pelagic-benthic coupling. Oceanography 24:220–231. https://doi.org/10.5670/oceanog.2011.74

Wiedmann I, et al. (2020) What feeds the Benthos in the Arctic Basins? Assembling a carbon budget for the deep Arctic Ocean. Front. Mar. Sci. 7:544386. https://doi.org/10.3389/fmars.2020.0022

5. BATHYMETRY, BENTHIC BIOLOGY AND BIOGEOCHEMISTRY

Christina Bienhold[1,2], Jakob Barz[1],
Lilian Böhringer[1], Antje Boetius[1,2], Frederic Bonk[4],
Ulrich Hoge[1], Felix Janssen[1,2],
Katharina Kohlenbach[3], Johannes Maring[1,2],
Axel Nordhausen[2], Malte Pallentin[1],
Autun Purser[1], Frederic Tardeck[5], Carolin Uhlir[4],
Frank Wenzhöfer[1,2,6]
not on board: Angelika Brandt[4], Saskia Brix[4],
Pedro Martinez-Arbizu[4], Andrey Vedenin[4]

[1]DE.AWI
[2]DE.MPIMM
[3]DE.UNI-BREMEN
[4]DE.SENCKENBERG
[5]DE.FIELAX
[6]DK.HADAL

Grant-No. AWI_PS138_01

Outline

Due to the difficult accessibility of the ice-covered Arctic basins, very little is known about the diversity, distribution and function of benthic communities. One of the central questions about the consequences of the shrinking sea-ice cover is to what extent primary production and subsequent export of organic matter to the seafloor will be affected, and how this will influence the structure and functioning of benthic communities in the Arctic. During PS138 we obtained data and samples for the assessment of the diversity of benthic communities across all size classes, i.e. megafauna, macrofauna, meiofauna, and microbes. A key task of this study is the comparison with the benthic biodiversity and foodweb at the same stations in 2012. In addition, our work included the mapping and exploration of largely unknown seafloor structures along the Gakkel and Lomonosov Ridges. Arctic benthic deep-sea communities depend on the sedimentation of particulate organic matter from the sea ice and the water column, which is in turn determined by temporal and spatial variations in sea-ice cover, hydrography, and surface production. Most of the sinking organic matter is recycled in the water column, and the fraction that ultimately reaches the seafloor is either remineralized or retained in the sediment record. The part that escapes remineralization is a key to the long-term storage of carbon in the oceans, facilitated by the biological carbon pump. Benthic oxygen fluxes help to provide a reliable and integrated measurement of the metabolic activity of surface sediments. During PS138, we determined benthic oxygen fluxes *in-situ* as well as *ex-situ* to quantify benthic carbon remineralization efficiency of deep-sea sediments in the central Arctic.

Objectives

Major objectives of our work include:

- High-resolution seafloor observations and the assessment of biodiversity and distribution of benthic megafauna, and epi- and suprabenthic macrofauna communities in the high Arctic
- Comparison of mega- and macrofauna foodweb structure and relation to sea-ice algal deposits

- Quantitative spatial and temporal comparisons of benthic macrofauna, as well as species descriptions based on morphological and genetic methods
- Assessment of temporal changes in the diversity and distribution of meiofauna and microbial communities at the Arctic deep-sea floor, as well as their functions in regions of varying sea-ice cover
- The characterization of the quantity and quality of deposited organic material and comparison to the past decades with stronger ice cover
- The quantification of pelagic export and benthic remineralization of organic carbon to assess links between surface production, benthic activity and burial of carbon.

5.1 Bathymetry

Most of the worlds' ocean topography has to date not been surveyed with echo sounders. Instead, much of the existing chart data, as used in the IBCAO and GEBCO datasets, is derived from satellite altimetry and gravimetric data. One objective of the PS138 mission was therefore to retrieve a full expedition track of multibeam bathymetry data, to contribute to the existing ocean datasets.

Technical introduction

The Teledyne Hydrosweep DS3 system is a hull-mounted multibeam echosounder on board Polarstern based on a sonar frequency between 14 kHz to 16 kHz and can record data from 10 m to more than 11,000 m water depth.

Work at sea

The Hydrosweep was in operation 24 hours per day. System parameters were regularly adjusted to the sea and ice conditions. Beam profile and backscatter data was recorded and visualized with Teledyne PDS. Water column data was not recorded as there were no relevant water column features visible. Vertical sound speed profiles from the CTD or XCTD casts were regularly applied. The acquired data was processed on board using Caris HIPS/SIPS Editor. The data was manually edited, filtered by applying matrix-based median filters and exported to grids and xyz soundings. Resulting grids were produced at different resolutions. These grids were regularly updated as background layers for the real-time mapping tool QGIS which was used for navigation and tracking of underwater instruments. In total, 37,442 km² of data in the Nansen Basin, Amundsen Basin and Gakkel Ridge were recorded during the leg.

Preliminary (expected) results

The collected bathymetry and sub-bottom data cover an area in the Nansen and Amundsen Basin, towards Lomonosov and Gakkel Ridge including transits from and to Svalbard (Fig. 5.1.1). After the first ice stations were performed in the Nansen Basin, a seamount west of the Gakkel Ridge, at 84° 46.83' N and 95° 6.61' E was investigated and mapped in detail to find the highest point (Fig. 5.1.2), for a planned instrument dive. A height difference of a couple of hundred meters to the GEBCO-Dataset could be recognised. During the transit to the North Pole an additional seamount at the Lomonosov Ridge was mapped at 1,580 m water depth. On the way back south, the northern part of the Langseth Seamount, north of the Gakkel Ridge, was mapped which had a height of approx. 2,490 m. The extent of the newly mapped area was 640 km².

During the 9 ice stations the ship drifted slowly between ice floes at a speed of not more than 0.7 kn. This resulted in a dense dataset of very good quality. Nevertheless, the individual beam footprint of 160 m at a depth of 4,000 m physically restricts a higher spatial resolution of bathymetric structures.

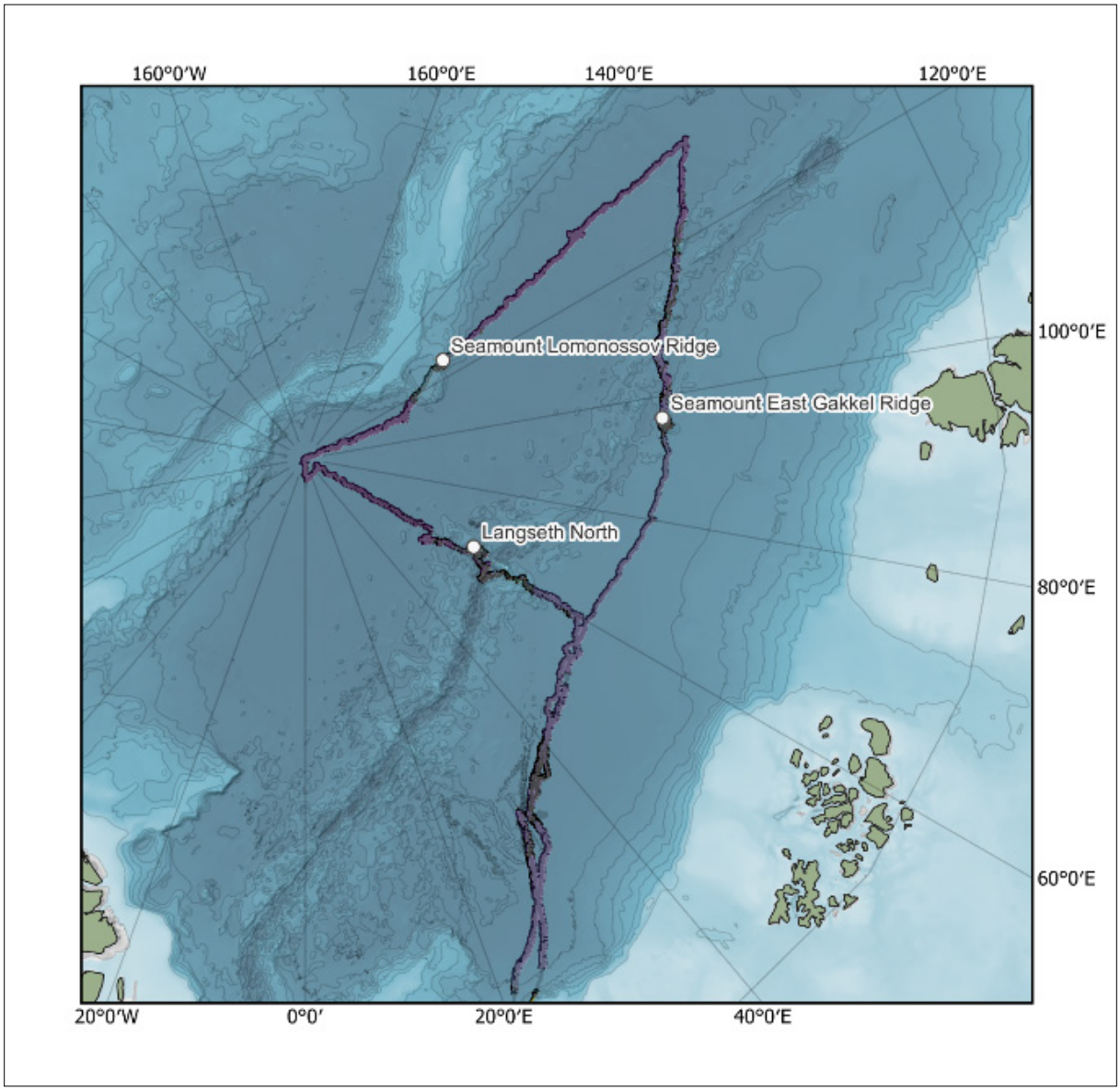

Fig. 5.1.1 Overview of bathymetry tracks during PS138

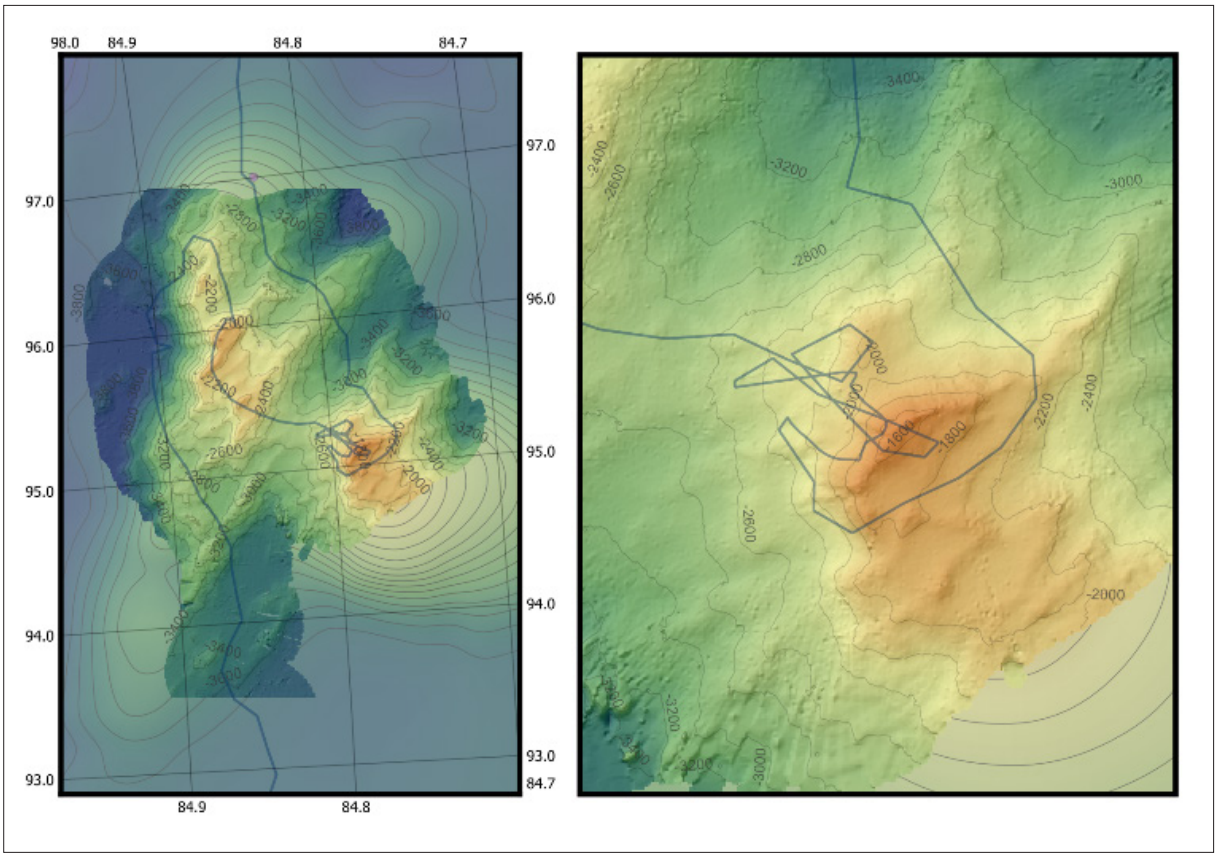

Fig. 5.1.2 Seamount west of the Gakkel Ridge mapped during PS138.

Data management

The bathymetry data set has been transferred to the AWI Geophysics / Bathymetry department and made available from World Data Center PANGAEA Data Publisher for Earth & Environmental Science (https://www.pangaea.de). The available data formats are S7K (from Teledyne PDS), ASD PHF/PHS (from Hydromap Control) and a grid in ESRI ASCII Grid and XYZ format as well as GeoTiffs projected in North Polar Projection.

This expedition was supported by the Helmholtz Research Programme “Changing Earth – Sustaining our Future” Topic 6, Subtopics 1, 2 and 3.

In all publications based on this expedition, the Grant No. AWI_PS138_01 will be quoted and the following publication will be cited:

Alfred-Wegener-Institut Helmholtz-Zentrum für Polar- und Meeresforschung (2017) Polar Research and Supply Vessel POLARSTERN Operated by the Alfred-Wegener-Institute. Journal of large-scale research facilities, 3, A119. http://dx.doi.org/10.17815/jlsrf-3-163.

5.2 Megabenthic ecology and high-resolution seafloor topography

Work at sea

During the PS138 expedition Ocean Floor Observation and Bathymetry Systems (OFOBS) (Purser et al. 2019; Rybakova et al. 2019) were deployed at all ice stations to assess the

seafloor megabenthic communities, and how these may have changed since the last central Arctic expedition with the Ocean Floor Observation System (OFOS) in 2012. Additional surveys of a site on the Lomonosov Ridge, across the northerly extent of the Langseth Ridge and at a newly mapped seamount on the Gakkel Ridge were performed. Two OFOBS systems were used, the 'OFOBS 1' and the newly constructed duplicate system, 'OFOBS 2' (for station PS138_216 only). Both systems integrated a 26 megapixel still image camera (iSiTEC, CANON EOS 5D Mark III) and HD video camera (iSiTEC, Sony FCB-H11). An EdgeTech multibeam system for high-resolution topographic mapping of seafloor structures was also mounted. The sidescan bathymetry sonars were interferometric EdgeTech 2205 AUV/ROV MPES (multiphase echosounder) with two sidescan frequencies. An additional compact CTD provided data on the chemical-physical composition of bottom waters during dives. Throughout all deployments the still camera system was programmed to take "TIMER" images automatically every 20 – 25 seconds, with additional "HOTKEY" images also taken of items or fauna of interest. A forward facing acoustic camera (Bluefin) recorded seafloor structure details throughout each deployment.

The OFOBS' were also equipped with a small ROV, which could be released at any time to conduct filming and small manipulations within 50 m of OFOBS, at up to 5,000 m depth. This device was used opportunistically during OFOBS dives to collect additional video data of seafloor features.

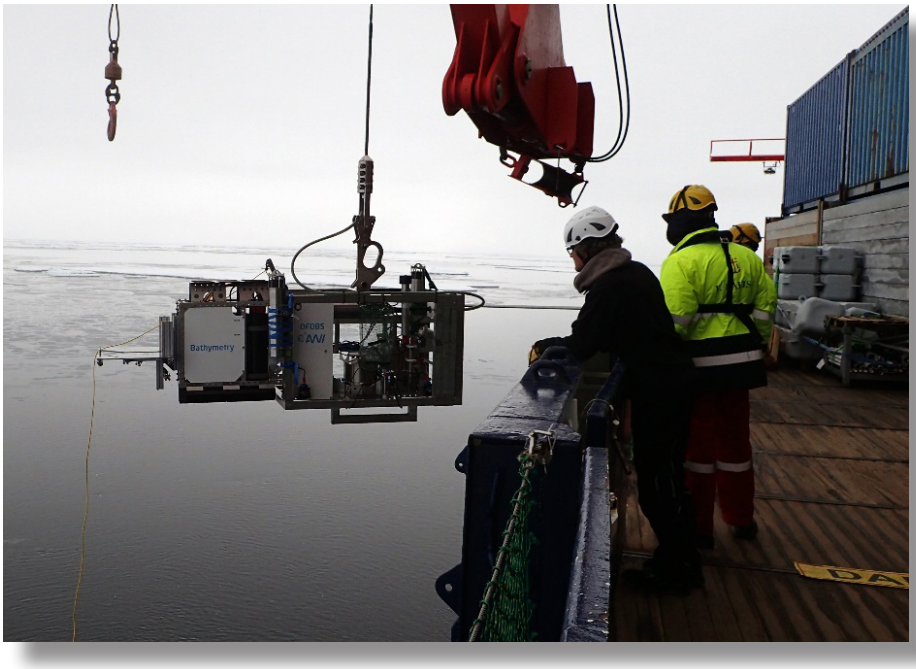

Fig. 5.2.1: Ocean Floor Observation and Bathymetry System (OFOBS)

The OFOBS 1 was equipped with a 12 L water sampling bottle, which was used to collect a bottom water sample for subsequent chemical analysis by colleagues on board.

The scientific aims of the OFOBS deployments were two-fold; Firstly, a number of the stations were repeat visits to those surveyed during the "IceArc" expedition with PS80 in 2012 with other dives surveying new sites of interest on the Gakkel Ridge, Lomonosov Ridge and elsewhere in the central Arctic. These dives were conducted to increase the general level of seafloor structural and fauna biodiversity knowledge across this remote region, and in particular to

allow a better description of central Arctic sponge distribution to be determined, following the discovery of a thick, sponge dominated ecosystem on the summits of the seamounts of the Langseth Ridge in 2016 (Morganti et al. 2022; Stratmann et al. 2022) and whether sponge mobility is high also in any other discovered central Arctic communities (Morganti et al. 2021).

Preliminary (expected) results

Table 5.2.1 gives an overview of the numbers of images collected during each deployment, and whether or not the small ROV was deployed, or water samples were collected.

Tab. 5.2.1: The numbers of "Time" and "Hotkey" images taken at each station during PS138.

Station	Date	Time first image (UTC)	Time final image (UTC)	Water column image No.	Benthic timer image No.	ROV ?	Water ?
PS138_10	08/08/2023	13:09:14	20:15:19	524	754		
PS138_34	15/08/2023	16:59:38	23:23:14	402	736		
PS138_51	18/08/2023	15:31:27	19:27:28	213	460		
PS138_53	19/08/2023	14:27:24	20:49:21	400	673	YES	
PS138_78	24/08/2023	15:48:14	20:53:08	344	556		
PS138_102	28/08/2023	11:06:54	10:59:40	497	961	YES	
PS138_126	02/09/2023	07:35:25	09:53:13	181	223	YES	
PS138_127	02/09/2023	10:42:18	13:52:56	83	452	YES	
PS138_132	03/09/2023	17:07:00	21:15:40	281	466	YES	
PS138_151	07/09/2023	09:31:17	16:14:30	488	496	YES	x
PS138_180	13/09/2023	13:07:55	19:03:55	569	498	YES	x
PS138_198	16/09/2023	12:19:21	15:01:42	339	159	YES	x
PS138_199	16/09/2023	16:30:16	19:41:06	244	289	YES	x
PS138_202	17/09/2023	07:17:30	11:25:08	142	358	YES	x
PS138_203	17/09/2023	12:13:00	17:26:58	361	568	YES	x
PS138_216	19/09/2023	17:21:33	21:33:12	605	282	YES	x

Brief description of each OFOBS station

PS138_10 OFOBS station 1

This station was of uniformly flat seafloor topography, with heavily worked sediments lightly covered by small, approx. 2 cm diameter or less algal aggregates. Crawling anemones and Kolga hyalima were the most abundant fauna observed, though there were numerous traces of emergent infauna and other surface reworking fauna observed. Octopus feeding traces were not uncommon, identical to those observed at the arctic Aurora seamount and elsewhere (Golikov et al. 2023), and a dumbo octopus was observed a few meters above the seafloor. Several fragmentary pieces of glass sponge stalk were observed, though very few living sponges were encountered during the deployment.

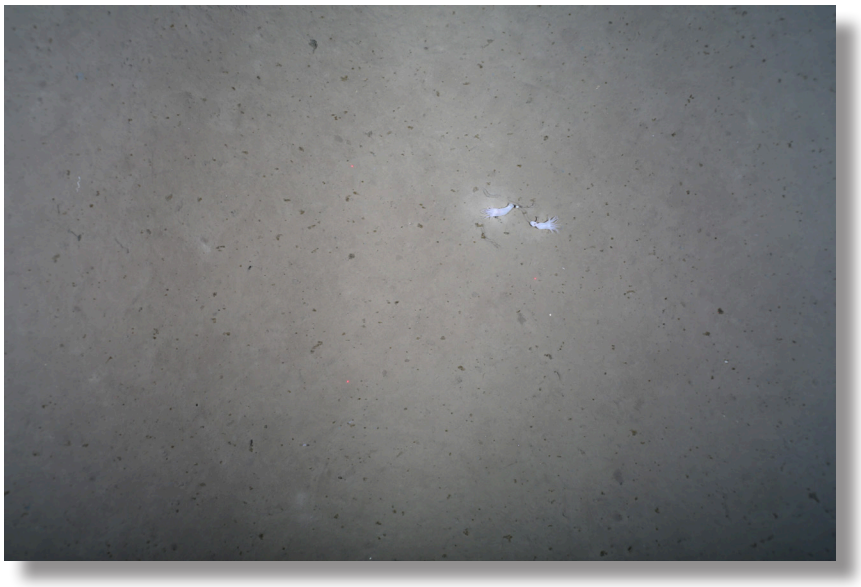

Fig. 5.2.2: A fine grained sedimentary seafloor was observed across the station images. Small aggregates of phytoplankton were observed scattered on the seafloor. In this image two apparently well fed anemones are using a piece of dead sponge as substrate. The three red dots in the centre of the image are laser points, with a spacing of 50 cm (please zoom in to see the laser points).

PS138_34 OFOBS station 2

This station was flat, with very occasional *Melosira arctica* patches observed. Sediments were highly reworked, though megafauna were not present in high abundance, with anemones being the most commonly observed.

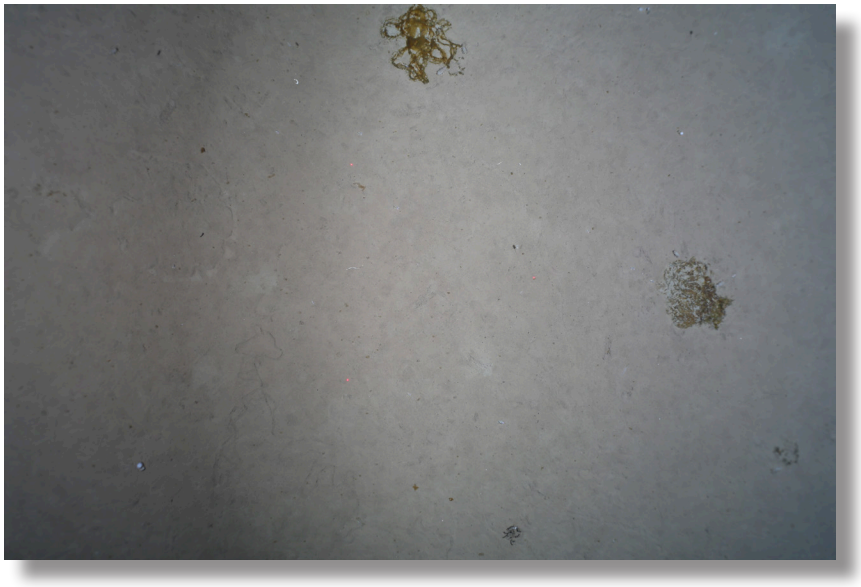

Fig. 5.2.3: A fine grained sedimentary seafloor was observed across the station images. Some scattered large aggregates of Melosira arctica were observed scattered on the seafloor, with two clumps visible in this image. On the left of the image an octagonal feeding trace of an octopus is visible. The three red dots in the centre of the image are laser points, with a spacing of 50 cm (please zoom in to see the laser points).

PS138_51 OFOBS station 3

This dive covered part of the flank and ridge summit of a seamount on the Gakkel Ridge. This was the first survey of this location with modern camera equipment, and an abundant sponge community was found to inhabit the summit of the seamount at 1,900 m depth, and the flanks at over 2,000 m. This is almost twice as deep as the sponge grounds discovered during the PS101 expedition to the Langseth Ridge on the Gakkel Ridge in 2016 (Morganti et al. 2022). As described from observations at the Langseth Ridge, budding and spicule trail deposition associated with sponge mobility (Morganti et al. 2021) were observed during this dive. The sponges at this seamount however were able to colonise steeper flank slopes than was achieved at the Langseth Ridge, with populations observed on 40° slopes. As with the Langseth Ridge sponge grounds, the sponges observed during PS138 at this site were also commonly supporting tube building worms on their exterior, and providing habitat niches for shrimp and small mobile fauna. Fish were also observed across the sponge grounds, and a dumbo octopus observed on the seamount flank. In contrast to the Langseth Ridge sponge grounds, this sponge ground was occupied by high densities of mobile crinoids, with any sharp variability in seafloor relief commonly correlating with a greatly increase in mobile crinoid abundance.

The geology underlying the sponge grounds was almost exclusively exposed basalt with some indications of erosion, but little sediment cover.

Fig. 5.2.4: The seafloor surveyed was predominantly made up of steep seamount flanks and intermittent ridges and crests. A typical flank area is shown here. Numerous sponges can be seen on a spicule substrate on this steep flank of approximately 40° slope angle. The cases of worms affixed to the sides of the sponges can occasionally be seen in the image (white lines). Toward the top of the image a dying sponge can be seen coated with a bacterial mat. The red dots in the centre of the image are laser points, with a spacing of 50 cm (please zoom in to see the laser points).

.

PS138_53 OFOBS station 4

Unique amongst the dives conducted during PS138, this area of low topography seafloor had regular aggregations of *Melosira algae*, with sizes of up to approximately 5 cm diameter present in almost every image. *Kolga hyalina* were regularly observed across the seafloor, often in close proximity of algae fragments, and some undergoing what appears to be stages of fissiparity. Infauna and fauna surface traces were common across all images, and in several cases emergent burrowing worms could be seen in images. *Elpidia heckeri* were also observed across images, as were anemones. In one instance an anemone could be seen consuming a large shrimp. Occasional woodfalls and dumbo octopus feeding traces were also observed.

Fig. 5.2.5: A fine grained sedimentary seafloor was observed across the station images. Small aggregates of phytoplankton were observed scattered on the seafloor. In this image a Kolga hyalina can be seen entering the frame from the bottom edge. A piece of wood of approximately 70 cm length is visible in the centre of the frame, with numerous small white gastropods, sea spiders and worms populating the woodfall and the surrounding sediment/wood interface. The three red dots in the centre of the image are laser points, with a spacing of 50 cm (please zoom in to see the laser points).

.

PS138_78 OFOBS station 5

The seafloor was of low relief, soft sediment topography, heavily reworked by surface deposit feeders and infauna. Anemones (crawling primarily) and *Kolga hyalina* were the most abundant megafauna, though occasional large, living glass sponges were also observed. Many of the *Kolga hyalina* appeared reddish with consumed food, and many were undergoing fissiparity. A plastic bag was observed, perhaps representing the most northerly such item yet captured on camera.

Fig. 5.2.6: A fine grained sedimentary seafloor was observed across the station images. Some white stains on the seafloor, perhaps indicative of previous algal falls, as in this image. In this image one of the very few living sponges observed is located within the centre of the frame, with an anemone, a sea spider and numerous amphipods using this as a substrate. A Kolga hyalina, apparently undergoing the process of fissiparity, is visible in the top of the image. The three red dots in the centre of the image are laser points, with a spacing of 50 cm (please zoom in to see the laser points).

.

PS138_102 OFOBS station 6

Though of generally low and flat relief, the region of seafloor surveyed during OFOBS dive 6 was also abundantly covered with pairs of mounds. These mound pairs consisted of one shallow mount (approx. 10 cm height) with a perfectly circular hole in the upper centre. The second mound in each pair was more chaotic, of approx. 20 cm height, and with no clear egress or ingress burrows. In some cases the round hole on the smaller mound was surrounded by radiating straight traces. In a few images the feeding apparatus of an infauna spoonworm could be seen stretched out across the seafloor surface, clearly responsible for forming the radial patterns by retracting food into the burrow. These hills formed a useful substrate for occupation by occasional isopods. The sediment surrounding these cone hills was reworked by a range of infauna and fauna, with both *Kolga hyalina* and *Elpidia heckeri* being observed across the surface, as well as occasional anemones and echinoids. A dumbo octopus was also observed. Small fragments of algae aggregates, perhaps *Melosira*, were seen in almost every image, with diameters of up to 5 cm. Larger white patches of sediment, perhaps indicative of previous larger algal falls, were visible across the surveyed area.

Fig. 5.2.7: A fine grained sedimentary seafloor was observed across the station images. Small aggregates of phytoplankton were observed scattered on the seafloor. In this image, white sediment staining indicating potential spots where previous algae patches have been eaten and degraded, can also be seen. A Kolga hyalina, apparently undergoing the process of fissiparity, is visible in the top of the image. The three red dots in the centre of the image are laser points, with a spacing of 50 cm (please zoom in to see the laser points).

.

PS138_126 OFOBS station 7

OFOBS dive 7 was conducted on top of the Lomonosov Ridge, several km from the rim of this large, central arctic feature. The survey was conducted from north to south, approaching the flank from the more central region of the ridge. The seafloor appeared generally of moderate relief, finely sedimented with clear indications of heavy reworking by fauna. Large burrows, not associated with hill structures, were commonly observed, of rough construction and diameters of up to 10 cm. Several large sponges were observed, reminiscent of those from OFOBS dive 3 (PS138_51) on the Gakkel Ridge seamount, from a similar depth. These sponges were also seen in association with a scattered spicule underlying mat, but sedimentation was much higher here on the Lomonosov Ridge, with the sponges themselves quite sediment dusted. As on the seamount, shrimp were observed to associate with the sponges, and mobile crinoids to be commonly spotted on their tops. Stalked crinoids and ophiuroids were observed here at greater density than elsewhere during the PS138 deployments, as well as occasional scaleworms and molluscs.

Fig. 5.2.8: A fine grained sedimentary seafloor was observed across the station images. In this image the darker patches are spicule produced by sponges, such as the large two observed in this image. As on the Gakkel Ridge, these sponges act as a substrate or vantage point for mobile fauna such as crinoids, and provide structural niches for the shrimp observed here. A large pycnogonid can be seen near the centre of the image, as well as a stalked crinoid on the right. The three red dots in the centre of the image are laser points, with a spacing of 50 cm (please zoom in to see the laser points).

.

PS138_127 OFOBS station 8

OFOBS dive 8 was conducted on the steep flank (slope angle up to 40°) of the Lomonosov Ridge, at depths of approx. 2,400 m. The seafloor was heavily sedimented, rather than of exposed rock, as was the case with the flanks of the Gakkel Ridge seamount (Morganti et al. 2022), dive OFOBS 3. There were some clear traces left on the sediments by fauna, but these traces were smooth and generally infilled, indicating probably high sedimentation rates. A few algal aggregates were observed, of up to 10 cm length, though these were far from abundant. A high abundance of *Kolga hyalina* was observed in almost every image collected, with occasional shrimp and fish also observed. There were small concentrations of sponges, reminiscent of those observed during dive 7, also present on the slope.

Fig. 5.2.9: A very fine grained and sloped sedimentary seafloor was observed across the station images. Numerous Kolga hyalina were observed, as in this image, with some indicating fissiparity ongoing. A fish can be seen toward the bottom of this image, though they were not abundant across the station. The three red dots in the centre of the image are laser points, with a spacing of 50 cm (please zoom in to see the laser points).

PS138_132 OFOBS station 9

The seafloor imaged during this dive was very flat, lightly reworked by fauna and wholly absent of algal aggregates. A large number of *Kolga hyalina* were observed and occasional crawling anemones. Some fresh infauna traces were present. There were some small white patches on the sediment perhaps indicative of previously settled algal material.

Fig. 5.2.10: A fine grained sedimentary seafloor was observed across the station images. Kolga hyalina and occasional anemones were observed throughout the dive. The three red dots in the centre of the image are laser points, with a spacing of 50 cm (please zoom in to see the laser points).

.

PS138_151 OFOBS station 10 North Pole Station

This dive was conducted at the North Pole, and collected images from a flat, sedimentary seafloor, highly reworked by fauna and almost wholly lacking in algal detritus. There were many pairs of hills observed, reminiscent of those observed during dive 6, but with far longer and more numerous worm feeding traces; some traces approaching 2 m in length at this station. Anemones and hydroids were the most common fauna observed, with occasional small *Kolga hyalina*. There were also abundant octopus feeding traces, of various diameters – which differs from seafloor observed elsewhere and in Golikov et al. (2023), where traces of roughly 40 cm diameter seem to be the most common. A small dumbo octopus, of about 10 cm diameter on the seafloor, was photographed actively feeding on the sediments.

Unfortunately, within a few hundred meters of the North Pole, a drink carton was observed during the dive, as was a collapsed array of what looked to be scientific equipment.

Fig. 5.2.11: A fine grained sedimentary seafloor was observed across the station images. Numerous pairs of small mounds, one approx. 10 cm high, the other 20 cm were observed, as in this image. Spoon worm feeding traces often radiated up to 60 cm from the centre of the shorter of the mounds, as in this image. Occasional anemones and sediment discolouration patches are present in this image and observed regularly across the surveyed area. The three red dots in the centre of the image are laser points, with a spacing of 50 cm (please zoom in to see the laser points).

.

PS138_180 OFOBS station 11

Station 11 was another flat region of arctic seafloor, highly sedimented, with very few algal aggregates present. The station was covered with very many small hill structures of two sizes. The larger, about 20 cm high, were quite broken up and irregular with many slit like burrows of approximately 3 to 5 cm length present near the summits. The smaller hills were approximately 10 cm in height and almost always a very light grey in colouration, perhaps indicating sediments extruded to the surface from depth by bioturbation. Between these hills and across the seafloor, white patches of sediment perhaps indicative of previous algal falls were not uncommon. *Kolga hyalina* and white amphipods were the most obvious fauna, though hydroids were also quite common. Several woodfalls were also observed, though less abundant in associate fauna than woodfalls observed on other dives during PS138.

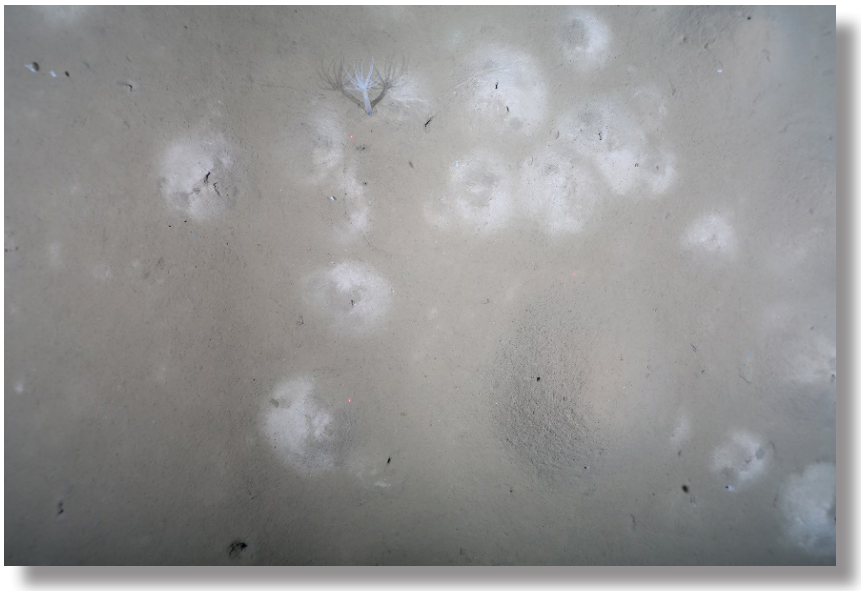

Fig. 5.2.12: A fine grained sedimentary seafloor was observed across the station images. Numerous mounds were observed across the seafloor, with 10 cm and 20 cm high mounds the main sizes. In this image many of the smaller mounds are white, perhaps indicating vertical displacement of deeper sediments by infauna. A hydroid is also present in this image. The three red dots in the centre of the image are laser points, with a spacing of 50 cm (please zoom in to see the laser points).

.

PS138_198 OFOBS station 12

OFOBS station 12 filmed the upper flank of the northern half of the Langseth Ridge, on the other side of the Gakkel Ridge to the southern half surveyed during the PS101 expedition (Morganti et al. 2022; Stratmann et al. 2022). In contrast to the southern half, the region surveyed in 2023 was far more heavily sedimented, though still clearly geologically composed of broken pillow basalts in steep steps. Fauna was not abundant, with filter feeding glass sponges, anemones and occasional shrimp the most commonly observed fauna. There were no *Geodia* sp. Or other bacteriosponges observed anywhere during the dive. Occasional fish were observed, as were small *Kolga hyalina* on the sedimented steps within the basalt slope.

Fig. 5.2.13: The majority of the dive covered steep, broken and fragmented pillow lavas. In this image numerous anemones are seen near a sedimented step in the steep lava wall. The three red dots in the centre of the image are lazer points, with a spacing of 50 cm (please zoom in to see the laser points).

.

PS138_199 OFOBS station 13

A fairly low relief area of sedimented seafloor was surveyed during dive 13, with occasional basalts observed and scattered small stone fragments in a matrix of soft sediments, heavily reworked by fauna. In contrast to the other sites surveyed during PS138, numerous bivalve shells were present in images, though no live bivalves observed. Both mobile and sessile crinoids were reasonably abundant across the seafloor. Occasional small *Kolga hyalina* were observed, though no algae appeared to be present on the seafloor.

Fig. 5.2.14: A fine grained sedimentary seafloor was observed across the station images. Small aggregates of phytoplankton were observed scattered on the seafloor. In this image various Kolga hyalina individuals can be seen on a very reworked sediment. A dead bivalve shell can be seen partially buried. The three red dots in the centre of the image are laser points, with a spacing of 50 cm (please zoom in to see the laser points).

.

PS138_202 OFOBS station 14

OFOBS dive 14 was the first conducted at the active hydrothermal mound within the Gakkel Ridge, first surveyed during PS101 in 2016. The seafloor throughout the dive mainly consisted of exposed basalts, exposed and broken pillow lava and some materials precipitated by small vents, present in some areas. A very few fish and anemones were observed. During both deployment and recovery, the OFOBS passed through two horizons of particulate heavy waters, indicative of black smoker output.

Fig. 5.2.15: Large pillow lava were common in the area, with a light sediment dusting and only occasional fauna observed. Here, a fish and shrimp can be seen near the centre of the image. The three red dots in the centre of the image are laser points, with a spacing of 50 cm (please zoom in to see the laser points).

.

PS138_203 OFOBS station 15

The second of the dives carried out on the active hydrothermal rise in the Gakkel Ridge, with this being conducted presumably closer to the currently active venting site. In addition to crossing regions of basalt outcrops and pillow lava, this second deployment imaged more areas of hydrothermal precipitates, including highly stained cliff and areas with small orange and yellow chimneys up to about 15 cm height. These were often covered by bacterial mats. Extended areas of seafloor were heavily broken and marked with these small chimneys, with filter feeding bryzoa or filamentous algae also present on the higher local topographies in these areas.

As with the previous dive, two horizons of smoky material were passed through with the OFOBS during deployment and recovery.

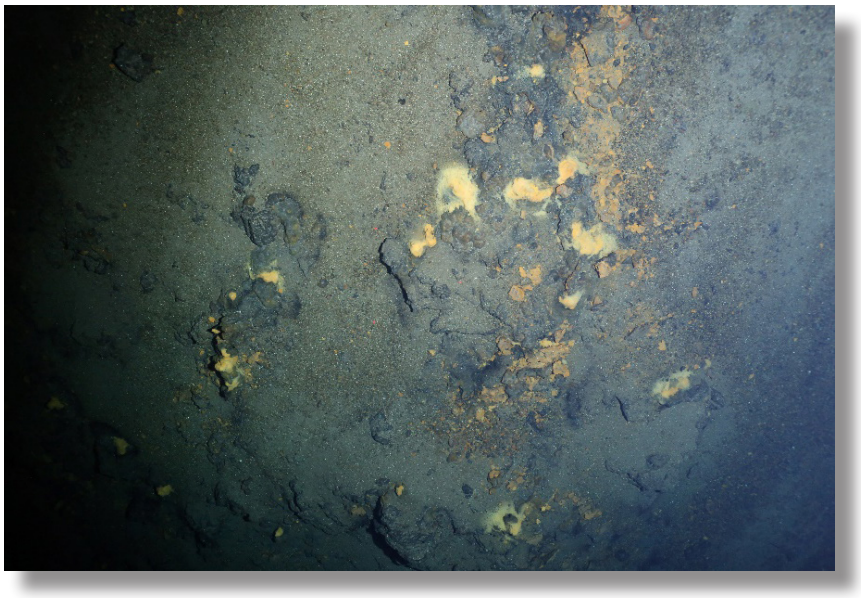

Fig. 5.2.16: Approaching the most active region of the vent site on the Gakkel Ridge. The seafloor in the image is comprised of small fragments of hydrothermally produced rocks and occasional small vents, most of which are covered with yellow precipitates and yellow bacterial mats. The three red dots in the centre of the image are lazer points, with a spacing of 50 cm (please zoom in to see the laser points).

.

PS138_216 OFOBS station 16

The final OFOBS deployment during the PS138 expedition surveyed an extremely flat sedimented area of seafloor, heavily reworked by epifauna. Dumbo octopus feeding traces were present, as well as small 1 or 2 cm aggregates of very degraded algae. Fauna were scarce, consisting primarily of crawling anemones.

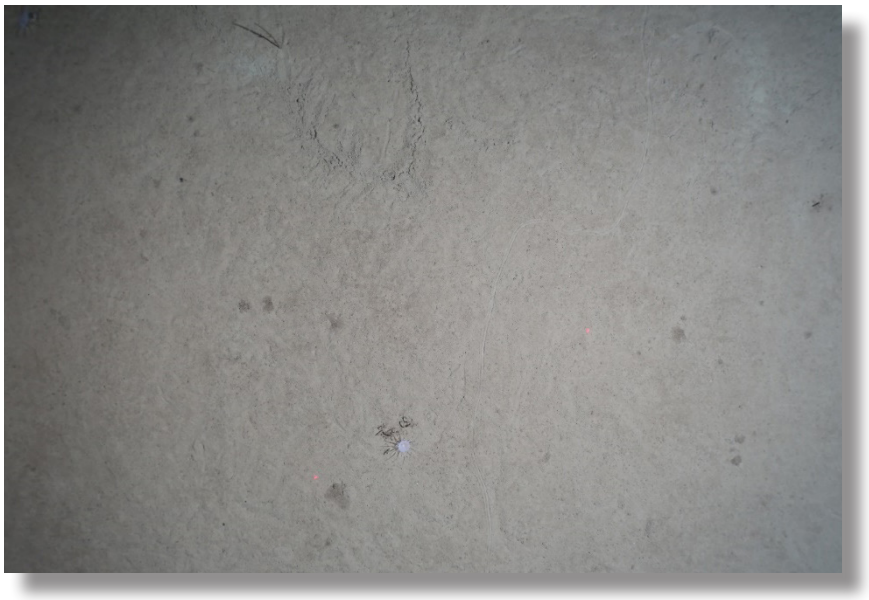

Fig. 5.2.17: A fine grained sedimentary seafloor was observed across the station images. Very small aggregates of phytoplankton were observed scattered on the seafloor, almost brown in colour and potentially highly degraded. The seafloor was heavily marked with the traces of movement left by deposit feeders and other epifauna. A small anemone is the only megafauna visible in the image, though in the top right an octagonal trace from previous octopus foraging can be seen. The three red dots in the centre of the image are laser points, with a spacing of 50 cm (please zoom in to see the laser points).

MINI ROV Videos

8 MINI-ROV deployments were made, and the video data from these is publically available.

3D Seafloor models

3D Models were prepared from OFOBS video frames using the Agisoft Metashape software application. These models give a 3D feel of the local seafloor rugosity of each deployment over a scale of mm. These models are publicly available.

Data management

All data collected with the OFOBS system will adhere to the FAIR principles proposed in Schoening et al. (2022).

All OFOBS still images, sidescan and forward sonar data will be archived to the World Data Center PANGAEA Data Publisher for Earth & Environmental Science (https://www.pangaea.de) within six months of cruise completion, and publically available either after two years, or following the first scientific publication based on results.

All miniROV videos and 3D models derived from OFOBS video data will be publically available from MENDELEY DATA within six months of cruise completion.

This expedition was supported by the Helmholtz Research Programme “Changing Earth – Sustaining our Future” Topic 6, Subtopics 1, 2 and 3.

In all publications based on this expedition, the Grant No. AWI_PS138_01 will be quoted and the following publication will be cited:

Alfred-Wegener-Institut Helmholtz-Zentrum für Polar- und Meeresforschung (2017) Polar Research and Supply Vessel POLARSTERN Operated by the Alfred-Wegener-Institute. Journal of large-scale research facilities, 3, A119. http://dx.doi.org/10.17815/jlsrf-3-163.

5.3 Macrofauna

Work at sea

The Giant Box Corer (BC; Hessler and Jumars 1974; Fig. 5.3.1) allows for a quantative sampling of the deep-sea macrofauna due to its fixed dimensions of 0.5 x 0.5 m which represents a sampling area of 0.25 m². The gear was deployed twice at all icestations (18 x in total, Tab. 5.3.1, Fig. 5.3.2), covering a total sampling area of 4.5 m^2. The BC deployment protocol was carried out as follows: the gear was lowered with 1.0 m/s and stopped 30 m above the ground to stop swinging. After three minutes, the BC was lowered with 0.5 m/s until lot depth. Subsequently, the speed was reduced to 0.2 m/s. Once the BC hit the ground, 5 m cable were added to compensate for the ship's movement. Then the BC was heaved out of the ground with 0.2 m/s to minimize the surface disturbance. Afterwards the speed was increased to 1.0 – 1.1 m/s.

Fig. 5.3.1: The Giant Box Corer back on deck after successful deployment from the aft of the vessel.

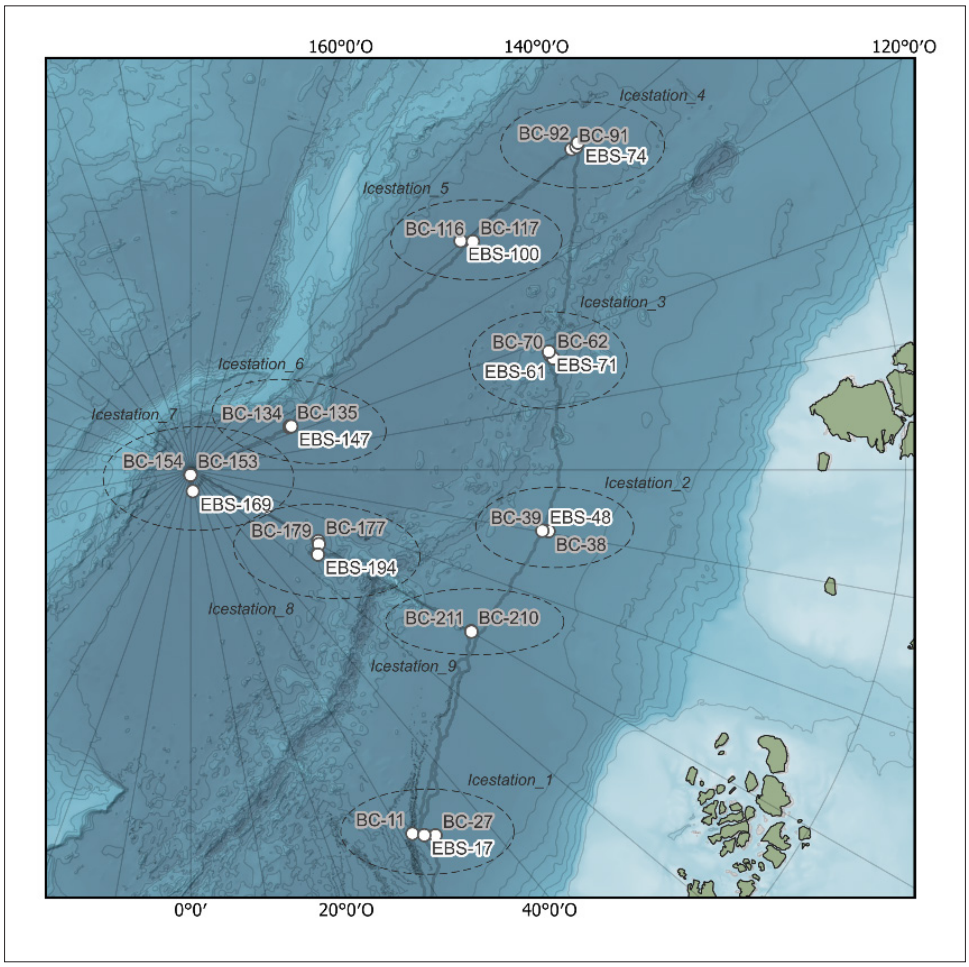

Fig. 5.3.2: EBS and BC station overview during PS138.

Once the gear was back on deck, the surface water was removed, filtered through a 300 µm sieve and fixed in 96 % ethanol. For the documentation of deployment success, a picture of the surface was taken. In total, each BC sample was divided into 12 sediment subsamples (each 0.03 m²): eight subsamples from the 0 – 4 cm layer and four subsamples from the 4 – 10 cm layer (Fig. 5.3.3). The sediment was mostly made up by very fine, muddy sediment. To allow for easier sieving, it was put into buckets with seawater and carefully dissolved. Each subsample was sieved on the DZMB sieving table with filtered seawater through a mesh size of 500 µm and 300 µm to divide the samples into different fractions. Results from the 500 µm fraction will be later compared to results from the multigrab device from IceArc 2012. Separated animals were handpicked and fixed into 96 % denatured ethanol. Out of the eight subsamples from the 0 – 4 cm layer, four were fixed in 96 % denatured ethanol. To ensure high quality of preservation, ethanol concentration was measured after 24 h and samples with a concentration below 90 % were re-fixed and stored at -20°C. All other samples were fixed in 4 % formosaline.

All BC deployments were successful. However, at station PS138-11, -153 and -154 only 2 out of 4 ethanol samples were taken due to a slightly tilted surface. At station PS138-210 the lids of the box were open when the gear came back on deck, so the surface water might contain some pelagic taxa.

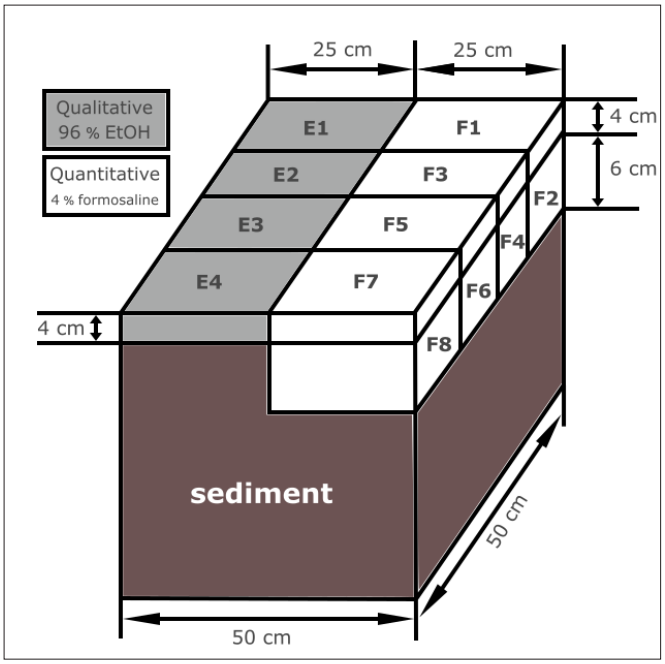

Fig. 5.3.3: Subsampling scheme for the box corer samples in order to allow comparison to the multigrab samples during IceArc in 2012; qualitative samples stored in 96 % denatured ethanol (E1-E4) were taken for molecular species identification, while quantitative samples in 4 % formosaline (F1-F8) will be used for benthic community analyses (modified from Soltwedel 2013).

Tab. 5.3.1: EBS and BC stations.

Area	Station	Gear	Date	Latitude [deg]	Longitude [deg]	Depth [m]	Trawling distance [m]
Icestation_1 (Nansen Basin)	**PS138-11**	BC	08/08/2023	84.033526	31.379373	3991	-
	PS138-17	EBS start EBS end	10/08/2023	83.921955 83.914214	32.526773 32.439297	3978 3978	1317
	PS138-27	BC	12/08/2023	83.840031	33.839940	4028	-
Icestation_2 (Nansen Basin)	**PS138-38**	BC	16/08/2023	84.911366	80.281106	3731	-
	PS138-39	BC	16/08/2023	84.910835	80.307331	3727	
	PS138-48	EBS start EBS end	17/08/2023	84.996723 84.993822	80.305903 80.440589	3743 3740	1420
Icestation_3 (Nansen Basin)	**PS138-61** (was repeated)	EBS start EBS end	20/08/2023 21/08/2023	84.692706 84.705323	107.097337 107.143968	3791 3667	2097
	PS138-62	BC	21/08/2023	84.709788	107.749790	3979	-
	PS138-70	BC	22/08/2023	84.711614	107.632998	3972	
	PS138-71	EBS start EBS end	22/08/2023	84.708769 84.706158	108.173665 108.054791	3976 3978	1735

Area	Station	Gear	Date	Latitude [deg]	Longitude [deg]	Depth [m]	Trawling distance [m]
Icestation_4 (Amundsen Basin)	**PS138-74**	EBS start EBS end	24/08/2023	82.894650 82.890680	130.170690 130.072777	4156 4158	1731
	PS138-91	BC	26/08/2023	83.025814	130.100095	4161	-
	PS138-92	BC	26/08/2023	82.952735	129.944874	4165	
Icestation_5 (Amundsen Basin)	**PS138-100**	EBS start EBS end	28/08/2023	85.034167 85.037079	130.280025 130.246852	4298 4299	1124
	PS138-116	BC	31/08/2023	84.930894	128.990948	4308	-
	PS138-117	BC	31/08/2023	84.911114	128.973251	4307	
Icestation_6 (Amundsen Basin)	**PS138-134**	BC	04/09/2023	88.489838	113.410359	4323	-
	PS138-135	BC	04/09/2023	88.483518	113.902132	4324	
	PS138-147	EBS start EBS end	05/09/2023	88.460529 88.452334	113.377957 113.030550	4323 4326	1594
Icestation_7 (North Pole)	**PS138-153**	BC	07/09/2023	89.929921	-4.893236	4239	-
	PS138-154	BC	08/09/2023	89.929049	-1.896208	4239	
	PS138-169	EBS start EBS end	11/09/2023	89.687348 89.698714	5.881338 4.637083	4248 4249	1450
Icestation_8 (Amundsen Basin)	**PS138-177**	BC	13/09/2023	87.950641	60.862116	4377	-
	PS138-179	BC	13/09/2023	87.923303	59.944336	4378	
	PS138-194	EBS start EBS end	15/09/2023	87.854307 87.853192	56.379335 56.696744	4375 4377	1335
Icestation_9 (Nansen Basin)	**PS138-210**	BC	19/09/2023	85.465686	60.136333	3885	-
	PS138-211	BC	19/09/2023	85.458590	60.063795	3882	

To sample benthic macrofauna living within and just above the seafloor, the Epibenthic Sledge named Berta (EBS; Brenke 2005) was deployed once per station (except twice at icestation 3) during PS138 (9x in total, Tab. 5.3.1) from the aft of the vessel (Fig. 5.3.4). It is trawled on the seafloor and catches the stirred-up sediments with two different nets: the supra and the epi net. Each net has a mesh size of 500 µm and the cod ends are equipped with net-buckets with 300 µm mesh windows. A mechanical opening-closing device prevents pelagic fauna to be caught while veering and hieving. The total area trawled covered 13,803 m of the seafloor. Trawling distance was calculated with following the formula:

$$s = v_1 * t_1 + v_2 * t_2 + v_3 * t_3$$

$$s = trawling\ distance;\ v_1 = \text{vessel trawl speed } \left(\frac{\text{m}}{\text{s}}\right);\ t_1 = \text{vessel trawl time (min)};$$
$$v_2 = \text{vessel haul speed } \left(\frac{\text{m}}{\text{s}}\right);\ t_2 = \text{vessel haul (min)};\ v_3 = \text{winch haul speed } \left(\frac{\text{m}}{\text{s}}\right);$$
$$t_3 = \text{winch haul time (min)}$$

Additionally, the gear was equipped with a SeaGuard RCM DW CTD (Aanderaa Data Instruments AS, Norway) to measure environmental parameters of pressure, temperature, salinity and turbidity on the seafloor.

Fig. 5.3.4: Deployment of the Epibenthic Sledge 'Berta' (Brenke 2005) from the aft of the vessel at the North Pole station PS138-169 (Icestation-7 area).

The EBS deployment protocol was carried out as follows: The gear was lowered with 1 m/s until 300 m above the ground. Then, the winch was stopped to stop swinging. After three minutes the ship started moving forward with 1 kt while the EBS was further lowered with 0.5 m/s. Once it landed on the ground, 1,000 m of cable wire were laid out with 0.5 m/s on the seafloor while the ship kept moving with 1 kt. To remove loops of the wire, the ship continued moving for 10 minutes while the winch was stopped. The EBS was trawled over the

ground with 0.3 m/s until it left the ground. Hieving was carried out with 1.0 m/s. At Icestation-5 (PS138-100) deployment was carried out in 'drift mode' from the aft while the vessel was attached to an icefloe. Ice drift velocity varied between 0.5 and 0.1 kt, thus, winch speed during landing and trawling was continually adapted to half of the drift velocity. At this station, 700 m cable wire were laid out. Ship speed during trawling time was according to the ice drift velocity.

Once the gear was back on deck, the cod ends as well as the supernatant sediment in the nets ("Überstand") were retrieved and sieved with filtered seawater through 1,000 µm, 500 µm and 300 µm mesh size. Larger specimens were hand-picked, placed into seawater and photographed on board in the 4°C laboratory. If multiple specimens of one morphospecies were present, two to five were rinsed with filtered milliQ water and wrapped into pre-rinsed aluminium foil for microplastic analysis (in collaboration with M. Bergmann, AWI). Blank controls were taken in parallel with the specimen picking. Additional specimens were fixed in RNA later. The rest was fixed in 96 % ethanol. If holothurians were present, around 5 individuals stayed in seawater for chlorophyll analysis of the gut later. The remaining samples were fixed in 96 % ethanol and stored at -20°C for at least 48h. During that time, samples were gently moved to avoid freezing. After 24h the ethanol concentration was checked. If it was below 90 %, additional ethanol was added. After 48h the sorting process started. Animals were identified to higher taxon level and the remaining sediment was stored for potential usage later. All deployments were successfull except of one EBS at icestation 3 where it was trawled 70 m hillupwards and filled with 2 tons of sediment. The cod ends and parts of the sediment in the nets were sieved. However, the deployment was repeated to allow for a better comparison with other stations.

Preliminary (expected) results

A total of 365 samples have been taken with the BC and 56 with the EBS from 3,727 – 4,379 m depth. Out of these, 66 were sorted on board. So far, 12,638 animals were found and sorted into higher taxa groups and 122 individuals were photographed for first identification (in correspondence with A. Vedenin, Senckenberg Fig. 5.3.5, Fig. 5.3.6). Current authoritative classification and associated original descriptions follow the catalogue World Register of Marine Species (WoRMS Editorial Board, 2023). Crustacea and Annelida were the most abundant groups followed by Mollusca. Further sample sorting, taxa identification, species abundance and biomass assessments will be performed in the laboratories after the cruise.

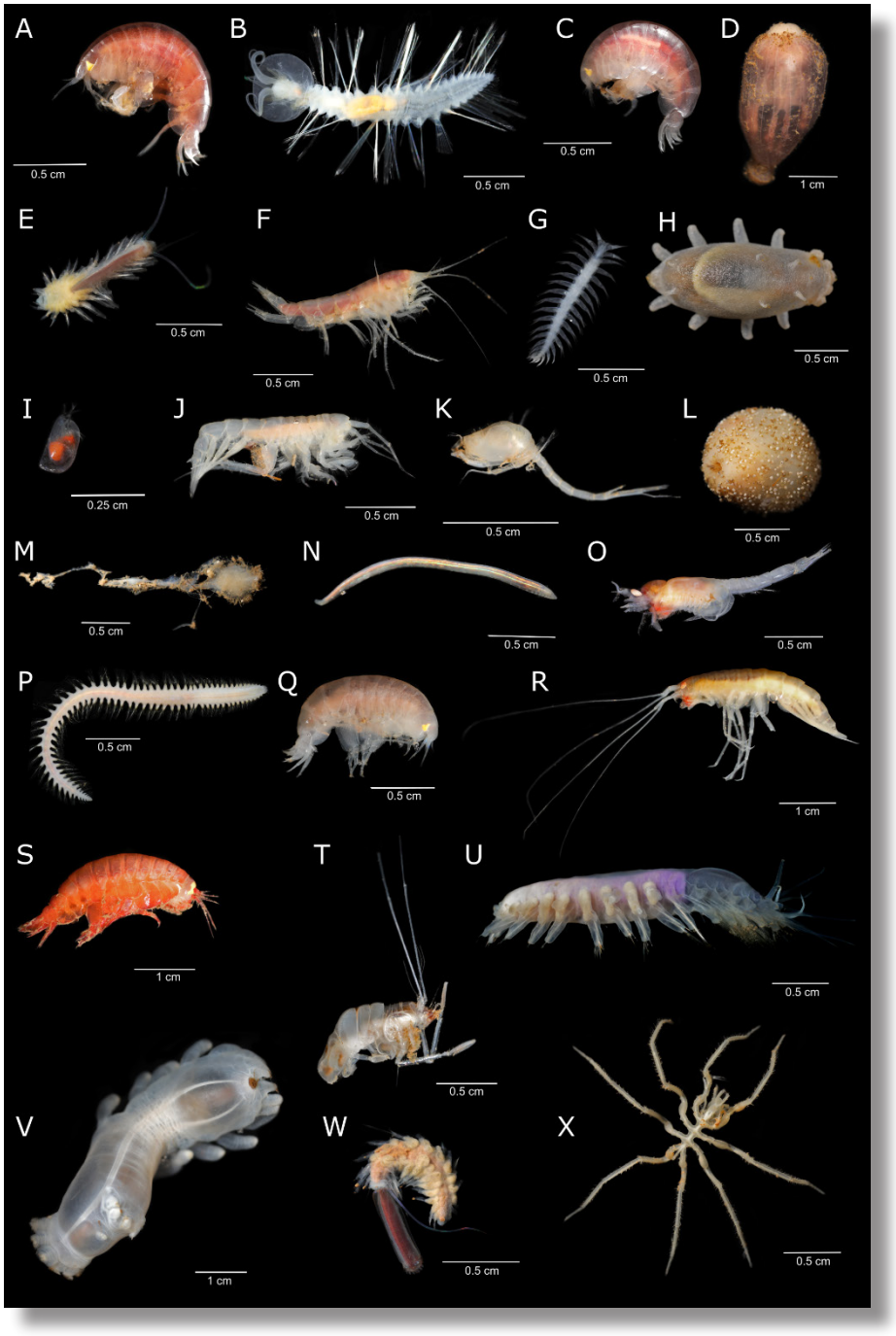

Fig. 5.3.5: First insight into the diversity of macrobenthic fauna sampled with the epibenthic sledge, photographed live at Icestation-1 (PS138-17, A: Lysianassoidea; B: Chauvinelia arctica Averincev, 1980; C: Lysianassoidea; D: Bathyphellia margaritacea (Danielssen, 1890); E: Bathypolaria carinata Levenstein, 1981), Icestation-2 (PS138-48, F: Liljeborgia caliginis d'Udekem d'Acoz & Vader, 2009; G: Lopadorrhynchidae; H: Elpidia heckeri Baranova, 1989, I: Ostracoda), Icestation-3 (PS138-71, J: Arrhis phyllonyx (M. Sars, 1858); K: Leptostylis sp.; L: Bathyphellia margaritacea (Danielssen, 1890); M: Porifera; N: Ophelina opisthobranchiata Wirén, 1901; O: Mysida; P: Aglaophamus malmgreni (Théel, 1879); Q: Lysianassoidea); Icestation-4 (PS138-74, R: Halirages sp.; S: Eurythenes gryllus (Lichtenstein in Mandt, 1822)), Icestation-5 (PS138-100, T: Munnopsurus giganteus (G. O. Sars, 1877); U: Macellicephala cf. longipalpa Uschakov, 1957) and Icestation-6 (PS138-147, V: Kolga hyalina Danielssen & Koren, 1879; W: Polychaeta; X: Ascorhynchus abyssi Sars, 1877).

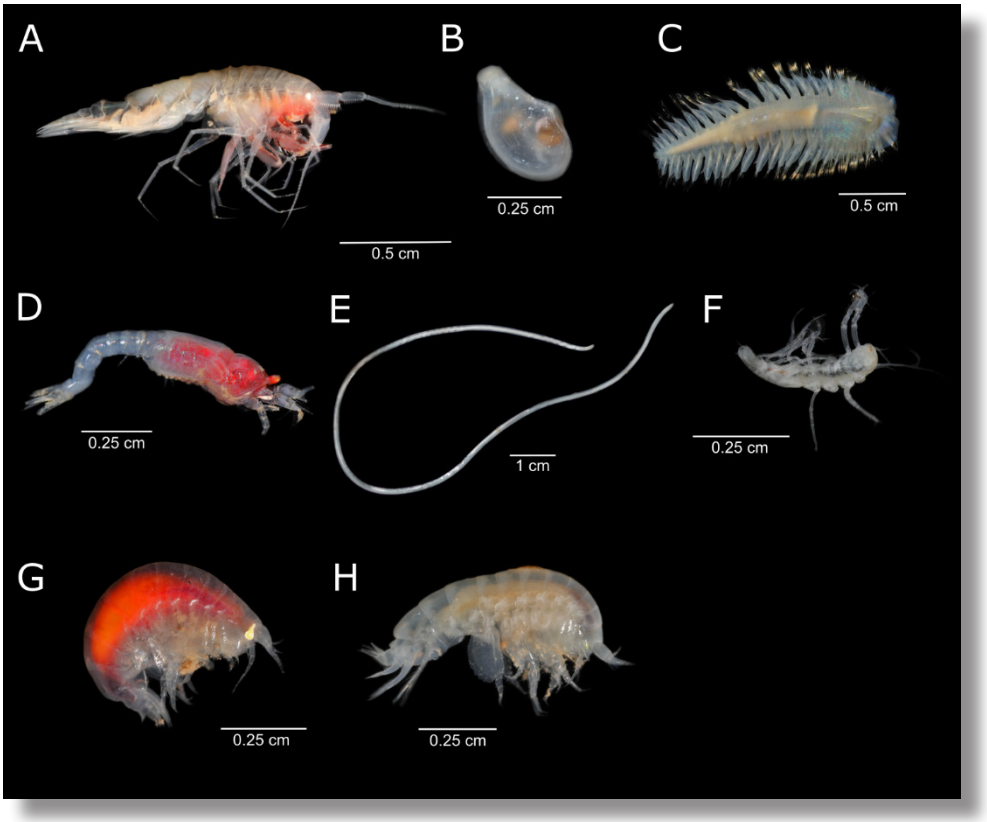

Fig. 5.3.6: First insight into the diversity of macrobenthic fauna sampled with the epibenthic sledge at Icestation-7 (PS138-169; A: Cleonardo appendiculatus (G.O. Sars, 1879); B: Cuspidaria centobi Bouchet & Warén, 1979; C: Macellicephalinae gen. sp.; D: Neobirsteiniamysis inermis (Willemoes-Suhm, 1875); E: Benthimermithidae) and Icestation-8 (PS138-194; F: Desmosomatidae; G: Lysianassoidea; H: Centromedon typhlops (G. O. Sars, 1879)).

Data management

All samples will be stored at the German Center for Marine Biodiversity (DZMB) in Hamburg and Wilhelmshaven. Once all samples are sorted to higher taxa level, groups will be handed over to taxonomic experts for further identification. Sample processing of microplastic specimens will be carried out at AWI. Molecular DNA and RNA data will be archived, published and disseminated within the publicly accessible repositories GenBank (https://www.ncbi.nlm.nih.gov/genbank/) and BOLD (https://www.boldsystems.org/index.php). After successful identification, records will be uploaded to the Ocean Biodiversity Information System (OBIS, https://obis.org) and the Global Biodiversity Information Facility (GBIF, https://www.gbif.org).

This expedition was supported by the Helmholtz Research Programme “Changing Earth – Sustaining our Future” Topic 6, Subtopics 1, 2 and 3.

In all publications based on this expedition, the Grant No. AWI_PS138_01 will be quoted and the following publication will be cited:

Alfred-Wegener-Institut Helmholtz-Zentrum für Polar- und Meeresforschung (2017) Polar Research and Supply Vessel POLARSTERN Operated by the Alfred-Wegener-Institute. Journal of large-scale research facilities, 3, A119. http://dx.doi.org/10.17815/jlsrf-3-163.

5.4 Meiofauna, microbial communities and biogeochemical parameters

Work at sea

A TV-guided multiple corer (TV-MUC, Fig. 5.4.1) was used to retrieve undisturbed sediment cores at all ice stations (Fig. 5.4.2); the TV-MUC was usually deployed two times at each ice station (Tab. 5.4.1). Low-resolution videos are available for all deployments, except for the first three deployments at ice station 1. On board, the sediment cores were documented and further processed for a variety of different analyses. Cores were subsampled in three depth layers (0 – 1 cm, 1 – 5 cm, 5 – 10 cm) using a custom-made core extruder and a steel plate. Sediment samples were further processed in the cooling container at 0°C (biogeochemistry and microbiology) or on deck (meiofauna). Subsamples were fixed for a range of meiofauna, microbiological and biogeochemical analyses that will be conducted in the home laboratory (Appendix Tab. A.6).

Replicate cores (3 – 5) were sampled for biogeochemistry and microbiology. This includes samples for microbial DNA/RNA extraction, microbial cell counts, phospholipid analyses, porosity, and the measurement of total organic carbon (Tab. 5.4.2). In addition, pore water was extracted from 2 cores per station using rhizones (0.2 µm) at the following resolution: the first ten centimeters in 1 cm resolution, 14 – 15 cm, 19 – 20 cm; additionally bottom water was sampled from the overlying water in the MUC cores. Porewater samples were fixed for the analysis of nutrients, DIC (dissolved inorganic carbon), alkalinity, and iron in the home laboratory. Measurements of extracellular enzymatic activities (beta-glucosidase, chitobiase, aminopeptidase, esterase) and chlorophyll pigment contents, i.e. chlorophyll-a and phaeopigments (as a proxy of organic matter availability) were conducted directly on board and measured according to Bienhold et al. 2022.

Three replicate cores were sampled and fixed for morphological (4 % buffered formalin) and molecular (95 % ethanol) analyses of meiofauna. Sample processing, identification and further analyses will be conducted in the home laboratories.

Additional cores were dedicated to *ex-situ* microprofiling on board (see section 5.5).

One core per station was sampled (upper 10 cm in bulk) and stored in aluminum foil at -20°C for later microplastic analyses (collaboration Melanie Bergmann, AWI).

Fig. 5.4.1: TV-guided Multicorer (TV-MUC) with 12 sediment cores. © Esther Horvath

Fig. 5.4.2: Sediment cores retrieved with the TV-MUC. © Esther Horvath

Tab. 5.4.1 Overview of Multicorer stations during PS138

Station	Date	Ice station	Latitude	Longitude	Depth [m]	Cores retrieved	Comment
PS138_15-1	2023-08-09	1	84.031516	31.708245	3987	10	
PS138_16-1	2023-08-09	1	84.000764	32.031351	3987	0	MUC did not close, no samples
PS138_28-1	2023-08-12	1	83.861852	33.55526	4035	11	
PS138_35-1	2023-08-16	2	84.911801	80.244023	3736	12	Many Melosira/algae aggregates in OFOBS. No aggregates retrieved in MUC cores
PS138_36-1	2023-08-16	2	84.90917	80.235543	3735	12	Melosira algae patches seen in OFOBS dive. Also with TV-MUC, but no algae retrieved in cores
PS138_59-1	2023-08-20	3	84.690258	107.301532	3726	9	Many algae patches at seafloor. Some Kolgas.
PS138_60-1	2023-08-20	3	84.685294	107.309302	3748	8	Many algae at seafloor
PS138_76-1	2023-08-24	4	82.912533	130.096683	4156	10	Many sponges!! Some anemones and a few Kolgas. Few algae patches.
PS138_77-1	2023-08-24	4	82.911933	130.217807	4154	10	No algae, but white patches on seaflooor. Anemones, sea cucumbers and a red amphipod following the light.
PS138_98-1	2023-08-27	5	85.049803	130.080338	4301	12	Many algae patches at the seafloor. Also many large white spots. Many anemones, sea cucumbers (Kolga). Mounds; in later OFOBS dives identified as belonging to spoon worms.
PS138_99-1	2023-08-27	5	85.04607	130.258397	4297	11	Many algae and white patches at seafloor. Mounds. Kolga, but not too many. Elpidia?
PS138_130-1	2023-09-03	6	88.494735	111.829615	4329	11	Many Kolgas and white patches at seafloor. One anemone and some small white sponges.
PS138_131-1	2023-09-03	6	88.494502	111.901256	4328	11	Many Kolgas, like PS138_130-1. Some anemones and some small white sponges
PS138_156-1	2023-09-08	7	89.941775	49.900195	4239	12	North Pole. Anemones, spoonworm mounds, Lebensspuren, amphipods
PS138_157-1	2023-09-08	7	89.937302	47.459924	4241	10	North Pole. Anemones, amphipods, no algae at seafloor

Station	Date	Ice station	Latitude	Longitude	Depth [m]	Cores retrieved	Comment
PS138_161-1	2023-09-09	7	89.906094	8.342745	4242	9	North Pole. Anemones, Lebensspuren, rarely small white balls (sponges?)
PS138_181-1	2023-09-13	8	87.900354	58.804405	4373	5	Few Kolgas, many white patches, mounds. At least 2 cores did not close.
PS138_182-1	2023-09-14	8	87.897831	58.325756	4365	9	Many white patches, small mounds, few Kolgas, sponge stalks, anemones
PS138_208-1	2023-09-18	9	85.492434	60.102286	3884	12	Small (dark) algae patches, anemones, no/ very few holothurians, tube like structure, one small Kolga
PS138_209-1	2023-09-18	9	85.481274	60.167596	3882	11	Many algae patches, few Kolgas, some small white balls (sponges?)

Tab. 5.4.2: Fixation of samples for microbiological and geochemical analyses. AODC – Acridine Orange Direct Counts. FISH – Fluorescence In Situ Hybridization. DIC – Dissolved inorganic carbon.

Method	Total no. of samples (incl. replicates)	Fixation / Storage
Sediment samples		
DNA extraction	134	-20°C
RNA extraction	27	-80°C
Cell counts	134 (AODC); 30 (FISH)	4°C in 4 % formaldehyde (AODC), -20°C in PBS/Ethanol (FISH)
Total organic carbon	134	-20°C
Phospholipids	134	-20°C
Porosity	134	4°C
Chlorophyll pigments	188	-20°C dark (most directly measured on board)
Extracellular enzymatic activities (beta-glucosidase, chitobiase, aminopeptidase, esterase)	4 x 155	measured on board
Meiofauna	92 (morphology) 81 (genetics)	4 % Formaldehyde for morphological analysis -20° in Ethanol for genetic analysis
Porewater samples		
DIC and alkalinity	229	4°C, no headspace
Nutrients	229	-20°C
Iron	229	4°C, in 1 M hydrochloric acid
sulfate/sulfide	229	4°C, in 2 % zinc acetate

Preliminary (expected) results

The retrieved sediment samples will provide further insights into the distribution and function of benthic life (meiofauna, microbes) in the Arctic. Chlorophyll pigment values (chloroplastic pigment equivalents – CPE) decreased with increasing sediment depth (from 0-1 cm to 5-10 cm) and were generally higher compared to 2012. They were on average 0.42 µg/ml in the first sediment horizon (0-1 cm) in 2012, and 0.71 µg/ml in 2023 (Fig. 5.4.3). Chlorophyll-a values however varied only slightly and were on average 0.13 µg/ml (0-1 cm) in both years, resulting in a lower proportion of chlorophyll-a to total chloroplastic pigments, indicating less fresh phytodetritus in 2023 compared to 2012. Estimates of extracellular enzymatic activities were also generally higher in 2023. Molecular analyses of sedimentary DNA will take place in the home laboratory and will be used to determine benthic microbial community composition across the central Arctic Ocean in comparison to samples from PS80 in 2012, and in the context of the different sea ice (see Chapter 2) and surface ocean conditions, including their physics, chemistry and biology (Chapters 3 and 4).

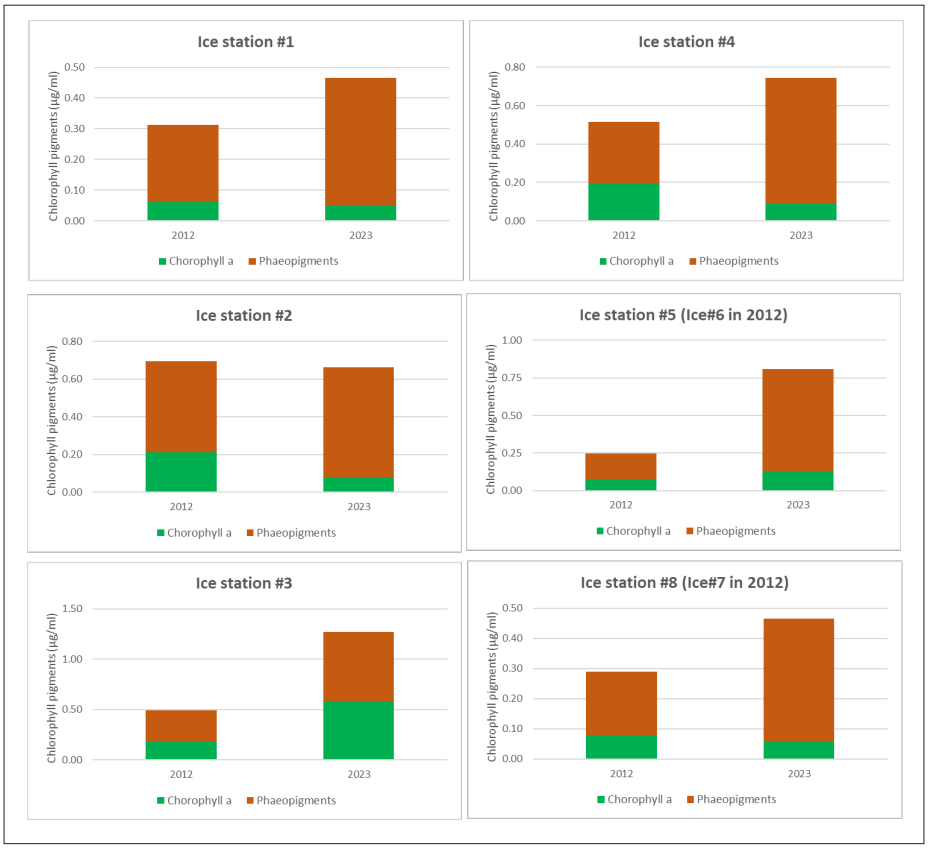

Fig. 5.4.3: Chlorophyll pigment measurements at those ice stations that were visited in both 2012 and 2023. Values are the average of 5 replicate measurements; standard deviations are not shown. Note that for Ice station #3, two of the replicate samples had much higher chlorophyll-a values (>1 µg/ml) compared to the other samples (<0.2 µg/ml), also coinciding with higher phaeopigment values, resulting in the average high chloroplastic pigment value.

Data management

Environmental data will be archived, published and disseminated according to international standards by the World Data Center PANGAEA Data Publisher for Earth & Environmental Science (https://www.pangaea.de) within two years after the end of the expedition at the latest.

By default, the CC-BY license will be applied.

Molecular data (DNA and RNA data) will be archived, published and disseminated within one of the repositories of the International Nucleotide Sequence Data Collaboration (INSDC, www.insdc.org) comprising of EMBL-EBI/ENA, GenBank and DDBJ.

This expedition was supported by the Helmholtz Research Programme “Changing Earth – Sustaining our Future” Topic 6, Subtopics 1, 2 and 3.

In all publications based on this expedition, the Grant No. AWI_PS138_01 will be quoted and the following publication will be cited:

Alfred-Wegener-Institut Helmholtz-Zentrum für Polar- und Meeresforschung (2017) Polar Research and Supply Vessel POLARSTERN Operated by the Alfred-Wegener-Institute. Journal of large-scale research facilities, 3, A119. http://dx.doi.org/10.17815/jlsrf-3-163.

5.5 *In-situ* benthic fluxes

Work at sea

The amount of organic material that escapes mineralization and is retained in the sediment record is the single most important factor determining the long-term O2 levels of the global ocean. Today we generally have a relatively good understanding of the processes that contribute to the mineralization of organic material and factors regulating the burial efficiency of organic material of most oceanic environments. However, the seafloor of the Arctic Ocean is largely unexplored but appears to be seriously impacted by climate change.

We planned to perform *in-situ* measurements using three moored Flux-Lander Systems, designed for under permanent sea-ice cover operations, to study benthic oxygen uptake and fluxes at the sediment water interface (Wenzhöfer & Glud; 2002; Boetius et al. 2013). Each Lander was equipped with one 2-axis microprofiler and 2-axis deep-profiler (Fig. 5.5.1).

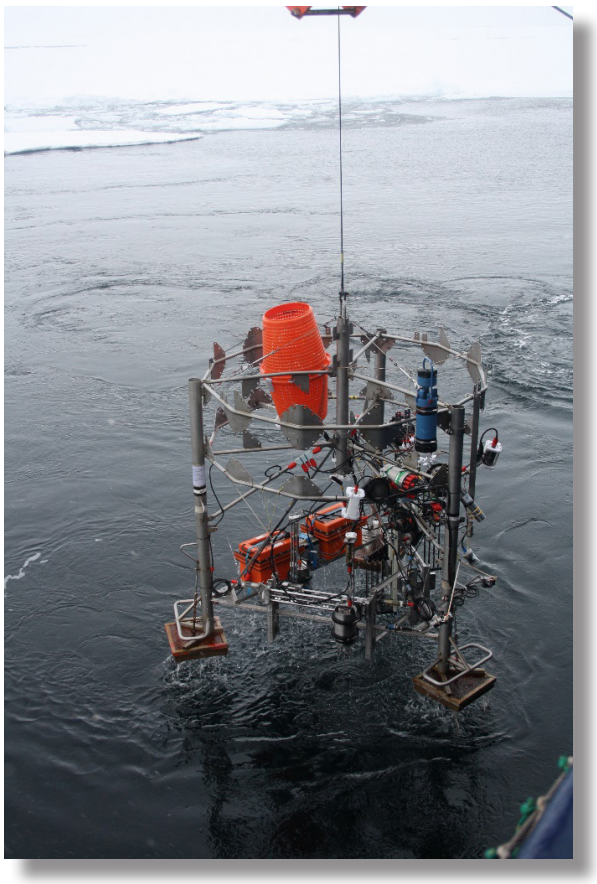

Fig. 5.5.1: Flux-Lander system recovery after a 24-h deployment. Due to high sea-ice concentration only one system was deployed that was equipped with two 2-axis mircroprofilers and two 2-axis fiberoptical deep profilers (Photo: Frank Wenzhöfer).

Both 2-axis profiler systems were used to perform multiple high-resolution vertical oxygen profiles across the sediment-water interface at different positions along a 50 cm long horizontal stretch. The 2-axis microprofilers were equipped with up to 10 custom-built O2 electrodes with typical tip diameters of < 50 µm. In addition, 1-2 conductivity sensors and 1 temperature sensor were mounted to the systems. Measurements across the sediment-water interface and within the upper sediment layer were performed with a vertical resolution of 100 µm and extended over a total length of 15 – 25 cm. The 2-axis fiberoptical deep profilers were used to record multiple, deeper oxygen profiles at lower spatial resolution. The deep profilers were equipped with 8 fiberoptical oxygen sensors based on 430 µm diameter bare fiber oxygen

sensors (OXB430-SUB, Pyroscience, Aachen, Germany). These were inserted into 0.8 µm diameter hypodermic needles attached to the end of 6 mm diameter carbon reinforced plastic tubes (total length approx. 430 mm). Individual profiles reached total lengths of typically 25 – 30 cm at a vertical resolution of 250 µm. All oxygen electrodes and fiberoptical sensors were calibrated before each deployment using air-saturated and chemically deoxygenated water kept at 0°C. Data recorded with both 2-axis profiler systems are used to quantify the diffusive oxygen uptake (DOU), which is generally assigned to microbial respiration. Depending on the sea-ice concentration present at the different stations, one or two lander systems were deployed (Tab. 5.5.1). In cases, where only one lander was used, two microprofilers and two deep profilers were attached to the lander frame. Fig. 5.5.2 shows the setup during deployment PS138_136-1 on station Ice-6.

Fig. 5.5.2 and fiberoptical profiler (right) and deep profiler (left) recording in-situ profiles at station Ice-6 (PS138_136-1)

In-situ benthic microprofiler measurements were complemented by *ex-situ* measurements performed in the laboratory. Three or more replicate oxygen profiles of approx. 60 mm length were recorded in Multicorer sediment cores from all stations (see overview of Multicorer samples in Tab. 5.5.1). Fiberoptical sensors with 50 µm tips (retractable fiber oxygen microsensor OXR50, Pyroscience, Aachen, Germany) were lowered at 100 µm steps into the sediments using lab microprofiling equipment and software provided by the same company (1-axis motorized micromanipulator MU1, optical oxygen meter FireSting®-O2, micro-profiling software Profix). In most cores, one up to 20 cm long profile was additionally obtained at 250 µm vertical resolution. Profiling was performed with a modified version of the fiberoptical profiler used with the moored landers in situ using the same sensors (430 µm diameter bare fiber oxygen sensors (OXB430-SUB, Pyroscience) inserted into 0.8 µm diameter hypodermic needles attached to 6mm diameter carbon reinforced plastic tubes (L~430 mm). During the

measurements the cores were kept in a water bath kept at 1° C, i.e., close to *in-situ* bottom water temperature (approx. -0.7° C) by means of a Refrigerated Circulating Water Bath (ECO series, LAUDA GMBH & CO. KG, Lauda-Königshofen, Germany). The overlying water in the cores was kept mixed by a stream of cold air blown at the water surface through a hypodermic needle attached to the rim of the core.

Preliminary (expected) results

In-situ oxygen profiles were completed at all ice-stations resulting in a total of 14 deployments (Tab. 5.5.1). Unfortunately, lander #1, deployed at station Ice-1 in harsh wind conditions, could not be recovered.

Tab. 5.5.1: Overview of all lander deployments

		DShip*						Posidonia (USBL)			
Deployment & station		**Event time***	**Device operation**	**Action**	**Latitude (N)***	**Longitude (E)***	**Depth (m)***	**Latitude (N)**	**Longitude (E)**	**Depth releaser (m) + 5m**	**Lander ID**
1	Ice-1	09.08.23 14:03	PS138_14-1	deployed	83° 57.627‘	032° 08.150‘	3984	83° 57.281‘	032° 04.281‘	*no data*	#1
		Recovery failed									
2	Ice-1	10.08.23 12:56	PS138_18_1	deployed	83° 53.948‘	033° 10.438‘	3977	*no data*	*no data*	*no data*	#2
		11.08.23 17:19	PS138_18_1	released	83° 55.261‘	033° 22.688‘	3995				
3	Ice-2	15.08.23 13:26	PS138_33-1	deployed	84° 56.246‘	080° 02.739‘	3724	84° 56.252‘	80° 03.344‘	3672	#2
		16.08.23 11:28	PS138_33-1	released	84° 56.146‘	080° 03.863‘	*no data*				
4	Ice-3	20.08.23 10:17	PS138_57-1	deployed	84° 42.415‘	107° 39.829‘	3971	84° 42.388‘	107° 40.191‘	3965	#2
		21.08.23 07:52	PS138_57-1	released	84° 42.480‘	107° 40.634‘	3971				
5	Ice-3	20.08.23 13:47	PS138_58-1	deployed	84° 43.368‘	107° 27.835‘	3971	84° 43.267‘	107° 28.281‘	3956	#3
		22.08.23 07:27	PS138_58-1	released	84° 43.330‘	107° 28.848‘	3971				
6	Ice-4	25.08.23 10:22	PS138_83-1	deployed	82° 59.694‘	129° 56.361‘	4163	82° 59.604‘	129° 55.374‘	4153	#2
		26.08.23 07:02	PS138_83-1	released	82° 59.669‘	129° 56.088‘	4162				
7	Ice-4	25.08.23 14:26	PS138_84-1	deployed	82° 59.522‘	130° 01.247‘	4161	82° 59.511‘	130° 01.091‘	4153	#3
		26.08.23 12:13	PS138_84-1	released	82° 59.509‘	130° 02.056‘	4162				
8	Ice-5	29.08.23 11:12	PS138_107-1	deployed	85° 01.768‘	130° 33.137‘	4298	85° 01.782‘	130° 32.680‘	4287	#2
		30.08.23 09:02	PS138_107-1	released	85° 01.695‘	130° 31.900‘	4294				
9	Ice-5	29.08.23 15:53	PS138_108-1	deployed	85° 01.749‘	130° 11.993‘	4300	85° 01.555‘	130° 14.004‘	4288	#3
		30.08.23 15:06	PS138_108-1	released	85° 01.774‘	!30° 13.169‘	4296				

Deployment & station		DShip* Event time*	Device operation	Action	Latitude (N)*	Longitude (E)*	Depth (m)*	Posidonia (USBL) Latitude (N)	Longitude (E)	Depth releaser (m) + 5m	Lander ID
10	Ice-6	04.09.23 10:35	PS138_136-1	deployed	88° 27.985‘	113° 44.055‘	4319	88° 28.075‘	113° 44.601‘	4309	#2
		05.09.23 09:45	PS138_136-1	released	88° 28.141‘	113° 50.976‘	4318				
11	Ice-6	04.09.23 14:11	PS138_137-1	deployed	88° 27.116‘	113° 58.767‘	4326	88° 27.115‘	114° 00.539‘	4307	#3
		06.09.23 06:59	PS138_137-1	released	88° 27.140‘	113° 58.430‘	4314				
12	Ice-7	09.09.23 09:20	PS138_160-1	deployed	89° 55.212‘	013° 53.713‘	4241	89° 55.239‘	015° 18.020‘	4230	#2
		10.09.23 15:22	PS138_160-1	released	89° 55.210‘	014° 13.857‘	4244				
13	Ice-8	14.09.23 10:50	PS138_185-1	deployed	87° 52.951‘	057° 02.544‘	4380	87° 52.787‘	057° 04.013‘	4364	#2
		15.09.23 12:40	PS138_185-1	released	87° 52.775‘	057° 05.094‘	4376				
14	Ice-9	19.09.23 10:29	PS138_212-1	deployed	85° 27.610‘	060° 03.580‘	3882	85° 27.671‘	060° 03.255‘	3875	#2
		20.09.23 16:50	PS138_212-1	released	85° 27.714‘	060° 01.424‘	3882				

** Station book / D-Ship times and positions in the table refer to Lander deployment (i.e., instrument's mooring line disconnected from the ship shortly after arrival at the seafloor) and release (sub-surface buoy is called acoustically to the surface to connect to mooring line and retrieve instrument). These station protocol entries are reported here as they most closely frame the instrument's deployment at the seafloor. Consequently, times and positions deviate from the Pangaea events reported in the PS138 station list that refer to start and end of the station work (i.e., start of mooring deployment until instrument recovery on deck).*

In-situ high-resolution microprofiles in the top sediment layer were performed at all stations and are used to calculate the oxygen uptake (DOU) across the sediment-water interface using the linear gradient in the diffusive boundary layer (DBL) above the sediment (Fig. 5.5.3). As measured in 2012, oxygen consumption was generally low and largely limited to the uppermost millimeters to centimeters.

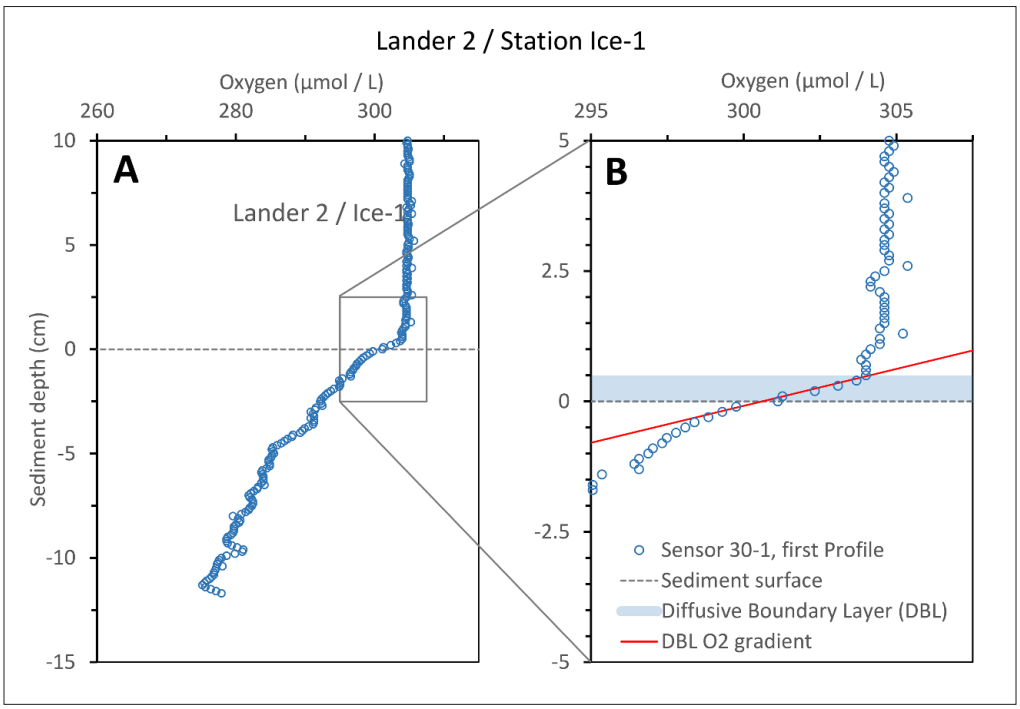

Fig. 5.5.3: A. Oxygen microprofile measured at ice station 1. B. Linear oxygen concentration gradient within the DBL used for DOU calculations.

Long *in-situ* profiles were successfully recorded with the 2-axis deep profiler at all ice stations except Ice-1. None of the profiles reached the oxygen penetration depth (i.e., the depth where oxygen is depleted) except for station Ice-9 (Lander mooring station PS138_212-1). In all fiberoptical profiles recorded at that station, oxygen showed an almost linear decrease in the top 15 cm and stayed at zero / very low concentration deeper down. At all other stations, a simple extrapolation of the profiles suggests oxygen penetration depths in the range of 0.5 to 1.2 m. At several stations, most pronounced at station Ice-3 and Ice-5, subsurface excursions to lower oxygen concentrations were observed with rounded bulges reaching down 5 to 10 cm (e.g., blue profile in Fig. 5.5.4). These bulges as well as sharper subsurface minima (e.g., green profile in Fig. 5.5.4) likely originate from elevated oxygen respiration rates in response to a recent deposition of organic matter at the sediment surface. A more detailed analysis of the data, including model-based assessments of volumetric respiration rates in different sediment horizons, is pending.

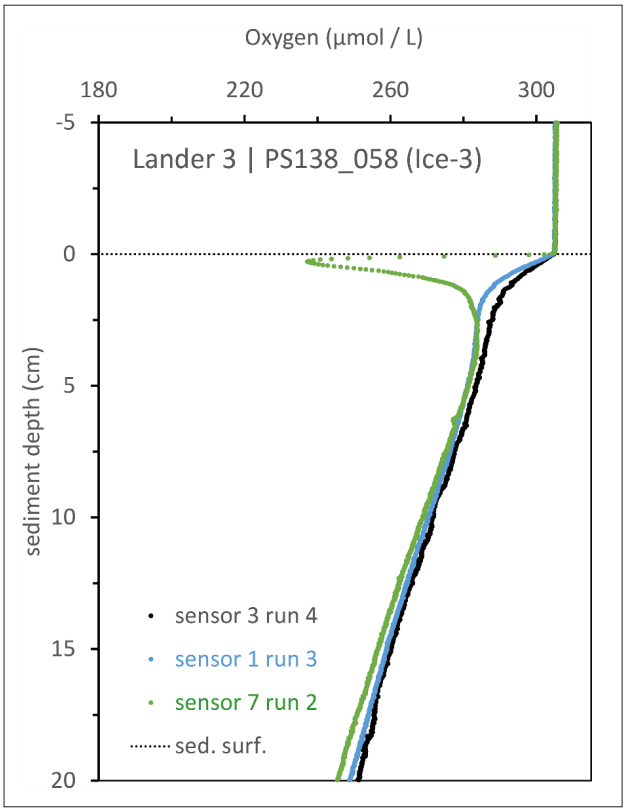

Fig. 5.5.4: Examples of profiles recorded in-situ at station Ice-3 during Lander 3 deployment PS138_058-1 by fiberoptical microprofiler. The subsurface excursions to lower oxygen levels in the colored profiles are indicative of a previous (blue) and very recent (green) deposition of organic matter.

Ex-situ profiles have been recorded to investigate specific features and for comparison to in situ profiles to assess lateral variability. Pronounced features observed in situ profiles from specific stations (e.g., shallow oxygen penetration at station Ice-9, sub-surface oxygen minima, especially at stations Ice-3 and -5) were similarly observed in the measurements obtained in Multicorer cores although sometimes altered (e.g., by oxygen levels gradually increasing in the overlying water upon air exposure during measurements). This added evidence that characteristics in oxygen distribution observed in lander deployments were also found at neighbouring sites (i.e., Multicorer sampling positions). *Ex-situ* profiles obtained in cores from stations Ice-3 (PS138_060-1, core7) and Ice-5 (PS138_098-1, core07 and PS138_099-1, core 10) with visible traces of algal patches at the surface showed that phytodetritus deposition events can lead to localized oxygen depletion in the upper sediment layer (Fig. 5.5.5). Observations of oxygen depletion to zero close to the sediment surface were missing in the in situ data obtained at random locations.

The results will add to our growing database of microbial carbon mineralization in deep-sea (Jørgensen et al. 2022) and polar regions (Boetius et al. 2013) and allow for comparisons over decadal time scales.

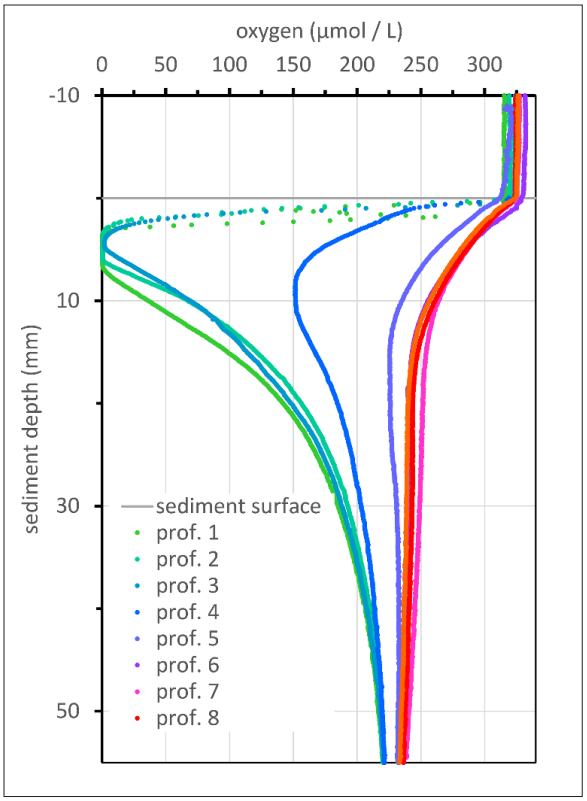

Fig. 5.5.5: Oxygen profiles obtained in a small algal patch (profiles 1-3) and at increasing lateral distance from the patch (profile 4: ~1.5 cm, profile 5: ~3 cm, profile 6: ~4.5 cm, profile 7, 8, and 9: ~6 cm) at the surface of core 7 from Multicorer deployment PS138_098-1. The first measurements took place in the overlying water above the sediment water interface (horizontal grey line).

Data management

Environmental data will be archived, published and disseminated according to international standards by the World Data Center PANGAEA Data Publisher for Earth & Environmental Science (https://www.pangaea.de) within two years after the end of the expedition at the latest. By default, the CC-BY license will be applied.

This expedition is supported by the Helmholtz Research Programme “Changing Earth – Sustaining our Future” Topic 6, Subtopics 1, 2 and 3.

In all publications based on this expedition, the **Grant No. AWI_PS138_01** will be quoted and the following publication will be cited:

Alfred-Wegener-Institut Helmholtz-Zentrum für Polar- und Meeresforschung (2017) Polar Research and Supply Vessel POLARSTERN Operated by the Alfred-Wegener-Institute. Journal of large-scale research facilities, 3, A119. http://dx.doi.org/10.17815/jlsrf-3-163.

References

Bienhold C, Schourup-Kristensen V, Krumpen T, Nöthig EM, Wenzhöfer F, Korhonen M et al. (2022) Effects of sea ice retreat and ocean warming on the Laptev Sea continental slope ecosystem (1993 vs 2012). Frontiers in Marine Science 9. https://doi.org/10.3389/fmars.2022.1004959

Boetius A, Albrecht S, Bakker K, Bienhold C, Felden J, Fernández-Méndez M, Hendricks S, Katlein C, Lalande C, Krumpen T, Nicolaus M, Peeken I, Rabe B, Rogacheva A, Rybakova E, Somavilla R, Wenzhöfer F, and the RV Polarstern ARK27-3-Shipboard Science Party (2013) Export of Algal Biomass from the Melting Arctic Sea Ice. Science 339:1430–1432. https://doi.org/10.1126/science.1231346

Brenke N (2005) An epibenthic sledge for operations on marine soft bottom and bedrock. Marine Technology Society Journal 39(2):10-21.

Golikov AV, Stauffer JB,Schindler SV, Taylor J, Boehringer L, Purser A,Sabirov RM, Hoving H-J. (2023) Miles down forlunch: deep-seain situobservations of Arcticfinned octopodsCirroteuthis muellerisuggestpelagic–benthic feeding migration. Proc. R. Soc. B290: 20230640. https://doi.org/10.1098/rspb.2023.0640

Hessler RR, Jumars PA (1974) Abyssal community analysis from replicate box cores in the central North Pacific. Deep-Sea Res 21:185– 209.

Jørgensen BB, Wenzhöfer F, Egger M, Glud RN (2022) Sediment oxygen consumption: Role in the global marine carbon cycle. Earth-Science Reviews 228:103987. https://doi.org/10.1016/j.earscirev.2022.103987

Morganti T, Purser A, Rapp HT, German C, Jakuba MV, Hehemann L, Blendl J, Slaby B, Boetius A (2021) In situ observation of sponge trails indicate common sponge locomotion in the deep central Arctic. Current Biology 31, 368-370.

Morganti T, Slaby B, De Kluijver A, Purser A, Busch K, Franzenburg S, Hentschel U, Rapp H T, Middelburg J, Boetius A (2022) Giant sponge grounds of Arctic seamounts apparently associated with extinct seep life (Langseth Ridge, 87°N, 61°E). Nature Communications 13, https://doi.org/10.1038/s41467-022-28129-7

Purser A, Marcon Y, Dreutter S, Hoge U, Sablotny B, Hehemann L, Lemburg J, Dorschel B, Biebow H, Boetius A (2019) Ocean Floor Observation and Bathymetry System (OFOBS): A New Towed Camera/Sonar System for Deep-Sea Habitat Surveys. IEEE Journal of Oceanic Engineering 44(1):87–99. https://doi.org/10.1109/JOE.2018.2794095

Rybakova E, Kremenetskaia A, Vedenin A, Boetius A, Gebruk A (2019) Deep-sea megabenthos communities of the Eurasian Central Arctic are influenced by ice-cover and sea-ice algal falls. PLoS One 14(7). https://doi.org/10.1371/journal.pone.0211009

Schoening T, Durden JM, Faber C, Felden J, Heger K, Hoving H-JT, Kiko R, Köser K, Krämmer C, Kwasnitschka T, Möller KO, Nakath D, Nass A, Nattkemper TW, Purser A, Zurowietz M (2022) Making marine image data FAIR. Sci. Data 9: 414. https://doi.org/10.1038/s41597-022-01491-3

Soltwedel T (2013) The expedition of the research vessel "Polarstern" to the Arctic in 2012 (ARK-XXVII/2). Berichte zur Polar und Meeresforschung 658. Bremerhaven: Alfred Wegener Institute for Polar and Marine Research.

Stratmann T, Simon-Lledo E, Morganti TM, de Kluijver A, Vedenin A, Purser A (2022) Habitat types and megabenthos composition from three sponge-dominated high-Arctic seamounts. Nature Scientific Reports, 12, 20610. https://doi.org/10.1038/s41598-022-25240-z

Wenzhöfer F, Glud RN (2002) Benthic carbon mineralization in the Atlantic: a synthesis based on in situ data from the last decade. Deep-Sea Research, Part I: Oceanographic Research Papers 49(7):1255–1279.

Wenzhöfer F, Lemburg J, Hofbauer M, Lehmenhecker S, Färber P (2016) „TRAMPER - An autonomous crawler for long-term benthic oxygen flux studies in remote deep sea ecosystems" OCEANS 2016 MTS/IEEE Monterey, 1–6. https://doi.org/10.1109/OCEANS.2016.7761217

WoRMS Editorial Board (2023). World Register of Marine Species. Available from https://www.marinespecies.org at VLIZ. Accessed 2023-09-26. https://doi.org./10.14284/170

6. AUTONOMOUS BUOY MEASUREMENTS

Mario Hoppmann[1], Marcel Nicolaus[1], Benjamin Rabe[1], Jacob Allerholt[1], Yusuke Kawaguchi[2], Ivan Kuznetsov[1], Ian Raphael[3], Daniel Scholz[1]
not on board: Olivier Desprez de Gesincourt[4], Joey Voermans[5], Jeff O'Brien[6], Bin Cheng[8], Ruibo Lei[9], Ignatius Rigor[7], Matthieu Labaste[10], Nathalie Sennechael[10]

[1]DE.AWI
[2]JP.UTOKYO
[3]EDU.DARTMOUTH
[4]FR.SHOM
[5]AUS.UMELBOURNE
[6]EDU.WHOI
[7]EDU.UWASHINGTON
[8]FI.FMI
[9]CN.PRIC
[10]FR.LOCEAN

Grant-No. AWI_PS138_03 and AWI_PS138_04

Objectives

The Arctic Ocean is a region of great importance for the ongoing global change. Examples are the significant sea-ice retreat (Intergovernmental Panel on Climate Change, 2022), an unprecedented rise in near-surface air temperature (nearly four times the global rate, Rantanen et al. 2022), and the more recently observed Atlantification in the Eurasian Basin (Polyakov et al. 2017). The Arctic Ocean is also closely linked to the adjacent oceans and seas, hence it has a profound impact on regional and even global ocean circulation patterns, atmospheric temperatures at lower latitudes (Wu et al. 2013), and ultimately, global climate (Koenigk et al. 2007). Pan-Arctic energy and heat budgets and circulation patterns are governed not only by basin-scale forcing, but also by many processes on the meso scale (von Appen et al. 2022) and even by small-scale turbulence (Rippeth and Fine 2022). Autonomous observations have gained more and more importance in the Arctic Ocean in recent times, and they yield great potential to fill many of the current knowledge gaps. Especially the development of advanced ice-tethered (profiling) systems that are able to measure and send data while drifting with the sea ice, have helped immensely to close significant gaps in seasonal and regional observing. Examples of these kinds of instruments include the Woods Hole Oceanographic Institution Ice-tethered Profiler (WHOI-ITP; Toole et al. 2011), the Naval Postgraduate School Autonomous Ocean Flux Buoys (AOFB; Stanton et al. 2012), the Ice-Atmosphere-Ocean Observation System (IAOOS; Athanase et al. 2019), along with several different kinds of sea-ice mass balance buoys (Richter-Menge et al. 2006; Jackson et al. 2013; Planck et al. 2019), CTD-chain buoys (Hoppmann et al. 2022), Snow Buoys (Nicolaus et al. 2021), and spectral radiation stations (Tao et al. submitted). Building on the success of the Multidisciplinary drifting Observatory for the Study of Arctic Climate (MOSAiC) experiment, during PS138 we aim to continuously observe a multitude of variables in the coupled atmosphere-ice-ocean system along the Transpolar Drift. We utilize many of the platforms also deployed during MOSAiC in 2019/20, and we expect that this dataset will provide an exciting opportunity to compare these new results with prior observations. Our buoy deployments are supported by the International Arctic Buoy Programme at the University of Washington (IABP; IABP, 2023), the overarching body coordinating the basin-wide deployments of autonomous ice-tethered instruments across the whole Arctic Ocean region, including regionally focused efforts in selected regions of the Arctic.

Work at sea

During PS138, we deployed the following buoy types:

Snow Buoy

The Snow Buoy (MetOcean, Canada) measures snow depth and basic meteorological parameters (Fig. 6.1a). It consists of a hull containing the batteries and electronics, along with a 1.5 m tall mast that is equipped with a barometer, air temperature sensor, GPS- and iridium antennas, and 4 ultrasonic pingers. During deployment, the hull is placed inside the ice. The 4 pingers mounted on the mast regularly measure the distance to the surface, providing the temporal evolution of snow depth around the buoy. Data is transmitted hourly via the iridium satellite network, and also contributes to the Global Telecommunication System (GTS).

Snow and Ice Mass Balance Array (SIMBA)

The SIMBA (SAMS Enterprise, Scotland) is a thermistor-chain ice mass balance buoy that measures the small-scale temperature gradient through the atmosphere-snow-ice-ocean boundary (Fig. 6.1b). The buoy consists of a small yellow pelicase that houses the battery, main electronics and auxiliary sensors, and a thermistor chain. A typical thermistor chain is 4.80 m long, with 240 thermistors at 0.02 m spacing. Additionally, the chain is equipped with 240 resistors that can actively heat the environment, which enables a better discrimination of the interfaces between the different media. These interfaces can be determined from temperature and heating profiles using manual or automated methods. Auxiliary sensors include GPS, barometric pressure, air temperature and tilt. The data is transmitted via iridium. Most SIMBAs are configured to measure and transmit 4 temperature and one heating profile per day.

CTD chain buoy

The CTD (chain) buoy (Pacific Gyre, USA) consists of an oval surface buoy containing the batteries and electronics, and a 100 m inductive tether with several instruments that measure physical (and optical) properties of the ocean (Fig. 6.1c). Most of the CTD buoys are equipped with 5 SBE37IMP MicroCATs mounted on the tether at 10, 20, 50, 75 and 100 m depth. They record seawater temperature, conductivity/salinity and pressure internally at 2-minute intervals. The surface buoy polls the individual sensors for a measurement every 10 minutes, which is then transmitted via iridium along with the GPS position. The position data is provided to the GTS.

Ocean Profilers (ITP, IAOOS)

The Woods Hole Ice-Tethered Profiler (Fig. 6.1e), and the LOCEAN IAOOS platform (Fig. 6.1c) are composed of a surface unit mounted in/on a large floatation, and an ocean profiler that climbs/descends along an 800 m inductive modem tether. The profilers are equipped with SeaBird CTDs as a standard, and optional optical sensors. Profiles are conducted 1-2 times per day. The data is transmitted via iridium.

Radiation stations

The Radiation Stations are equipped with 3 Ramses (Trios) spectral radiometers to detect incoming, reflected and transmitted light through the ice (Fig. 6.1f). Spectra are recorded every 10 minutes for the non-iridium version (built by AWI), and transmitted every 4 hours by the two iridium versions (built by Bruncin, Croatia). The latter are also equipped with light chains, snow pingers, webcams and sensors for basic meteorological parameters.

Sidekick camera buoy

The Sidekick camera buoy (Pacific Gyre, USA) consists of a pelicase with two integrated webcams facing in opposite directions (Fig. 6.1g). They record images at variable intervals and transmit these via the Iridium network. This buoy was contributed by the International Arctic Buoy Programme.

SIMB

The Seasonal Ice Mass balance Buoy (SIMB, Cryosphere Innovations, USA) is a several meter long cylinder-shaped buoy that detects surface and bottom ice/snow accumulation and ablation using ultrasonic pingers above and below the ice (Fig. 6.1h). Some models are also equipped with a thermistor chain, and a small CTD at the bottom. Data is transmitted at hourly intervals via the Iridium satellite network.

SnowTATOS

The SnowTATOS buoy (Dartmouth College, USA) is a prototype of a newly developed snow pinger network, consisting of several snow pingers mounted on poles and distributed along a transect (Fig. 6.1i). They report their measurements to a close-by base station, which in turn transmits the collected data via irdium.

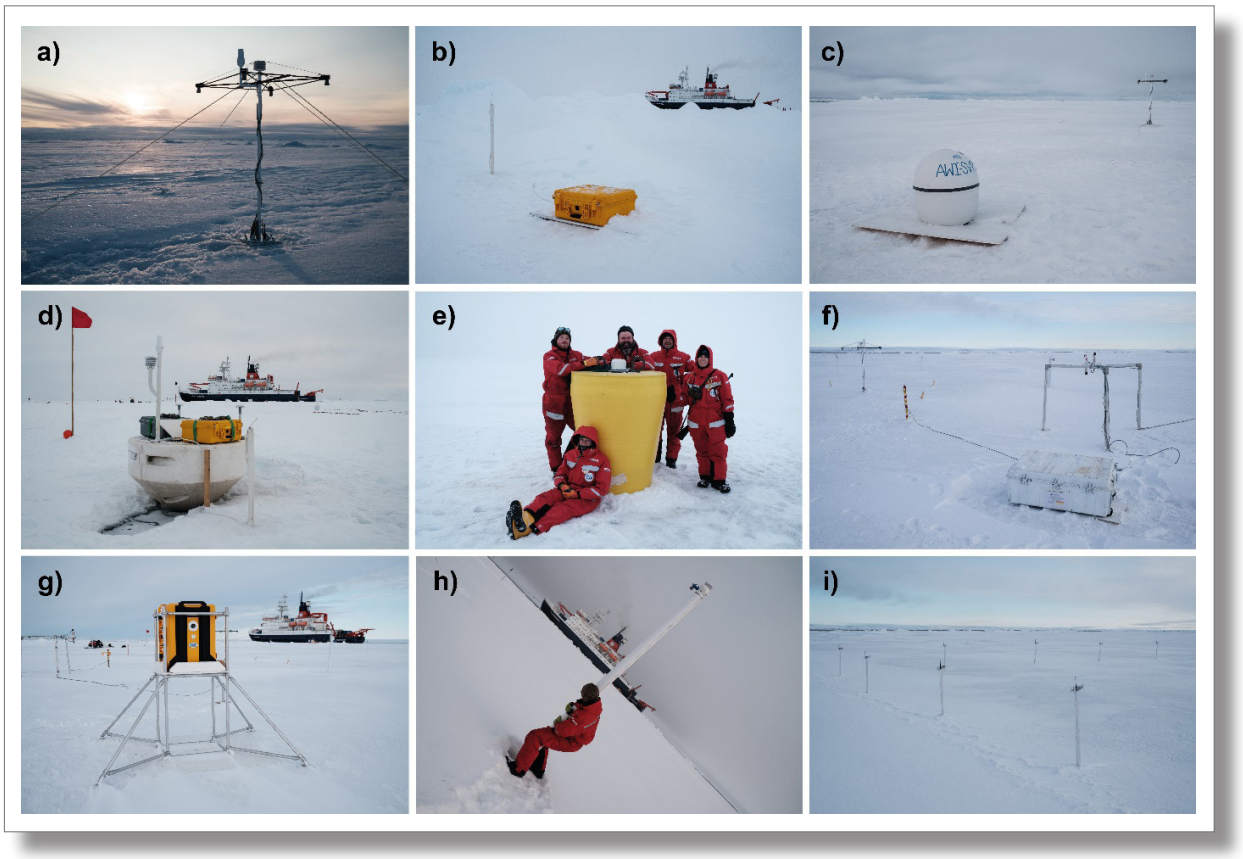

Fig. 6.1: Exemplary buoys deployed during regular ice stations: a) MetOcean Snow Buoy 2023S100; b) SAMS SIMBA 2023T110; c) Pacific Gyre CTD Buoy 2023O22; d) LOCEAN IAOOS; e) WHOI ITP135 (2023W5); f) Bruncin Radiation Station 2023R25; g) Pacific Gyre SideKick Buoy 2023K1; h) Cryosphere Innovations SIMB 2023I10; i) Dartmouth College SnowTATOS

GPS buoys with meteorological sensors

We deployed different types of GPS drifters that were partly also equipped with barometric pressure and surface temperature sensors. These included three TRUSTED buoys (NKE Instrumentation, France) with barometric pressure and high-accuracy surface temperature sensors for satellite remote sensing data validation, 8 SVP-B buoys (MetOcean, Canada) with barometric pressure sensors, and several Universal- and Ice Trackers (Pacific Gyre, USA), two of which also contained barometric pressure sensors. Data of all these buoys are reported to the GTS. The NKE and MetOcean buoys were provided by SHOM/MeteoFrance, and 4 of the Pacific Gyre buoys were contributed by the International Arctic Buoy Programme.

Wavelogger and OpenMetBuoy

We deployed two types of wave buoys. The four waveloggers determine wave height and power spectra using high-accuracy pressure differences, whereas the single OpenMetBuoy detects waves based on an inertial motion unit. These five units were provided by the University of Melbourne.

Buoy deployments during regular ice stations

As part of the regular ice station work programme, a number of autonomous instruments were deployed on each ice floe at a location referred to as “buoy site”. The locations of these sites were determined during the floe exploration phase, and were commonly situated around ~300 m from the ship’s anchoring spot. The site was also chosen not to consist of ice thicker than ~1.5 m, to facilitate the deployment of the instrumentation through holes in the ice. The number and types of instruments varied greatly among ice stations, and was mostly determined based on the region of the ice station, i.e., more instruments were deployed further upstream the Transpolar Drift. Tables 6.1 (ICE1) and 6.2 (ICE2 – ICE9) present a summary of all buoys deployed during regular ice stations.

Revisit Ice floe

The buoy plan also included a revisit of the first ice station (ICE1), to perform repeat surveys and to recover some instruments that only store their data internally. A summary of all deployments during ICE1 is given in Table 6.1 (please see the end oft the chapter). Unfortunately, the floe could not be revisited due to logistical constraints. Consequently, data from several instruments (ADCP, AWS, Radiation Station & Waveloggers) could not be recovered during PS138 and are potentially lost. In case the floe and instruments survive the winter, a recovery could be attempted in 2024.

Post-MOSAiC Distributed Network

As part of the regular ice station plan, we installed a suite of instruments at the original MOSAiC Leg 1 starting location. The installations on the central node (ICE5) included an ITP, a CTD chain buoy, a Bruncin radiation station with 3 RAMSES spectral radiometers and light chain, a Snow Buoy, a Seasonal Ice Mass Balance Buoy with a snow sensor network prototype, a SIMBA-type IMB, and were complemented by a Sidekick camera buoy. A time lapse camera was installed on the ITP in case of a recovery at any given opportunity. Based on the MOSAiC concept, we also complemented the installations on the central node by a small Distributed Network within a radius of ~5 km (ICE5-N1 to ICE5-N3, Tab. 6.3 – please see the end oft the chapter). These side nodes each included a CTD-chain buoy, a Snow Buoy, and a SIMBA-type IMB.

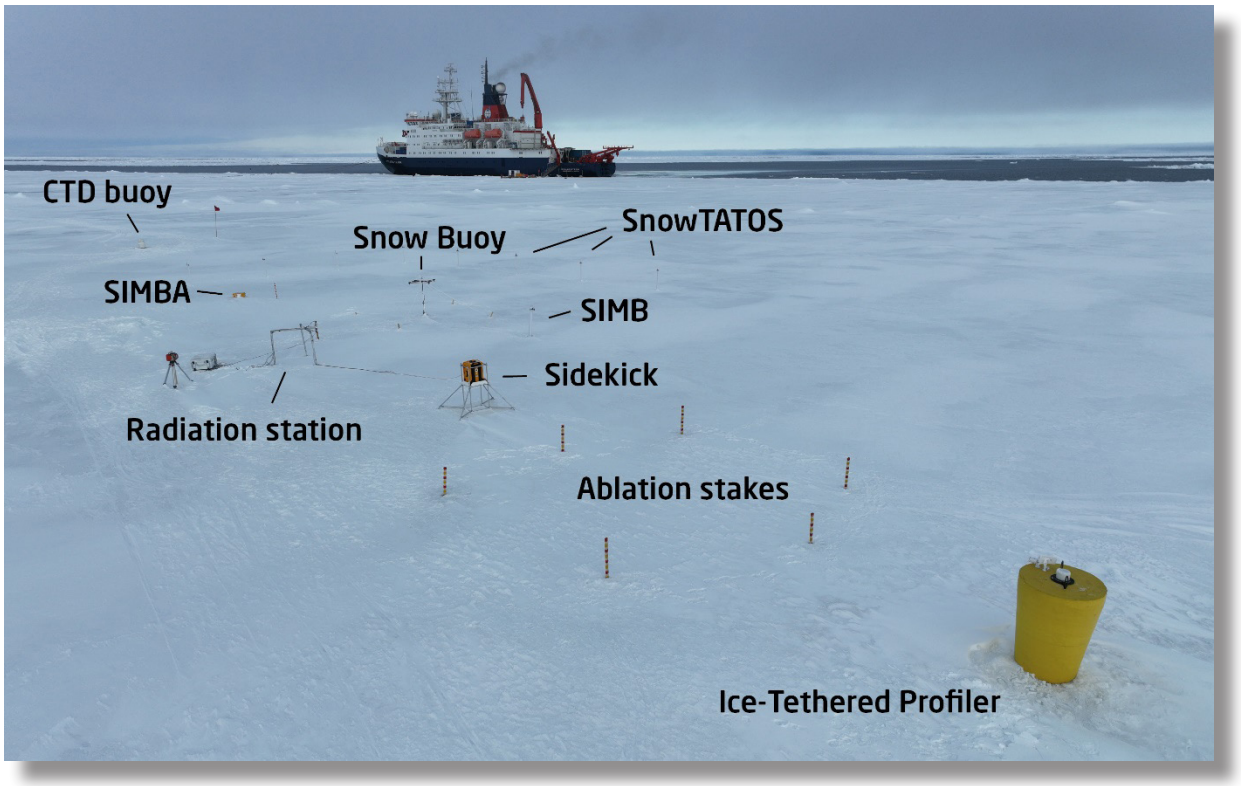

Fig. 6.2: Aerial image of the ICE5 buoy site

Along-track buoy deployments

A number of GPS drifters, partly also equipped with surface temperature and barometric pressure sensors, were deployed along the PS138 cruise track on a regular basis as a complement to the instruments deployed during the ice stations. These buoys included 3 Trusted buoys (NKE, France), 8 SVP-Bs (MetOcean, Canada), 2 Universal Trackers with pressure (Pacific Gyre, USA), 2 Ice Trackers without pressure (Pacific Gyre, USA) and 5 Universal trackers without pressure (Pacific Gyre, USA).

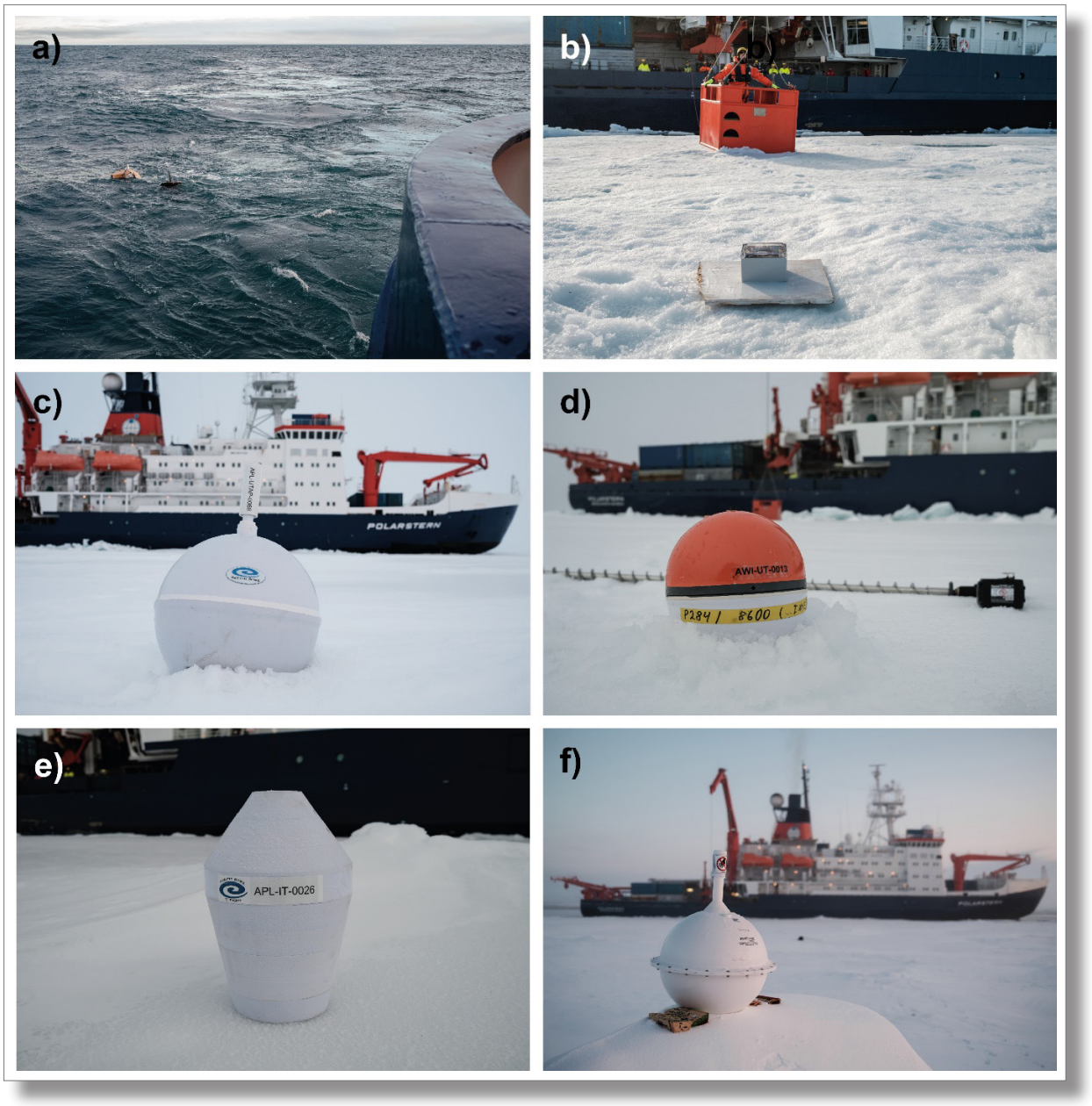

Fig. 6.3: Overview of different GPS buoys deployed during transit: a) NKE Trusted Buoy 2023P270; b) OpenMetBuoy 2023X16; c) Pacific Gyre Universal Tracker 2023P288; d) Pacific Gyre Universal Tracker 2023P284; e) Pacific Gyre Ice Tracker 2023P289; f) MetOcean SVP-B 2023P267

The main aim of these deployments was to achieve a better coverage of barometric pressure measurements in the notoriously under-sampled Arctic Ocean for the improvement of weather forecasts also in lower latitudes. These buoys were deployed in different areas along the cruise track, spaced apart at least 100 km for maximum coverage. They were deployed mostly by mummy chair from the ship. Between these deployments, gaps were filled with regular GPS drifters. Finally, one OpenMetBuoy (OMB), which is equipped with an IMU unit to detect waves in ice, was deployed in the marginal ice zone close to Svalbard during transit into the ice. An overview of the along-track deployments is given in Table 6.4 (please see the end oft the chapter).

Float Your Boat Outreach activity

As part of the FloatYourBoat Outreach activity led by the International Arctic Buoy Programme, we deployed a large number of wooden boats along with our buoys at the North Pole station ICE7. These numbered boats were painted by school classes and students, and are traceable, when found, via floatboat.org. These were complemented by a smaller number of boats painted by cruise participants (the “ARCWATCH” logo in Fig. 6.4).

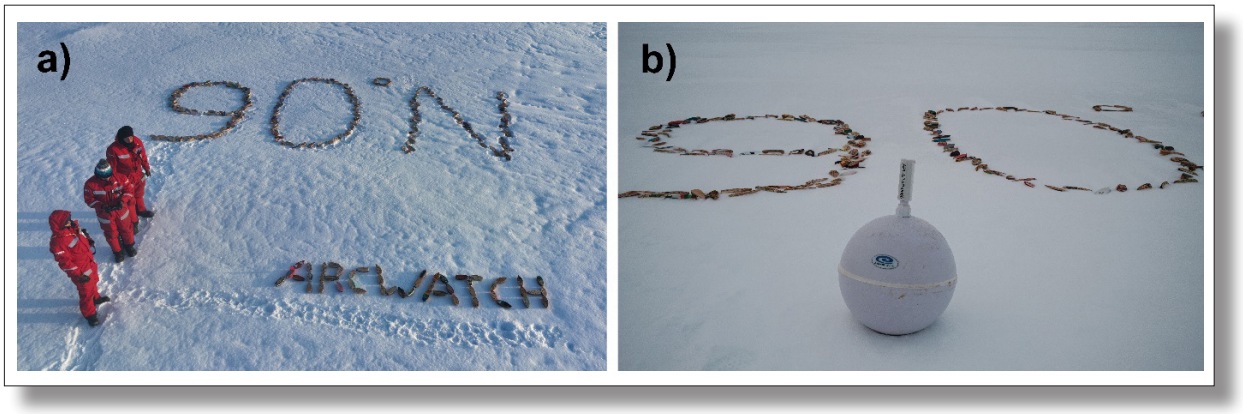

Fig. 6.4: Deployment of FloatBoats close to ICE7 buoy site. a) Aerial view; b) Buoy 2023P286 was deployed right next to the FloatBoats to track their trajectory through the Arctic Ocean.

Please see Tab. 6.1 to 6.4 at the end of the chapter for further information.

Preliminary results

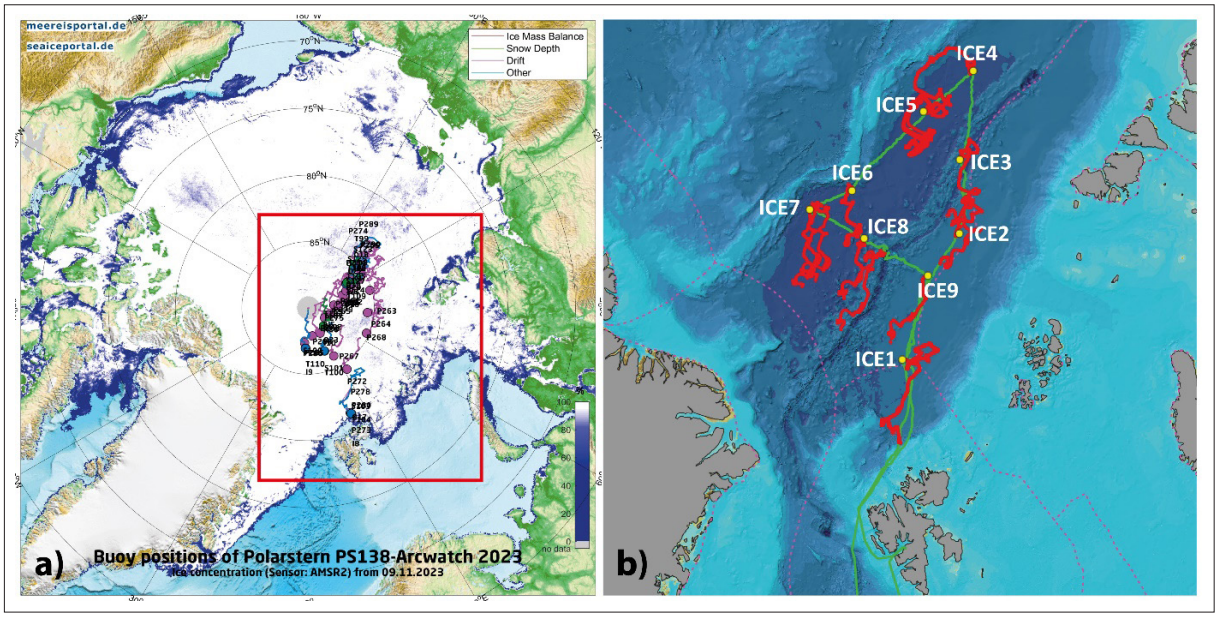

Fig. 6.5: Overview of study area and buoy deployments. a) Map of the entire Arctic Ocean and drift trajectories of all PS138 buoys as of 09 November 2023 (www.meereisportal.de); b) Map of the central Arctic Basin, location of the nine main ice stations (yellow circles), and subsequent drift trajectories of selected buoys deployed on the respective floes (red) as of 07 November 2023. The Polarstern cruise track is indicated in green.

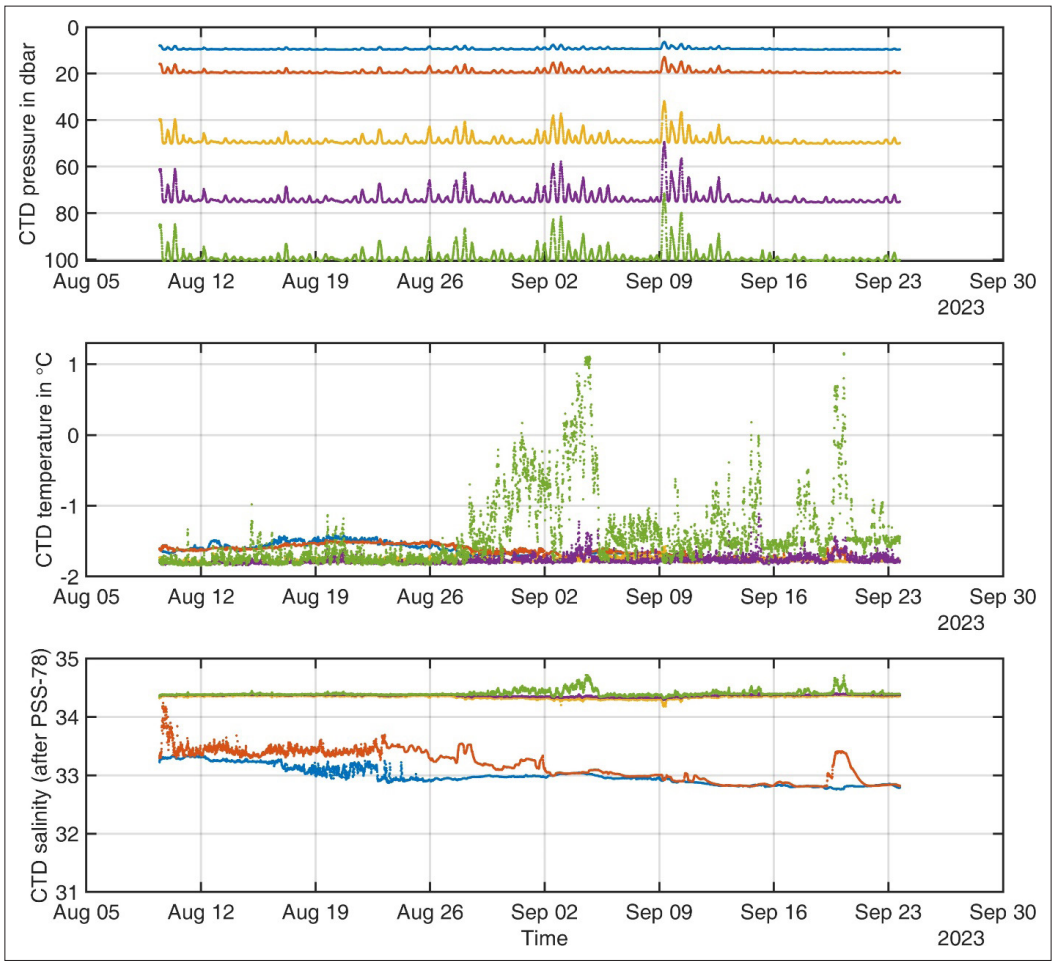

Fig. 6.6: Exemplary oceanographic data transmitted by CTD chain buoy 2023O17 deployed on ICE1

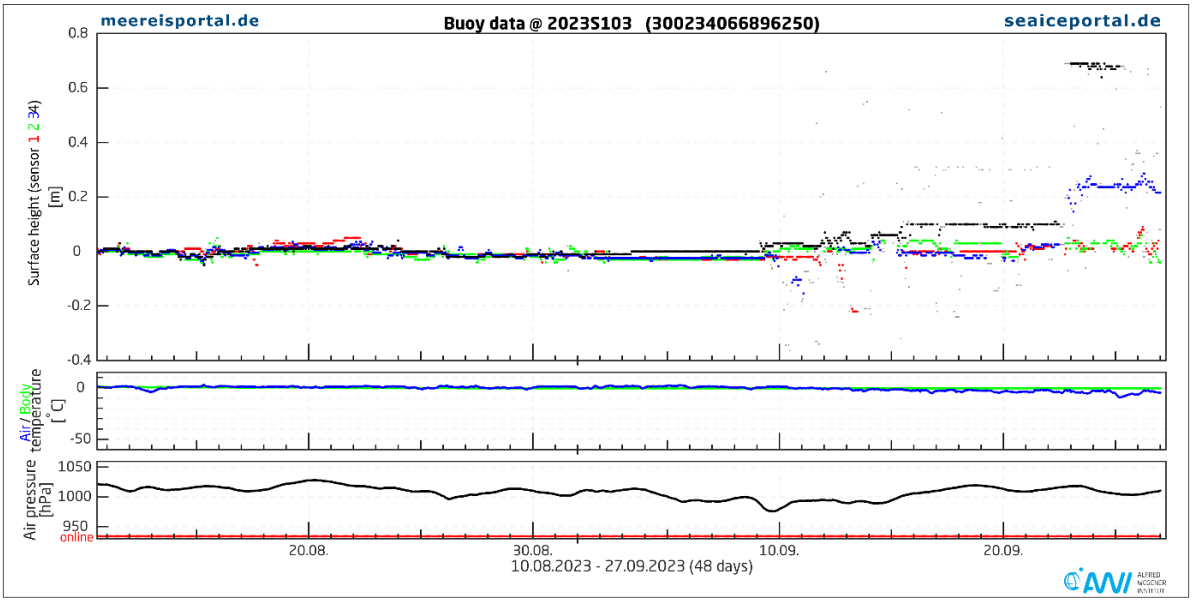

Fig. 6.7: Exemplary data transmitted by Snow Buoy 2023S103 deployed on ICE1

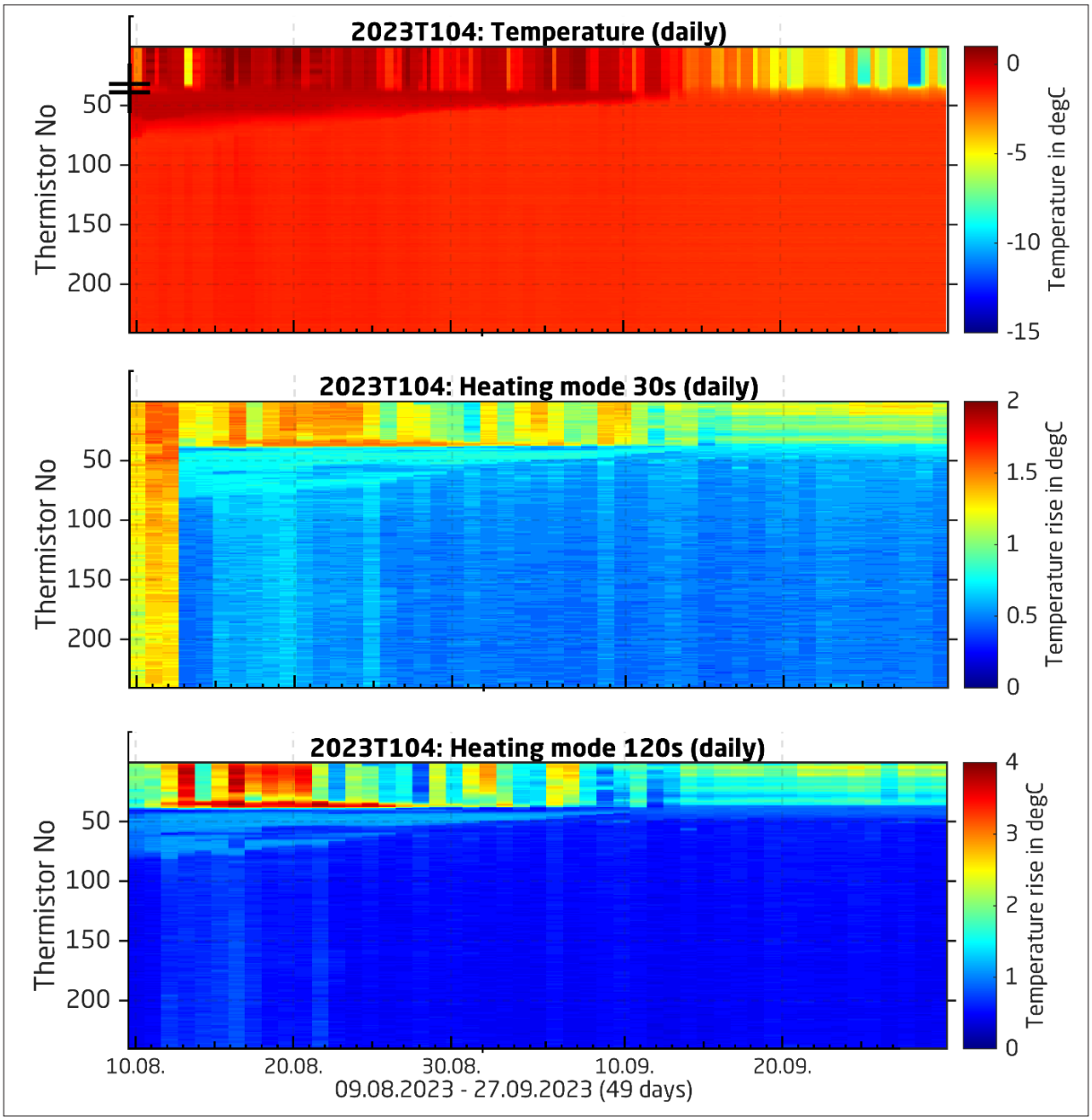

Fig. 6.8: Exemplary data transmitted by SIMBA 2023T104 deployed on ICE1

Data management

All buoy data are transmitted via the iridium satellite network, and decoded and stored on dedicated servers of the respective buoy manufacturer. Most of the data are provided, displayed and updated daily on the data portal section of meereisportal.de. The provided information includes deployment sheets, buoy metadata, maps, and the measured parameters themselves. Additionally, selected buoy data is fed into the database of the International Arctic Buoy Programme (IABP) and the WMO's Global Telecommunications System (GTS), from where they are immediately available for public use.

The data will be archived, published, and disseminated according to international standards and FAIR principles by the World Data Center PANGAEA Data Publisher for Earth & Environmental

Science (https://www.pangaea.de) one year after a buoy ceased operation. By default, the CC-BY license will be applied.

Any other data will be submitted to an appropriate long-term archive that provides unique and stable identifiers for the datasets and allows open online access to the data.

We acknowledge financial support by the USIABP and Ignatius Rigor for covering a large part of the buoys' iridium costs.

This expedition was supported by the Helmholtz Research Programme "Changing Earth – Sustaining our Future" Topic 2, Subtopics 1 and 4

In all publications based on this expedition, the Grant No. **AWI_PS138_03** and **AWI_PS138_04** will be quoted.

References

Athanase M, Sennéchael N, Garric G, Koenig Z, Boles E, Provost C (2019) New Hydrographic Measurements of the Upper Arctic Western Eurasian Basin in 2017 Reveal Fresher Mixed Layer and Shallower Warm Layer Than 2005–2012 Climatology. J Geophys Res Oceans 124(2): 1091–1114. https://doi.org/10.1029/2018JC014701

Hoppmann M, Kuznetsov I, Fang Y-C, Rabe B (2022) Mesoscale observations of temperature and salinity in the Arctic Transpolar Drift: a high-resolution dataset from the MOSAiC Distributed Network. Earth Syst Sci Data 14(11): 4901–4921. https://doi.org/10.5194/essd-14-4901-2022

IABP. 2023: https://iabp.apl.uw.edu/, last accessed 30 June, 2023

Intergovernmental Panel On Climate Change (IPCC) (2022) The Ocean and Cryosphere in a Changing Climate: Special Report of the Intergovernmental Panel on Climate Change. 1st ed. Cambridge University Press. https://doi.org/10.1017/9781009157964

Jackson K, Wilkinson J, Maksym T, Meldrum D, Beckers J, Haas C, Mackenzie D (2013) A Novell and Low-Cost Sea Ice Mass Balance Buoy. Journal of Atmospheric and Oceanic Technology 30(11): 2676–2688. https://doi.org/10.1175/JTECH-D-13-00058.1

Koenigk T, Mikolajewicz U, Haak H, Jungclaus J (2007) Arctic freshwater export in the 20th and 21st centuries: ARCTIC FRESHWATER EXPORT FROM 1900 TO 2100. J Geophys Res 112(G4): https://doi.org/10.1029/2006JG000274

Nicolaus M, Hoppmann M, Arndt S, Hendricks S, Katlein C, Nicolaus A, Rossmann L, Schiller M, Schwegmann S (2021) Snow Depth and Air Temperature Seasonality on Sea Ice Derived From Snow Buoy Measurements. Front Mar Sci 8: 655446. https://doi.org/10.3389/fmars.2021.65544

Planck CJ, Whitlock J, Polashenski C, Perovich D (2019) The evolution of the seasonal ice mass balance buoy. Cold Regions Science and Technology 165: 102792. https://doi.org/10.1016/j.coldregions.2019.102792

Polyakov IV, Pnyushkov AV, Alkire MB, Ashik IM, Baumann TM, Carmack EC, Goszczko I, Guthrie J, Ivanov VV, Kanzow T, et al. (2017) Greater role for Atlantic inflows on sea-ice loss in the Eurasian Basin of the Arctic Ocean. Science 356(6335): 285–291. https://doi.org/10.1126/science.aai8204

Rantanen M, Karpechko AYu, Lipponen A, Nordling K, Hyvärinen O, Ruosteenoja K, Vihma T, Laaksonen A (2022) The Arctic has warmed nearly four times faster than the globe since 1979. Commun Earth Environ 3(1): 168. https://doi.org/10.1038/s43247-022-00498-3

Richter-Menge JA, Perovich DK, Elder BC, Claffey K, Rigor I, Ortmeyer M (2006) Ice mass- balance buoys: a tool for measuring and attributing changes in the thickness of the Arctic sea-ice cover. Ann Glaciol 44: 205–210. https://doi.org/10.3189/172756406781811727

Rippeth T, Fine E (2022) Turbulent Mixing in a Changing Arctic Ocean. Oceanog, in press. https://doi.org/10.5670/oceanog.2022.103

Stanton TP, Shaw WJ, Hutchings JK (2012) Observational study of relationships between incoming radiation, open water fraction, and ocean-to-ice heat flux in the Transpolar Drift: 2002-2010: OCEAN/ICE FLUXES IN THE ARCTIC. J Geophys Res 117(C7): https://doi.org/10.1029/2011JC007871

Tao R, Nicolaus M, Katlein C, Anhaus P, Hoppmann M, Spreen G, Niehaus H, Jäkel E, Wendisch M, Haas C (2023) Seasonality of spectral radiative fluxes and optical properties of Arctic sea ice. Submitted to Elementa.: Science of the Anthropocene

Toole J, Krishfield R, Timmermans M-L, Proshutinsky A (2011) The Ice-Tethered Profiler: Argo of the Arctic. Oceanog 24(3): 126–135. https://doi.org/10.5670/oceanog.2011.64

von Appen W-J, Baumann T, Janout M, Koldunov N, Lenn Y-D, Pickart R, Scott R, Wang Q (2022) Eddies and the Distribution of Eddy Kinetic Energy in the Arctic Ocean. Ocean. https://doi.org/10.5670/oceanog.2022.122

Wu B, Handorf D, Dethloff K, Rinke A, Hu A (2013) Winter Weather Patterns over Northern Eurasia and Arctic Sea Ice Loss. Monthly Weather Review 141(11): 3786–3800. https://doi.org/10.1175/MWR-D-13-00046.1

Tab. 6.1: Overview of buoys deployed during ICE1

Short name	Type / Description	IMEI	Original name	WMO id	Deployment time (UTC)	Deployment Latitude	Deployment Longitude	Device Operation	Additional Info
2023A6	Automatic Weather Station				09.08.2023 16:00	83° 57.000’ N	032° 19.200’ E	PS138_9_ Buoy_001	
2023R27	Radiation station	100000000000080	Radstation AWI #4		10.08.2023 19:30	83° 51.600’ N	033° 29.400’ E	PS138_9_ Buoy_002	core length 0.98 m, sensor 2 m below ice surface
2023T104	SIMBA	300234068527600	PRIC 10 07		09.08.2023 13:00	83° 59.556’ N	032° 21.300’ E	PS138_9_ Buoy_006	ice thickness 0.98m, scattering layer 0.03m, freeboard 0.15m; sensor 32 at surface
2023O17	Pacific Gyre CTD buoy	300234068166760	AWI-SVP5S-0004	4804099	09.08.2023 11:00	84° 00.960’ N	032° 16.073’ E	PS138_9_ Buoy_007	ice thickness 1m; Includes 3 HOBO loggers @3, 5, 7 m
2023S103	Snow buoy	300234066896250		2802061	10.08.2023 13:35	83° 52.080’ N	033° 31.104’ E	PS138_9_ Buoy_008	scattering layer 0.02 m, no snow
2023I8	SIMB (no thermistor chain)	300434064564590	AWI#1		10.08.2023 17:45	83° 51.643’ N	033° 29.781’ E	PS138_9_ Buoy_009	scattering layer 0.03 m, no snow; ice thickness 0.98 m,
2023P273	Pacific Gyre Universal tracker	300534064261600	AWI-UT-0002	5802074	09.08.2023 12:35	83° 59.556’ N	032° 21.295’ E	PS138_9_ Buoy_010	atttached to ADCP
2023P278	Pacific Gyre Universal tracker	300534064264600	AWI-UT-0007	4804097	11.08.2023 19:15	83° 58.348’ N	032° 21.630’ E	PS138_9_ Buoy_011	deployed next to 2023WaveLogger4

Short name	Type / Description	IMEI	Original name	WMO id	Deployment time (UTC)	Deployment Latitude	Deployment Longitude	Device Operation	Additional Info
2023P280	Pacific Gyre Universal tracker	300534064264620	AWI-UT-0009	6801881	11.08.2023 19:38	83° 51.965' N	033° 54.284' E	PS138_9_ Buoy_012	deployed next to 2023WaveLogger1
2023WaveLogger1	Pressure Wave logger		Wavelogger 1		11.08.2023 19:38	83° 51.965' N	033° 54.284' E	PS138_9_ Buoy_013	deployed next to 2023P280
2023WaveLogger2	Pressure Wave logger		Wavelogger 2		09.08.2023 11:00	83° 59.863' N	032° 20.533' E	PS138_9_ Buoy_014	on ablation shield of 2023O17
2023WaveLogger3	Pressure Wave logger		Wavelogger 3		11.08.2023 16:03	83° 50.882' N	034° 02.593' E	PS138_9_ Buoy_015	deployed behind ridge, on palette
2023WaveLogger4	Pressure Wave logger		Wavelogger 4		11.08.2023 19:15	83° 51.778' N	033° 53.648' E	PS138_9_ Buoy_016	deployed next to 2023P278
ADCP_ WH600_12668	RDI 600 kHz ADCP SN 12668				09.08.2023 12:35	83° 59.556' N	032° 21.295' E	PS138_9_ Buoy_017	2023P273 attached
my_iceBTC40_ ps138	Marlin Yug iceBTC1 1/40	300234061116910T			09.08.2023 11:00	83° 59.864' N	032° 20.532' E	PS138_9_ Buoy_018	ice thickness 0.98 m, scattering layer 0.01 m, freeboard 0,13 m

Tab. 6.2: Overview of buoys deployed during ICE2 – ICE9

Station	Short name	Type / Description	IMEI	Original name	WMO id	Deployment time (UTC)	Deployment Latitude	Deployment Longitude	Device Operation
ICE2	2023P268	MetOcean SVP-B	300534063489680		6203668	15.08.2023 08:00	84° 56.938‘ N	080° 09.276‘ E	PS138_31_ Buoy_001
ICE3	2023P264	MetOcean SVP-B	300534063486700		6203666	21.08.2023 09:40	84° 41.403‘ N	107° 17.302‘ E	PS138_52_ Buoy_001
ICE4	2023S123	Snow buoy	300234060543140		2802063	25.08.2023 12:45	83° 00.908‘ N	130° 09.270‘ E	PS138_75_ Buoy_004
	2023I12	SIMB	300434066151920	DARTMOUTH 2023 #4		24.08.2023 16:00	82° 54.930‘ N	130° 10.847‘ E	PS138_75_ Buoy_005
	2023T99	SAMS Ice Mass Balance Buoy	300534061345540	AWI 09 07		25.08.2023 13:10	83° 00.842‘ N	130° 09.342‘ E	PS138_75_ Buoy_006
	2023O18	Pacific Gyre CTD buoy	300234068514740	AWI-SVP5S-0006	6801883	25.08.2023 14:00	83° 00.659‘ N	130° 09.158‘ E	PS138_75_ Buoy_007
ICE5	2023O20	Pacific Gyre CTD buoy (6 CTDs + 1 Triplet)	300534060151880	AWI-SVP6S-0001	1801781	28.08.2023 13:00	85° 02.009‘ N	130° 24.226‘ E	PS138_101_ Buoy_001
	2023I11	SIMB	300434066254600	DARTMOUTH 2023 #3		29.08.2023 12:00	85° 54.930‘ N	130° 10.847‘ E	PS138_101_ Buoy_003
	2023W6	WHOI Ice Tethered Profiler*	300025060518220	ITP140		28.08.2023 16:40	85° 01.842‘ N	130° 18.449‘ E	PS138_101_ Buoy_004
	2023S126	Snow buoy	300234060729780		2802066	28.08.2023 13:20	85° 01.933‘ N	130° 23.971‘ E	PS138_101_ Buoy_005
	2023T106	SIMBA	300534063056460	AWI 11-02 long chain		28.08.2023 13:45	85° 01.880‘ N	130° 23.466‘ E	PS138_101_ Buoy_006
	2023R25	Radiation station, Bruncin	300025060615750	BOS089		30.08.2023 16:00	85° 01.500‘ N	130° 10.500‘ E	PS138_101_ Buoy_007

Station	Short name	Type / Description	IMEI	Original name	WMO id	Deployment time (UTC)	Deployment Latitude	Deployment Longitude	Device Operation
	Snowtatos1	SnowTATOS	300434068070720			29.08.2023 12:00	85° 54.930‘ N	130° 10.847‘ E	PS138_101_ Buoy_008
	2023K1	Sidekick Camera Buoy	300534062721510	APL-SK-0003	4701551	29.08.2023 12:00	85° 54.930‘ N	130° 10.847‘ E	PS138_101_ Buoy_009
ICE6	2023I10	SIMB	300434066159880	DARTMOUTH 2023 #1		04.09.2023 18:45	88° 26.050‘ N	114° 11.700‘ E	PS138_129_ Buoy_001
	2023R26	Radiation station, Bruncin	300025010736890	IMB090		04.09.2023 19:00	88° 26.030‘ N	114° 08.210‘ E	PS138_129_ Buoy_002
	2023S102	Snow buoy	300234066893230		3801665	04.09.2023 11:30	88° 27.930‘ N	114° 18.756‘ E	PS138_129_ Buoy_003
	2023T107	SIMBA	300534063050430	AWI 11-03		03.09.2023 12:00	88° 27.830‘ N	114° 21.700‘ E	PS138_129_ Buoy_004
	2023W5	WHOI Ice Tethered Profiler*	300025060513230	ITP135		03.09.2023 12:40	88° 29.771‘ N	111° 56.903‘ E	PS138_129_ Buoy_005
	2023T102	SIMBA	300234068701300	PRIC 09-03		04.09.2023 20:00	88° 25.980‘ N	113° 56.280‘ E	PS138_129_ Buoy_007
	2023O23	Pacific Gyre CTD buoy	300534064368480	AWI-SVP5S-0012	4804090	03.09.2023 14:45	88° 29.562‘ N	012° 02.892‘ E	PS138_129_ Buoy_008
ICE7	2023S100	Snow buoy	300234066088170		1801768	09.09.2012 12:45	89° 54.993‘ N	000° 44.130‘ E	PS138_152_ Buoy_001
	2023W7	LOCEAN IAOOS*	300250103413 20	IAOOS#21		09.09.2012 11:20	89° 55.269‘ N	004° 15.759‘ E	PS138_152_ Buoy_002
	2023I9	SIMB (no thermistor chain)	300434064565670	AWI 2022 #2		09.09.2012 11:50	89° 55.157‘ N	002° 54.080‘ E	PS138_152_ Buoy_003
	2023T115	SIMBA	300234066296810	LOCEAN 07-04		10.09.2023 09:00	89° 49.035‘ N	002° 26.799‘ W	PS138_152_ Buoy_004

Station	Short name	Type / Description	IMEI	Original name	WMO id	Deployment time (UTC)	Deployment Latitude	Deployment Longitude	Device Operation
	2023T110	SIMBA	300534061780910	PRIC 12-02		10.09.2023 07:50	89° 49.349‘ N	002° 38.452‘ W	PS138_152_ Buoy_005
	2023P286	Pacific Gyre Universal tracker	300534063804280	APL-UTAP-0066	4701554	10.09.2023 06:50	89° 49.576‘ N	002° 54.083‘ W	PS138_152_ Buoy_006
	2023P285	Pacific Gyre Universal tracker	300534064468030	AWI-UT-0014	6801884	07.09.2023 16:00	89° 52.260‘ N	059° 24.240‘ W	PS138_152_ Buoy_007
ICE8	2023S101	Snow buoy	300234066797650		1801769	13.09.2023 14:15	87° 55.209‘ N	059° 25.737‘ E	PS138_178_ Buoy_001
	2023T100	SIMBA	300534061348580	AWI 09-09		13.09.2023 13:45	87° 55.242‘ N	059° 29.418‘ E	PS138_178_ Buoy_002
ICE9	2023P272	Pacific Gyre Universal tracker	300534064260620	AWI-UT-0001	4804100	19.09.2023 14:40	85° 27.383‘ N	060° 02.413‘ E	PS138_213_ Buoy_001

Tab. 6.3: Overview of buoys deployed around ICE5

Station	Short name	Type / Description	IMEI	Original name	WMO id	Deployment time (UTC)	Deployment Latitude	Deployment Longitude	Device Operation
ICE5-N1	2023O16	Pacific Gyre CTD buoy	300234068164710	AWI-SVP5S-0003	5802075	29.08.2023 15:10	85° 00.920’ N	129° 51.172’ E	PS138_Heli_ Buoy_001
	2023T109	SIMBA	300534061784850	PRIC 12-01		29.08.2023 15:30	85° 00.941’N	129° 49.490’ E	PS138_Heli_ Buoy_002
	2023S124	Snow buoy	300234060726880		2802064	30.08.2023 08:00	84° 59.361’ N	129° 02.407’ E	PS138_Heli_ Buoy_003
ICE5-N2	2023O22	Pacific Gyre CTD buoy	300534064364470	AWI-SVP5S-0011	3801666	30.08.2023 17:40	84° 56.568’ N	129° 21.349’ E	PS138_Heli_ Buoy_004
	2023S125	Snow buoy	300234060727760		2802065	30.08.2023 17:50	84° 56.568’ N	129° 21.346’ E	PS138_Heli_ Buoy_005
	2023T103	SIMBA	300234065171790	FMI 05 10		30.08.2023 18:05	84° 56.568’ N	129° 21.346’ E	PS138_Heli_ Buoy_006
ICE5-N3	2023O19	Pacific Gyre CTD buoy	300534060057710	AWI-SVP5S-0009	4804098	31.08.2023 22:00	84° 56.200’ N	129° 22.100’ E	PS138_120-1
	2023T105	SIMBA	300534063054440	AWI 11-01		31.08.2023 22:00	84° 56.200’ N	129° 22.100’ E	PS138_120-2
	2023S122	Snow buoy	300234060330560		2802062	31.08.2023 22:00	84° 56.200’ N	129° 22.100’ E	PS138_120-3

Tab. 6.4: Overview of buoys deployed during transit by mummy chair or helicopter

Short name	Type / Description	IMEI	Original name	WMO id	Deployment time (UTC)	Deployment Latitude	Deployment Longitude	Device Operation
2023P270	NKE Trusted Buoy	300534063315650		6401594	07.08.2023 00:05	81° 25.785’ N	021° 07.559’ E	PS138_6-1
2023X16	Open MetBuoy	300434066297280			07.08.2023 13:30	82° 30.101’ N	027° 05.913’ E	PS138_8-1
2023P263	MetOcean SVP-B	300534063488690		6203666	23.08.2023 11:45	83° 38.614’ N	122° 07.967’ E	PS138_73-1
2023P289	Pacific Gyre Ice Tracker	300534062124450	APL-IT-0026	4701552	26.08.2023 23:00	83° 24.060’ N	129° 56.274’ E	PS138_95-1
2023P266	MetOcean SVP-B	300534063488690		6203666	27.08.2023 04:00	83° 53.341’ N	129° 43.039’ E	PS138_96-1
2023P290	Pacific Gyre Ice Tracker	300534062125830	APL-IT-0027	4701553	27.08.2023 08:55	84° 22.491’ N	130° 02.104’ E	PS138_97-1
2023P274	Pacific Gyre Universal tracker	300534064261620	AWI-UT-0003	5802073	29.08.2023 09:20	85° 00.920’ N	129° 51.172’ E	PS138_Heli_ Buoy_007
2023P284	Pacific Gyre Universal tracker	300534064268600	AWI-UT-0013	6801885	01.09.2023 00:30	85° 26.472’ N	128° 39.040’ E	PS138_121-1
2023P261	MetOcean SVP-B	300534063482680		6203657	01.09.2023 08:00	85° 56.700’ N	128° 10.686’ E	PS138_122-1
2023P283	Pacific Gyre Universal tracker	300534064267620	AWI-UT-0012	6801882	01.09.2023 14:30	86° 29.759’ N	127° 08.973’ E	PS138_121-4
2023P279	Pacific Gyre Universal tracker	300534064264610	AWI-UT-0008	1801780	01.09.2023 19:10	86° 56.530’ N	126° 33.979’ E	PS138_123-1
2023P265	MetOcean SVP-B	300534063487700		6203664	02.09.2023 01:50	87° 25.230’ N	125° 25.934’ E	PS138_124-1

Short name	Type / Description	IMEI	Original name	WMO id	Deployment time (UTC)	Deployment Latitude	Deployment Longitude	Device Operation
2023P275	Pacific Gyre Universal tracker	300534064262600	AWI-UT-0004	2802080	02.09.2023 20:10	87° 59.888' N	121° 33.440' E	PS138_128-1
2023P262	MetOcean SVP-B	300534063485680		6203661	06.09.2023 16:15	88° 59.167' N	112° 45.731' E	PS138_148-1
2023P288	Pacific Gyre Universal tracker	300534063806270	APL-UTAP-0068	4701555	06.09.2023 22:20	89° 28.536' N	111° 00.040' E	PS138_150-1
2023P267	MetOcean SVP-B	300534063488700		6203667	16.09.2023 20:00	87° 13.161' N	062° 41.014' E	PS138_200-1
2023P269	NKE Trusted Buoy	300534063313650		6401593	24.09.2023 16:00	77° 56.413' N	007° 07.528' E	PS138_224-1
2023P271	NKE Trusted Buoy	300534063318640		6401595	25.09.2023 01:40	75° 35.708' N	006° 39.176 'E	PS138_225-1

APPENDIX

A.1 TEILNEHMENDE INSTITUTE / PARTICIPATING INSTITUTES

A.2 FAHRTTEILNEHMER:INNEN / CRUISE PARTICIPANTS

A.3 SCHIFFSBESATZUNG / SHIP‘S CREW

A.4. STATIONSLISTE / STATION LIST

A.5 ICE STATION MAPS

A.6 OVERVIEW OF MULTICORER CORES RETRIEVED DURING PS138

A.1 TEILNEHMENDE INSTITUTE / PARTICIPATING INSTITUTES

Affiliation	Address
On board	

AU.UTAS	University of Tasmania 20 Castray Esplanade 7004 Battery Point Australia
DE.AWI	Alfred-Wegener-Institut Helmholtz-Zentrum für Polar- und Meeresforschung Postfach 120161 27515 Bremerhaven Germany
DE.DWD	Deutscher Wetterdienst Seewetteramt Bernhard-Nocht-Str. 76 20359 Hamburg Germany
DE.DRF	DRF Luftrettung gAG Laval Avenue E312 77836 Rheinmünster Germany
DE.FIELAX	Fielax Gesellschaft für wissenschaftliche Datenverarbeitung mbH Schleusenstraße 14 27568 Bremerhaven Germany
DE.K*	Tim Kalvelage Freier Wissenschaftsjournalist Admiralstraße 134 28215 Bremen Germany

Affiliation	Address
DE.MARUM	MARUM Zentrum für Marine Umweltwissenschaftern der Universität Bremen Leobener Str. 8 28359 Bremen Germany
DE.MPIMM	Max-Planck-Institut für Marine Mikrobiologie Celsiusstraße 1 28359 Bremen Germany
DE.NHC	Northern HeliCopter GmbH Gorch-Fock-Str., 103 26721 Emden Germany
DE.SENCKENBERG	Senckenberg Forschungsinstitut und Naturmuseum Südstrand 40 26382 Wilhelmshaven Germany
DE.UNI-BREMEN	Universität Bremen Leobener Straße, NW2a 28359 Bremen Germany
DE.UNI-FREIBURG	Albrecht-Ludwigs-Universität Freiburg Friedrichstr. 39 79098 Freiburg Germany
DE.UFA documentary	UFA Documentary GmbH Osloer Straße 118 13359 Berlin Germany
DE.OVGU	Otto-von-Guericke Universität Magdeburg Universitätsplatz 2 39106 Magdeburg Germany
DK.HADAL	Danish Center for Hadal Research – HADAL University of Southern Denmark – Dept Biology Campusvej 55 5320 Odense M Denmark

Affiliation	Address
EDU.DARTMOUTH	Dartmouth College 14 Engineering Dr. 3755 Hanover United States
JP.UTOKYO	The University of Tokyo 5-1-5, Kashiwa-no-ha 277-8564 Kashiwa Japan
UX.UE	University of Exeter Prince of Wales – Hatherly building EX4 4PS Exeter United Kindgom

Not on board	
AU.UMELBOURNE	The University of Melbourne Department of Civil Engineering Grattan Street, Parkville, 3010 Victoria Australia
DE.BSH	Bundesamt für Seeschifffahrt und Hydrographie Bundesbehörde im Geschäftsbereich des Bundesministeriums für Digitales und Verkehr Bernhard-Nocht-Str. 78 20359 Hamburg Germany
FR.SHOM	Météo France Centre de Météorologie Marine Site du SHOM 13 rue du Chatallier 29200 BREST France
NO.NGI	Norwegian Geotechnical Institute Sandakerveien 140 0484 Oslo Norway
USA.UWASHINGTON	Polar Science Center Applied Physics Laboratory University of Washington 1013 NE 40th Street, Box 355640, Seattle WA 98105-6698 United States

Affiliation	Address
USA.WHOI	Woods Hole Oceanographic Institution 266 Woods Hole Roead MS #2 Woods Hole MA 02543 United States

A.2 FAHRTTEILNEHMER:INNEN / CRUISE PARTICIPANTS

Name/ Last name	Vorname/ First name	Institut/ Institute	Beruf/ Profession	Fachrichtung/ Discipline
Allerholt	Jacob	DE.AWI	Technician	Oceanography
Allhusen	Erika	DE.AWI	Technician	Biology
Barz	Jakob	DE.AWI	Technician	Chemistry
Bienhold	Christina Andrea	DE.AWI	Scientist	Biology
Boetius	Antje	DE.AWI	Scientist	Biology
Böhringer	Lilian	DE.AWI	PhD student	Biology
Bonk	Frederic	DE.SENCKENBERG	PhD student	Biology
Brauer	Jens	DE.NHC	Pilot	Helicopter Service
Bryan	Natasha Anne	DE.AWI	Student (Master)	Biology
Bußmann	Frederik Alexander	DE.AWI	PhD student	Chemistry
Cimoli	Emiliano	AU.UTAS	Scientist	Physics
Cook	Kathryn	UX.UE	Scientist	Oceanography
Eggers	Sarah Lena	DE.AWI	Technician	Biology
Ernst	Manuel	DE.UFA documentary	Journalist	Public Outreach
Geibert	Walter	DE.AWI	Scientist	Geochemistry
Hoge	Ulrich	DE.AWI	Engineer	Engineering Sciences
Hoppmann	Mario	DE.AWI	Scientist	Oceanography
Horvath	Esther	DE.AWI	Photographer	Public Outreach
Iversen	Morten Hvitfeldt	DE.AWI	Scientist	Biology
Janssen	Felix	DE.AWI	Scientist	Biology
Kalvelage	Tim	DE.K*	Journalist	Public Outreach
Kawaguchi	Yusuke	JP.UTOKYO	Scientist	Oceanography
Koch	Boris	DE.AWI	Scientist	Chemistry
Kohlenbach	Katharina Renate Gisela	DE.UNI-BREMEN	Student (Master)	Biology
Kuznetsov	Ivan	DE.AWI	Scientist	Oceanography
McOscar	Dwayne	DE.DRF	Technician	Helicopter Service
Mehlmann	Carolin	DE.OVGU	Scientist	Mathematics
Miehe	Kai	DE.DRF	Technician	Helicopter Service
Nicolaus	Marcel	DE.AWI	Scientist	Geophysics
Nordhausen	Axel	DE.MPIMM	Technician	Engineering Sciences
Otte	Frank	DE.DWD	Scientist	Meteorology
Oziel	Laurent	DE.AWI	Scientist	Oceanography

Name/ Last name	Vorname/ First name	Institut/ Institute	Beruf/ Profession	Fachrichtung/ Discipline
Pallentin	Malte	DE.AWI	Engineer	Biology
Purser	Autun	DE.AWI	Scientist	Biology
Quintanilla Zurita	Alejandra	DE.AWI	PhD student	Oceanography
Rabe	Benjamin	DE.AWI	Scientist	Oceanography
Raphael	Ian	EDU.DARTMOUTH	PhD student	Engineering Sciences
Regnery	Julia	DE.AWI	Scientist	Logistics
Richter	Thomas Michael	DE.OVGU	Scientist	Mathematics
Rohde	Jan	DE.AWI	Engineer	Engineering Sciences
Scholz	Daniel	DE.AWI	Engineer	Chemistry
Schulte-Hillen	Ruben Lennart	DE.UNI-FREIBURG	Student (Master)	Biology
Tardeck	Frederic	DE.FIELAX	Technician	Engineering Sciences
Thielecke	Antonia	DE.AWI	PhD student	Biology
Torres-Valdés	Sinhué	DE.AWI	Scientist	Oceanography
Uhlir	Carolin	DE.SENCKENBERG	Scientist	Biology
Vane	Kim	DE.AWI	Scientist	Biology
Vaupel	Lars	DE.NHC	Pilot	Helicopter Service
Vogt	Nils	DE.UFA documentary	Journalist	Public Outreach
Wenzel	Anna Julia	DE.DWD	Scientist	Meteorology
Wenzhoefer	Frank	DE.AWI	Scientist	Biology
Wietz	Matthias	DE.AWI	Scientist	Biology
Zimmer	Florian	DE.AWI	Student	Engineering Sciences

A.3 SCHIFFSBESATZUNG / SHIP‘S CREW

No.	Name / Last Name	Vorname / First Name	Position / Rank
1	Schwarze	Stefan	Master
2	Westphal	Henning	Chief
3	Lauber	Felix Thomas	1st Mate
4	Dmoch	René Pascal	2nd Mate
5	Strauß	Erik	2nd Mate
6	Hofmann	Jörg Walter	CommOffc
7	Gößmann-Lange	Petra	Ships doc
8	Baehler	Stefanie	2nd Eng.
9	Beyer	Mario	2nd Eng.
10	Brose	Thomas Christian	2nd Eng.
11	Redmer	Jens Dirk	E-Eng.
12	Jäger	Vladimir	ELO
13	Kliemann	Olaf	ELO
14	Nasis	Ilias	ELO
15	Zohrabyan	David Rubeni	ELO
16	Meier	Jan	Bosun
17	Neisner	Winfried	Carpen.
18	Cornelsen	Robert	MP Rat.
19	Ehm	Lars Ole	MP Rat.
20	Klähn	Anton	MP Rat.
21	Klee	Philipp	MP Rat.
22	Mahlmann	Oliver Karl-Heinz	MP Rat.
23	Reiche	Julian Dominik	MP Rat.
24	Bäcker	Andreas	AB
25	Burzan	Gerd-Ekkehard	AB
26	Kistenmacher	Mario André	AB
27	Plehn	Marco Markus	Storek.
28	Hänert	Ove	MP Rat

No.	Name / Last Name	Vorname / First Name	Position / Rank
29	Klinger	Dana Maria	MP Rat
30	Münzenberger	Börge	MP Rat
31	Rhau	Lars-Peter	MP Rat
32	Schwarz	Uwe	MP Rat
33	Hofmann	Werner	Cook
34	Dietrich	Emilia Felizitas	Cooksm.
35	Silinski	Frank	Cooksm.
36	Wöckener	Martina	Nurse
37	Arendt	René	2nd Stew.
38	Brändli	Monika	2nd Stew.
39	Chen	Dansheng	2nd Stew.
40	Cheng	Qi	2nd Stew.
41	Dibenau	Torsten	2nd Stew.
42	Krause	Tomasz	2nd Stew.
43	Silinski	Carmen	2nd Stew.

A.4 STATIONSLISTE / STATION LIST PS138

Station list of expedition PS138 from Tromsoe – Bremerhaven;
the list details the action log for all stations along the cruise track.

See https://www.pangaea.de/expeditions/events/PS138 to display the station (event) list for expedition PS138.
This version contains Uniform Resource Identifiers for all sensors listed under https://sensor.awi.de. See https://www.awi.de/en/about-us/service/computing-centre/data-flow-framework.html for further information about AWI's data flow framework from sensor observations to

Event label	Optional label	Date / Time	Latitude	Longitude	Depth [m]	Gear	Action	Comment
PS138-track		2023-08-02 T00:00:00	69.67800	18.98980		CT	Station start	Tromsø – Bremerhaven
PS138-track		2023-10-01 T00:00:00	53.56750	8.55480		CT	Station end	Tromsø – Bremerhaven
PS138_0_Underway-51		2023-08-02 T13:17:01	69.74732	19.14245		SWEAS	Station start	
PS138_0_Underway-51		2023-09-29 T10:40:03	56.76223	5.56896	43	SWEAS	Station end	
PS138_0_Underway-30		2023-08-03 T08:36:43	69.74730	19.14246		ECHO	Station start	
PS138_0_Underway-30		2023-09-29 T10:40:03	56.76223	5.56896	43	ECHO	Station end	
PS138_0_Underway-52		2023-08-03 T12:00:00	69.74731	19.14245		GOPRO	Station start	
PS138_0_Underway-52		2023-09-20 T23:01:00	85.38898	57.09751	3899	GOPRO	Station end	
PS138_0_Underway-39		2023-08-03 T19:26:32	70.68825	20.04741	154	PS	Station start	
PS138_0_Underway-39		2023-09-28 T12:24:48	59.27775	3.54755	219	PS	Station end	

** Comments are limited to 130 characters. See https://www.pangaea.de/expeditions/events/PS138 to show full comments in conjunction with the station (event) list for expedition PS138*

Event label	Optional label	Date / Time	Latitude	Longitude	Depth [m]	Gear	Action	Comment
PS138_0_Underway-42		2023-08-03 T19:30:27	70.70390	20.03271	168	SNDVELPR	Station start	
PS138_0_Underway-42		2023-09-29 T10:40:18	56.76184	5.56979	43	SNDVELPR	Station end	
PS138_0_Underway-31		2023-08-03 T19:31:13	70.70691	20.03020	165	NEUMON	Station start	
PS138_0_Underway-31		2023-09-29 T10:40:12	56.76200	5.56945	43	NEUMON	Station end	
PS138_0_Underway-11		2023-08-03 T19:33:36	70.71573	20.02187	172	MYON	Station start	
PS138_0_Underway-11		2023-09-29 T10:40:20	56.76179	5.56990	43	MYON	Station end	
PS138_0_Underway-23		2023-08-03 T19:36:05	70.72456	20.01439	174	MAG	Station start	
PS138_0_Underway-23		2023-09-29 T10:39:09	56.76363	5.56604	43	MAG	Station end	
PS138_0_Underway-24		2023-08-03 T19:36:27	70.72591	20.01319	172	GRAV	Station start	
PS138_0_Underway-24		2023-09-29 T10:39:56	56.76242	5.56858	43	GRAV	Station end	
PS138_0_Underway-43		2023-08-03 T19:44:54	70.75535	19.98666	182	TSG	Station start	Keel 1
PS138_0_Underway-43		2023-09-29 T10:40:12	56.76200	5.56945	43	TSG	Station end	Keel 1
PS138_0_Underway-44		2023-08-03 T19:45:17	70.75666	19.98548	180	TSG	Station start	Keel 2
PS138_0_Underway-44		2023-09-29 T10:40:12	56.76200	5.56945	43	TSG	Station end	Keel 2
PS138_0_Underway-13		2023-08-03 T19:46:13	70.75987	19.98272	179	FBOX	Station start	

Event label	Optional label	Date / Time	Latitude	Longitude	Depth [m]	Gear	Action	Comment
PS138_0_Underway-13		2023-09-29 T10:40:12	56.76200	5.56945	43	FBOX	Station end	
PS138_0_Underway-35		2023-08-03 T19:47:24	70.76391	19.97923	181	pCO2	Station start	
PS138_0_Underway-35		2023-09-29 T10:40:12	56.76200	5.56945	43	pCO2	Station end	
PS138_0_Underway-34		2023-08-03 T19:47:43	70.76506	19.97825	180	pCO2	Station start	
PS138_0_Underway-34		2023-09-29 T10:40:34	56.76143	5.57067	42	pCO2	Station end	
PS138_0_Underway-28		2023-08-03 T19:49:39	70.77160	19.97210		DS3	Station start	Event shows start/end point (date/time & coordinates) of first/last data record using Atlas Hydrographic Hydrosweep DS 3 multibeam…
PS138_0_Underway-28		2023-09-29 T07:45:14	57.02940	5.04144		DS3	Station end	Event shows start/end point (date/time & coordinates) of first/last data record using Atlas Hydrographic Hydrosweep DS 3 multibeam…
PS138_0_Underway-50		2023-08-03 T19:50:29	70.77441	19.96957	181	W-RADAR	Station start	
PS138_0_Underway-50		2023-09-29 T10:40:33	56.76145	5.57062	42	W-RADAR	Station end	

Event label	Optional label	Date / Time	Latitude	Longitude	Depth [m]	Gear	Action	Comment
PS138_0_Underway-3		2023-08-03 T20:14:30	70.85520	19.88671	183	ADCP	Station start	
PS138_0_Underway-3		2023-09-29 T10:40:12	56.76200	5.56945	43	ADCP	Station end	
PS138_0_Underway-53		2023-08-04 T12:20:00	74.13489	16.07072	748	RAMSES_ ACC-VIS	Station start	
PS138_0_Underway-53		2023-09-24 T10:11:00	79.11262	7.93955	1099	RAMSES_ ACC-VIS	Station end	
PS138_1-1		2023-08-06 T12:00:34	80.94910	15.35803	1966	POS	Station start	Posidonia system and transponder Test
PS138_1-1		2023-08-06 T14:29:27	80.94960	15.34787	2034	POS	Station end	Posidonia system and transponder Test
PS138_2-1		2023-08-06 T15:38:56	80.94810	15.35065	2028	CTD-RO	max depth	at max depth
PS138_2_DRONE_001	UAV_PS	2023-08-06 T15:57:00	80.94900	15.35100		UAV	max depth	Photogrammetry grid
PS138_3-1		2023-08-06 T16:25:40	80.94749	15.34817	2031	ARGOFL	Station start	
PS138_3-1		2023-08-06 T16:25:43	80.94749	15.34818	2031	ARGOFL	Station end	
PS138_4-1		2023-08-06 T17:01:06	80.94584	15.34677	2035	POS	Station start	Posidonia system and transponder Test
PS138_4-1		2023-08-06 T18:13:08	80.94511	15.33724	2027	POS	Station end	Posidonia system and transponder Test
PS138_5-1		2023-08-06 T18:24:59	80.94571	15.33794	2030	hCTD	max depth	
PS138_0_Underway-55		2023-08-06 T21:30:00	81.14135	18.12673	414	ICEOBS	Station start	

Event label	Optional label	Date / Time	Latitude	Longitude	Depth [m]	Gear	Action	Comment
PS138_0_Underway-55		2023-09-23 T18:00:05	81.33794	18.97241	577	ICEOBS	Station end	
PS138_6-1	2023P270	2023-08-07 T00:02:54	81.42641	21.04192	1415	ISVP	Station start	2023P270 NKE Trusted Buoy 300534063315650
PS138_6-1	2023P270	2023-08-07 T00:02:56	81.42643	21.04227	1415	ISVP	Station end	2023P270 NKE Trusted Buoy 300534063315650
PS138_7-1		2023-08-07 T03:19:00	81.80359	24.04494	2607	XCTD	Station start	
PS138_7-1		2023-08-07 T03:27:22	81.80779	24.08809	720	XCTD	Station end	
PS138_7-2		2023-08-07 T05:48:53	81.98893	25.12195	3659	XCTD	Station start	
PS138_7-2		2023-08-07 T05:54:43	81.99291	25.15490	3638	XCTD	Station end	
PS138_Heli_EM-Bird_001	Embird_awi-bird	2023-08-07 T07:33:00	82.15242	25.67650		EMB	max depth	Short flight in the marginal ice zone that had to aborted due to bad weather.
PS138_7-3		2023-08-07 T08:04:37	82.15233	25.59735	3756	XCTD	Station start	
PS138_7-3		2023-08-07 T08:10:20	82.15384	25.61263	3775	XCTD	Station end	
PS138_SBLA_20230807T093300		2023-08-07 T09:33:00	82.14520	25.62339		SBLA	Station start	
PS138_SBLA_20230807T093300		2023-08-07 T09:33:00	82.14705	25.77754		SBLA	Station end	
PS138_7-4		2023-08-07 T11:00:51	82.32919	26.44822	3837	XCTD	Station start	

Event label	Optional label	Date / Time	Latitude	Longitude	Depth [m]	Gear	Action	Comment
PS138_7-4		2023-08-07 T11:02:30	82.33018	26.44904	3838	XCTD	Station end	
PS138_8-1	2023X16	2023-08-07 T13:26:08	82.50240	27.09597	3879	BUOY	Station start	2023X16 Open MetBuoy
PS138_8-1	2023X16	2023-08-07 T13:32:36	82.50182	27.09800	3879	BUOY	Station end	2023X16 Open MetBuoy
PS138_7-5		2023-08-07 T13:32:53	82.50179	27.09807	3880	XCTD	Station start	
PS138_7-5		2023-08-07 T13:41:51	82.50180	27.09793	3878	XCTD	Station end	
PS138_7-6		2023-08-07 T15:27:28	82.65300	27.32435	3886	XCTD	Station start	
PS138_7-6		2023-08-07 T15:34:38	82.65927	27.33071	3888	XCTD	Station end	
PS138_7-7		2023-08-07 T20:23:06	82.97497	27.98806	3931	XCTD	Station start	
PS138_7-7		2023-08-07 T20:28:40	82.97308	27.99511	3931	XCTD	Station end	
PS138_9_1_hobo_ u20_21248543-001	hobo_ u20_21248543	2023-08-08 T00:00:00	84.07357	31.21155		HOBO_ON	max depth	IceStation #1
PS138_9_1_hobo_ u24_21309010-001	hobo_ u24_21309010	2023-08-08 T00:00:00	84.07357	32.21155		HOBO_ON	max depth	IceStation #1
PS138_9_1_hobo_ u24_21308995-001	hobo_ u24_21308995	2023-08-08 T00:00:00	84.07357	31.21155		HOBO_ON	max depth	IceStation #1
PS138_9_1_hobo_ u24_21309009-001	hobo_ u24_21309009	2023-08-08 T00:00:00	84.07357	31.21155		HOBO_ON	max depth	IceStation #1
PS138_7-8		2023-08-08 T00:47:35	83.32100	29.17338	3952	XCTD	Station start	
PS138_7-8		2023-08-08 T00:48:07	83.32116	29.17192	3953	XCTD	Station end	

Event label	Optional label	Date / Time	Latitude	Longitude	Depth [m]	Gear	Action	Comment
PS138_7-9		2023-08-08 T04:40:59	83.65348	30.16154	3985	XCTD	Station start	
PS138_7-9		2023-08-08 T04:46:52	83.65470	30.20123	3989	XCTD	Station end	
PS138_9-1		2023-08-08 T10:40:45	84.07357	31.21155	3993	ICE	Station start	IceStation #1
PS138_9-1		2023-08-12 T02:05:18	83.84814	34.10190		ICE	Station end	IceStation #1
PS138_9_1_RINKO-EC_16		2023-08-08 T10:40:45	84.07356	31.21155		TP	max depth	IceStation #1
PS138_10-1		2023-08-08 T13:00:33	84.05679	31.33170	3991	OFOBS	Station start	IceStation #1
PS138_10-1		2023-08-08 T20:17:36	84.03045	31.33188	3992	OFOBS	Station end	IceStation #1
PS138_Heli_EM-Bird_002	Embird_awi-bird	2023-08-08 T13:26:00	84.06541	31.00610		EMB	max depth	Flight near the first IceStation.
PS138_9_MSS_1	mss_90L_097	2023-08-08 T14:17:00	84.04070	31.35540		MSS	max depth	MSS 097 series of 7 profiles; IceStation #1
PS138_9_ICEADCP300_1	300kHzADCP	2023-08-08 T14:17:00	84.04070	31.35540		ADCP	max depth	Under-ice RDI 300 KHz ADCP time series; IceStation #1
PS138_SBLA_20230808T153000		2023-08-08 T15:30:00	84.06257	31.26607		SBLA	Station start	
PS138_SBLA_20230808T153000		2023-08-08 T15:30:00	84.31807	28.52007		SBLA	Station end	
PS138_SBLA_20230808T155700		2023-08-08 T15:57:00	84.26699	28.37682		SBLA	Station start	
PS138_SBLA_20230808T155700		2023-08-08 T15:57:00	84.02096	28.30546		SBLA	Station end	

Event label	Optional label	Date / Time	Latitude	Longitude	Depth [m]	Gear	Action	Comment
PS138_ SBLA_20230808T161800		2023-08-08 T16:18:00	84.01348	28.96779		SBLA	Station start	
PS138_ SBLA_20230808T161800		2023-08-08 T16:18:00	84.05013	31.90095		SBLA	Station end	
PS138_9_Chemistry-001	snow_sampler_ glove	2023-08-08 T16:41:00	83.87799	33.48234		SSG	max depth	Snow sample; IceStation #1
PS138_9_Coring-001	SI_corer_9cm	2023-08-08 T16:53:13	84.07357	31.21155		MARKII	max depth	Biocore_1; IceStation #1
PS138_9_Coring-002	SI_corer_9cm	2023-08-08 T16:53:33	84.07357	31.21155		MARKII	max depth	Biocore_2; IceStation #1
PS138_9_Coring-003	SI_corer_9cm	2023-08-08 T16:54:13	84.07357	31.21155		MARKII	max depth	Biocore_3; IceStation #1
PS138_9_Coring-004	SI_corer_9cm	2023-08-08 T16:54:37	84.07357	31.21155		MARKII	max depth	Biocore_4; IceStation #1
PS138_9_Coring-005	SI_corer_9cm	2023-08-08 T16:56:34	84.07357	31.21155		MARKII	max depth	Biocore_5; IceStation #1
PS138_9_Coring-006	SI_corer_9cm	2023-08-08 T16:56:44	84.07357	31.21155		MARKII	max depth	Biocore_6; IceStation #1
PS138_9-1_ISCA-002	ISCA	2023-08-08 T17:00:00	84.07357	31.21155		ISCA	max depth	IceStation #1
PS138_9-1_ISCA-001	ISCA	2023-08-08 T17:00:00	84.07357	31.21155		ISCA	max depth	IceStation #1
PS138_9_Coring-007	SI_corer_9cm	2023-08-08 T17:00:03	84.07357	31.21155		MARKII	max depth	Biocore_7; IceStation #1
PS138_9_Coring-008	SI_corer_9cm	2023-08-08 T17:01:25	84.07357	31.21155		MARKII	max depth	Biocore_8; IceStation #1
PS138_9_Coring-009	SI_corer_9cm	2023-08-08 T17:02:15	84.07357	31.21155		MARKII	max depth	Biocore_9; IceStation #1
PS138_9_Coring-010	SI_corer_9cm	2023-08-08 T17:02:31	84.07357	31.21155		MARKII	max depth	Biocore_10; IceStation #1

Event label	Optional label	Date / Time	Latitude	Longitude	Depth [m]	Gear	Action	Comment
PS138_9_Coring-011	SI_corer_9cm	2023-08-08 T17:04:26	84.07357	31.21155		MARKII	max depth	SIP_Archive; IceStation #1
PS138_9_Coring-012	SI_corer_9cm	2023-08-08 T17:04:37	84.07357	31.21155		MARKII	max depth	SIP_Texture; IceStation #1
PS138_9_Coring-013	hand_pump	2023-08-08 T17:06:10	84.07357	31.21155		HP	max depth	Under Ice Water; IceStation #1
PS138_9_Coring-014	hand_pump	2023-08-08 T17:06:46	84.07357	31.21155		HP	max depth	Melt Pond Water; IceStation #1
PS138_9_Coring-015	snow_sampler_glove	2023-08-08 T17:08:00	84.07357	31.21155		SSG	max depth	Snow sample; IceStation #1
PS138_9_Coring-016	snow_sampler_glove	2023-08-08 T17:08:10	84.07357	31.21155		SSG	max depth	Snow sample; IceStation #1
PS138_0_Underway-54		2023-08-08 T21:05:00	84.03719	31.26087	3992	CAME	Station start	IceStation #1
PS138_0_Underway-54		2023-09-21 T13:45:46	84.89616	44.97113	3959	CAME	Station end	IceStation #1
PS138_11-1		2023-08-08 T23:24:10	84.03353	31.37937	3991	GKG	max depth	IceStation #1
PS138_12-1		2023-08-09 T01:28:16	84.02522	31.49789	3988	MSN	Station start	IceStation #1
PS138_12-1		2023-08-09 T04:25:50	84.02526	31.49588	3990	MSN	Station end	IceStation #1
PS138_13-1		2023-08-09 T04:38:52	84.02339	31.51649	3990	MSN	Station start	IceStation #1
PS138_13-1		2023-08-09 T06:22:23	84.04755	31.68771	3988	MSN	Station end	IceStation #1
PS138_9_MSS_2	mss_90L_097	2023-08-09 T09:13:00	84.04480	32.24850		MSS	max depth	MSS 097 series of 3 profiles; IceStation #1
PS138_9_GEM_001	gem2-512	2023-08-09 T09:39:00	84.06667	31.21667		BES	max depth	IceStation #1

Event label	Optional label	Date / Time	Latitude	Longitude	Depth [m]	Gear	Action	Comment
PS138_9_ASD_001	Dart_ASD	2023-08-09 T11:00:00	84.06667	31.21667		ALBEDOM	max depth	IceStation #1
PS138_9_Buoy_007	2023O17	2023-08-09 T11:00:00	84.01600	32.26788		BUOY_CTD	max depth	Includes 3 HOBO loggers at 3. 5. 7 m; IceStation #1
PS138_9_Buoy_014	2023WaveLogger2	2023-08-09 T11:00:00	83.99772	32.34222		WLOG	max depth	on ablation shield of 2023O17; IceStation #1
PS138_9_nortek_ s1000_102149-001	nortek_ s1000_102149	2023-08-09 T12:00:00	84.07357	31.21155		BUOY_ ADCP	max depth	IceStation #1
PS138_9_Buoy_018	my_iceBTC40_ ps138	2023-08-09 T12:00:00	84.07357	31.21155		BUOY	max depth	IceStation #1
PS138_9_ Vector_5418-001	Vector_5418	2023-08-09 T12:00:00	69.67800	18.98980		CM	max depth	IceStation #1
PS138_9_Buoy_010	2023P273	2023-08-09 T12:35:00	83.99260	32.35492		ISVP	max depth	attached to ADCP; IceStation #1
PS138_9_Buoy_017	ADCP_ WH600_12668	2023-08-09 T12:35:00	83.99260	32.35492		BUOY_ ADCP	max depth	Beam 3 directed to ROV hole (GPS station 8 and 2023P280). 2023P273 attached to it; IceStation #1
PS138_9_Buoy_006	2023T104	2023-08-09 T13:00:00	83.99260	32.35492		SIMBA	max depth	ice thickness 0.98m. scattering layer 0.03m. freeboard 0.15m. thermistor 32 at surface. level first-year ice co-deployed with 2023…

Event label	Optional label	Date / Time	Latitude	Longitude	Depth [m]	Gear	Action	Comment
PS138_14-1		2023-08-09 T14:03:00	83.95468	32.07135		B_LANDER	max depth	Flux Lander #1. IceStation #1. Lander not found; Posidonia Position
PS138_9_Buoy_001	2023A6	2023-08-09 T16:00:00	83.95000	32.32000		M-AWS	max depth	IceStation #1
PS138_9_IT_001	PS138_9-1_IT_ssl-001	2023-08-09 T16:45:00	84.07357	31.21155		STRAP_ICE	max depth	Deployment of ice sediment traps equipped with gel traps; Ice station #1
PS138_15-1		2023-08-09 T18:21:23	84.03731	31.54825	3992	TVMUC	Station start	IceStation #1
PS138_15-1		2023-08-09 T21:44:56	84.02353	31.84900	3991	TVMUC	Station end	IceStation #1
PS138_16-1		2023-08-09 T21:46:07	84.02339	31.85134	3988	TVMUC	Station start	IceStation #1
PS138_16-1		2023-08-10 T01:52:42	83.97671	32.07949	3989	TVMUC	Station end	IceStation #1
PS138_17-1		2023-08-10 T02:49:06	83.92843	32.61157	3982	EBS	Station start	IceStation #1
PS138_17-1		2023-08-10 T08:16:24	83.90268	32.58994	3979	EBS	Station end	IceStation #1
PS138_9_CTD001	rbr_concerto_210909	2023-08-10 T11:44:33	83.88572	33.38706		hCTD	max depth	4 casts with uprising ctd at ROV hole for Morten and Boris; IceStation #1

Event label	Optional label	Date / Time	Latitude	Longitude	Depth [m]	Gear	Action	Comment
PS138_9_IT_002	PS138_9-1_IT_ssl-002	2023-08-10 T11:50:00	84.07357	31.21155		STRAP_ICE	max depth	Recovery of ice sediment traps equipped with gel traps; Ice station #1
PS138_9_MSS_3	MSS_90D_075	2023-08-10 T12:32:00	83.87800	33.46130		MSS	max depth	MSS 075 series of 14n profiles; IceStation #1
PS138_18-1		2023-08-10 T12:56:00	83.89913	33.17397	3977	B_LANDER	Station start	Flux Lander #2. IceStation #1; Posidonia Position
PS138_18-1		2023-08-11 T17:19:00	83.92102	33.37813	3995	B_LANDER	Station end	Flux Lander #2. IceStation #1; Posidonia Position
PS138_9_KEF_001	PS138_9-1_KEF_ssl-003	2023-08-10 T13:10:00	84.07357	31.21155		STRAP_ICE	max depth	Deployment of ice sediment traps for biogeochemistry; Ice station #1
PS138_9_Buoy_008	2023S103	2023-08-10 T13:35:00	83.86800	33.51840		BUOY_SNOW	max depth	scattering layer 0.02m at all pingers. level first-year ice. no snow. co-deployed with 2023T104; IceStation #1
PS138_009_SUNAprofil_001	Nitrate_profiler	2023-08-10 T13:38:56	83.87630	33.47840		NO3	max depth	7 profiles; IceStation #1
PS138_9_Chemistry-003	hand_pump	2023-08-10 T14:00:00	83.87799	33.48234		HP	max depth	Melt Pond Water; IceStation #1
PS138_9_Chemistry-002	hand_pump	2023-08-10 T14:00:00	83.87799	33.48234		HP	max depth	Melt Pond Water; IceStation #1

Event label	Optional label	Date / Time	Latitude	Longitude	Depth [m]	Gear	Action	Comment
PS138_9_Chemistry-004	snow_sampler_glove	2023-08-10 T14:02:00	83.87799	33.48234		SSG	max depth	Snow sample; IceStation #1
PS138_19-1		2023-08-10 T16:38:39	83.86830	33.20881	3976	CTD-RO	max depth	IceStation #1. at max depth
PS138_20-1		2023-08-10 T17:07:14	83.87129	33.20454	3975	BONGO	Station start	IceStation #1
PS138_20-1		2023-08-10 T17:17:03	83.87237	33.20417	3973	BONGO	Station end	IceStation #1
PS138_21-1		2023-08-10 T17:19:30	83.87262	33.20383	3975	HN	Station start	IceStation #1
PS138_21-1		2023-08-10 T17:33:51	83.87409	33.20130	3977	HN	Station end	IceStation #1
PS138_9_Buoy_009	2023I8	2023-08-10 T17:45:00	83.86071	33.49634		SIMB	max depth	scattering layer 0.03 m. distance pinger to surface 1.07m; IceStation #1
PS138_22-1		2023-08-10 T18:11:50	83.87706	33.16962	3976	CTD-RO	max depth	IceStation #1. at max depth
PS138_23-1		2023-08-10 T19:01:31	83.88244	33.18431	3974	MSC	max depth	IceStation #1
PS138_24-1		2023-08-10 T19:23:42	83.88586	33.21185	3977	MSC	max depth	IceStation #1
PS138_9_DRONE_001	UAV_PS	2023-08-10 T19:29:00	84.06667	31.21667		UAV	max depth	Photogrammetry grid over floe; IceStation #1

Event label	Optional label	Date / Time	Latitude	Longitude	Depth [m]	Gear	Action	Comment
PS138_9_Buoy_002	2023R27	2023-08-10 T19:30:00	83.86000	33.49000		BRS	max depth	sensor 50A4 upward looking. sensor 50A2 downward looking. sensor 50A3 under ice. core length 0.98 m. sensor 2 m below ice surface;…
PS138_25-1		2023-08-10 T19:30:44	83.88716	33.22642	3975	ROSINA	Station start	IceStation #1
PS138_25-1		2023-08-10 T21:20:02	83.89309	33.38321	3980	ROSINA	Station end	IceStation #1
PS138_9_DRONE_002	UAV_PS	2023-08-10 T19:37:00	84.06667	31.21667		UAV	max depth	Photo-grammetry grid over ROV area; IceStation #1
PS138_9_ROV_001	BEAST	2023-08-10 T19:54:00	84.06667	31.21667		BEAST	max depth	20230810_1; IceStation #1
PS138_9_Buoy_003	2023Reolink11	2023-08-10 T21:00:00	84.06667	31.21667		CAME	max depth	deployed at CTD buoy facing towards buoy site; IceStation #1
PS138_9_Buoy_004	2023Reolink12	2023-08-10 T21:20:00	84.06667	31.21667		CAME	max depth	deployed at Radstation facing towards buoy site; IceStation #1
PS138_9_Buoy_005	2023Reolink13	2023-08-10 T21:40:00	84.06667	31.21667		CAME	max depth	deployed at AWS facing towards buoy site; IceStation #1

Event label	Optional label	Date / Time	Latitude	Longitude	Depth [m]	Gear	Action	Comment
PS138_9_Core_002	SI_corer_14cm	2023-08-11 T00:00:00	84.06667	31.21667		MARKV	max depth	OPT. HI scan. no bio samples; IceStation #1
PS138_9_Core_001	SI_corer_14cm	2023-08-11 T00:00:00	84.06667	31.21667		MARKV	max depth	OPT. HI scan. no bio samples; IceStation #1
PS138_26-1_1	ISP_Franky	2023-08-11 T00:19:00	83.87184	34.08649	3974	ISP	Station start	IceStation #1
PS138_26-1_1	ISP_Franky	2023-08-11 T06:12:00	83.86024	33.91330	3969	ISP	Station end	IceStation #1
PS138_26-1_2	ISP_Seb	2023-08-11 T01:07:00	83.86343	34.11553	3971	ISP	Station start	IceStation #1
PS138_26-1_2	ISP_Seb	2023-08-11 T06:12:00	83.86024	33.91330	3969	ISP	Station end	IceStation #1
PS138_26-1_3	ISP_Frauke	2023-08-11 T01:43:00	83.85735	34.11913	3971	ISP	Station start	IceStation #1
PS138_26-1_3	ISP_Frauke	2023-08-11 T06:12:00	83.86024	33.91330	3969	ISP	Station end	IceStation #1
PS138_26-1		2023-08-11 T01:55:47	83.85607	34.11768	3970	CTD-RO	Station start	IceStation #1. at max depth
PS138_26-1		2023-08-11 T02:17:20	83.85325	34.10632	3969	CTD-RO	Station end	IceStation #1. at max depth
PS138_26-1_4	ISP_Hulda	2023-08-11 T02:13:00	83.85366	34.10755	3967	ISP	Station start	failed -- sudden pressure release; IceStation #1
PS138_26-1_4	ISP_Hulda	2023-08-11 T06:12:00	83.86024	33.91330	3969	ISP	Station end	failed -- sudden pressure release; IceStation #1
PS138_9_Buoy_015	2023 WaveLogger3	2023-08-11 T16:03:00	83.84803	34.04322		WLOG	max depth	deployed behind ridge. on palette

Event label	Optional label	Date / Time	Latitude	Longitude	Depth [m]	Gear	Action	Comment
PS138_9_MSS_4	MSS_90D_075	2023-08-11 T17:09:00	83.84930	33.95910		MSS	max depth	MSS 075 series of 14 profiles; IceStation #1
PS138_9_ROV_002	BEAST	2023-08-11 T17:27:00	84.06667	31.21667		BEAST	max depth	20230811_1; IceStation #1
PS138_9_Buoy_011	2023P278	2023-08-11 T19:15:00	83.86297	33.89413		ISVP	max depth	deployed next to 2023WaveLogger4. MSS site; IceStation #1
PS138_9_Buoy_016	2023 WaveLogger4	2023-08-11 T19:15:00	83.86297	33.89413		WLOG	max depth	deployed next to 2023P278; IceStation #1
PS138_9_ROV_003	BEAST	2023-08-11 T19:22:00	84.06667	31.21667		BEAST	max depth	20230811_2; IceStation #1
PS138_9_Buoy_013	2023 WaveLogger1	2023-08-11 T19:38:00	83.86608	33.90473		WLOG	max depth	deployed next to 2023P280; IceStation #1
PS138_9_Buoy_012	2023P280	2023-08-11 T19:38:00	83.86608	33.90473		ISVP	max depth	deployed next to 2023WaveLogger1. ROV hole; IceStation #1
PS138_9_KEF_002	PS138_9-1_ KEF_ssl-004	2023-08-12 T00:35:00	84.07357	31.21155		STRAP_ICE	max depth	Recovery of ice sediment traps for biogeochemistry; Ice station #1
PS138_27-1		2023-08-12 T04:26:19	83.84003	33.83994	4028	GKG	max depth	IceStation #1
PS138_28-1		2023-08-12 T06:00:35	83.84469	33.65722	4030	TVMUC	Station start	IceStation #1
PS138_28-1		2023-08-12 T09:29:58	83.87609	33.54158	3976	TVMUC	Station end	IceStation #1

Event label	Optional label	Date / Time	Latitude	Longitude	Depth [m]	Gear	Action	Comment
PS138_29-1		2023-08-12 T21:29:00	84.30664	35.75028	3982	XCTD	Station start	
PS138_29-1		2023-08-12 T21:44:16	84.31082	35.84801	3981	XCTD	Station end	
PS138_29-2		2023-08-13 T07:42:04	84.58882	39.42776	3970	XCTD	Station start	
PS138_29-2		2023-08-13 T07:48:25	84.59131	39.52572	3968	XCTD	Station end	
PS138_HELI_ FishingRod_1	CTD_48M_1459	2023-08-13 T12:08:00	84.87000	43.58000		CTD_fishrod	max depth	
PS138_29-3		2023-08-13 T18:48:43	85.15657	48.55479	3929	XCTD	Station start	
PS138_29-3		2023-08-13 T18:59:42	85.15732	48.66383	3926	XCTD	Station end	
PS138_29-4		2023-08-14 T00:38:47	85.39281	54.10000	3905	XCTD	Station start	
PS138_29-4		2023-08-14 T00:46:34	85.38779	54.19656	3902	XCTD	Station end	
PS138_30-1		2023-08-14 T06:42:07	85.34925	59.94552	3867	POS	Station start	Posidonia system and transponder Test
PS138_30-1		2023-08-14 T12:41:36	85.34567	59.90037	3867	POS	Station end	Posidonia system and transponder Test
PS138_29-5		2023-08-14 T13:19:19	85.34972	60.46959	3861	XCTD	Station start	
PS138_29-5		2023-08-14 T13:38:21	85.34594	60.61436	3857	XCTD	Station end	
PS138_29-8		2023-08-14 T16:21:41	85.32303	64.87820	3825	XCTD	Station start	

Event label	Optional label	Date / Time	Latitude	Longitude	Depth [m]	Gear	Action	Comment
PS138_29-8		2023-08-14 T23:04:11	85.17804	72.48155	3767	XCTD	Station end	
PS138_29-6		2023-08-14 T17:36:35	85.28001	66.95265	3805	XCTD	Station start	
PS138_29-6		2023-08-14 T17:42:43	85.28087	67.01409	3805	XCTD	Station end	
PS138_29-7		2023-08-14 T17:57:00	85.28319	67.26108	3801	XCTD	Station start	
PS138_29-7		2023-08-14 T18:04:05	85.28527	67.32142	3800	XCTD	Station end	
PS138_31-1		2023-08-15 T06:08:15	84.94969	80.14008	3727	ICE	Station start	IceStation #2
PS138_31-1		2023-08-17 T10:17:19	84.95631	80.11085	3736	ICE	Station end	IceStation #2
PS138_31_Chemistry-002	snow_sampler_ glove	2023-08-15 T07:55:00	84.90831	80.24779		SSG	max depth	Snow sample; IceStation #2
PS138_31_nortek_ s1000_102149-001	nortek_ s1000_102149	2023-08-15 T08:00:00	84.94969	80.14008		BUOY_ ADCP	max depth	IceStation #2
PS138_31_Buoy_001	2023P268	2023-08-15 T08:00:00	84.94897	80.15367		ISVP	max depth	deployed next to ridge. ice floe 1 nm diameter. 1-2 m thickness; IceStation #2
PS138_31_ Vector_5418-001	Vector_5418	2023-08-15 T08:00:00	69.67800	18.98980		CM	max depth	IceStation #2
PS138_31_Chemistry-003	snow_sampler_ glove	2023-08-15 T08:18:00	84.90208	80.24348		SSG	max depth	Snow Sample; IceStation #2
PS138_32-1		2023-08-15 T08:22:07	84.94899	80.13405	3723	MSN	Station start	IceStation #2
PS138_32-1		2023-08-15 T10:07:14	84.94403	80.15884	3725	MSN	Station end	IceStation #2

Event label	Optional label	Date / Time	Latitude	Longitude	Depth [m]	Gear	Action	Comment
PS138_31_KEF_001	PS138_31-1_KEF_ssl-007	2023-08-15 T08:45:00	84.94969	80.14008		STRAP_ICE	max depth	Deployment of ice sediment traps for biogeochemistry; Ice station #2
PS138_31_Chemistry-004	snow_sampler_glove	2023-08-15 T09:00:00	84.90208	80.24348		SSG	max depth	Snow sample; IceStation #2
PS138_031_SUNAprofil_002	Nitrate_profiler	2023-08-15 T09:16:00	84.94760	80.15280		NO3	max depth	14 profiles; IceStation #2
PS138_31_MSS_1	MSS_90D_075	2023-08-15 T10:36:00	84.94100	80.19180		MSS	max depth	MSS 075 series of 17 profiles; IceStation #2
PS138_31_ICEADCP300_1	300kHzADCP	2023-08-15 T10:36:00	84.94100	80.19180		ADCP	max depth	Under-ice RDI 300 KHz ADCP time series; IceStation #2
PS138_31_GEM_001	gem2-512	2023-08-15 T10:50:00	84.95000	80.13333		BES	max depth	IceStation #2
PS138_31_Chemistry-001	hand_pump	2023-08-15 T11:00:00	84.90831	80.24779		HP	max depth	Melt Pond Water; IceStation #2
PS138_31_Coring-001	SI_corer_9cm	2023-08-15 T12:22:37	84.94969	80.14008		MARKII	max depth	Biocore_1; IceStation #2
PS138_31_Coring-002	SI_corer_9cm	2023-08-15 T12:24:55	84.94969	80.14008		MARKII	max depth	Biocore_2; IceStation #2
PS138_31_Coring-003	SI_corer_9cm	2023-08-15 T12:25:15	84.94969	80.14008		MARKII	max depth	Biocore_3; IceStation #2
PS138_31_Coring-004	SI_corer_9cm	2023-08-15 T12:25:26	84.94969	80.14008		MARKII	max depth	Biocore_4; IceStation #2
PS138_31_Coring-005	SI_corer_9cm	2023-08-15 T12:25:35	84.94969	80.14008		MARKII	max depth	Biocore_5; IceStation #2
PS138_31_Coring-006	SI_corer_9cm	2023-08-15 T12:25:50	84.94969	80.14008		MARKII	max depth	Biocore_6; IceStation #2

Event label	Optional label	Date / Time	Latitude	Longitude	Depth [m]	Gear	Action	Comment
PS138_31_Coring-007	SI_corer_9cm	2023-08-15 T12:26:00	84.94969	80.14008		MARKII	max depth	Biocore_7; IceStation #2
PS138_31_Coring-008	SI_corer_9cm	2023-08-15 T12:26:17	84.94969	80.14008		MARKII	max depth	Biocore_8; IceStation #2
PS138_31_Coring-009	SI_corer_9cm	2023-08-15 T12:26:31	84.94969	80.14008		MARKII	max depth	Biocore_9; IceStation #2
PS138_31_Coring-010	SI_corer_9cm	2023-08-15 T12:27:26	84.94969	80.14008		MARKII	max depth	SIP-Archive; IceStation #2
PS138_31_Coring-011	SI_corer_9cm	2023-08-15 T12:27:40	84.94969	80.14008		MARKII	max depth	SIP-Texture; IceStation #2
PS138_31_Coring-012	hand_pump	2023-08-15 T12:28:51	84.94969	80.14008		HP	max depth	Under Ice Water; IceStation #2
PS138_31_Coring-013	hand_pump	2023-08-15 T12:29:16	84.94969	80.14008		HP	max depth	Melt Pond Water; IceStation #2
PS138_31-1_ISCA-002	ISCA	2023-08-15 T13:00:00	84.94969	80.14008		ISCA	max depth	IceStation #2
PS138_31-1_ISCA-001	ISCA	2023-08-15 T13:00:00	84.94969	80.14008		ISCA	max depth	IceStation #2
PS138_33-1		2023-08-15 T13:26:00	84.93753	80.05573	3672	B_LANDER	Station start	Flux Lander #2. IceStation #2; Posidonia Position
PS138_33-1		2023-08-16 T11:28:00	84.93577	80.06438		B_LANDER	Station end	Flux Lander #2. IceStation #2; Posidonia Position
PS138_31_ROV_001	BEAST	2023-08-15 T15:22:00	84.95000	80.13333		BEAST	max depth	20230815_1; IceStation #2
PS138_31_DRONE_001	UAV_PS	2023-08-15 T16:12:00	84.95000	80.13333		UAV	max depth	Photogrammetry grid over ROV area; IceStation #2
PS138_34-1		2023-08-15 T18:03:30	84.92903	80.09829	3736	OFOBS	Station start	IceStation #2

Event label	Optional label	Date / Time	Latitude	Longitude	Depth [m]	Gear	Action	Comment
PS138_34-1		2023-08-15 T22:10:52	84.92396	80.21904	3736	OFOBS	Station end	IceStation #2
PS138_31_IT_001	PS138_31-1_ IT_ssl-005	2023-08-15 T19:24:00	84.94969	80.14008		STRAP_ICE	max depth	Deployment of ice sediment traps equipped with gel traps; Ice station #2
PS138_35-1		2023-08-15 T23:47:20	84.91837	80.24886	3736	TVMUC	Station start	IceStation #2
PS138_35-1		2023-08-16 T03:37:35	84.90974	80.23959	3734	TVMUC	Station end	IceStation #2
PS138_31_Core_002	SI_corer_14cm	2023-08-16 T00:00:00	84.95000	80.13333		MARKV	max depth	OPT. HI scan. HPLC filter bot 3 cm (0); IceStation #2
PS138_31_Core_001	SI_corer_14cm	2023-08-16 T00:00:00	84.95000	80.13333		MARKV	max depth	OPT. HI scan. HPLC filter bot 3 cm (0); IceStation #2
PS138_36-1		2023-08-16 T03:37:58	84.90973	80.23958	3734	TVMUC	Station start	IceStation #2
PS138_36-1		2023-08-16 T06:16:31	84.90943	80.24276	3732	TVMUC	Station end	IceStation #2
PS138_37-1		2023-08-16 T06:20:40	84.90946	80.24352	3733	ROSINA	Station start	IceStation #2
PS138_37-1		2023-08-16 T09:35:06	84.90847	80.28180	3727	ROSINA	Station end	IceStation #2
PS138_31_IT_002	PS138_31-1_ IT_ssl-006	2023-08-16 T06:55:00	84.94969	80.14008		STRAP_ICE	max depth	Recovery of ice sediment traps equipped with gel traps; Ice station #2

Event label	Optional label	Date / Time	Latitude	Longitude	Depth [m]	Gear	Action	Comment
PS138_31_ASD_001	Dart_ASD	2023-08-16 T07:30:00	84.95000	80.13333		ALBEDOM	max depth	IceStation #2
PS138_31_UpperOcean IceFloeTransect_1	CTD_48M_1459	2023-08-16 T07:30:00	84.91000	80.23000		CTD_fishrod	max depth	Ice floe transect with the fishing rod and upriser.; IceStation #2
PS138_31_Kipps_001	Dart_Kipps	2023-08-16 T07:30:00	84.95000	80.13333		ALBEDOM	max depth	IceStation #2
PS138_31_Chemistry-005	hand_pump	2023-08-16 T08:12:00	84.90208	80.24348		HP	max depth	Ice Edge Water; IceStation #2
PS138_31_MSS_2	MSS_90D_075	2023-08-16 T08:59:00	84.90680	80.29440		MSS	max depth	MSS 075 series of 18 profiles; IceStation #2
PS138_31_Chemistry-007	hand_pump	2023-08-16 T09:36:00	84.90831	80.24779		HP	max depth	Under Ice Water; IceStation #2
PS138_31_Chemistry-006	hand_pump	2023-08-16 T09:41:00	84.90831	80.24779		HP	max depth	Melt Pond Water Experiment; IceStation #2
PS138_31_DRONE_002	UAV_PS	2023-08-16 T10:22:00	84.95000	80.13333		UAV	max depth	Photogrammetry grid over ROV area; IceStation #2
PS138_31_ROV_003	BEAST	2023-08-16 T10:41:00	84.95000	80.13333		BEAST	max depth	20230816_2; IceStation #2
PS138_31_ROV_002	BEAST	2023-08-16 T10:41:00	84.95000	80.13333		BEAST	max depth	20230816_1; IceStation #2

Event label	Optional label	Date / Time	Latitude	Longitude	Depth [m]	Gear	Action	Comment
PS138_Heli_EM-Bird_003	Embird_awi-bird	2023-08-16 T11:13:00	84.90896	80.22300		EMB	max depth	Flight near second IceStation.No wind. sunshine. a lot of open water. During the whole survey. no laser response over open water. …
PS138_Heli_EM-Bird_004	Embird_awi-bird	2023-08-16 T13:09:00	84.93280	80.22000		EMB	max depth	Second flight near second IceStation. A short flight over the IceStation. Pilot flew a lot of steep turns. Watch height and pitch/…
PS138_SBLA_20230816T132000		2023-08-16 T13:20:00	84.86281	80.72304		SBLA	Station start	
PS138_SBLA_20230816T132000		2023-08-16 T13:20:00	84.66822	82.86374		SBLA	Station end	
PS138_SBLA_20230816T134000		2023-08-16 T13:40:00	84.65907	83.15311		SBLA	Station start	
PS138_SBLA_20230816T134000		2023-08-16 T13:40:00	85.05045	84.39423		SBLA	Station end	
PS138_SBLA_20230816T141000		2023-08-16 T14:10:00	85.07694	83.97290		SBLA	Station start	
PS138_SBLA_20230816T141000		2023-08-16 T14:10:00	84.93258	80.88607		SBLA	Station end	
PS138_SBLA_20230816T143000		2023-08-16 T14:30:00	84.90816	80.38153		SBLA	Station start	
PS138_SBLA_20230816T143000		2023-08-16 T14:30:00	84.91124	80.30970		SBLA	Station end	

Event label	Optional label	Date / Time	Latitude	Longitude	Depth [m]	Gear	Action	Comment
PS138_31_ROV_004	BEAST	2023-08-16 T14:51:00	84.95000	80.13333		BEAST	max depth	20230816_3; IceStation #2
PS138_31_KEF_002	PS138_31-1_ KEF_ssl-008	2023-08-16 T19:00:00	84.94969	80.14008		STRAP_ICE	max depth	Recovery of ice sediment traps for biogeochemistry; Ice station #2
PS138_38-1		2023-08-16 T19:54:38	84.91137	80.28111	3731	GKG	max depth	IceStation #2
PS138_39-1		2023-08-16 T23:05:20	84.91084	80.30733	3727	GKG	max depth	IceStation #2
PS138_40-1_1	ISP_Seb	2023-08-17 T00:56:00	84.91108	80.28902	3727	ISP	Station start	IceStation #2
PS138_40-1_1	ISP_Seb	2023-08-17 T05:29:00	84.92897	80.20185	3737	ISP	Station end	IceStation #2
PS138_40-1_2	ISP_Franky	2023-08-17 T01:46:00	84.91282	80.27162	3733	ISP	Station start	failed -- minimum flow reached; IceStation #2
PS138_40-1_2	ISP_Franky	2023-08-17 T05:35:00	84.92952	80.19990	3738	ISP	Station end	failed -- minimum flow reached; IceStation #2
PS138_40-1_3	ISP_Frauke	2023-08-17 T02:25:00	84.91479	80.25845	3737	ISP	Station start	IceStation #2
PS138_40-1_3	ISP_Frauke	2023-08-17 T06:13:00	84.93314	80.18132	3738	ISP	Station end	IceStation #2
PS138_40-1		2023-08-17 T02:37:23	84.91551	80.25443	3736	CTD-RO	max depth	IceStation #2. at max depth
PS138_40-1_4	ISP_Hulda	2023-08-17 T02:48:00	84.91620	80.25089	3736	ISP	Station start	failed -- minimum flow reached; IceStation #2

Event label	Optional label	Date / Time	Latitude	Longitude	Depth [m]	Gear	Action	Comment
PS138_40-1_4	ISP_Hulda	2023-08-17 T06:58:00	84.93756	80.15780	3734	ISP	Station end	failed -- minimum flow reached; IceStation #2
PS138_42-1		2023-08-17 T06:39:09	84.93567	80.16776	3737	HN	Station start	IceStation #2
PS138_42-1		2023-08-17 T06:51:31	84.93691	80.16110	3736	HN	Station end	IceStation #2
PS138_41-1		2023-08-17 T07:01:57	84.93796	80.15589	3737	MSN	Station start	IceStation #2
PS138_41-1		2023-08-17 T09:02:18	84.94970	80.12233	3735	MSN	Station end	IceStation #2
PS138_43-1		2023-08-17 T09:32:10	84.95238	80.11886	3732	CTD-RO	max depth	IceStation #2. at max depth
PS138_44-1		2023-08-17 T10:41:46	84.95645	80.04676	3736	MSC	max depth	IceStation #2
PS138_45-1		2023-08-17 T11:00:09	84.95621	80.04594	3738	MSC	max depth	IceStation #2
PS138_46-1		2023-08-17 T11:19:53	84.95589	80.04145	3739	BONGO	Station start	IceStation #2
PS138_46-1		2023-08-17 T11:30:55	84.95579	80.04059	3737	BONGO	Station end	IceStation #2
PS138_47-1		2023-08-17 T12:08:11	84.95626	80.03796	3737	CTD-RO	max depth	IceStation #2. at max depth
PS138_47-2		2023-08-17 T12:56:21	84.95666	80.02832	3738	CTD-RO	max depth	IceStation #2. at max depth
PS138_48-1		2023-08-17 T13:46:08	84.99868	80.19650	3749	EBS	Station start	IceStation #2
PS138_48-1		2023-08-17 T19:09:37	85.00331	80.58311	3744	EBS	Station end	IceStation #2
PS138_49-1		2023-08-17 T21:22:43	84.92776	84.14347	3734	XCTD	Station start	

Event label	Optional label	Date / Time	Latitude	Longitude	Depth [m]	Gear	Action	Comment
PS138_49-1		2023-08-17 T21:28:01	84.91933	84.20118	3736	XCTD	Station end	
PS138_49-2		2023-08-18 T03:48:02	84.80271	91.08123	3706	XCTD	Station start	
PS138_49-2		2023-08-18 T03:54:53	84.80597	91.14794	3707	XCTD	Station end	
PS138_50-2		2023-08-18 T09:17:08	84.87337	96.66717	2945	PS	Station start	
PS138_50-2		2023-08-18 T15:01:51	84.80900	95.22351	2504	PS	Station end	
PS138_50-1		2023-08-18 T09:33:37	84.85832	96.57589	2322	DS3	Station start	
PS138_50-1		2023-08-18 T15:00:41	84.80900	95.22427	2511	DS3	Station end	
PS138_49-3		2023-08-18 T13:12:16	84.78594	95.28715	1998	XCTD	Station start	
PS138_49-3		2023-08-18 T13:18:04	84.78765	95.30262	2021	XCTD	Station end	
PS138_51-1		2023-08-18 T15:24:59	84.78951	95.22078	1919	OFOBS	Station start	
PS138_51-1		2023-08-18 T20:34:59	84.80110	95.15898	2328	OFOBS	Station end	
PS138_52_nortek_ s1000_102149-001	nortek_ s1000_102149	2023-08-19 T00:00:00	84.76114	107.79211		BUOY_ ADCP	max depth	IceStation #3
PS138_52_ Vector_5418-001	Vector_5418	2023-08-19 T00:00:00	69.67800	18.98980		CM	max depth	IceStation #3
PS138_49-4		2023-08-19 T03:34:47	84.73196	100.31047	3973	XCTD	Station start	
PS138_49-4		2023-08-19 T03:40:41	84.72712	100.34119	3969	XCTD	Station end	

Event label	Optional label	Date / Time	Latitude	Longitude	Depth [m]	Gear	Action	Comment
PS138_49-5		2023-08-19 T08:30:00	84.73764	105.36718	3946	XCTD	Station start	
PS138_49-5		2023-08-19 T08:36:14	84.73985	105.41267	3949	XCTD	Station end	
PS138_52-1		2023-08-19 T12:00:11	84.76114	107.79211	3857	ICE	Station start	IceStation #3
PS138_52-1		2023-08-21 T20:02:36	84.68355	107.71274	3825	ICE	Station end	IceStation #3
PS138_052_ SUNAprofil_003	Nitrate_profiler	2023-08-19 T14:26:00	84.74690	107.70750		NO3	max depth	10 profiles
PS138_52_KEF_001	PS138_52-1_ KEF_ssl-011	2023-08-19 T14:53:00	84.76114	107.79211		STRAP_ICE	max depth	Deployment of ice sediment traps for biogeochemistry; Ice station #3
PS138_53-1		2023-08-19 T15:42:57	84.75133	107.71773	3971	OFOBS	Station start	IceStation #3
PS138_53-1		2023-08-19 T19:38:30	84.73715	107.69658	3978	OFOBS	Station end	IceStation #3
PS138_52_ ICEADCP300_1	300kHzADCP	2023-08-19 T15:51:00	84.74840	107.71470		ADCP	max depth	Under-ice RDI 300 kHz ADCP time series; IceStation #3
PS138_52_MSS_1	mss_90L_097	2023-08-19 T15:51:00	84.74840	107.71470		MSS	max depth	MSS 097 series of 6 profiles; IceStation #3
PS138_52_DRONE_001	UAV_PS	2023-08-19 T16:24:00	84.76667	107.78333		UAV	max depth	Photogrammetry grid over floe; IceStation #3
PS138_52_GEM_001	gem2-512	2023-08-19 T16:46:00	84.76667	107.78333		BES	max depth	IceStation #3

Event label	Optional label	Date / Time	Latitude	Longitude	Depth [m]	Gear	Action	Comment
PS138_52_Magna_001	magnaprobe-steffi	2023-08-19 T16:48:00	84.76667	107.78333		MAGNA	max depth	IceStation #3
PS138_52_Chemistry-002	hand_pump	2023-08-19 T17:00:00	84.75238	107.73031		HP	max depth	Under Ice Water; IceStation #3
PS138_52_Chemistry-001	snow_sampler_glove	2023-08-19 T17:00:00	84.75238	107.73031		SSG	max depth	Snow sample; IceStation #3
PS138_52_Coring-001	SI_corer_9cm	2023-08-19 T17:26:16	84.76114	107.79211		MARKII	max depth	Biocore_1; IceStation #3
PS138_52_Coring-002	SI_corer_9cm	2023-08-19 T17:26:32	84.76114	107.79211		MARKII	max depth	Biocore_2; IceStation #3
PS138_52_Coring-003	SI_corer_9cm	2023-08-19 T17:26:46	84.76114	107.79211		MARKII	max depth	Biocore_3; IceStation #3
PS138_52_Coring-004	SI_corer_9cm	2023-08-19 T17:26:56	84.76114	107.79211		MARKII	max depth	Biocore_4; IceStation #3
PS138_52_Coring-005	SI_corer_9cm	2023-08-19 T17:27:03	84.76114	107.79211		MARKII	max depth	Biocore_5; IceStation #3
PS138_52_Coring-006	SI_corer_9cm	2023-08-19 T17:27:11	84.76114	107.79211		MARKII	max depth	Biocore_6; IceStation #3
PS138_52_Coring-007	SI_corer_9cm	2023-08-19 T17:27:18	84.76114	107.79211		MARKII	max depth	Biocore_7; IceStation #3
PS138_52_Coring-008	SI_corer_9cm	2023-08-19 T17:27:28	84.76114	107.79211		MARKII	max depth	Biocore_8; IceStation #3
PS138_52_Coring-009	SI_corer_9cm	2023-08-19 T17:27:37	84.76114	107.79211		MARKII	max depth	Biocore_9; IceStation #3
PS138_52_Coring-010	SI_corer_9cm	2023-08-19 T17:34:10	84.76114	107.79211		MARKII	max depth	SIP-Texture; IceStation #3
PS138_52_Coring-011	SI_corer_9cm	2023-08-19 T17:34:45	84.76114	107.79211		MARKII	max depth	SIP-Archive; IceStation #3
PS138_52_Chemistry-003	snow_sampler_glove	2023-08-19 T17:35:00	84.74833	107.72472		SSG	max depth	Snow sample; IceStation #3

Event label	Optional label	Date / Time	Latitude	Longitude	Depth [m]	Gear	Action	Comment
PS138_52_Coring-012	SI_corer_9cm	2023-08-19 T17:35:35	84.76114	107.79211		MARKII	max depth	Biocore at ice edge of floe; IceStation #3
PS138_52_Coring-013	hand_pump	2023-08-19 T17:36:15	84.76114	107.79211		HP	max depth	Under Ice Water; IceStation #3
PS138_52_Coring-014	snow_sampler_ glove	2023-08-19 T17:37:06	84.76114	107.79211		SSG	max depth	Snow Sample; IceStation #3
PS138_52_Coring-015	falcon_tube	2023-08-19 T17:38:01	84.76114	107.79211		WS	max depth	Algae fishing at ice edge of floe; IceStation #3
PS138_52-1_ISCA-001	ISCA	2023-08-19 T18:00:00	84.76114	107.79211		ISCA	max depth	IceStation #3
PS138_52_Chemistry-005	hand_pump	2023-08-19 T18:30:00	84.75238	107.73031		HP	max depth	Algae Experiment; IceStation #3
PS138_52_IT_001	PS138_52-1_ IT_ssl-009	2023-08-19 T18:53:00	84.76114	107.79211		STRAP_ICE	max depth	Deployment of ice sediment traps equipped with gel traps; Ice station #3
PS138_52_Chemistry-004	snow_sampler_ glove	2023-08-19 T19:08:00	84.74861	107.71444		SSG	max depth	Snow sample; IceStation #3
PS138_54-1		2023-08-19 T21:30:56	84.72721	107.69422	3978	ROSINA	Station start	IceStation #3
PS138_54-1		2023-08-20 T01:38:18	84.70617	107.65608	3968	ROSINA	Station end	IceStation #3
PS138_52_Core_002	SI_corer_14cm	2023-08-20 T00:00:00	84.76667	107.78333		MARKV	max depth	1x OPT. HI scan. no bio samples; IceStation #3
PS138_52_Core_001	SI_corer_14cm	2023-08-20 T00:00:00	84.76667	107.78333		MARKV	max depth	1x OPT. HI scan. 1 x HPLC/Fluo filter bot 3 cm (1); IceStation #3

Event label	Optional label	Date / Time	Latitude	Longitude	Depth [m]	Gear	Action	Comment
PS138_55-1		2023-08-20 T01:39:16	84.70610	107.65581	3968	MSN	Station start	IceStation #3
PS138_55-1		2023-08-20 T03:38:48	84.69935	107.63245	3853	MSN	Station end	IceStation #3
PS138_56-1		2023-08-20 T03:39:53	84.69930	107.63239	3845	MSN	Station start	IceStation #3
PS138_56-1		2023-08-20 T05:22:21	84.69603	107.63071	3758	MSN	Station end	IceStation #3
PS138_52_ASD_001	Dart_ASD	2023-08-20 T06:13:00	84.76667	107.78333		ALBEDOM	max depth	IceStation #3
PS138_52_Kipps_001	Dart_Kipps	2023-08-20 T06:13:00	84.76667	107.78333		ALBEDOM	max depth	IceStation #3
PS138_52_MSS_2	MSS_90D_075	2023-08-20 T06:30:00	84.69300	107.64540		MSS	max depth	MSS 075 series of 17 profiles; IceStation #3
PS138_Heli_EM-Bird_005	Embird_awi-bird	2023-08-20 T07:50:00				EMB	max depth	Calibration measurement inside the helicopter hangar. The difference between laser heigth and coil plane is measured.; IceStation …
PS138_52_ROV_001	BEAST	2023-08-20 T08:19:00	84.76667	107.78333		BEAST	max depth	20230820_1; IceStation #3
PS138_52_UpperOcean IceFloeTransect_1	CTD_48M_1459	2023-08-20 T08:30:00	84.69000	107.57000		CTD_fishrod	max depth	Ice floe transect with the fishing rod and upriser.; IceStation #3

Event label	Optional label	Date / Time	Latitude	Longitude	Depth [m]	Gear	Action	Comment
PS138_57-1		2023-08-20 T10:17:00	84.70647	107.66985	3965	B_LANDER	Station start	Flux Lander #2. IceStation #3; Posidonia Position
PS138_57-1		2023-08-21 T07:52:00	84.70800	107.67723	3971	B_LANDER	Station end	Flux Lander #2. IceStation #3; Posidonia Position
PS138_58-1		2023-08-20 T13:47:00	84.72112	107.47135	3956	B_LANDER	Station start	Flux Lander #3. IceStation #3; Posidonia Position
PS138_58-1		2023-08-22 T07:27:00	84.72217	107.48080	3971	B_LANDER	Station end	Flux Lander #3. IceStation #3; Posidonia Position
PS138_59-1		2023-08-20 T15:30:05	84.69045	107.30669	3726	TVMUC	Station start	IceStation #3
PS138_59-1		2023-08-20 T18:30:42	84.68854	107.30758	3731	TVMUC	Station end	IceStation #3
PS138_52_ROV_002	BEAST	2023-08-20 T15:41:00	84.76667	107.78333		BEAST	max depth	20230820_2; IceStation #3
PS138_52_DRONE_002	UAV_PS	2023-08-20 T16:27:00	84.76667	107.78333		UAV	max depth	Photogrammetry survey and floe and ship shot; IceStation #3
PS138_52_Coring-016	falcon_tube	2023-08-20 T16:31:00	84.76114	107.79211		WS	max depth	Algae fishing trap hole; IceStation #3
PS138_52_IT_002	PS138_52-1_ IT_ssl-010	2023-08-20 T18:00:00	84.76114	107.79211		STRAP_ICE	max depth	Recovery of ice sediment traps equipped with gel traps; Ice station #3

Event label	Optional label	Date / Time	Latitude	Longitude	Depth [m]	Gear	Action	Comment
PS138_52_KEF_002	PS138_52-1_ KEF_ssl-012	2023-08-20 T18:20:00	84.76114	107.79211		STRAP_ICE	max depth	Recovery of ice sediment traps for biogeochemistry; Ice station #3
PS138_60-1		2023-08-20 T18:31:11	84.68852	107.30763	3731	TVMUC	Station start	IceStation #3
PS138_60-1		2023-08-20 T21:29:07	84.68364	107.29687	3787	TVMUC	Station end	IceStation #3
PS138_61-1		2023-08-20 T22:14:44	84.68212	107.10598	3952	EBS	Station start	IceStation #3
PS138_61-1		2023-08-21 T04:19:09	84.72895	107.13916	3606	EBS	Station end	IceStation #3
PS138_52_MSS_3	MSS_90D_075	2023-08-21 T07:04:00	84.69020	107.25840		MSS	max depth	MSS 075 series of 16 profiles; IceStation #3
PS138_52_ROV_003	BEAST	2023-08-21 T08:19:00	84.76667	107.78333		BEAST	max depth	20230821_1; IceStation #3
PS138_52_Buoy_001	2023P264	2023-08-21 T09:40:00	84.69005	107.28837		ISVP	max depth	MSS site; IceStation #3
PS138_62-1		2023-08-21 T13:35:27	84.70979	107.74979	3979	GKG	max depth	IceStation #3
PS138_64-1		2023-08-21 T16:51:33	84.69183	107.52553	3500	HN	Station start	IceStation #3
PS138_64-1		2023-08-21 T17:12:35	84.69119	107.55118	3555	HN	Station end	IceStation #3
PS138_63-1		2023-08-21 T16:57:34	84.69166	107.53294	3528	CTD-RO	max depth	IceStation #3. at max depth
PS138_65-1		2023-08-21 T17:35:18	84.69040	107.57726	3608	BONGO	Station start	IceStation #3
PS138_65-1		2023-08-21 T17:41:43	84.69016	107.58452	3618	BONGO	Station end	IceStation #3

Event label	Optional label	Date / Time	Latitude	Longitude	Depth [m]	Gear	Action	Comment
PS138_66-1		2023-08-21 T18:48:37	84.68741	107.65937	3751	CTD-RO	max depth	IceStation #3. at max depth
PS138_67-1		2023-08-21 T19:28:59	84.68557	107.70804	3783	MSC	max depth	IceStation #3
PS138_68-1		2023-08-21 T19:43:39	84.68493	107.72434	3786	MSC	max depth	IceStation #3
PS138_69-1_1	ISP_Seb	2023-08-21 T21:24:00	84.73336	107.57680	3977	ISP	Station start	IceStation #3
PS138_69-1_1	ISP_Seb	2023-08-22 T03:29:00	84.71742	107.57176	3973	ISP	Station end	IceStation #3
PS138_69-1_2	ISP_Frauke	2023-08-21 T22:15:00	84.73318	107.56997	3977	ISP	Station start	IceStation #3
PS138_69-1_2	ISP_Frauke	2023-08-22 T02:39:00	84.72321	107.55995	3974	ISP	Station end	IceStation #3
PS138_69-1_3	ISP_Franky	2023-08-21 T22:52:00	84.73317	107.57064	3975	ISP	Station start	IceStation #3
PS138_69-1_3	ISP_Franky	2023-08-22 T02:00:00	84.72648	107.54926	3976	ISP	Station end	IceStation #3
PS138_69-1		2023-08-21 T23:02:45	84.73307	107.57279	3977	CTD-RO	max depth	IceStation #3. at max depth
PS138_69-1_4	ISP_Hulda	2023-08-21 T23:15:00	84.73346	107.57417	3976	ISP	Station start	failed -- minimum flow reached; IceStation #3
PS138_69-1_4	ISP_Hulda	2023-08-22 T01:51:00	84.72727	107.55386	3976	ISP	Station end	failed -- minimum flow reached; IceStation #3
PS138_70-1		2023-08-22 T05:26:02	84.71161	107.63300	3972	GKG	max depth	IceStation #3
PS138_71-1		2023-08-22 T11:56:53	84.71411	108.28314	3872	EBS	Station start	IceStation #3

Event label	Optional label	Date / Time	Latitude	Longitude	Depth [m]	Gear	Action	Comment
PS138_71-1		2023-08-22 T16:32:52	84.69837	108.05872	3977	EBS	Station end	IceStation #3
PS138_72-1		2023-08-22 T21:45:57	84.40093	111.98967	2574	XCTD	Station start	
PS138_72-1		2023-08-22 T22:00:11	84.40287	112.11097	2761	XCTD	Station end	
PS138_72-2		2023-08-23 T02:36:42	84.10857	116.15888	3961	XCTD	Station start	
PS138_72-2		2023-08-23 T02:42:15	84.10567	116.18010	3962	XCTD	Station end	
PS138_72-3		2023-08-23 T07:43:50	83.84287	120.24894	3448	XCTD	Station start	
PS138_72-3		2023-08-23 T07:55:40	83.83739	120.30725	3451	XCTD	Station end	
PS138_73-1	2023P263	2023-08-23 T11:41:49	83.64411	122.13010	4051	ISVP	Station start	2023P263 MetOcean SVP-B 300534063488690
PS138_73-1	2023P263	2023-08-23 T11:49:09	83.64343	122.13392	4054	ISVP	Station end	2023P263 MetOcean SVP-B 300534063488690
PS138_HELI_ FishingRod_2	CTD_48M_1459	2023-08-23 T13:50:00	83.52000	123.79000		CTD_fishrod	max depth	
PS138_72-4		2023-08-23 T18:44:45	83.22496	127.23622	4201	XCTD	Station start	
PS138_72-4		2023-08-23 T18:50:50	83.22189	127.22157	4201	XCTD	Station end	
PS138_74-1		2023-08-23 T23:09:57	82.90035	130.18408	4155	EBS	Station start	IceStation #4
PS138_74-1		2023-08-24 T04:04:55	82.88666	130.05530	4156	EBS	Station end	IceStation #4

Event label	Optional label	Date / Time	Latitude	Longitude	Depth [m]	Gear	Action	Comment
PS138_75_Core_002	SI_corer_14cm	2023-08-24 T00:00:00	82.90200	129.99300		MARKV	max depth	1x OPT. HI scan. no bio samples; IceStation #4
PS138_75_ Vector_5418-001	Vector_5418	2023-08-24 T00:00:00	84.07357	31.21155		CM	max depth	IceStation #4
PS138_75_nortek_ s1000_102149-001	nortek_ s1000_102149	2023-08-24 T00:00:00	82.90224	129.99332		BUOY_ ADCP	max depth	IceStation #4
PS138_75_Core_001	SI_corer_14cm	2023-08-24 T00:00:00	82.90200	129.99300		MARKV	max depth	1x OPT. HI scan. 1 x HPLC/Fluo filter bot 3 cm (1); IceStation #4
PS138_75_Kipps_001	Dart_Kipps	2023-08-24 T03:30:00	82.90200	129.99300		ALBEDOM	max depth	IceStation #4
PS138_75_ASD_001	Dart_ASD	2023-08-24 T03:30:00	82.90200	129.99300		ALBEDOM	max depth	IceStation #4
PS138_75-1		2023-08-24 T06:32:18	82.90224	129.99332	4160	ICE	Station start	IceStation #4
PS138_75-1		2023-08-26 T18:26:20	82.95848	129.87187	4164	ICE	Station end	IceStation #4
PS138_76-1		2023-08-24 T08:20:48	82.90815	130.02605	4157	TVMUC	Station start	IceStation #4
PS138_76-1		2023-08-24 T11:32:35	82.91407	130.17055	4157	TVMUC	Station end	IceStation #4
PS138_75_Chemistry-004	hand_pump	2023-08-24 T09:00:00	82.90548	130.00163		HP	max depth	Under Ice Water; IceStation #4
PS138_75_Chemistry-002	hand_pump	2023-08-24 T09:00:00	82.90895	130.05508		HP	max depth	Ice Edge Water; IceStation #4
PS138_75_Chemistry-003	hand_pump	2023-08-24 T09:00:00	82.90548	130.00163		HP	max depth	Melt Pond Water; IceStation #4

Event label	Optional label	Date / Time	Latitude	Longitude	Depth [m]	Gear	Action	Comment
PS138_Heli_EM-Bird_006	Embird_awi-bird	2023-08-24 T09:31:00	82.91170	130.07050		EMB	max depth	Flight near the fourth IceStation.; IceStation #4
PS138_75_IT_001	PS138_75-1_IT_ssl-013	2023-08-24 T10:00:00	82.90224	129.99332		STRAP_ICE	max depth	Deployment of ice sediment traps equipped with gel traps; Ice station #4
PS138_75_Chemistry-001	snow_sampler_glove	2023-08-24 T10:00:00	82.90548	130.00163		SSG	max depth	Snow sample; IceStation #4
PS138_75_KEF_001	PS138_75-1_KEF_ssl-015	2023-08-24 T10:34:00	82.90224	129.99332		STRAP_ICE	max depth	Deployment of ice sediment traps for biogeochemistry; Ice station #4
PS138_77-1		2023-08-24 T11:33:10	82.91407	130.17099	4156	TVMUC	Station start	IceStation #4
PS138_77-1		2023-08-24 T14:35:09	82.91063	130.20413	4156	TVMUC	Station end	IceStation #4
PS138_SBLA_20230824T113400		2023-08-24 T11:34:00	82.87642	130.71237		SBLA	Station start	
PS138_SBLA_20230824T113400		2023-08-24 T11:34:00	82.98818	130.58651		SBLA	Station end	
PS138_75_DRONE_001	UAV_PS	2023-08-24 T11:40:00	82.90200	129.99300		UAV	max depth	Photogrammetry grid over floe; IceStation #4
PS138_SBLA_20230824T115700		2023-08-24 T11:57:00	82.97267	130.69414		SBLA	Station start	
PS138_SBLA_20230824T115700		2023-08-24 T11:57:00	82.91083	130.74962		SBLA	Station end	
PS138_SBLA_20230824T122100		2023-08-24 T12:21:00	82.97367	130.68492		SBLA	Station start	

Event label	Optional label	Date / Time	Latitude	Longitude	Depth [m]	Gear	Action	Comment
PS138_ SBLA_20230824T122100		2023-08-24 T12:21:00	82.98491	130.53946		SBLA	Station end	
PS138_ SBLA_20230824T124200		2023-08-24 T12:42:00	82.99778	130.40258		SBLA	Station start	
PS138_ SBLA_20230824T124200		2023-08-24 T12:42:00	82.97351	130.30659		SBLA	Station end	
PS138_75_Chemistry-005	snow_sampler_ glove	2023-08-24 T14:00:00	82.92832	130.14766		SSG	max depth	Snow sample; IceStation #4
PS138_75_Chemistry-006	snow_sampler_ glove	2023-08-24 T14:00:00	82.91458	130.24198		SSG	max depth	Snow sample; IceStation #4
PS138_78-1		2023-08-24 T15:44:49	82.91245	130.16156	4157	OFOBS	Station start	IceStation #4
PS138_78-1		2023-08-24 T22:23:59	82.96801	130.12882	4161	OFOBS	Station end	IceStation #4
PS138_75_Buoy_002	2023I12	2023-08-24 T16:00:00	82.91550	130.18078		SIMB	max depth	IceStation #4
PS138_75_MSS_1	MSS_90D_075	2023-08-24 T16:08:00	82.91440	130.16020		MSS	max depth	MSS 075 series of 4 profiles; IceStation #4
PS138_75_ICEADCP_1	300kHzADCP	2023-08-24 T16:08:00	82.91440	130.16020		ADCP	max depth	Under-ice RDI 300 kHz ADCP time series; IceStation #4
PS138_75_ROV_001	BEAST	2023-08-24 T16:26:00	82.90200	129.99300		BEAST	max depth	20230824_1; IceStation #4
PS138_75_Coring-001	SI_corer_9cm	2023-08-24 T16:33:09	82.90224	129.99332		MARKII	max depth	Biocore_1; IceStation #4
PS138_75_Coring-002	SI_corer_9cm	2023-08-24 T16:35:22	82.90224	129.99332		MARKII	max depth	Biocore_2; IceStation #4
PS138_75_Coring-003	SI_corer_9cm	2023-08-24 T16:35:35	82.90224	129.99332		MARKII	max depth	Biocore_3; IceStation #4

Event label	Optional label	Date / Time	Latitude	Longitude	Depth [m]	Gear	Action	Comment
PS138_75_Coring-004	SI_corer_9cm	2023-08-24 T16:35:44	82.90224	129.99332		MARKII	max depth	Biocore_4; IceStation #4
PS138_75_Coring-005	SI_corer_9cm	2023-08-24 T16:35:52	82.90224	129.99332		MARKII	max depth	Biocore_5; IceStation #4
PS138_75_Coring-006	SI_corer_9cm	2023-08-24 T16:36:03	82.90224	129.99332		MARKII	max depth	Biocore_6; IceStation #4
PS138_75_Coring-007	SI_corer_9cm	2023-08-24 T16:36:09	82.90224	129.99332		MARKII	max depth	Biocore_7; IceStation #4
PS138_75_Coring-008	SI_corer_9cm	2023-08-24 T16:36:16	82.90224	129.99332		MARKII	max depth	Biocore_8; IceStation #4
PS138_75_Coring-009	SI_corer_9cm	2023-08-24 T16:36:26	82.90224	129.99332		MARKII	max depth	Biocore_9; IceStation #4
PS138_75_Coring-010	SI_corer_9cm	2023-08-24 T16:36:35	82.90224	129.99332		MARKII	max depth	SIP-texture; IceStation #4
PS138_75_Coring-011	SI_corer_9cm	2023-08-24 T16:37:08	82.90224	129.99332		MARKII	max depth	SIP-archive; IceStation #4
PS138_75_Coring-012	SI_corer_9cm	2023-08-24 T16:37:22	82.90224	129.99332		MARKII	max depth	SIP-salinity; IceStation #4
PS138_75_Coring-013	hand_pump	2023-08-24 T16:37:36	82.90224	129.99332		HP	max depth	Under Ice Water; IceStation #4
PS138_75_Coring-014	hand_pump	2023-08-24 T16:38:04	82.90224	129.99332		HP	max depth	Melt Pond Water; IceStation #4
PS138_75_Coring-015	snow_sampler_ glove	2023-08-24 T16:38:38	82.90224	129.99332		SSG	max depth	Snow Sample; IceStation #4
PS138_75-1_ISCA-002	ISCA	2023-08-24 T17:00:00	82.90224	129.99332		ISCA	max depth	IceStation #4
PS138_75-1_ISCA-001	ISCA	2023-08-24 T17:00:00	82.90224	129.99332		ISCA	max depth	IceStation #4
PS138_75-1_ISCA-003	ISCA	2023-08-24 T17:00:00	82.90224	129.99332		ISCA	max depth	IceStation #4

Event label	Optional label	Date / Time	Latitude	Longitude	Depth [m]	Gear	Action	Comment
PS138_79-1		2023-08-24 T17:20:58	82.92138	130.08649	4156	HN	Station start	IceStation #4
PS138_79-1		2023-08-24 T17:35:10	82.92335	130.07619	4157	HN	Station end	IceStation #4
PS138_80-1		2023-08-24 T22:24:30	82.96805	130.12925	4160	ROSINA	Station start	IceStation #4
PS138_80-1		2023-08-25 T01:21:53	82.96954	130.21135	4157	ROSINA	Station end	IceStation #4
PS138_81-1		2023-08-25 T01:23:01	82.96950	130.21114	4157	MSN	Station start	IceStation #4
PS138_81-1		2023-08-25 T03:14:29	82.96750	130.14790	4159	MSN	Station end	IceStation #4
PS138_82-1		2023-08-25 T03:15:03	82.96751	130.14742	4159	MSN	Station start	IceStation #4
PS138_82-1		2023-08-25 T04:58:42	82.97286	130.05065	4160	MSN	Station end	IceStation #4
PS138_075_ SUNAprofil_004	Nitrate_profiler	2023-08-25 T05:09:00	83.01560	130.11960		NO3	max depth	7 profiles; IceStation #4
PS138_75_MSS_2	MSS_90D_075	2023-08-25 T07:09:00	82.98940	129.99390		MSS	max depth	MSS 075 series of 14 profiles; IceStation #4
PS138_75_ROV_002	BEAST	2023-08-25 T07:51:00	82.90200	129.99300		BEAST	max depth	20230825_1; IceStation #4
PS138_83-1		2023-08-25 T10:22:00	82.99340	129.92290	4153	B_LANDER	Station start	Flux Lander #2. IceStation #4; Posidonia Position
PS138_83-1		2023-08-26 T07:02:00	82.99448	129.93480	4162	B_LANDER	Station end	Flux Lander #2. IceStation #4; Posidonia Position

Event label	Optional label	Date / Time	Latitude	Longitude	Depth [m]	Gear	Action	Comment
PS138_75_Buoy_001	2023S123	2023-08-25 T12:45:00	83.01513	130.15450		BUOY_ SNOW	max depth	scattering layer 0.03m at all pingers. second-year ice patch on FYI floe; co-deployed with 2023T99; IceStation #4
PS138_75_Buoy_003	2023T99	2023-08-25 T13:10:00	83.01403	130.15570		SIMBA	max depth	ice thickness 2.06m. freeboard: 0.31m. scattering layer: 0.03m. thermistor 26 at surface. second-year ice patch on FYI floe; co-de…
PS138_75_Buoy_004	2023O18	2023-08-25 T14:00:00	83.01098	130.15263		BUOY_CTD	max depth	IceStation #4
PS138_84-1		2023-08-25 T14:26:00	82.99185	130.01818	4153	B_LANDER	Station start	Flux Lander #3. IceStation #4; Posidonia Position
PS138_84-1		2023-08-26 T12:13:00	82.99182	130.03427	4162	B_LANDER	Station end	Flux Lander #3. IceStation #4; Posidonia Position
PS138_75_GEM_001	gem2-512	2023-08-25 T14:31:00	82.90200	129.99300		BES	max depth	IceStation #4
PS138_86-1		2023-08-25 T16:28:23	83.00463	129.96980	4164	HN	Station start	IceStation #4
PS138_86-1		2023-08-25 T16:38:16	83.00489	129.95702	4163	HN	Station end	IceStation #4
PS138_85-1		2023-08-25 T16:29:37	83.00466	129.96820	4164	CTD-RO	max depth	IceStation #4. at max depth

Event label	Optional label	Date / Time	Latitude	Longitude	Depth [m]	Gear	Action	Comment
PS138_87-1		2023-08-25 T16:58:00	83.00567	129.93172	4163	MSC	max depth	IceStation #4
PS138_88-1		2023-08-25 T17:35:02	83.00832	129.88582	4163	CTD-RO	max depth	IceStation #4. at max depth
PS138_89-1		2023-08-25 T18:01:02	83.01118	129.85705	4166	BONGO	Station start	IceStation #4
PS138_89-1		2023-08-25 T18:07:09	83.01196	129.85091	4166	BONGO	Station end	IceStation #4
PS138_90-1		2023-08-25 T18:09:35	83.01227	129.84857	4168	CTD-RO	max depth	IceStation #4. at max depth
PS138_75_IT_002	PS138_75-1_ IT_ssl-014	2023-08-25 T18:58:00	82.90224	129.99332		STRAP_ICE	max depth	Recovery of ice sediment traps equipped with gel traps; Ice station #4
PS138_90-1_1	ISP_Seb	2023-08-25 T19:14:00	83.02235	129.80317	4166	ISP	Station start	IceStation #4
PS138_90-1_1	ISP_Seb	2023-08-26 T01:31:00	83.03682	130.09742	4166	ISP	Station end	IceStation #4
PS138_75_KEF_002	PS138_75-1_ KEF_ssl-016	2023-08-25 T19:37:00	82.90224	129.99332		STRAP_ICE	max depth	Recovery of ice sediment traps for biogeochemistry; Ice station #4
PS138_90-1_2	ISP_Franky	2023-08-25 T20:12:00	83.03197	129.79940	4169	ISP	Station start	IceStation #4
PS138_90-1_2	ISP_Franky	2023-08-26 T00:36:00	83.04242	130.06035	4165	ISP	Station end	IceStation #4
PS138_90-1_3	ISP_Frauke	2023-08-25 T20:58:00	83.03872	129.82149	4168	ISP	Station start	IceStation #4
PS138_90-1_3	ISP_Frauke	2023-08-25 T23:57:00	83.04539	130.02068	4165	ISP	Station end	IceStation #4

Event label	Optional label	Date / Time	Latitude	Longitude	Depth [m]	Gear	Action	Comment
PS138_90-1_4	ISP_Hulda	2023-08-25 T21:25:00	83.04179	129.84248	4168	ISP	Station start	used with controller of pump ISP_Jimmy; IceStation #4
PS138_90-1_4	ISP_Hulda	2023-08-25 T23:46:00	83.04600	130.00816	4166	ISP	Station end	used with controller of pump ISP_Jimmy; IceStation #4
PS138_91-1		2023-08-26 T03:22:51	83.02581	130.10010	4161	GKG	max depth	IceStation #4
PS138_92-1		2023-08-26 T16:49:54	82.95274	129.94487	4165	GKG	max depth	IceStation #4
PS138_93-1		2023-08-26 T19:00:13	83.01356	130.01174	4163	ARGOFL	Station start	
PS138_93-1		2023-08-26 T19:16:01	83.03358	129.94997	4168	ARGOFL	Station end	
PS138_94-1		2023-08-26 T22:46:13	83.40243	129.88500	4201	XCTD	Station start	
PS138_94-1		2023-08-26 T23:14:06	83.40099	129.93802	4199	XCTD	Station end	
PS138_95-1	2023P289	2023-08-26 T22:46:47	83.40241	129.88609	4203	ISVP	Station start	2023P289 Pacific Gyre Ice Tracker 300534062124450
PS138_95-1	2023P289	2023-08-26 T22:55:54	83.40199	129.90364	4200	ISVP	Station end	2023P289 Pacific Gyre Ice Tracker 300534062124450
PS138_96-1	2023P266	2023-08-27 T03:45:06	83.88587	129.72259	4257	ISVP	Station start	2023P266 MetOcean SVP-B 300534063488690
PS138_96-1	2023P266	2023-08-27 T03:59:30	83.88672	129.72057	4256	ISVP	Station end	2023P266 MetOcean SVP-B 300534063488690

Event label	Optional label	Date / Time	Latitude	Longitude	Depth [m]	Gear	Action	Comment
PS138_94-2		2023-08-27 T04:08:40	83.88723	129.71994	4257	XCTD	Station start	
PS138_94-2		2023-08-27 T04:16:29	83.88846	129.71888	4257	XCTD	Station end	
PS138_97-1	2023P290	2023-08-27 T08:10:21	84.36813	130.04485	4278	BUOY_ICE_ TRACK	Station start	2023P290 Pacific Gyre Ice Tracker 300534062125830
PS138_97-1	2023P290	2023-08-27 T08:52:29	84.37486	130.03148	4282	BUOY_ICE_ TRACK	Station end	2023P290 Pacific Gyre Ice Tracker 300534062125830
PS138_94-3		2023-08-27 T08:42:48	84.37461	130.02022	4281	XCTD	Station start	
PS138_94-3		2023-08-27 T08:56:01	84.37485	130.03587	4279	XCTD	Station end	
PS138_Heli_EM-Bird_007	Embird_awi-bird	2023-08-27 T11:48:00	84.59560	130.16290		EMB	max depth	Short flight during Transit that had to be aborted due to bad weather.; IceStation #5
PS138_98-1		2023-08-27 T17:40:15	85.04653	130.00547	4298	TVMUC	Station start	IceStation #5
PS138_98-1		2023-08-27 T20:58:08	85.04979	130.16616	4298	TVMUC	Station end	IceStation #5
PS138_99-1		2023-08-27 T20:58:40	85.04978	130.16662	4299	TVMUC	Station start	IceStation #5
PS138_99-1		2023-08-28 T00:19:57	85.03983	130.29999	4298	TVMUC	Station end	IceStation #5
PS138_101_nortek_ s1000_102149-001	nortek_ s1000_102149	2023-08-28 T00:00:00	85.04528	130.35034		BUOY_ ADCP	max depth	station 5; IceStation #5

Event label	Optional label	Date / Time	Latitude	Longitude	Depth [m]	Gear	Action	Comment
PS138_101_Core_001	SI_corer_14cm	2023-08-28 T00:00:00	85.04500	130.35000		MARKV	max depth	1x OPT. HI scan. no bio samples; IceStation #5
PS138_101_ Vector_5418-001	Vector_5418	2023-08-28 T00:00:00	84.94969	80.14008		CM	max depth	IceStation #5
PS138_100-1		2023-08-28 T00:21:23	85.03974	130.30046	4298	EBS	Station start	IceStation #5
PS138_100-1		2023-08-28 T06:39:01	85.04526	130.26842	4301	EBS	Station end	IceStation #5
PS138_101-1		2023-08-28 T09:25:07	85.04528	130.35034	4298	ICE	Station start	IceStation #5
PS138_101-1		2023-08-31 T20:36:26	84.94013	129.40775	4303	ICE	Station end	IceStation #5
PS138_101_ Chemistry-004	snow_sampler_ glove	2023-08-28 T11:38:00	85.03618	130.37361		SSG	max depth	Snow sample; IceStation #5
PS138_101_ Chemistry-001	hand_pump	2023-08-28 T11:39:00	85.03689	130.36995		HP	max depth	Ice Edge Water; IceStation #5
PS138_102-1		2023-08-28 T12:06:23	85.03908	130.42073	4295	OFOBS	Station start	IceStation #5
PS138_102-1		2023-08-28 T19:58:51	85.04092	130.33575	4298	OFOBS	Station end	IceStation #5
PS138_101_ Chemistry-005	snow_sampler_ glove	2023-08-28 T12:32:00	85.03611	130.40722		SSG	max depth	Snow sample; IceStation #5
PS138_101_Coring-001	SI_corer_9cm	2023-08-28 T12:48:00	85.04528	130.35034		MARKII	max depth	Biocore_1; IceStation #5
PS138_101_Coring-002	SI_corer_9cm	2023-08-28 T12:48:05	85.04528	130.35034		MARKII	max depth	Biocore_2; IceStation #5
PS138_101_Coring-003	SI_corer_9cm	2023-08-28 T12:48:10	85.04528	130.35034		MARKII	max depth	Biocore_3; IceStation #5
PS138_101_Coring-004	SI_corer_9cm	2023-08-28 T12:48:15	85.04528	130.35034		MARKII	max depth	Biocore_4; IceStation #5

Event label	Optional label	Date / Time	Latitude	Longitude	Depth [m]	Gear	Action	Comment
PS138_101_Coring-005	SI_corer_9cm	2023-08-28 T12:48:20	85.04528	130.35034		MARKII	max depth	Biocore_5; IceStation #5
PS138_101_Coring-006	SI_corer_9cm	2023-08-28 T12:48:25	85.04528	130.35034		MARKII	max depth	Biocore_6; IceStation #5
PS138_101_Coring-007	SI_corer_9cm	2023-08-28 T12:48:30	85.04528	130.35034		MARKII	max depth	Biocore_7; IceStation #5
PS138_101_Coring-008	SI_corer_9cm	2023-08-28 T12:48:35	85.04528	130.35034		MARKII	max depth	Biocore_8; IceStation #5
PS138_101_Coring-009	SI_corer_9cm	2023-08-28 T12:48:40	85.04528	130.35034		MARKII	max depth	Biocore_9; IceStation #5
PS138_101_Coring-010	SI_corer_9cm	2023-08-28 T12:48:45	85.04528	130.35034		MARKII	max depth	SIP-Texture; IceStation #5
PS138_101_Coring-011	SI_corer_9cm	2023-08-28 T12:48:50	85.04528	130.35034		MARKII	max depth	SIP-Archive; IceStation #5
PS138_101_Coring-012	SI_corer_9cm	2023-08-28 T12:48:55	85.04528	130.35034		MARKII	max depth	SIP-Salinity; IceStation #5
PS138_101_Coring-013	hand_pump	2023-08-28 T12:49:00	85.04528	130.35034		HP	max depth	Under Ice Water; IceStation #5
PS138_101_ Chemistry-002	hand_pump	2023-08-28 T12:49:00	85.03626	130.40304		HP	max depth	Melt Pond Water; IceStation #5
PS138_101_Coring-014	hand_pump	2023-08-28 T12:49:05	85.04528	130.35034		HP	max depth	Melt Pond Water; IceStation #5
PS138_101_Coring-015	snow_sampler_ glove	2023-08-28 T12:49:10	85.04528	130.35034		SSG	max depth	Snow Sample; IceStation #5
PS138_101_ Chemistry-003	hand_pump	2023-08-28 T12:55:00	85.03626	130.40304		HP	max depth	Under Ice Water; IceStation #5
PS138_101-1_ISCA-002	ISCA	2023-08-28 T13:00:00	85.04528	130.35034		ISCA	max depth	IceStation #5
PS138_101-1_ISCA-003	ISCA	2023-08-28 T13:00:00	85.04528	130.35034		ISCA	max depth	IceStation #5

Event label	Optional label	Date / Time	Latitude	Longitude	Depth [m]	Gear	Action	Comment
PS138_101_Buoy_001	2023O20	2023-08-28 T13:00:00	85.03348	130.40377		BUOY_CTD	max depth	IceStation #5
PS138_101-1_ISCA-001	ISCA	2023-08-28 T13:00:00	85.04528	130.35034		ISCA	max depth	IceStation #5
PS138_101_ Chemistry-006	snow_sampler_ glove	2023-08-28 T13:19:00	85.03116	130.37218		SSG	max depth	Snow sample; IceStation #5
PS138_101_Buoy_005	2023S127	2023-08-28 T13:20:00	85.03222	130.39952		BUOY_ SNOW	max depth	level second year-ice; co-deployed with 2023R25; IceStation #5
PS138_101_ Chemistry-007	snow_sampler_ glove	2023-08-28 T13:28:00	85.03220	130.38649		SSG	max depth	Snow sample; IceStation #5
PS138_101_Buoy_006	2023T106	2023-08-28 T13:45:00	85.03133	130.39110		SIMBA	max depth	ice thickness 1.52m. freeboard: 0.2m. snow/ cattering layer: 0.03m. thermistor 29 at surface. level second year-ice; IceStation #5
PS138_101_DRONE_001	UAV_PS	2023-08-28 T14:02:00	85.04500	130.35000		UAV	max depth	Photogrammetry grid over floe; IceStation #5
PS138_101_ROV_001	BEAST	2023-08-28 T14:30:00	85.04500	130.35000		BEAST	max depth	20230828_1; IceStation #5
PS138_101_ SUNAprofil_005	Nitrate_profiler	2023-08-28 T15:03:00	85.03820	130.30660		NO3	max depth	10 profiles; IceStation #5
PS138_101_Buoy_004	2023W6	2023-08-28 T16:40:00	85.03070	130.30748		BUOY_ITP	max depth	IceStation #5

Event label	Optional label	Date / Time	Latitude	Longitude	Depth [m]	Gear	Action	Comment
PS138_101_ICEADCP_1	300kHzADCP	2023-08-28 T16:52:00	85.03820	130.21510		ADCP	max depth	Under-ice RDI 300 kHz ADCP time series; IceStation #5
PS138_101_MSS_1	MSS_90D_075	2023-08-28 T16:52:00	85.03820	130.21510		MSS	max depth	MSS 075 one profile; IceStation #5
PS138_101_KEF_001	PS138_101-1_ KEF_ssl-019	2023-08-28 T17:12:00	85.04528	130.35034		STRAP_ICE	max depth	Deployment of ice sediment traps for biogeochemistry; Ice station #5
PS138_101_IT_001	PS138_101-1_IT_ssl-017	2023-08-28 T17:50:00	85.04528	130.35034		STRAP_ICE	max depth	Deployment of ice sediment traps equipped with gel traps; Ice station #5
PS138_103-1		2023-08-28 T19:59:46	85.04094	130.33616	4299	MSN	Station start	IceStation #5
PS138_103-1		2023-08-28 T22:08:21	85.04083	130.40145	4295	MSN	Station end	IceStation #5
PS138_104-1		2023-08-28 T22:09:15	85.04080	130.40186	4297	MSN	Station start	IceStation #5
PS138_104-1		2023-08-28 T23:56:13	85.03551	130.42602	4298	MSN	Station end	IceStation #5
PS138_101_Core_002	SI_corer_14cm	2023-08-29 T00:00:00	85.04500	130.35000		MARKV	max depth	IceStation #5
PS138_105-1		2023-08-29 T00:00:39	85.03525	130.42568	4299	ROSINA	Station start	IceStation #5
PS138_105-1		2023-08-29 T02:51:42	85.02888	130.34376	4296	ROSINA	Station end	IceStation #5

Event label	Optional label	Date / Time	Latitude	Longitude	Depth [m]	Gear	Action	Comment
PS138_101_ASD_001	Dart_ASD	2023-08-29 T03:40:00	85.04500	130.35000		ALBEDOM	max depth	IceStation #5
PS138_101_Kipps_001	Dart_Kipps	2023-08-29 T03:40:00	85.04500	130.35000		ALBEDOM	max depth	IceStation #5
PS138_101_DRONE_002	UAV_PS	2023-08-29 T05:11:00	85.04500	130.35000		UAV	max depth	Photogrammetry grid over ROV area; IceStation #5
PS138_106-1		2023-08-29 T06:19:53	85.03697	130.24600	4297	ZODIAC	Station start	Zodiac Luisa. IceStation #5
PS138_106-1		2023-08-29 T07:33:55	85.04113	130.25894	4300	ZODIAC	Station end	Zodiac Luisa. IceStation #5
PS138_101_MSS_2	MSS_90D_075	2023-08-29 T06:55:00	85.03820	130.21510		MSS	max depth	MSS 075 series of 11 profiles; IceStation #5
PS138_101_ROV_002	BEAST	2023-08-29 T07:26:00	85.04500	130.35000		BEAST	max depth	20230829_1; IceStation #5
PS138_Heli_Buoy_007	2023P274	2023-08-29 T09:20:00	85.03300	130.51700		ISVP	max depth	IceStation #5
PS138_107-1		2023-08-29 T11:12:00	85.02970	130.54467	4287	B_LANDER	Station start	Flux Lander #2. IceStation #5; Posidonia Position
PS138_107-1		2023-08-30 T09:02:00	85.02825	130.53167	4294	B_LANDER	Station end	Flux Lander #2. IceStation #5; Posidonia Position
PS138_101_Buoy_003	2023I11	2023-08-29 T12:00:00	85.03502	130.34337		SIMB	max depth	IceStation #5
PS138_101_Buoy_008	SnowTATOS1	2023-08-29 T12:00:00	85.91550	130.18078		SR	max depth	IceStation #5
PS138_101_Buoy_009	2023K1	2023-08-29 T12:00:00	85.91550	130.18078		CAME	max depth	IceStation #5

Event label	Optional label	Date / Time	Latitude	Longitude	Depth [m]	Gear	Action	Comment
PS138_Heli_Buoy_001	2023O16	2023-08-29 T15:10:00	85.01533	129.85287		BUOY_CTD	max depth	IceStation #5
PS138_Heli_Buoy_002	2023T109	2023-08-29 T15:30:00	85.01568	129.82483		SIMBA	max depth	ice thickness 1.4m. freeboard: 0.2m. snow/ scattering layer: 0.05m. thermistor 25 at surface. probably level second year-ice; co-de…
PS138_108-1		2023-08-29 T15:53:00	85.02592	130.23340	4288	B_LANDER	Station start	Flux Lander #3. IceStation #5; Posidonia Position
PS138_108-1		2023-08-30 T15:06:00	85.02957	130.21948	4296	B_LANDER	Station end	Flux Lander #3. IceStation #5; Posidonia Position
PS138_110-1		2023-08-29 T17:15:11	85.03307	130.02117	4301	HN	Station start	IceStation #5
PS138_110-1		2023-08-29 T17:22:03	85.03337	130.01558	4302	HN	Station end	IceStation #5
PS138_109-1		2023-08-29 T17:25:16	85.03349	130.01315	4301	CTD-RO	max depth	IceStation #5. at max depth
PS138_111-1		2023-08-29 T18:03:37	85.03527	129.98850	4301	MSC	max depth	IceStation #5
PS138_112-1		2023-08-29 T18:15:38	85.03586	129.98278	4301	MSC	max depth	IceStation #5
PS138_113-1		2023-08-29 T19:20:40	85.03876	129.96767	4302	CTD-RO	max depth	IceStation #5. at max depth
PS138_114-1		2023-08-29 T19:52:51	85.03962	129.96768	4301	BONGO	Station start	IceStation #5

Event label	Optional label	Date / Time	Latitude	Longitude	Depth [m]	Gear	Action	Comment
PS138_114-1		2023-08-29 T19:59:38	85.03973	129.96794	4300	BONGO	Station end	IceStation #5
PS138_101_IT_002	PS138_101-1_IT_ssl-018	2023-08-29 T20:05:00	85.04528	130.35034		STRAP_ICE	max depth	Recovery of ice sediment traps equipped with gel traps; Ice station #5
PS138_115-1_1	ISP_Seb	2023-08-29 T20:59:00	85.03939	129.97044	4303	ISP	Station start	IceStation #5
PS138_115-1_1	ISP_Seb	2023-08-30 T03:20:00	85.00919	129.56313	4304	ISP	Station end	IceStation #5
PS138_115-1_2	ISP_Frauke	2023-08-29 T22:10:00	85.03548	129.96266	4300	ISP	Station start	IceStation #5
PS138_115-1_2	ISP_Frauke	2023-08-30 T02:20:00	85.01180	129.65987	4307	ISP	Station end	IceStation #5
PS138_115-1_3	ISP_Franky	2023-08-29 T22:34:00	85.03349	129.95404	4302	ISP	Station start	failed -- minimum flow reached; IceStation #5
PS138_115-1_3	ISP_Franky	2023-08-30 T01:35:00	85.01520	129.73930	4303	ISP	Station end	failed -- minimum flow reached; IceStation #5
PS138_115-1		2023-08-29 T22:46:06	85.03239	129.94762	4303	CTD-RO	max depth	IceStation #5. at max depth
PS138_115-1_4	ISP_Jimmy	2023-08-29 T22:56:00	85.03141	129.94099	4301	ISP	Station start	IceStation #5
PS138_115-1_4	ISP_Jimmy	2023-08-30 T01:26:00	85.01591	129.75381	4302	ISP	Station end	IceStation #5
PS138_Heli_Buoy_003	2023S124	2023-08-30 T08:00:00	84.98935	129.04012		BUOY_ SNOW	max depth	co-deployed with 2023T109; IceStation #5

Event label	Optional label	Date / Time	Latitude	Longitude	Depth [m]	Gear	Action	Comment
PS138_101_ROV_003	BEAST	2023-08-30 T08:00:00	85.04500	130.35000		BEAST	max depth	20230830_1; IceStation #5
PS138_101_GEM_001	gem2-512	2023-08-30 T13:26:00	85.04500	130.35000		BES	max depth	IceStation #5
PS138_101_Magna_001	magnaprobe-steffi	2023-08-30 T13:32:00	85.04500	130.35000		MAGNA	max depth	IceStation #5
PS138_101_UpperOceanIceFloeTransect_1	CTD_48M_1459	2023-08-30 T14:50:00	89.82000	2.08000		CTD_fishrod	max depth	IceStation #5
PS138_101_Buoy_007	2023R25	2023-08-30 T16:00:00	85.02500	130.17500		BRS	max depth	Ramses under ice: depth: 3.4m. draft 1.35m. Ramses over ice 0.97m. snow depth under Ramses reflected 3cm. photos of optics core; c…
PS138_101_Buoy_002	2023Reolink15	2023-08-30 T16:30:00	85.04500	130.35000		CAME	max depth	IceStation #5
PS138_Heli_Buoy_004	2023O22	2023-08-30 T17:40:00	84.94280	129.35582		BUOY_CTD	max depth	
PS138_Heli_Buoy_005	2023S125	2023-08-30 T17:50:00	84.94280	129.35577		BUOY_SNOW	max depth	scattering layer 0.03m at all pingers plus snow: SH1: 2cm. SH2: 1cm SH3: 1cm. SH2: 3cm. level second year-ice; co-deployed with 20…

Event label	Optional label	Date / Time	Latitude	Longitude	Depth [m]	Gear	Action	Comment
PS138_Heli_Buoy_006	2023T103	2023-08-30 T18:05:00	84.94280	129.35577		SIMBA	max depth	ice thickness 1.95m. freeboard: 0.3m. snow/ scattering layer: 0.05m. thermistor 34 at surface. level second year-ice; co-deployed w…
PS138_101_KEF_002	PS138_101-1_ KEF_ssl-020	2023-08-30 T18:35:00	85.04528	130.35034		STRAP_ICE	max depth	Recovery of ice sediment traps for biogeochemistry; Ice station #5
PS138_116-1		2023-08-30 T22:50:27	84.93089	128.99095	4308	GKG	max depth	IceStation #5
PS138_117-1		2023-08-31 T02:02:35	84.91111	128.97325	4307	GKG	max depth	IceStation #5
PS138_118-1	CAO1-01	2023-08-31 T07:13:58	84.90760	128.95269	4304	MOOR	Station start	Arctic Mooring #1 CAO1-01 deployment
PS138_118-1	CAO1-01	2023-08-31 T12:35:31	84.90771	129.25582	4302	MOOR	Station end	Arctic Mooring #1 CAO1-01 deployment
PS138_119-1	CAO2-01	2023-08-31 T13:18:18	84.89257	129.49371	4302	MOOR	Station start	CAO2-01 deployment
PS138_119-1	CAO2-01	2023-08-31 T18:24:12	84.88718	129.63022	4300	MOOR	Station end	CAO2-01 deployment
PS138_120-1		2023-08-31 T19:36:20	84.93997	129.32709	4308	BUOY_CTD	Station start	138-120_ Buoy_001 - 2023O19 138-120_Buoy_002 - 2023T105 138-120_Buoy_003 - 2023S122

Event label	Optional label	Date / Time	Latitude	Longitude	Depth [m]	Gear	Action	Comment
PS138_120-1		2023-08-31 T20:35:37	84.94015	129.40669	4305	BUOY_CTD	Station end	138-120_ Buoy_001 - 2023O19 138-120_Buoy_002 - 2023T105 138-120_Buoy_003 - 2023S122
PS138_120-2	2023T105	2023-08-31 T20:30:00	84.94022	129.39884	4308	SIMBA	Station start	2023T105
PS138_120-2	2023T105	2023-08-31 T20:30:20	84.94022	129.39931	4305	SIMBA	Station end	2023T105
PS138_120-3	2023S122	2023-08-31 T20:30:30	84.94022	129.39954	4309	BUOY_ SNOW	Station start	Snow Buoy 2023S122
PS138_120-3	2023S122	2023-08-31 T20:30:50	84.94021	129.40000	4306	BUOY_ SNOW	Station end	Snow Buoy 2023S122
PS138_121-1	2023P284	2023-09-01 T02:18:48	85.44131	128.65159	4318	ISVP	Station start	2023P284 Pacific Gyre Universal tracker 300534064268600
PS138_121-1	2023P284	2023-09-01 T02:38:04	85.44116	128.65079	4321	ISVP	Station end	2023P284 Pacific Gyre Universal tracker 300534064268600
PS138_121-2		2023-09-01 T02:39:11	85.44117	128.65073	4321	XCTD	Station start	
PS138_121-2		2023-09-01 T02:57:26	85.44117	128.64779	4318	XCTD	Station end	
PS138_121-3		2023-09-01 T07:50:11	85.94439	128.15839	4325	XCTD	Station start	
PS138_121-3		2023-09-01 T08:05:52	85.94501	128.17767	4325	XCTD	Station end	

Event label	Optional label	Date / Time	Latitude	Longitude	Depth [m]	Gear	Action	Comment
PS138_122-1	2023P261	2023-09-01 T07:51:10	85.94460	128.16470	4325	ISVP	Station start	2023P261 MetOcean SVP-B 300534063482680
PS138_122-1	2023P261	2023-09-01 T08:05:21	85.94500	128.17746	4326	ISVP	Station end	2023P261 MetOcean SVP-B 300534063482680
PS138_121-4	2023P283	2023-09-01 T14:22:23	86.44687	127.15109	4322	ISVP	Station start	2023P283 Pacific Gyre Universal tracker 300534064267620
PS138_121-4	2023P283	2023-09-01 T14:33:48	86.44600	127.14959	4321	ISVP	Station end	2023P283 Pacific Gyre Universal tracker 300534064267620
PS138_121-5		2023-09-01 T14:34:21	86.44597	127.14953	4321	XCTD	Station start	
PS138_121-5		2023-09-01 T14:39:58	86.44572	127.14879	4321	XCTD	Station end	
PS138_121-6		2023-09-01 T19:02:15	86.94339	126.57914	4177	XCTD	Station start	
PS138_121-6		2023-09-01 T19:15:35	86.94223	126.56853	4177	XCTD	Station end	
PS138_123-1	2023P279	2023-09-01 T19:02:58	86.94331	126.57905	4182	ISVP	Station start	2023P279 Pacific Gyre Universal tracker 300534064264610
PS138_123-1	2023P279	2023-09-01 T19:15:54	86.94222	126.56806	4179	ISVP	Station end	2023P279 Pacific Gyre Universal tracker 300534064264610

Event label	Optional label	Date / Time	Latitude	Longitude	Depth [m]	Gear	Action	Comment
PS138_124-1	2023P265	2023-09-02 T01:36:29	87.42415	125.49505	3266	lSVP	Station start	2023P265 MetOcean SVP-B 300534063487700
PS138_124-1	2023P265	2023-09-02 T01:55:23	87.42276	125.47499	3267	lSVP	Station end	2023P265 MetOcean SVP-B 300534063487700
PS138_121-7		2023-09-02 T01:57:20	87.42262	125.47273	3269	XCTD	Station start	
PS138_121-7		2023-09-02 T02:03:26	87.42216	125.46544	3268	XCTD	Station end	
PS138_125-1		2023-09-02 T03:47:50	87.57255	125.68090	1638	DS3	Station start	
PS138_125-1		2023-09-02 T05:45:14	87.64723	124.57734	1703	DS3	Station end	
PS138_Heli_EM-Bird_008	Embird_awi-bird	2023-09-02 T07:26:00	87.62560	124.43850		EMB	max depth	Flight during transit.
PS138_126-1		2023-09-02 T08:10:28	87.62761	124.41325	1739	OFOBS	Station start	
PS138_126-1		2023-09-02 T09:22:37	87.62998	124.38517	1747	OFOBS	Station end	
PS138_SBLA_20230902T092900		2023-09-02 T09:29:00	87.63525	124.36032		SBLA	Station start	
PS138_SBLA_20230902T092900		2023-09-02 T09:29:00	87.58737	127.83160		SBLA	Station end	
PS138_SBLA_20230902T095300		2023-09-02 T09:53:00	87.52048	127.56806		SBLA	Station start	
PS138_SBLA_20230902T095300		2023-09-02 T09:53:00	87.69165	120.45547		SBLA	Station end	
PS138_SBLA_20230902T101400		2023-09-02 T10:14:00	87.70092	119.31468		SBLA	Station start	

Event label	Optional label	Date / Time	Latitude	Longitude	Depth [m]	Gear	Action	Comment
PS138_ SBLA_20230902T101400		2023-09-02 T10:14:00	87.63269	124.61738		SBLA	Station end	
PS138_127-1		2023-09-02 T11:23:04	87.62186	123.81288	2455	OFOBS	Station start	
PS138_127-1		2023-09-02 T14:02:02	87.62334	124.16927	1962	OFOBS	Station end	
PS138_128-1	2023P275	2023-09-02 T20:04:25	87.99375	121.72985	3157	ISVP	Station start	2023P275 Pacific Gyre Universal tracker 300534064262600
PS138_128-1	2023P275	2023-09-02 T20:10:28	87.99371	121.72358	3156	ISVP	Station end	2023P275 Pacific Gyre Universal tracker 300534064262600
PS138_121-8		2023-09-02 T20:12:12	87.99382	121.71137	3155	XCTD	Station start	
PS138_121-8		2023-09-02 T20:23:54	87.99675	121.69312	3155	XCTD	Station end	
PS138_129_1_jfe_ct-logger_34-001	jfe_ct-logger_34	2023-09-03 T00:00:00	88.49402	111.92883		COND	max depth	IceStation #6
PS138_129_ Vector_5418-001	Vector_5418	2023-09-03 T00:00:00	84.76114	107.79211		CM	max depth	IceStation #6
PS138_129_nortek_ s1000_102149-001	nortek_ s1000_102149	2023-09-03 T00:00:00	88.49402	111.92883		BUOY_ ADCP	max depth	IceStation #6
PS138_129-1		2023-09-03 T06:39:30	88.49578	112.03753	4330	ICE	Station start	IceStation #6
PS138_129-1		2023-09-06 T09:49:28	88.45852	114.50837	4314	ICE	Station end	IceStation #6
PS138_130-1		2023-09-03 T08:31:04	88.49402	111.90437	4328	TVMUC	Station start	IceStation #6

Event label	Optional label	Date / Time	Latitude	Longitude	Depth [m]	Gear	Action	Comment
PS138_130-1		2023-09-03 T11:45:04	88.49587	111.80597	4327	TVMUC	Station end	IceStation #6
PS138_129_ Chemistry-003	snow_sampler_ glove	2023-09-03 T10:35:00	88.49355	111.88368		SSG	max depth	Snow sample; IceStation #6
PS138_129_ Chemistry-004	snow_sampler_ glove	2023-09-03 T10:50:00	88.49707	111.85769		SSG	max depth	Snow sample; IceStation #6
PS138_129_ Chemistry-001	hand_pump	2023-09-03 T11:00:00	88.49707	111.85769		HP	max depth	Ice Edge Water; IceStation #6
PS138_129_ Chemistry-002	hand_pump	2023-09-03 T11:00:00	88.49707	111.85769		HP	max depth	Under Ice Water; IceStation #6
PS138_129_ Chemistry-005	snow_sampler_ glove	2023-09-03 T11:01:00	88.49583	111.91222		SSG	max depth	Snow sample; IceStation #6
PS138_129_ Chemistry-006	snow_sampler_ glove	2023-09-03 T11:45:00	88.49472	111.87944		SSG	max depth	Snow sample; IceStation #6
PS138_131-1		2023-09-03 T11:47:07	88.49588	111.80638	4330	TVMUC	Station start	IceStation #6
PS138_131-1		2023-09-03 T15:11:52	88.49196	112.00348	4332	TVMUC	Station end	IceStation #6
PS138_129_Buoy_004	2023T107	2023-09-03 T12:00:00	88.46383	114.36167		SIMBA	max depth	hole filled with slush and new snow on top. 10 m from snow buoy; ice thickness 1.6 m. freeboard 0.12 m. snow depth 0.1 m. thermist…
PS138_129_Buoy_005	2023W5	2023-09-03 T12:40:00	88.49618	111.94838		BUOY_ITP	max depth	IceStation #6
PS138_129_ Chemistry-007	snow_sampler_ glove	2023-09-03 T12:53:00	88.49444	111.92361		SSG	max depth	Snow sample; IceStation #6

Event label	Optional label	Date / Time	Latitude	Longitude	Depth [m]	Gear	Action	Comment
PS138_129_ SUNAprofil_006	Nitrate_profiler	2023-09-03 T13:11:19	88.48970	112.12610		NO3	max depth	7 profiles; IceStation #6
PS138_129_MSS_1	MSS_90D_075	2023-09-03 T14:15:00	88.49230	112.01770		MSS	max depth	MSS 075 series of 5 profiles; IceStation #6
PS138_129_ICEADCP_1	300kHzADCP	2023-09-03 T14:15:00	88.49230	112.01770		ADCP	max depth	Under-ice RDI 300 kHz ADCP time series; IceStation #6
PS138_129_DRONE_001	UAV_PS	2023-09-03 T14:16:00	88.49600	112.03800		UAV	max depth	Photogrammetry grid over floe; IceStation #6
PS138_129_ROV_001	BEAST	2023-09-03 T14:42:00	88.49600	112.03800		BEAST	max depth	20230903_1; IceStation #6
PS138_129_Buoy_008	2023O23	2023-09-03 T14:45:00	88.49270	112.04820		BUOY_CTD	max depth	100m from ITP135; IceStation #6
PS138_129_Coring-001	SI_corer_9cm	2023-09-03 T16:42:01	88.49578	112.03753		MARKII	max depth	Biocore_1; IceStation #6
PS138_129_Coring-002	SI_corer_9cm	2023-09-03 T16:43:24	88.49578	112.03753		MARKII	max depth	Biocore_2; IceStation #6
PS138_129_Coring-003	SI_corer_9cm	2023-09-03 T16:43:33	88.49578	112.03753		MARKII	max depth	Biocore_3; IceStation #6
PS138_129_Coring-004	SI_corer_9cm	2023-09-03 T16:43:43	88.49578	112.03753		MARKII	max depth	Biocore_4; IceStation #6
PS138_129_Coring-005	SI_corer_9cm	2023-09-03 T16:43:50	88.49578	112.03753		MARKII	max depth	Biocore_5; IceStation #6
PS138_129_Coring-006	SI_corer_9cm	2023-09-03 T16:43:55	88.49578	112.03753		MARKII	max depth	Biocore_6; IceStation #6
PS138_129_Coring-007	SI_corer_9cm	2023-09-03 T16:44:01	88.49578	112.03753		MARKII	max depth	Biocore_7; IceStation #6

Event label	Optional label	Date / Time	Latitude	Longitude	Depth [m]	Gear	Action	Comment
PS138_129_Coring-008	SI_corer_9cm	2023-09-03 T16:44:08	88.49578	112.03753		MARKII	max depth	Biocore_8; IceStation #6
PS138_129_Coring-009	SI_corer_9cm	2023-09-03 T16:44:14	88.49578	112.03753		MARKII	max depth	Biocore_9; IceStation #6
PS138_129_Coring-010	SI_corer_9cm	2023-09-03 T16:44:20	88.49578	112.03753		MARKII	max depth	SIP-Texture; IceStation #6
PS138_129_Coring-011	SI_corer_9cm	2023-09-03 T16:45:00	88.49578	112.03753		MARKII	max depth	SIP-Archive; IceStation #6
PS138_129_Coring-012	SI_corer_9cm	2023-09-03 T16:45:11	88.49578	112.03753		MARKII	max depth	SIP-Salinity; IceStation #6
PS138_129_Coring-013	hand_pump	2023-09-03 T16:45:22	88.49578	112.03753		HP	max depth	Under Ice Water; IceStation #6
PS138_129_Coring-014	snow_sampler_ glove	2023-09-03 T16:45:38	88.49578	112.03753		SSG	max depth	Snow Sample; IceStation #6
PS138_129-1_ISCA-001	ISCA	2023-09-03 T17:00:00	88.49578	112.03753		ISCA	max depth	IceStation #6
PS138_132-1		2023-09-03 T17:22:20	88.48905	112.18954	4330	OFOBS	Station start	IceStation #6
PS138_132-1		2023-09-03 T19:44:44	88.48809	112.44029	4326	OFOBS	Station end	IceStation #6
PS138_133-1		2023-09-03 T21:33:35	88.48887	112.71652	4325	MSN	Station start	IceStation #6
PS138_133-1		2023-09-03 T23:37:31	88.48974	113.09731	4325	MSN	Station end	IceStation #6
PS138_129_Core_001	SI_corer_14cm	2023-09-04 T00:00:00	88.49600	112.03800		MARKV	max depth	IceStation #6
PS138_129_Core_002	SI_corer_14cm	2023-09-04 T00:00:00	88.49600	112.03800		MARKV	max depth	1x OPT. HI scan. no bio samples; IceStation #6
PS138_134-1		2023-09-04 T01:20:08	88.48984	113.41036	4323	GKG	max depth	IceStation #6

Event label	Optional label	Date / Time	Latitude	Longitude	Depth [m]	Gear	Action	Comment
PS138_129_ASD_001	Dart_ASD	2023-09-04 T04:15:00	88.49600	112.03800		ALBEDOM	max depth	IceStation #6
PS138_129_Kipps_001	Dart_Kipps	2023-09-04 T04:15:00	88.49600	112.03800		ALBEDOM	max depth	IceStation #6
PS138_135-1		2023-09-04 T04:38:33	88.48352	113.90213	4324	GKG	max depth	IceStation #6
PS138_129_IT_001	PS138_129-1_IT_ssl-021	2023-09-04 T06:50:00	88.49578	112.03753		STRAP_ICE	max depth	Deployment of ice sediment traps equipped with gel traps; Ice station #6
PS138_129_KEF_001	PS138_129-1_KEF_ssl-023	2023-09-04 T06:58:00	88.49578	112.03753		STRAP_ICE	max depth	Deployment of ice sediment traps for biogeochemistry; Ice station #6
PS138_129_PiCam_001	PS138_129_PiCam_001	2023-09-04 T07:20:00	88.49578	112.03753		VIDEO	max depth	Deployment of time-lapse camera under the ice; Ice station #6
PS138_129_ROV_002	BEAST	2023-09-04 T08:16:00	88.49600	112.03800		BEAST	max depth	20230904_1; IceStation #6
PS138_136-1		2023-09-04 T10:35:00	88.46792	113.74335	4309	B_LANDER	Station start	Flux Lander #2. IceStation #6; Posidonia Position
PS138_136-1		2023-09-05 T09:45:00	88.46902	113.84960	4318	B_LANDER	Station end	Flux Lander #2. IceStation #6; Posidonia Position

Event label	Optional label	Date / Time	Latitude	Longitude	Depth [m]	Gear	Action	Comment
PS138_129_Buoy_003	2023S102	2023-09-04 T11:30:00	88.46550	114.31260		BUOY_ SNOW	max depth	20 m from ITP135. co-deployed with 2023T107; SH1: 0.07m. SH2: 0.06 m. SH3: 0.15 m. SH4: 0.1 m. level second year-ice; IceStation #…
PS138_137-1		2023-09-04 T14:11:00	88.45192	114.00898	4307	B_LANDER	Station start	Flux Lander #3. IceStation #6; Posidonia Position
PS138_137-1		2023-09-06 T06:59:00	88.45233	113.97383	4314	B_LANDER	Station end	Flux Lander #3. IceStation #6; Posidonia Position
PS138_129_GEM_001	gem2-512	2023-09-04 T14:55:00	88.49600	112.03800		BES	max depth	IceStation #6
PS138_129_Magna_001	magnaprobe-steffi	2023-09-04 T15:00:00	88.49600	112.03800		MAGNA	max depth	IceStation #6
PS138_138-1		2023-09-04 T15:52:59	88.44357	114.41639	4308	MSN	Station start	IceStation #6
PS138_138-1		2023-09-04 T17:31:11	88.43677	114.24905	4311	MSN	Station end	IceStation #6
PS138_129_ Chemistry-008	snow_sampler_ glove	2023-09-04 T17:00:00	88.44357	114.41639		SSG	max depth	Snow sample; IceStation #6
PS138_140-1		2023-09-04 T17:57:02	88.43552	114.19677	4315	HN	Station start	IceStation #6
PS138_140-1		2023-09-04 T18:09:33	88.43500	114.17091	4313	HN	Station end	IceStation #6
PS138_139-1		2023-09-04 T18:02:40	88.43528	114.18497	4315	CTD-RO	max depth	IceStation #6. at max depth
PS138_141-1		2023-09-04 T18:30:39	88.43428	114.12648	4312	MSC	max depth	IceStation #6

Event label	Optional label	Date / Time	Latitude	Longitude	Depth [m]	Gear	Action	Comment
PS138_142-1		2023-09-04 T18:41:22	88.43399	114.10303	4312	MSC	max depth	IceStation #6
PS138_129_Buoy_001	2023I10	2023-09-04 T18:45:00	88.43417	114.19500		SIMB	max depth	scattering layer: 0.05 m. distance from pinger to surface: 1.01 m; IceStation #6
PS138_129_Buoy_002	2023R26	2023-09-04 T19:00:00	88.43383	114.13683		BRS	max depth	incoming RAMSES 85A9. reflected RAMSES 85A7. transmitted RAMSES 511E. snow depth under reflected RAMSES: 0.14 m. distance from sen…
PS138_129_Buoy_006	2023Reolink14	2023-09-04 T19:00:00	88.49600	112.03800		CAME	max depth	mounted on top of ITP floatation; IceStation #6
PS138_143-1		2023-09-04 T19:21:24	88.43347	114.01510	4315	CTD-RO	max depth	IceStation #6. at max depth
PS138_144-1		2023-09-04 T19:58:37	88.43376	113.94058	4316	BONGO	Station start	IceStation #6
PS138_144-1		2023-09-04 T20:06:57	88.43391	113.92536	4316	BONGO	Station end	IceStation #6
PS138_129_Buoy_007	2023T102	2023-09-04 T20:00:00	88.43330	113.93830		SIMBA	max depth	thin ice close to ship; IceStation #6
PS138_145-1_1	ISP_Seb	2023-09-04 T21:20:00	88.43610	113.83033	4318	ISP	Station start	IceStation #6
PS138_145-1_1	ISP_Seb	2023-09-05 T03:31:00	88.43585	114.33369	4307	ISP	Station end	IceStation #6

Event label	Optional label	Date / Time	Latitude	Longitude	Depth [m]	Gear	Action	Comment
PS138_145-1_2	ISP_Frauke	2023-09-04 T22:30:00	88.43889	113.80546	4319	ISP	Station start	IceStation #6
PS138_145-1_2	ISP_Frauke	2023-09-05 T02:33:00	88.43782	114.26306	4312	ISP	Station end	IceStation #6
PS138_145-1_3	ISP_Franky	2023-09-04 T23:06:00	88.44014	113.83080	4319	ISP	Station start	IceStation #6
PS138_145-1_3	ISP_Franky	2023-09-05 T01:54:00	88.43923	114.19176	4314	ISP	Station end	IceStation #6
PS138_145-1		2023-09-04 T23:16:59	88.44042	113.84400	4320	CTD-RO	Station start	IceStation #6. at max depth
PS138_145-1		2023-09-04 T23:31:21	88.44075	113.86727	4318	CTD-RO	Station end	IceStation #6. at max depth
PS138_145-1_4	ISP_Jimmy	2023-09-04 T23:28:00	88.44069	113.86247	4318	ISP	Station start	IceStation #6
PS138_145-1_4	ISP_Jimmy	2023-09-05 T01:49:00	88.43942	114.17999	4310	ISP	Station end	IceStation #6
PS138_146-1		2023-09-05 T03:34:52	88.43575	114.33667	4308	ROSINA	Station start	IceStation #6
PS138_146-1		2023-09-05 T06:15:37	88.43573	114.35049	4308	ROSINA	Station end	IceStation #6
PS138_129_IT_002	PS138_129-1_IT_ssl-022	2023-09-05 T06:20:00	88.49578	112.03753		STRAP_ICE	max depth	Recovery of ice sediment traps equipped with gel traps; Ice station #6
PS138_129_KEF_002	PS138_129-1_KEF_ssl-024	2023-09-05 T06:40:00	88.49578	112.03753		STRAP_ICE	max depth	Recovery of ice sediment traps for biogeochemistry; Ice station #6
PS138_147-1		2023-09-05 T20:17:06	88.46259	113.44457	4319	EBS	Station start	IceStation #6

Event label	Optional label	Date / Time	Latitude	Longitude	Depth [m]	Gear	Action	Comment
PS138_147-1		2023-09-06 T01:51:04	88.46681	113.84627	4319	EBS	Station end	IceStation #6
PS138_148-1	2023P262	2023-09-06 T16:10:46	88.98538	112.72888	4306	ISVP	Station start	2023P262 MetOcean SVP-B 300534063485680
PS138_148-1	2023P262	2023-09-06 T16:22:30	88.98552	112.74661	4310	ISVP	Station end	2023P262 MetOcean SVP-B 300534063485680
PS138_149-1		2023-09-06 T16:23:25	88.98550	112.74854	4307	XCTD	Station start	
PS138_149-1		2023-09-06 T16:44:41	88.98561	112.77420	4309	XCTD	Station end	
PS138_150-1	2023P288	2023-09-06 T22:11:14	89.47611	110.86330	4277	ISVP	Station start	2023P288 Pacific Gyre Universal tracker 300534063806270
PS138_150-1	2023P288	2023-09-06 T22:29:06	89.47577	110.93691	4276	ISVP	Station end	2023P288 Pacific Gyre Universal tracker 300534063806270
PS138_149-2		2023-09-06 T22:29:38	89.47576	110.93899	4275	XCTD	Station start	
PS138_149-2		2023-09-06 T22:40:39	89.47549	110.98271	4276	XCTD	Station end	
PS138_152_ Vector_5418-001	Vector_5418	2023-09-07 T00:00:00	88.49402	111.92883		CM	max depth	IceStation #7
PS138_152_nortek_ s1000_102149-001	nortek_ s1000_102149	2023-09-07 T00:00:00	89.93587	-15.22256		BUOY_ ADCP	max depth	IceStation #7
PS138_151-1		2023-09-07 T10:49:41	89.99832	64.18903	4231	OFOBS	Station start	IceStation #7

Event label	Optional label	Date / Time	Latitude	Longitude	Depth [m]	Gear	Action	Comment
PS138_151-1		2023-09-07 T14:17:34	89.98275	24.22233	4232	OFOBS	Station end	IceStation #7
PS138_Heli_EM-Bird_009	Embird_awi-bird	2023-09-07 T13:05:00	89.99120	-32.18520		EMB	max depth	Flight at the North Pole
PS138_ SBLA_20230907T151500		2023-09-07 T15:15:00	89.96395	-66.61977		SBLA	Station start	
PS138_ SBLA_20230907T151500		2023-09-07 T15:15:00	89.68936	-76.17935		SBLA	Station end	
PS138_ SBLA_20230907T153400		2023-09-07 T15:34:00	89.66408	-74.01977		SBLA	Station start	
PS138_ SBLA_20230907T153400		2023-09-07 T15:34:00	89.69092	-11.20630		SBLA	Station end	
PS138_ SBLA_20230907T155200		2023-09-07 T15:52:00	89.68641	-9.88897		SBLA	Station start	
PS138_ SBLA_20230907T155200		2023-09-07 T15:52:00	89.90823	-176.81160		SBLA	Station end	
PS138_152_Buoy_007	2023P285	2023-09-07 T16:00:00	89.87100	-59.40400		ISVP	max depth	IceStation #7
PS138_152-1		2023-09-07 T19:56:36	89.93587	-15.22256	4233	ICE	Station start	IceStation #7
PS138_152-1		2023-09-11 T15:01:28	89.68855	3.77865	4245	ICE	Station end	IceStation #7
PS138_153-1		2023-09-07 T22:45:20	89.92992	-4.89324	4239	GKG	max depth	IceStation #7
PS138_154-1		2023-09-08 T01:59:44	89.92905	-1.89621	4239	GKG	max depth	IceStation #7
PS138_155-1		2023-09-08 T06:35:58	89.94568	13.02200	4236	ROSINA	Station start	IceStation #7
PS138_155-1		2023-09-08 T09:20:25	89.94643	29.12187	4245	ROSINA	Station end	IceStation #7

Event label	Optional label	Date / Time	Latitude	Longitude	Depth [m]	Gear	Action	Comment
PS138_Heli_EM-Bird_010	Embird_awi-bird	2023-09-08 T07:11:00	89.92380	32.57040		EMB	max depth	Second flight at the North Pole and flight over the IceStation.
PS138_152_Coring-001	SI_corer_9cm	2023-09-08 T07:25:00	89.93587	-15.22256		MARKII	max depth	Biocore_1; IceStation #7
PS138_152_Coring-002	SI_corer_9cm	2023-09-08 T07:25:05	89.93587	-15.22256		MARKII	max depth	Biocore_2; IceStation #7
PS138_152_Coring-003	SI_corer_9cm	2023-09-08 T07:25:10	89.93587	-15.22256		MARKII	max depth	Biocore_3; IceStation #7
PS138_152_Coring-004	SI_corer_9cm	2023-09-08 T07:26:00	89.93587	-15.22256		MARKII	max depth	Biocore_4; IceStation #7
PS138_152_Coring-005	SI_corer_9cm	2023-09-08 T07:26:05	89.93587	-15.22256		MARKII	max depth	Biocore_5; IceStation #7
PS138_152_Coring-006	SI_corer_9cm	2023-09-08 T07:26:10	89.93587	-15.22256		MARKII	max depth	Biocore_6; IceStation #7
PS138_152_Coring-007	SI_corer_9cm	2023-09-08 T07:27:00	89.93587	-15.22256		MARKII	max depth	Biocore_7; IceStation #7
PS138_152_Coring-008	SI_corer_9cm	2023-09-08 T07:27:05	89.93587	-15.22256		MARKII	max depth	Biocore_8; IceStation #7
PS138_152_Coring-009	SI_corer_9cm	2023-09-08 T07:27:10	89.93587	-15.22256		MARKII	max depth	Biocore_9; IceStation #7
PS138_152_Coring-010	SI_corer_9cm	2023-09-08 T07:28:00	89.93587	-15.22256		MARKII	max depth	SIP-Texture; IceStation #7
PS138_152_Coring-011	SI_corer_9cm	2023-09-08 T07:29:00	89.93587	-15.22256		MARKII	max depth	SIP-Archive; IceStation #7
PS138_152_Coring-012	SI_corer_9cm	2023-09-08 T07:29:05	89.93587	-15.22256		MARKII	max depth	SIP-Salinity; IceStation #7
PS138_152_Coring-013	hand_pump	2023-09-08 T07:30:00	89.93587	-15.22256		HP	max depth	Under Ice Water; IceStation #7

Event label	Optional label	Date / Time	Latitude	Longitude	Depth [m]	Gear	Action	Comment
PS138_152_Coring-014	hand_pump	2023-09-08 T07:30:05	89.93587	-15.22256		HP	max depth	Melt Pond Water; IceStation #7
PS138_152_Coring-015	snow_sampler_ glove	2023-09-08 T07:31:00	89.93587	-15.22256		SSG	max depth	Snow Sample; IceStation #7
PS138_152_ Chemistry-005	snow_sampler_ glove	2023-09-08 T08:00:00	89.94917	15.33222		SSG	max depth	Snow sample; IceStation #7
PS138_152_ Chemistry-009	snow_sampler_ glove	2023-09-08 T08:00:00	89.94710	21.56457		SSG	max depth	Snow sample; IceStation #7
PS138_152_ Chemistry-008	snow_sampler_ glove	2023-09-08 T08:00:00	89.94944	15.91611		SSG	max depth	Snow sample; IceStation #7
PS138_152_ Chemistry-007	snow_sampler_ glove	2023-09-08 T08:00:00	89.94720	21.60373		SSG	max depth	Snow sample; IceStation #7
PS138_152_ Chemistry-006	snow_sampler_ glove	2023-09-08 T08:00:00	89.95000	19.04361		SSG	max depth	Snow sample; IceStation #7
PS138_152_ Chemistry-001	hand_pump	2023-09-08 T08:00:00	89.94441	13.17547		HP	max depth	Ice Edge Water; IceStation #7
PS138_152_ Chemistry-002	hand_pump	2023-09-08 T08:00:00	89.94762	14.72547		HP	max depth	Melt Pond Water; IceStation #7
PS138_152_ Chemistry-003	hand_pump	2023-09-08 T08:00:00	89.94762	14.72547		HP	max depth	Under Ice Water; IceStation #7
PS138_152_ Chemistry-004	snow_sampler_ glove	2023-09-08 T08:00:00	89.94441	13.17547		SSG	max depth	Snow sample; IceStation #7
PS138_152-1_ISCA-003	ISCA	2023-09-08 T09:00:00	89.93587	-15.22256		ISCA	max depth	IceStation #7
PS138_152-1_ISCA-002	ISCA	2023-09-08 T09:00:00	89.93587	-15.22256		ISCA	max depth	IceStation #7
PS138_152-1_ISCA-001	ISCA	2023-09-08 T09:00:00	89.93587	-15.22256		ISCA	max depth	IceStation #7
PS138_ SBLA_20230908T091400		2023-09-08 T09:14:00	89.97952	-77.96180		SBLA	Station start	

Event label	Optional label	Date / Time	Latitude	Longitude	Depth [m]	Gear	Action	Comment
PS138_ SBLA_20230908T091400		2023-09-08 T09:14:00	89.80652	96.10514		SBLA	Station end	
PS138_ SBLA_20230908T093600		2023-09-08 T09:36:00	89.76000	97.49938		SBLA	Station start	
PS138_ SBLA_20230908T093600		2023-09-08 T09:36:00	89.79198	37.37154		SBLA	Station end	
PS138_ SBLA_20230908T095200		2023-09-08 T09:52:00	89.78272	31.73554		SBLA	Station start	
PS138_ SBLA_20230908T095200		2023-09-08 T09:52:00	89.80322	-148.17034		SBLA	Station end	
PS138_ SBLA_20230908T101400		2023-09-08 T10:14:00	89.75807	-148.43816		SBLA	Station start	
PS138_ SBLA_20230908T101400		2023-09-08 T10:14:00	89.78333	-88.46044		SBLA	Station end	
PS138_ SBLA_20230908T103100		2023-09-08 T10:31:00	89.76880	-80.97296		SBLA	Station start	
PS138_ SBLA_20230908T103100		2023-09-08 T10:31:00	89.96120	86.06847		SBLA	Station end	
PS138_ SBLA_20230908T104800		2023-09-08 T10:48:00	89.91570	103.49420		SBLA	Station start	
PS138_ SBLA_20230908T104800		2023-09-08 T10:48:00	89.96179	42.66195		SBLA	Station end	
PS138_156-1		2023-09-08 T17:00:00	89.94503	47.19160	4238	TVMUC	Station start	IceStation #7
PS138_156-1		2023-09-08 T20:39:58	89.93942	49.43894	4239	TVMUC	Station end	IceStation #7
PS138_157-1		2023-09-08 T20:40:36	89.93940	49.43085	4240	TVMUC	Station start	IceStation #7
PS138_157-1		2023-09-09 T00:09:34	89.93666	43.70829	4239	TVMUC	Station end	IceStation #7

Event label	Optional label	Date / Time	Latitude	Longitude	Depth [m]	Gear	Action	Comment
PS138_158-1		2023-09-09 T00:10:15	89.93666	43.67348	4241	MSN	Station start	IceStation #7
PS138_158-1		2023-09-09 T02:35:11	89.93721	35.45159	4247	MSN	Station end	IceStation #7
PS138_159-1		2023-09-09 T02:36:33	89.93721	35.36548	4244	MSN	Station start	IceStation #7
PS138_159-1		2023-09-09 T04:25:52	89.93701	28.65568	4241	MSN	Station end	IceStation #7
PS138_152_ROV_001	BEAST	2023-09-09 T09:01:00	89.93600	-15.22300		BEAST	max depth	IceStation #7
PS138_160-1		2023-09-09 T09:20:00	89.92065	15.30033	4230	B_LANDER	Station start	Flux Lander #2. IceStation #7; Posidonia Position
PS138_160-1		2023-09-10 T15:22:00	89.92017	14.23095	4244	B_LANDER	Station end	Flux Lander #2. IceStation #7; Posidonia Position
PS138_161-1		2023-09-09 T10:31:29	89.91112	12.83219	4244	TVMUC	Station start	IceStation #7
PS138_161-1		2023-09-09 T13:43:38	89.90086	5.43917	4242	TVMUC	Station end	IceStation #7
PS138_152_ SUNAprofil_007	Nitrate_profiler	2023-09-09 T10:45:54	89.91440	0.63220		NO3	max depth	4 profiles; IceStation #7
PS138_152_Buoy_002	2023W7	2023-09-09 T11:20:00	89.92115	4.26265		BUOY	max depth	IceStation #7
PS138_152_Buoy_003	2023I9	2023-09-09 T11:50:00	89.91900	2.90100		SIMB	max depth	distance from pinger to surface 1.07 m; IceStation #7

Event label	Optional label	Date / Time	Latitude	Longitude	Depth [m]	Gear	Action	Comment
PS138_152_Buoy_001	2023S100	2023-09-09 T12:45:00	89.91700	0.73600		BUOY_ SNOW	max depth	SH1: 0.2 m. SH2: 0.18 m. SH3: 0.18 m. SH4: 0.17 m. probably first-year ice; Co-deployed with IAOOS IMB; IceStation #7
PS138_152_MSS_1	MSS_90D_075	2023-09-09 T13:16:00	89.90250	6.07930		MSS	max depth	MSS 075 series of 7 profiles; IceStation #7
PS138_152_ICEADCP_1	300kHzADCP	2023-09-09 T13:16:00	89.90250	6.07930		ADCP	max depth	Under-ice RDI 300 kHz ADCP time series; IceStation #7
PS138_152_DRONE_001	UAV_PS	2023-09-09 T16:02:00	89.93600	-15.22300		UAV	max depth	Photogrammetry grid over floe; IceStation #7
PS138_152_IT_001	PS138_152-1_IT_ssl-025	2023-09-09 T16:17:00	89.93587	-15.22256		STRAP_ICE	max depth	Deployment of ice sediment traps equipped with gel traps; Ice station #7
PS138_152_KEF_001	PS138_152-1_KEF_ssl-027	2023-09-09 T16:25:00	89.93587	-15.22256		STRAP_ICE	max depth	Deployment of ice sediment traps for biogeochemistry; Ice station #7
PS138_152_PiCam_001	PS138_152_PiCam_001	2023-09-09 T17:00:00	89.93587	-15.22256		VIDEO	max depth	Deployment of time-lapse camera under the ice; Ice station #7
PS138_152_Core_001	SI_corer_14cm	2023-09-10 T00:00:00	89.93600	-15.22300		MARKV	max depth	IceStation #7

Event label	Optional label	Date / Time	Latitude	Longitude	Depth [m]	Gear	Action	Comment
PS138_152_Core_002	SI_corer_14cm	2023-09-10 T00:00:00	89.93600	-15.22300		MARKV	max depth	1x OPT. HI scan. no bio samples; IceStation #7
PS138_152_Kipps_001	Dart_Kipps	2023-09-10 T06:45:00	89.93600	-15.22300		ALBEDOM	max depth	IceStation #7
PS138_152_ASD_001	Dart_ASD	2023-09-10 T06:45:00	89.93600	-15.22300		ALBEDOM	max depth	IceStation #7
PS138_152_Buoy_006	2023P286	2023-09-10 T06:50:00	89.82627	-2.90138		ISVP	max depth	floatboat site. Floe size bigger than 2km; IceStation #7
PS138_152_GEM_001	gem2-512	2023-09-10 T06:52:00	89.93600	-15.22300		BES	max depth	IceStation #7
PS138_152_Magna_001	magnaprobe-steffi	2023-09-10 T06:57:00	89.93600	-15.22300		MAGNA	max depth	IceStation #7
PS138_152_UpperOcean IceFloeTransect_1	CTD_48M_1459	2023-09-10 T07:00:00	84.95000	129.04000		CTD_fishrod	max depth	IceStation #7
PS138_152_ROV_002	BEAST	2023-09-10 T07:25:00	89.93600	-15.22300		BEAST	max depth	IceStation #7
PS138_152_MSS_2	MSS_90D_075	2023-09-10 T07:25:00	89.82420	-1.76870		MSS	max depth	MSS 075 series of 7 profiles; IceStation #7
PS138_152_Buoy_005	2023T110	2023-09-10 T07:50:00	89.82200	-2.64100		SIMBA	max depth	ridge around 50 m from buoy site. deployed on ridge flank. hole filled with slush; ice thickness 2.82 m. freeboard 0.15 m. snow de…

Event label	Optional label	Date / Time	Latitude	Longitude	Depth [m]	Gear	Action	Comment
PS138_152_Buoy_004	2023T115	2023-09-10 T09:00:00	89.81725	-2.44665		SIMBA	max depth	ICE7. deployed on IAOOS. ice thickness 1.34 m. freeboard 0.17 m. no snow. thermistor 29 at surface. hole filled with slush; IceSta…
PS138_163-1		2023-09-10 T21:08:16	89.77242	-1.92753	4244	HN	Station start	IceStation #7
PS138_163-1		2023-09-10 T21:31:39	89.77055	-1.98709	4242	HN	Station end	IceStation #7
PS138_162-1		2023-09-10 T21:13:40	89.77198	-1.94057	4242	CTD-RO	max depth	IceStation #7. at max depth
PS138_164-1		2023-09-10 T21:47:05	89.76934	-2.02830	4242	MSC	max depth	IceStation #7
PS138_165-1		2023-09-10 T22:02:16	89.76818	-2.06917	4244	MSC	max depth	IceStation #7
PS138_166-1		2023-09-10 T22:50:33	89.76461	-2.19523	4244	CTD-RO	max depth	IceStation #7. at max depth
PS138_167-1		2023-09-10 T23:18:27	89.76264	-2.27216	4244	BONGO	Station start	IceStation #7
PS138_167-1		2023-09-10 T23:26:21	89.76210	-2.29078	4243	BONGO	Station end	IceStation #7
PS138_168-1_1	ISP_Seb	2023-09-11 T00:24:00	89.75839	-2.39429	4244	ISP	Station start	IceStation #7
PS138_168-1_1	ISP_Seb	2023-09-11 T06:32:00	89.73038	-0.08134	4249	ISP	Station end	IceStation #7
PS138_168-1_2	ISP_Frauke	2023-09-11 T01:20:00	89.75494	-2.35945	4243	ISP	Station start	IceStation #7

Event label	Optional label	Date / Time	Latitude	Longitude	Depth [m]	Gear	Action	Comment
PS138_168-1_2	ISP_Frauke	2023-09-11 T05:33:00	89.73595	-0.65436	4246	ISP	Station end	IceStation #7
PS138_168-1_3	ISP_Franky	2023-09-11 T01:58:00	89.75247	-2.23726	4244	ISP	Station start	IceStation #7
PS138_168-1_3	ISP_Franky	2023-09-11 T04:54:00	89.73919	-1.00242	4246	ISP	Station end	IceStation #7
PS138_168-1		2023-09-11 T02:08:19	89.75181	-2.19389	4242	CTD-RO	max depth	IceStation #7. at max depth
PS138_168-1_4	ISP_Jimmy	2023-09-11 T02:17:00	89.75118	-2.14732	4244	ISP	Station start	battery failed; IceStation #7
PS138_168-1_4	ISP_Jimmy	2023-09-11 T04:49:00	89.73963	-1.04720	4245	ISP	Station end	battery failed; IceStation #7
PS138_152_KEF_002	PS138_152-1_ KEF_ssl-028	2023-09-11 T06:20:00	89.93587	-15.22256		STRAP_ICE	max depth	Recovery of ice sediment traps for biogeochemistry; Ice station #7
PS138_152_IT_002	PS138_152-1_IT_ssl-026	2023-09-11 T06:40:00	89.93587	-15.22256		STRAP_ICE	max depth	Recovery of ice sediment traps equipped with gel traps; Ice station #7
PS138_169-1		2023-09-11 T09:02:24	89.70044	5.68107	4250	EBS	Station start	IceStation #7
PS138_169-1		2023-09-11 T15:00:08	89.68638	3.85116	4247	EBS	Station end	IceStation #7
PS138_170-1		2023-09-11 T09:37:47	89.69840	5.59566	4251	ZODIAC	Station start	Zodiac Luisa. IceStation #7
PS138_170-1		2023-09-11 T10:14:46	89.69201	5.95824	4251	ZODIAC	Station end	Zodiac Luisa. IceStation #7
PS138_171-1		2023-09-11 T17:19:24	89.81759	57.71303	4263	XCTD	Station start	

Event label	Optional label	Date / Time	Latitude	Longitude	Depth [m]	Gear	Action	Comment
PS138_171-1		2023-09-11 T17:28:02	89.81732	57.63654	4265	XCTD	Station end	
PS138_172-1		2023-09-11 T21:18:13	89.64759	57.33221	4283	CTD-RO	max depth	at max depth
PS138_171-2		2023-09-12 T00:34:07	89.50142	60.51670	4306	XCTD	Station start	
PS138_171-2		2023-09-12 T00:39:44	89.49562	60.03624	4306	XCTD	Station end	
PS138_173-1		2023-09-12 T03:07:51	89.33937	59.19928	4325	CTD-RO	max depth	at max depth
PS138_171-3		2023-09-12 T05:25:13	89.16690	60.20895	4343	XCTD	Station start	
PS138_171-3		2023-09-12 T05:32:15	89.16288	60.26435	4344	XCTD	Station end	
PS138_174-1		2023-09-12 T09:24:10	88.99530	59.61131	4356	CTD-RO	max depth	at max depth
PS138_171-4		2023-09-12 T12:59:53	88.83079	59.32194	4367	XCTD	Station start	
PS138_171-4		2023-09-12 T13:04:28	88.82797	59.47175	4367	XCTD	Station end	
PS138_175-1		2023-09-12 T15:44:18	88.67074	60.18934	4372	CTD-RO	max depth	at max depth
PS138_171-5		2023-09-12 T18:02:01	88.51250	60.21698	4376	XCTD	Station start	
PS138_171-5		2023-09-12 T18:08:49	88.51007	60.38630	4376	XCTD	Station end	
PS138_176-1		2023-09-12 T21:57:21	88.33404	59.61516	4372	CTD-RO	max depth	at max depth
PS138_178_nortek_ s1000_102149-001	nortek_ s1000_102149	2023-09-13 T00:00:00	87.92839	60.32250		BUOY_ ADCP	max depth	IceStation #8; IceStation #8

Event label	Optional label	Date / Time	Latitude	Longitude	Depth [m]	Gear	Action	Comment
PS138_178_ Vector_5418-001	Vector_5418	2023-09-13 T00:00:00	69.67800	18.98980		CM	max depth	IceStation #8
PS138_171-6		2023-09-13 T01:32:43	88.16889	59.75198	4379	XCTD	Station start	
PS138_171-6		2023-09-13 T01:38:52	88.16559	59.74602	4378	XCTD	Station end	
PS138_177-1		2023-09-13 T05:33:40	87.95064	60.86212	4377	GKG	max depth	IceStation #8
PS138_178_ASD_001	Dart_ASD	2023-09-13 T07:15:00	87.92800	60.23200		ALBEDOM	max depth	IceStation #8
PS138_178_Kipps_001	Dart_Kipps	2023-09-13 T07:15:00	87.92800	60.23200		ALBEDOM	max depth	IceStation #8
PS138_178-1		2023-09-13 T08:30:09	87.92839	60.32250	4375	ICE	Station start	IceStation #8
PS138_178-1		2023-09-15 T15:46:49	87.88227	56.91070	4374	ICE	Station end	IceStation #8
PS138_178_ SUNAprofil_008	Nitrate_profiler	2023-09-13 T09:28:00	87.92390	59.85580		NO3	max depth	5 profiles; IceStation #8
PS138_178_ICEADCP_1	300kHzADCP	2023-09-13 T10:42:00	87.92410	59.94510		ADCP	max depth	Under-ice RDI 300 kHz ADCP time series; IceStation #8
PS138_178_MSS_1	MSS_90D_075	2023-09-13 T10:42:00	87.92410	59.94510		MSS	max depth	MSS 075 series of 16 profiles; IceStation #8
PS138_178_ Chemistry-001	hand_pump	2023-09-13 T11:00:00	87.92371	59.89226		HP	max depth	Ice Edge Water; IceStation #8
PS138_178_ Chemistry-009	snow_sampler_ glove	2023-09-13 T11:00:00	87.92194	59.72639		SSG	max depth	Snow sample; IceStation #8
PS138_178_ Chemistry-002	hand_pump	2023-09-13 T11:00:00	87.92253	59.77014		HP	max depth	Melt Pond Water; IceStation #8

Event label	Optional label	Date / Time	Latitude	Longitude	Depth [m]	Gear	Action	Comment
PS138_178_ Chemistry-003	hand_pump	2023-09-13 T11:00:00	87.92253	59.77014		HP	max depth	Under Ice Water; IceStation #8
PS138_178_ Chemistry-004	snow_sampler_ glove	2023-09-13 T11:00:00	87.92371	59.89226		SSG	max depth	Snow sample; IceStation #8
PS138_178_ Chemistry-006	snow_sampler_ glove	2023-09-13 T11:00:00	87.92083	59.63278		SSG	max depth	Snow sample; IceStation #8
PS138_178_ Chemistry-007	snow_sampler_ glove	2023-09-13 T11:00:00	87.91972	59.59194		SSG	max depth	Snow sample; IceStation #8
PS138_178_ Chemistry-008	snow_sampler_ glove	2023-09-13 T11:00:00	87.92250	59.76472		SSG	max depth	Snow sample; IceStation #8
PS138_178_ Chemistry-005	snow_sampler_ glove	2023-09-13 T11:00:00	87.92194	59.70472		SSG	max depth	Snow sample; IceStation #8
PS138_179-1		2023-09-13 T11:05:26	87.92330	59.94434	4378	GKG	max depth	IceStation #8
PS138_178_DRONE_001	UAV_PS	2023-09-13 T11:50:00	87.92800	60.23200		UAV	max depth	Photogrammetry grid over floe; IceStation #8
PS138_178_ROV_001	BEAST	2023-09-13 T13:37:00	87.92800	60.23200		BEAST	max depth	IceStation #8
PS138_178_Buoy_002	2023T100	2023-09-13 T13:45:00	87.92100	59.49000		SIMBA	max depth	ice thickness: 0.96 m. freeboard: 0.04 m. snow depth: 0.1 m. thermistor 37 at surface. level first-year ice; Co-deployed with 2023…

Event label	Optional label	Date / Time	Latitude	Longitude	Depth [m]	Gear	Action	Comment
PS138_178_Buoy_001	2023S101	2023-09-13 T14:15:00	87.92000	59.42900		BUOY_ SNOW	max depth	SH1: 0.06 m. SH2: 0.08 m. SH3: 0.11 m. SH4: 0.09 m. level first-year ice; Co-deployed with IMB 2023T100; IceStation #8
PS138_180-1		2023-09-13 T14:34:40	87.92005	59.45906	4374	OFOBS	Station start	IceStation #8
PS138_180-1		2023-09-13 T17:24:15	87.91427	59.21190	4377	OFOBS	Station end	IceStation #8
PS138_178_Coring-001	SI_corer_9cm	2023-09-13 T15:11:14	87.92839	60.32250		MARKII	max depth	Biocore_1; IceStation #8
PS138_178_Coring-002	SI_corer_9cm	2023-09-13 T15:12:16	87.92839	60.32250		MARKII	max depth	Biocore_2; IceStation #8
PS138_178_Coring-003	SI_corer_9cm	2023-09-13 T15:12:25	87.92839	60.32250		MARKII	max depth	Biocore_3; IceStation #8
PS138_178_Coring-004	SI_corer_9cm	2023-09-13 T15:12:30	87.92839	60.32250		MARKII	max depth	Biocore_4; IceStation #8
PS138_178_Coring-005	SI_corer_9cm	2023-09-13 T15:12:36	87.92839	60.32250		MARKII	max depth	Biocore_5; IceStation #8
PS138_178_Coring-006	SI_corer_9cm	2023-09-13 T15:12:41	87.92839	60.32250		MARKII	max depth	Biocore_6; IceStation #8
PS138_178_Coring-007	SI_corer_9cm	2023-09-13 T15:12:46	87.92839	60.32250		MARKII	max depth	Biocore_7; IceStation #8
PS138_178_Coring-008	SI_corer_9cm	2023-09-13 T15:12:50	87.92839	60.32250		MARKII	max depth	Biocore_8; IceStation #8
PS138_178_Coring-009	SI_corer_9cm	2023-09-13 T15:12:55	87.92839	60.32250		MARKII	max depth	Biocore_9; IceStation #8
PS138_178_Coring-010	SI_corer_9cm	2023-09-13 T15:12:59	87.92839	60.32250		MARKII	max depth	SIP-Texture; IceStation #8

Event label	Optional label	Date / Time	Latitude	Longitude	Depth [m]	Gear	Action	Comment
PS138_178_Coring-011	SI_corer_9cm	2023-09-13 T15:13:32	87.92839	60.32250		MARKII	max depth	SIP-Archive; IceStation #8
PS138_178_Coring-012	SI_corer_9cm	2023-09-13 T15:13:44	87.92839	60.32250		MARKII	max depth	SIP-Salinity; IceStation #8
PS138_178_Coring-013	hand_pump	2023-09-13 T15:13:53	87.92839	60.32250		HP	max depth	Under Ice Water; IceStation #8
PS138_178_Coring-014	hand_pump	2023-09-13 T15:14:22	87.92839	60.32250		HP	max depth	Melt Pond Water; IceStation #8
PS138_178_Coring-015	snow_sampler_ glove	2023-09-13 T15:14:36	87.92839	60.32250		SSG	max depth	Snow Sample; IceStation #8
PS138_178-1_ISCA-001	ISCA	2023-09-13 T16:00:00	87.92839	60.32250		ISCA	max depth	IceStation #8
PS138_178-1_ISCA-002	ISCA	2023-09-13 T16:00:00	87.92839	60.32250		ISCA	max depth	IceStation #8
PS138_178-1_ISCA-003	ISCA	2023-09-13 T16:00:00	87.92839	60.32250		ISCA	max depth	IceStation #8
PS138_181-1		2023-09-13 T19:21:28	87.90777	59.04668	4359	TVMUC	Station start	IceStation #8
PS138_181-1		2023-09-13 T23:03:51	87.89687	58.60224	4375	TVMUC	Station end	IceStation #8
PS138_182-1		2023-09-13 T23:04:45	87.89685	58.60033	4374	TVMUC	Station start	IceStation #8
PS138_182-1		2023-09-14 T03:05:45	87.90257	58.20776	4287	TVMUC	Station end	IceStation #8
PS138_178_Core_002	SI_corer_14cm	2023-09-14 T00:00:00	87.92800	60.23200		MARKV	max depth	2x OPT no scan. no bio sample. only amphipod count; IceStation #8
PS138_178_Core_001	SI_corer_14cm	2023-09-14 T00:00:00	87.92800	60.23200		MARKV	max depth	IceStation #8

Event label	Optional label	Date / Time	Latitude	Longitude	Depth [m]	Gear	Action	Comment
PS138_183-1		2023-09-14 T03:26:02	87.90363	58.19201	4285	MSN	Station start	IceStation #8
PS138_183-1		2023-09-14 T05:06:52	87.90842	58.13775	4257	MSN	Station end	IceStation #8
PS138_184-1		2023-09-14 T05:07:38	87.90846	58.13744	4252	MSN	Station start	IceStation #8
PS138_184-1		2023-09-14 T06:57:49	87.91247	58.05773	4296	MSN	Station end	IceStation #8
PS138_178_KEF_001	PS138_178-1_ KEF_ssl-031	2023-09-14 T05:10:00	87.92839	60.32250		STRAP_ICE	max depth	Deployment of ice sediment traps for biogeochemistry; Ice station #8
PS138_178_IT_001	PS138_178-1_IT_ssl-029	2023-09-14 T05:20:00	87.92839	60.32250		STRAP_ICE	max depth	Deployment of ice sediment traps equipped with gel traps; Ice station #8
PS138_178_PiCam_001	PS138_178_ PiCam_001	2023-09-14 T05:30:00	87.92839	60.32250		VIDEO	max depth	Deployment of time-lapse camera under the ice; Ice station #8
PS138_178_ROV_002	BEAST	2023-09-14 T07:58:00	87.92800	60.23200		BEAST	max depth	IceStation #8
PS138_178_GEM_001	gem2-512	2023-09-14 T08:55:00	87.92800	60.23200		BES	max depth	IceStation #8
PS138_178_Magna_001	magnaprobe-steffi	2023-09-14 T09:02:00	87.92800	60.23200		MAGNA	max depth	IceStation #8
PS138_185-1		2023-09-14 T10:50:00	87.87978	57.06688	4364	B_LANDER	Station start	Flux Lander #2. IceStation #8; Posidonia Position

Event label	Optional label	Date / Time	Latitude	Longitude	Depth [m]	Gear	Action	Comment
PS138_185-1		2023-09-15 T12:40:00	87.87958	57.08490	4376	B_LANDER	Station end	Flux Lander #2. IceStation #8; Posidonia Position
PS138_187-1		2023-09-14 T12:28:29	87.94389	57.12600	4374	HN	Station start	IceStation #8
PS138_187-1		2023-09-14 T12:47:14	87.94686	57.06678	4377	HN	Station end	IceStation #8
PS138_186-1		2023-09-14 T12:29:24	87.94404	57.12312	4376	CTD-RO	max depth	IceStation #8. at max depth
PS138_178_MSS_2	MSS_90D_075	2023-09-14 T12:42:00	87.94610	57.02140		MSS	max depth	MSS 075 series of 10 profiles; IceStation #8
PS138_188-1		2023-09-14 T13:04:47	87.94972	57.01057	4377	MSC	max depth	IceStation #8
PS138_189-1		2023-09-14 T13:20:48	87.95236	56.96558	4379	MSC	max depth	IceStation #8
PS138_190-1		2023-09-14 T14:10:15	87.96007	56.85070	4376	CTD-RO	max depth	IceStation #8. at max depth
PS138_191-1		2023-09-14 T14:39:50	87.96431	56.79381	4374	BONGO	Station start	IceStation #8
PS138_191-1		2023-09-14 T14:48:36	87.96549	56.77871	4374	BONGO	Station end	IceStation #8
PS138_192-1		2023-09-14 T15:25:52	87.96990	56.72423	4375	ROSINA	Station start	IceStation #8
PS138_192-1		2023-09-14 T18:17:53	87.97750	56.63097	4375	ROSINA	Station end	IceStation #8
PS138_193-1_1	ISP_Seb	2023-09-14 T19:00:00	87.97727	56.61908	4375	ISP	Station start	IceStation #8
PS138_193-1_1	ISP_Seb	2023-09-15 T01:01:00	87.97255	55.32796	4383	ISP	Station end	IceStation #8

Event label	Optional label	Date / Time	Latitude	Longitude	Depth [m]	Gear	Action	Comment
PS138_193-1_2	ISP_Frauke	2023-09-14 T19:45:00	87.97727	56.61908	4375	ISP	Station start	IceStation #8
PS138_193-1_2	ISP_Frauke	2023-09-15 T01:01:00	87.97255	55.32796	4383	ISP	Station end	IceStation #8
PS138_193-1_3	ISP_Franky	2023-09-14 T20:15:00	87.97727	56.61908	4375	ISP	Station start	IceStation #8
PS138_193-1_3	ISP_Franky	2023-09-15 T01:01:00	87.97255	55.32796	4383	ISP	Station end	IceStation #8
PS138_193-1		2023-09-14 T20:28:36	87.97118	56.36937	4374	CTD-RO	max depth	IceStation #8. at max depth
PS138_193-1_4	ISP_Jimmy	2023-09-14 T20:40:00	87.97727	56.61908	4375	ISP	Station start	IceStation #8
PS138_193-1_4	ISP_Jimmy	2023-09-15 T01:01:00	87.97255	55.32796	4383	ISP	Station end	IceStation #8
PS138_178_KEF_002	PS138_178-1_ KEF_ssl-032	2023-09-15 T05:45:00	87.92839	60.32250		STRAP_ICE	max depth	Recovery of ice sediment traps for biogeochemistry; Ice station #8
PS138_178_IT_002	PS138_178-1_IT_ssl-030	2023-09-15 T05:59:00	87.92839	60.32250		STRAP_ICE	max depth	Recovery of ice sediment traps equipped with gel traps; Ice station #8
PS138_194-1		2023-09-15 T06:01:56	87.85770	56.38790	4378	EBS	Station start	IceStation #8
PS138_194-1		2023-09-15 T11:25:07	87.85506	56.53285	4377	EBS	Station end	IceStation #8
PS138_171-7		2023-09-15 T17:11:41	87.77244	58.10122	4324	XCTD	Station start	
PS138_171-7		2023-09-15 T17:20:24	87.76388	58.20662	4598	XCTD	Station end	

Event label	Optional label	Date / Time	Latitude	Longitude	Depth [m]	Gear	Action	Comment
PS138_195-1		2023-09-15 T20:45:51	87.66163	59.77246	4067	CTD-RO	max depth	at max depth
PS138_171-8		2023-09-15 T23:52:47	87.51736	59.47881	4102	XCTD	Station start	
PS138_171-8		2023-09-16 T00:03:30	87.50782	59.54781	3955	XCTD	Station end	
PS138_196-1		2023-09-16 T03:31:33	87.33866	59.92238	3505	CTD-RO	max depth	at max depth
PS138_197-1		2023-09-16 T06:59:12	87.28004	62.40352	3241	DS3	Station start	
PS138_197-1		2023-09-16 T11:02:47	87.09485	61.89875	3297	DS3	Station end	
PS138_Heli_EM-Bird_011	Embird_awi-bird	2023-09-16 T10:43:00	87.10220	61.93560		EMB	max depth	Flight during transit.Experiment for new calibration.
PS138_198_DRONE_001	UAV_PS	2023-09-16 T12:44:00	87.12300	62.35400		UAV	max depth	Photogrammetry grid
PS138_ SBLA_20230916T124600		2023-09-16 T12:46:00	87.14853	62.36687		SBLA	Station start	
PS138_ SBLA_20230916T124600		2023-09-16 T12:46:00	87.17885	68.95100		SBLA	Station end	
PS138_ SBLA_20230916T130800		2023-09-16 T13:08:00	87.16824	69.59152		SBLA	Station start	
PS138_ SBLA_20230916T130800		2023-09-16 T13:08:00	86.85013	66.30693		SBLA	Station end	
PS138_198-1		2023-09-16 T13:16:22	87.12427	62.36973	2653	OFOBS	Station start	
PS138_198-1		2023-09-16 T14:09:26	87.12642	62.40883	2573	OFOBS	Station end	
PS138_ SBLA_20230916T133000		2023-09-16 T13:30:00	86.81866	65.77177		SBLA	Station start	

Event label	Optional label	Date / Time	Latitude	Longitude	Depth [m]	Gear	Action	Comment
PS138_SBLA_20230916T133000		2023-09-16 T13:30:00	87.12568	61.48715		SBLA	Station end	
PS138_199-1		2023-09-16 T17:18:50	87.22806	62.73248	2499	OFOBS	Station start	
PS138_199-1		2023-09-16 T18:55:02	87.22089	62.68028	2515	OFOBS	Station end	
PS138_200-1	2023P267	2023-09-16 T19:56:09	87.21952	62.66411	2623	ISVP	Station start	2023P267 MetOcean SVP-B 300534063488700
PS138_200-1	2023P267	2023-09-16 T20:09:21	87.21937	62.65969	2651	ISVP	Station end	2023P267 MetOcean SVP-B 300534063488700
PS138_171-9		2023-09-16 T21:50:17	87.17720	60.03518	3968	XCTD	Station start	
PS138_171-9		2023-09-16 T21:59:27	87.16991	59.95051	3993	XCTD	Station end	
PS138_201-1		2023-09-17 T02:01:40	86.97768	60.02103	4207	CTD-RO	max depth	at max depth
PS138_Heli_EM-Bird_012	Embird_awi-bird	2023-09-17 T08:08:00	86.95880	55.79670		EMB	max depth	Flight during transit.
PS138_202-1		2023-09-17 T08:50:28	86.95905	55.80277	3168	OFOBS	Station start	
PS138_202-1		2023-09-17 T10:33:58	86.95154	55.74147	3084	OFOBS	Station end	
PS138_202_DRONE_001	UAV_PS	2023-09-17 T09:42:00	86.95900	55.79300		UAV	max depth	Photogrammetry grid
PS138_202_DRONE_002	UAV_PS	2023-09-17 T09:52:00	86.95900	55.79300		UAV	max depth	Photogrammetry grid
PS138_SBLA_20230917T101100		2023-09-17 T10:11:00	86.93008	55.70877		SBLA	Station start	

Event label	Optional label	Date / Time	Latitude	Longitude	Depth [m]	Gear	Action	Comment
PS138_ SBLA_20230917T101100		2023-09-17 T10:11:00	86.93044	48.90780		SBLA	Station end	
PS138_ SBLA_20230917T103200		2023-09-17 T10:32:00	86.92489	48.31744		SBLA	Station start	
PS138_ SBLA_20230917T103200		2023-09-17 T10:32:00	86.64101	51.23072		SBLA	Station end	
PS138_ SBLA_20230917T105100		2023-09-17 T10:51:00	86.60678	51.61962		SBLA	Station start	
PS138_ SBLA_20230917T105100		2023-09-17 T10:51:00	86.95501	56.26669		SBLA	Station end	
PS138_203-1		2023-09-17 T13:12:21	86.96081	55.76195	3252	OFOBS	Station start	
PS138_203-1		2023-09-17 T17:36:07	86.95811	55.76008	3151	OFOBS	Station end	
PS138_171-10		2023-09-17 T20:00:29	86.83223	58.72485	3571	XCTD	Station start	
PS138_171-10		2023-09-17 T20:16:45	86.83006	58.83525	3500	XCTD	Station end	
PS138_204-1		2023-09-17 T23:33:45	86.66052	60.06168	1854	CTD-RO	max depth	at max depth
PS138_171-11		2023-09-18 T01:50:01	86.50665	60.02328	1886	XCTD	Station start	
PS138_171-11		2023-09-18 T01:56:27	86.50201	59.96438	1793	XCTD	Station end	
PS138_205-1		2023-09-18 T05:02:56	86.33017	60.06175	2764	CTD-RO	max depth	at max depth
PS138_171-12		2023-09-18 T08:13:57	86.17059	60.13684	3857	XCTD	Station start	
PS138_171-12		2023-09-18 T08:24:54	86.16648	60.07147	3864	XCTD	Station end	

Event label	Optional label	Date / Time	Latitude	Longitude	Depth [m]	Gear	Action	Comment
PS138_206_DRONE_001	UAV_PS	2023-09-18 T10:28:00	86.00300	60.41700		UAV	max depth	Photogrammetry grid
PS138_206-1		2023-09-18 T11:06:42	85.99917	60.43570	3868	CTD-RO	max depth	at max depth
PS138_171-13		2023-09-18 T13:44:45	85.83457	60.12206	3878	XCTD	Station start	
PS138_171-13		2023-09-18 T13:50:43	85.83171	60.09339	3880	XCTD	Station end	
PS138_207-1		2023-09-18 T16:40:36	85.65768	60.11230	3885	CTD-RO	max depth	at max depth
PS138_208-1		2023-09-18 T20:18:04	85.49452	60.07646	3886	TVMUC	Station start	IceStation #9
PS138_208-1		2023-09-18 T23:05:43	85.48914	60.13368	3882	TVMUC	Station end	IceStation #9
PS138_209-1		2023-09-18 T23:06:54	85.48907	60.13416	3883	TVMUC	Station start	IceStation #9
PS138_209-1		2023-09-19 T02:25:34	85.47435	60.16508	3884	TVMUC	Station end	IceStation #9
PS138_213_Core_002	SI_corer_14cm	2023-09-19 T00:00:00	85.46400	59.97000		MARKV	max depth	3x OPT scan. gypsum samples IceStation #9
PS138_213_ Vector_5418-001	Vector_5418	2023-09-19 T00:00:00	69.67800	18.98980		CM	max depth	IceStation #9
PS138_213_nortek_ s1000_102149-001	nortek_ s1000_102149	2023-09-19 T00:00:00	85.46397	59.96956		BUOY_ ADCP	max depth	IceStation #9IceStation #9
PS138_213_Core_001	SI_corer_14cm	2023-09-19 T00:00:00	85.46400	59.97000		MARKV	max depth	no samples IceStation #9
PS138_213_Core_003	SI_corer_14cm	2023-09-19 T00:00:00	85.46400	59.97000		MARKV	max depth	3x OPT scan. gypsum samples IceStation #9

Event label	Optional label	Date / Time	Latitude	Longitude	Depth [m]	Gear	Action	Comment
PS138_210-1		2023-09-19 T04:25:49	85.46569	60.13633	3885	GKG	max depth	IceStation #9
PS138_211-1		2023-09-19 T07:15:57	85.45859	60.06379	3882	GKG	max depth	IceStation #9
PS138_Heli_EM-Bird_013	Embird_awi-bird	2023-09-19 T07:37:00	85.45370	60.04180		EMB	max depth	Flight near IceStation 9.IceStation #9
PS138_ SBLA_20230919T094000		2023-09-19 T09:40:00	85.43939	59.71947		SBLA	Station start	
PS138_ SBLA_20230919T094000		2023-09-19 T09:40:00	85.83429	57.47869		SBLA	Station end	
PS138_ SBLA_20230919T100500		2023-09-19 T10:05:00	85.84593	57.40353		SBLA	Station start	
PS138_ SBLA_20230919T100500		2023-09-19 T10:05:00	85.44933	54.76208		SBLA	Station end	
PS138_ SBLA_20230919T102900		2023-09-19 T10:29:00	85.42102	54.56746		SBLA	Station start	
PS138_ SBLA_20230919T102900		2023-09-19 T10:29:00	85.43111	60.28988		SBLA	Station end	
PS138_212-1		2023-09-19 T10:29:00	85.46118	60.05425	3875	B_LANDER	Station start	Flux Lander #2. IceStation #9; Posidonia Position
PS138_212-1		2023-09-20 T16:50:00	85.46190	60.02373	3882	B_LANDER	Station end	Flux Lander #2. IceStation #9; Posidonia Position
PS138_213-1		2023-09-19 T12:38:32	85.46397	59.96956	3883	ICE	Station start	IceStation #9
PS138_213-1		2023-09-20 T19:50:04	85.47198	59.98317	3883	ICE	Station end	IceStation #9
PS138_213_ SUNAprofil_009	Nitrate_profiler	2023-09-19 T13:03:23	85.44560	60.01430		NO3	max depth	15 profiles IceStation #9

Event label	Optional label	Date / Time	Latitude	Longitude	Depth [m]	Gear	Action	Comment
PS138_214-1		2023-09-19 T13:32:13	85.46039	59.99377	3884	MSN	Station start	IceStation #9
PS138_214-1		2023-09-19 T15:18:10	85.45257	60.01107	3882	MSN	Station end	IceStation #9
PS138_Heli_EM-Bird_014	Embird_awi-bird	2023-09-19 T13:58:00	85.45490	59.89290		EMB	max depth	Second flight near IceStation #9. survey of the ice floe.IceStation #9
PS138_213_KEF_001	PS138_213-1_ KEF_ssl-035	2023-09-19 T14:00:00	85.46397	59.96956		STRAP_ICE	max depth	Deployment of ice sediment traps for biogeochemistry; Ice station #9
PS138_213_IT_001	PS138_213-1_IT_ssl-033	2023-09-19 T14:15:00	85.46397	59.96956		STRAP_ICE	max depth	Deployment of ice sediment traps equipped with gel traps; Ice station #9
PS138_213_MSS_1	MSS_90D_075	2023-09-19 T14:24:00	85.45700	60.03750		MSS	max depth	MSS 075 series of 18 profiles IceStation #9
PS138_213_ICEADCP_1	300kHzADCP	2023-09-19 T14:24:00	85.45700	60.03750		ADCP	max depth	Under-ice RDI 300 kHz ADCP time series IceStation #9
PS138_213_PiCam_001	PS138_213_ PiCam_001	2023-09-19 T14:30:00	85.46397	59.96956		VIDEO	max depth	Deployment of time-lapse camera under the ice; Ice station #9
PS138_213_Buoy_001	2023P272	2023-09-19 T14:40:00	85.45638	60.04022		ISVP	max depth	IceStation #9

Event label	Optional label	Date / Time	Latitude	Longitude	Depth [m]	Gear	Action	Comment
PS138_213_DRONE_001	UAV_PS	2023-09-19 T15:04:00	85.46400	59.97000		UAV	max depth	Photogrammetry grid over entire floeIceStation #9
PS138_213_DRONE_002	UAV_PS	2023-09-19 T15:19:00	85.46400	59.97000		UAV	max depth	Photogrammetry grid over ROV arealceStation #9
PS138_215-1		2023-09-19 T15:23:51	85.45217	60.01079	3885	MSN	Station start	IceStation #9
PS138_215-1		2023-09-19 T17:11:21	85.44584	59.98751	3882	MSN	Station end	IceStation #9
PS138_213_ Chemistry-006	snow_sampler_ glove	2023-09-19 T15:30:00	85.44894	60.04095		SSG	max depth	Snow sample IceStation #9
PS138_213_ Chemistry-009	snow_sampler_ glove	2023-09-19 T15:30:00	85.44778	59.99139		SSG	max depth	Snow sample IceStation #9
PS138_213_ Chemistry-008	snow_sampler_ glove	2023-09-19 T15:30:00	85.44880	60.04279		SSG	max depth	Snow sample IceStation #9
PS138_213_ Chemistry-001	hand_pump	2023-09-19 T15:30:00	85.44920	60.03257		HP	max depth	Ice Edge Water IceStation #9
PS138_213_ Chemistry-003	hand_pump	2023-09-19 T15:30:00	85.45149	60.02464		HP	max depth	Under Ice Water IceStation #9
PS138_213_ Chemistry-007	snow_sampler_ glove	2023-09-19 T15:30:00	85.45222	60.01972		SSG	max depth	Snow sample IceStation #9
PS138_213_ Chemistry-002	hand_pump	2023-09-19 T15:30:00	85.45149	60.02464		HP	max depth	Melt Pond Water IceStation #9
PS138_213_ Chemistry-005	snow_sampler_ glove	2023-09-19 T15:30:00	85.44920	60.03257		SSG	max depth	Snow sample IceStation #9
PS138_213_ Chemistry-004	snow_sampler_ glove	2023-09-19 T15:30:00	85.45149	60.02464		SSG	max depth	Snow sample IceStation #9
PS138_213_GEM_001	gem2-512	2023-09-19 T17:06:00	85.46400	59.97000		BES	max depth	IceStation #9

Event label	Optional label	Date / Time	Latitude	Longitude	Depth [m]	Gear	Action	Comment
PS138_213_Magna_001	magnaprobe-steffi	2023-09-19 T17:08:00	85.46400	59.97000		MAGNA	max depth	IceStation #9
PS138_213_Coring-001	SI_corer_9cm	2023-09-19 T17:43:00	85.46397	59.96956		MARKII	max depth	Biocore_1 IceStation #9
PS138_213_Coring-002	SI_corer_9cm	2023-09-19 T17:43:53	85.46397	59.96956		MARKII	max depth	Biocore_2 IceStation #9
PS138_213_Coring-003	SI_corer_9cm	2023-09-19 T17:43:59	85.46397	59.96956		MARKII	max depth	Biocore_3 IceStation #9
PS138_213_Coring-004	SI_corer_9cm	2023-09-19 T17:44:04	85.46397	59.96956		MARKII	max depth	Biocore_4 IceStation #9
PS138_213_Coring-005	SI_corer_9cm	2023-09-19 T17:44:08	85.46397	59.96956		MARKII	max depth	Biocore_5 IceStation #9
PS138_213_Coring-006	SI_corer_9cm	2023-09-19 T17:44:12	85.46397	59.96956		MARKII	max depth	Biocore_6 IceStation #9
PS138_213_Coring-007	SI_corer_9cm	2023-09-19 T17:44:16	85.46397	59.96956		MARKII	max depth	Biocore_7 IceStation #9
PS138_213_Coring-008	SI_corer_9cm	2023-09-19 T17:44:21	85.46397	59.96956		MARKII	max depth	Biocore_8 IceStation #9
PS138_213_Coring-009	SI_corer_9cm	2023-09-19 T17:44:25	85.46397	59.96956		MARKII	max depth	Biocore_9 IceStation #9
PS138_213_Coring-010	SI_corer_9cm	2023-09-19 T17:44:31	85.46397	59.96956		MARKII	max depth	SIP-TextureIceStation #9
PS138_213_Coring-011	SI_corer_9cm	2023-09-19 T17:45:25	85.46397	59.96956		MARKII	max depth	SIP-ArchiveIceStation #9
PS138_213_Coring-012	SI_corer_9cm	2023-09-19 T17:45:34	85.46397	59.96956		MARKII	max depth	SIP-SalinityIceStation #9
PS138_213_Coring-013	hand_pump	2023-09-19 T17:45:45	85.46397	59.96956		HP	max depth	Under Ice WaterIceStation #9
PS138_213_Coring-014	snow_sampler_glove	2023-09-19 T17:46:09	85.46397	59.96956		SSG	max depth	Snow SampleIceStation #9

Event label	Optional label	Date / Time	Latitude	Longitude	Depth [m]	Gear	Action	Comment
PS138_213_ROV_001	BEAST	2023-09-19 T17:50:00	85.46400	59.97000		BEAST	max depth	IceStation #9
PS138_213-1_ISCA-001	ISCA	2023-09-19 T18:00:00	85.46397	59.96956		ISCA	max depth	IceStation #9
PS138_216-1		2023-09-19 T18:32:01	85.44315	59.96603	3886	OFOBS	Station start	IceStation #9
PS138_216-1		2023-09-19 T19:48:42	85.44250	59.95789	3884	OFOBS	Station end	IceStation #9
PS138_217-1		2023-09-19 T21:44:42	85.44268	59.97245	3884	ROSINA	Station start	IceStation #9
PS138_217-1		2023-09-20 T01:12:13	85.43790	60.05913	3883	ROSINA	Station end	IceStation #9
PS138_218-1_1	ISP_Seb	2023-09-20 T01:30:00	85.43702	60.06426	3880	ISP	Station start	IceStation #9
PS138_218-1_1	ISP_Seb	2023-09-20 T07:12:00	85.43194	59.98973	3881	ISP	Station end	IceStation #9
PS138_218-1_2	ISP_Frauke	2023-09-20 T02:16:00	85.43473	60.07184	3880	ISP	Station start	IceStation #9
PS138_218-1_2	ISP_Frauke	2023-09-20 T07:12:00	85.43194	59.98973	3881	ISP	Station end	IceStation #9
PS138_218-1_3	ISP_Franky	2023-09-20 T02:53:00	85.43306	60.07130	3881	ISP	Station start	IceStation #9
PS138_218-1_3	ISP_Franky	2023-09-20 T07:12:00	85.43194	59.98973	3881	ISP	Station end	IceStation #9
PS138_218-1		2023-09-20 T03:01:38	85.43273	60.07040	3881	CTD-RO	max depth	IceStation #9. at max depth
PS138_218-1_4	ISP_Jimmy	2023-09-20 T03:10:00	85.43240	60.06924	3880	ISP	Station start	IceStation #9
PS138_218-1_4	ISP_Jimmy	2023-09-20 T07:12:00	85.43194	59.98973	3881	ISP	Station end	IceStation #9

Event label	Optional label	Date / Time	Latitude	Longitude	Depth [m]	Gear	Action	Comment
PS138_213_MSS_2	MSS_90D_075	2023-09-20 T04:32:00	85.43070	60.07800		MSS	max depth	MSS 075 series of 12 profiles IceStation #9
PS138_213_ROV_002	BEAST	2023-09-20 T04:43:00	85.46400	59.97000		BEAST	max depth	IceStation #9
PS138_219-1		2023-09-20 T07:35:01	85.43286	59.98448	3880	MSC	max depth	IceStation #9
PS138_220-1		2023-09-20 T07:48:22	85.43347	59.98203	3881	MSC	max depth	IceStation #9
PS138_221-1		2023-09-20 T08:01:13	85.43408	59.98054	3883	BONGO	Station start	IceStation #9
PS138_221-1		2023-09-20 T08:06:22	85.43432	59.98020	3880	BONGO	Station end	IceStation #9
PS138_213_ASD_001	Dart_ASD	2023-09-20 T08:30:00	85.46400	59.97000		ALBEDOM	max depth	IceStation #9
PS138_213_Kipps_001	Dart_Kipps	2023-09-20 T08:30:00	85.46400	59.97000		ALBEDOM	max depth	IceStation #9
PS138_223-1		2023-09-20 T08:39:10	85.43595	59.98177	3882	HN	Station start	IceStation #9
PS138_223-1		2023-09-20 T08:54:08	85.43662	59.98482	3883	HN	Station end	IceStation #9
PS138_222-1		2023-09-20 T08:57:11	85.43676	59.98555	3884	CTD-RO	max depth	at max depth
PS138_213_KEF_002	PS138_213-1_ KEF_ssl-036	2023-09-20 T11:00:00	85.46397	59.96956		STRAP_ICE	max depth	Recovery of ice sediment traps for biogeochemistry; Ice station #9

Event label	Optional label	Date / Time	Latitude	Longitude	Depth [m]	Gear	Action	Comment
PS138_213_IT_002	PS138_213-1_IT_ssl-034	2023-09-20 T11:15:00	85.46397	59.96956		STRAP_ICE	max depth	Recovery of ice sediment traps equipped with gel traps; Ice station #9
PS138_Heli_EM-Bird_015	Embird_awi-bird	2023-09-21 T08:05:00	85.02870	48.52010		EMB	max depth	Transit back to area of IceStation #1.
PS138_ SBLA_20230921T100800		2023-09-21 T10:08:00	85.01898	48.38941		SBLA	Station start	
PS138_ SBLA_20230921T100800		2023-09-21 T10:08:00	84.84015	43.77036		SBLA	Station end	
PS138_ SBLA_20230921T103300		2023-09-21 T10:33:00	84.82049	43.30523		SBLA	Station start	
PS138_ SBLA_20230921T103300		2023-09-21 T10:33:00	85.23214	43.73576		SBLA	Station end	
PS138_ SBLA_20230921T105700		2023-09-21 T10:57:00	85.27265	43.77371		SBLA	Station start	
PS138_ SBLA_20230921T105700		2023-09-21 T10:57:00	85.05116	47.90553		SBLA	Station end	
PS138_Heli_EM-Bird_016	Embird_awi-bird	2023-09-22 T08:36:00	83.95670	32.04230		EMB	max depth	Back at area of IceStation #1.
PS138_ SBLA_20230922T103900		2023-09-22 T10:39:00	83.96312	32.40052		SBLA	Station start	
PS138_ SBLA_20230922T103900		2023-09-22 T10:39:00	83.91088	33.39799		SBLA	Station end	
PS138_ SBLA_20230922T105900		2023-09-22 T10:59:00	83.87881	33.35414		SBLA	Station start	
PS138_ SBLA_20230922T105900		2023-09-22 T10:59:00	84.03929	30.73302		SBLA	Station end	

Event label	Optional label	Date / Time	Latitude	Longitude	Depth [m]	Gear	Action	Comment
PS138_ SBLA_20230922T111800		2023-09-22 T11:18:00	84.04502	30.32328		SBLA	Station start	
PS138_ SBLA_20230922T111800		2023-09-22 T11:18:00	83.96120	32.27328		SBLA	Station end	
PS138_224-1	2023P271	2023-09-24 T16:01:47	77.94461	7.12650	2646	ISVP	max depth	2023P271 NKE TRUSTED buoy SVP-BRST
PS138_225-1	2023P269	2023-09-25 T01:45:16	75.60058	6.65350	2054	ISVP	Station start	2023P269 NKE TRUSTED buoy SVP-BRST
PS138_225-1	2023P269	2023-09-25 T01:45:43	75.59873	6.65319	2038	ISVP	Station end	

** Comments are limited to 130 characters. See https://www.pangaea.de/expeditions/events/PS138 to show full comments in conjunction with the station (event) list for expedition PS138*

Abbreviation	Method/Device
ADCP	Acoustic Doppler Current Profiler
ALBEDOM	Albedometer
ARGOFL	Argo float
BEAST	Remotely operated sensor platform BEAST
BES	Broadband electromagnetic sensor
BONGO	Bongo net
BRS	Buoy, radiation station
BUOY	Buoy
BUOY_ADCP	Buoy, acoustic doppler current profiler
BUOY_CTD	Buoy, CTD
BUOY_ICE_TRACK	Buoy, ice tracker
BUOY_ITP	Ice-Tethered Profiler Buoy
BUOY_SNOW	Snow buoy
B_LANDER	Bottom lander
CAME	Camera
CM	Current meter
COND	Conductivity meter
CT	Underway cruise track measurements
CTD-RO	CTD/Rosette
CTD-twoyo	CTD, towed system
CTD_fishrod	CTD fishing rod, Sea and Sun Technology
DS3	Swath-mapping system Atlas Hydrosweep DS-3
EBS	Epibenthic sledge
ECHO	Echosounder
EMB	Electro-magnetic Bird (EM-Bird)
FBOX	FerryBox
GKG	Giant box corer
GOPRO	Digital Camera, GoPro
GRAV	Gravimetry
HN	Hand net
HOBO_ON	Onset HOBO data logger
HP	Hand pump
ICE	Ice station
ICEOBS	Ice observation
ISCA	In-situ chemotaxis chamber
ISP	In situ pump
ISVP	Surface velocity profiler
M-AWS	Mobile Automatic Weather Station
MAG	Magnetometer
MAGNA	Magnaprobe
MARKII	Mark II motorized coring device, Kovacs Enterprise Inc
MARKV	Mark V motorized coring device, Kovacs Enterprise Inc

Abbreviation	Method/Device
MOOR	Mooring
MSC	Marine snow catcher
MSN	Multiple opening/closing net
MSS	Micro structure probe
MYON	DESY Myon Detector
NEUMON	Neutron monitor
NO3	Nitrate profiler
OFOBS	Ocean Floor Observation and Bathymetry System
POS	Posidonia positioning system
PS	ParaSound
RAMSES_ACC-VIS	Hyperspectral UV-VIS Radiometer, TriOS, RAMSES-ACC-VIS
ROSINA	Remotely ObServing INsitu camera for Aggregates
SIMB	Seasonal Ice Mass Balance buoy
SIMBA	SAMS Ice Mass Balance buoy
SNDVELPR	Sound velocity probe
SR	Sonic ranger
SSG	Snow sampler glove
SWEAS	Ship Weather Station
TP	Temperature probe
TSG	Thermosalinograph
TVMUC	Multicorer with television
UAV	Unmanned aerial vehicle
W-RADAR	Wave Radar System
WRIDER	Waverider
WS	Water sample
XCTD	Expendable CTD
ZODIAC	Rubber boat, Zodiac
hCTD	CTD, handheld
pCO2	pCO2 sensor

A.5 ICE STATION MAPS

This chapter shows maps of the ICE stations, when the vessel was anchored to the ice for parts of the station time. Maps are available for ICE1 to ICE3 and ICE6 to ICE9. No maps were created for ICE4 and ICE5. The geographic position of each station along the cruise track is shown in Figure 2.1 and the main characteristics and statistics of each ICE station are summarized in Table 2.1. The distances are estimated from known distances between markers and installations and contain uncertainties within a few meters. In addition, distortions in the images from the stitching processes may occur.

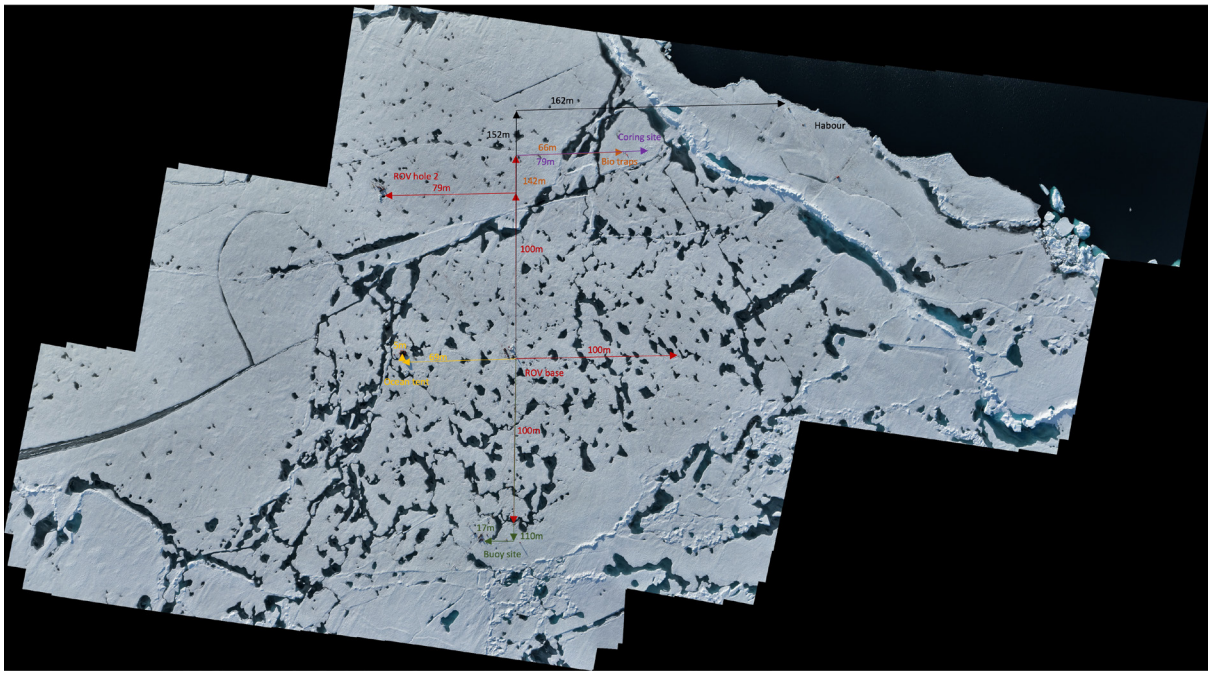

Fig. A.5.1: Station map of station ICE1. The map is based on a panorama image taken on 10 August 2023.

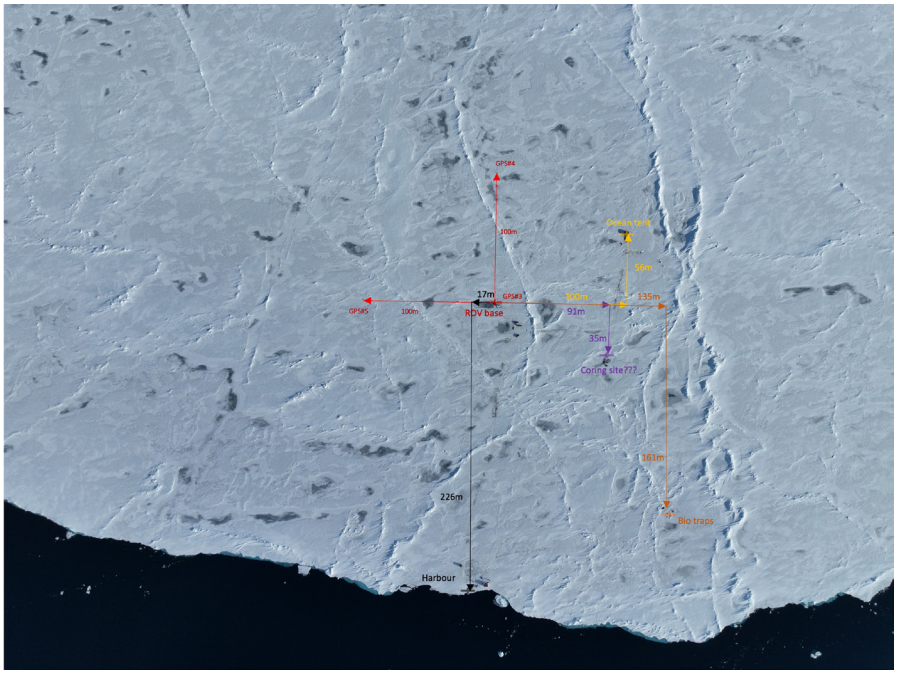

Fig. A.5.2: Station map of station ICE2. The map is based on a panorama image taken on 16 August 2023.

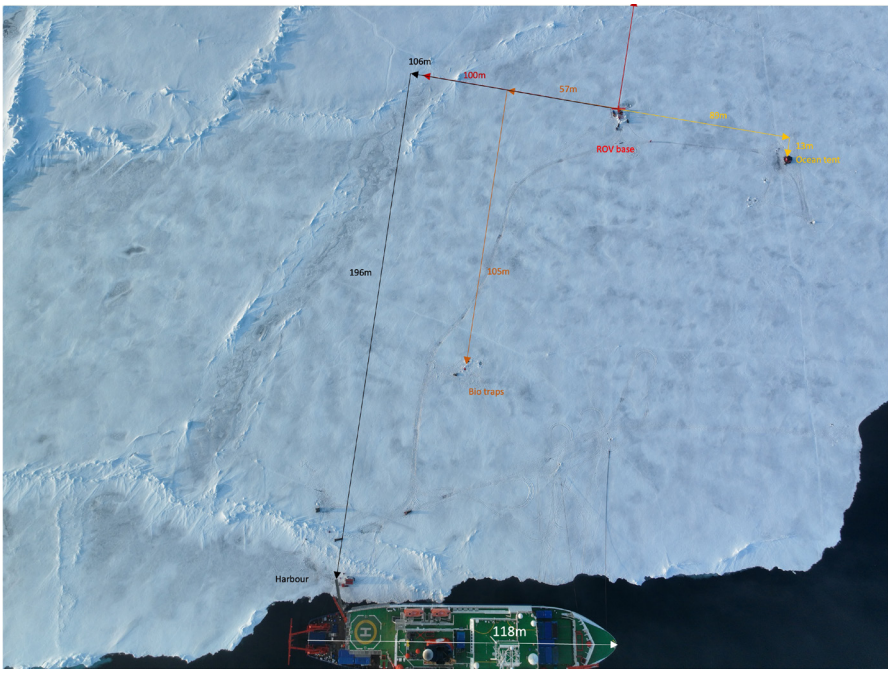

Fig. A.5.3: Station map of station ICE3. The map is based on a panorama image taken on 20 August 2023.

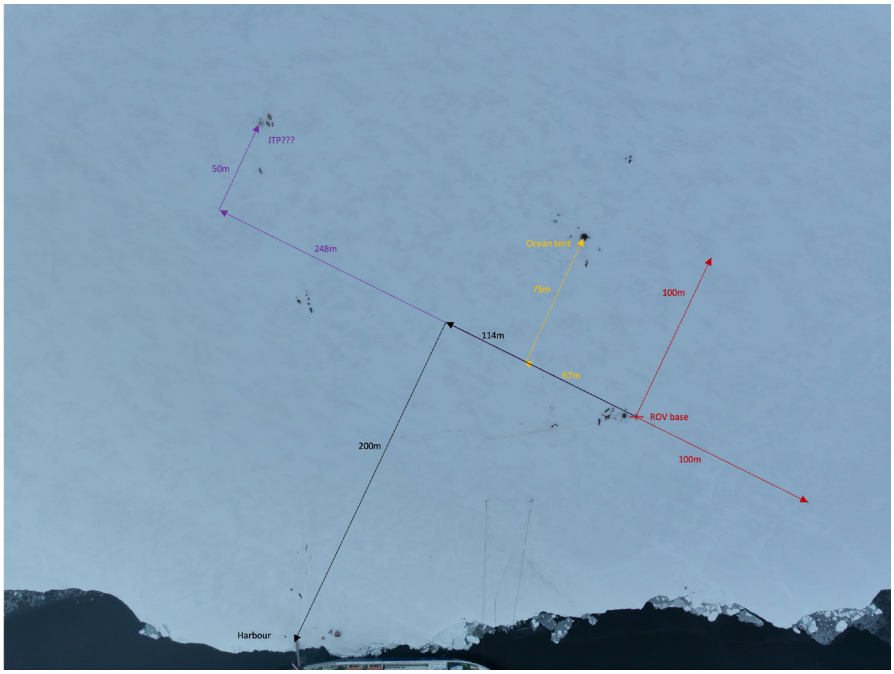

Fig. A.5.4: Station map of station ICE6. The map is based on a panorama image taken on 03 September 2023.

Fig. A.5.5: Station map of station ICE7. The map is based on a panorama image taken on 08 September 2023.

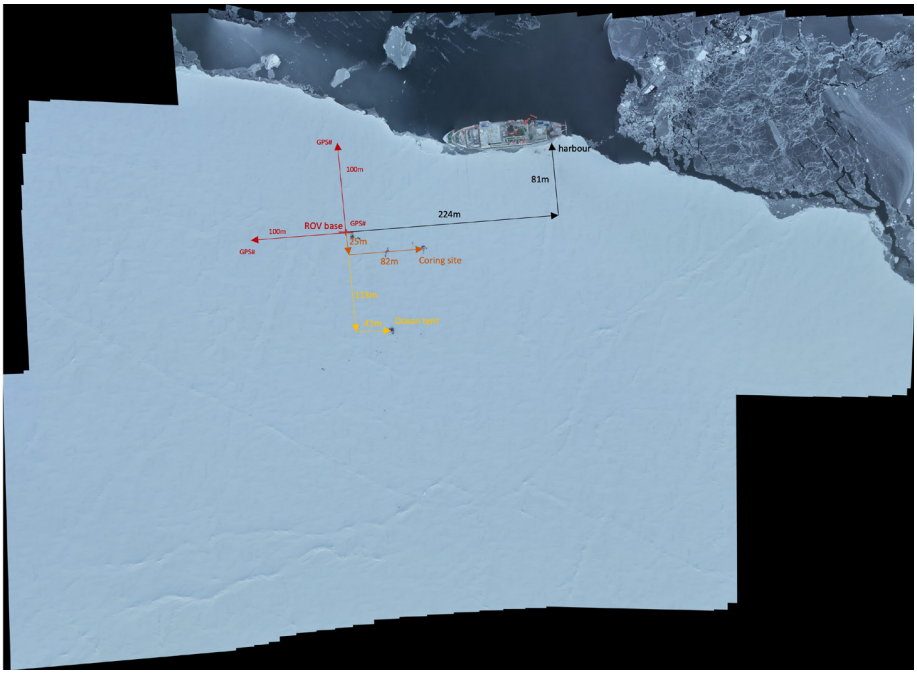

Fig. A.5.6: Station map of station ICE8. The map is based on a panorama image taken on 13 September 2023.

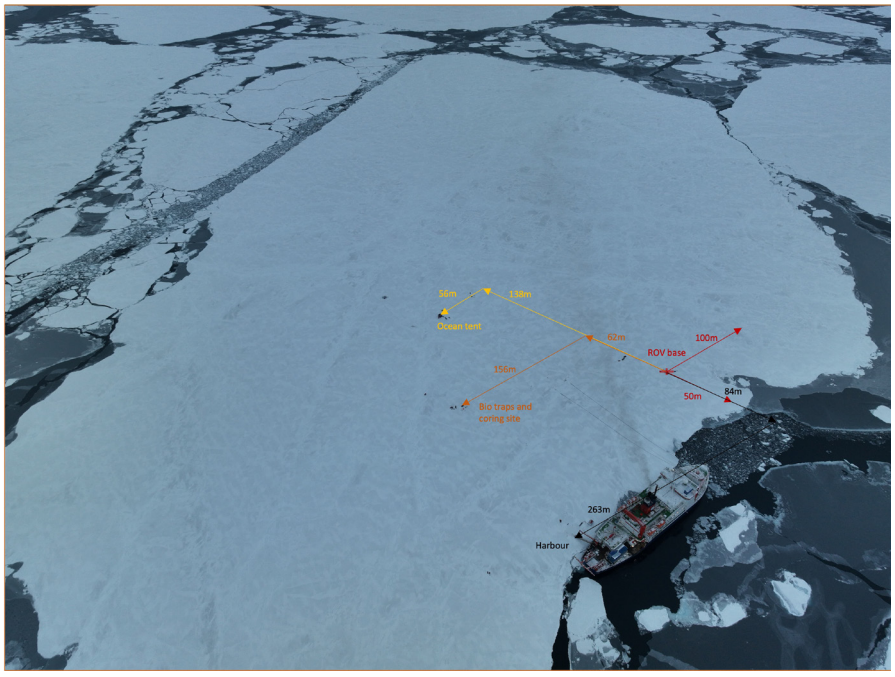

Fig. A.5.7: Station map of station ICE9. The map is based on a panorama image taken on 19 September 2023.

A.6 OVERVIEW OF MULTICORER CORES RETRIEVED DURING PS138

Tab. A.6.1: Overview of multicorer cores retrieved during PS138 and their distribution to scientists for different types of analyses

AODC – Acridine Orange Direct Counts, DIC – Dissolved inorganic carbon, FISH – Fluorescence In Situ Hybridization, MiBio/Biogeo – Microbiology/Biogeochemistry, NA – Not Available

Station	Ice station	Core Number	Core length [cm]	Distributed to	Methods	Comments
PS138_15-1	1	1	–	NA	NA	leaked out, failed
PS138_15-1	1	2	24	F. Bonk, P. Martínez Arbizu (DZMB)	Meiofauna	4% Formaldehyde for morphological analysis
PS138_15-1	1	3	31	F. Bonk, P. Martínez Arbizu (DZMB)	Meiofauna	4% Formaldehyde for morphological analysis
PS138_15-1	1	4	27	C. Bienhold (AWI/MPI)	Porewater	pore water (DIC, alkalinity, nutrients, iron, sulfate/ sulfide)
PS138_15-1	1	5	25	C. Bienhold (AWI/MPI)	Porewater	pore water (DIC, alkalinity, nutrients, iron, sulfate/ sulfide)
PS138_15-1	1	6	25	C. Bienhold (AWI/MPI)	MiBio/Biogeo	DNA, RNA, AODC/FISH, TOC, Chlorophyll, Enzyme activity, porosity, phospholipids
PS138_15-1	1	7	26	C. Bienhold (AWI/MPI)	MiBio/Biogeo	DNA, RNA, AODC/FISH, TOC, Chlorophyll, Enzyme activity, porosity, phospholipids

Station	Ice station	Core Number	Core length [cm]	Distributed to	Methods	Comments
PS138_15-1	1	8	30	C. Bienhold (AWI/MPI)	MiBio/Biogeo	DNA, RNA, AODC/FISH, TOC, Chlorophyll, Enzyme activity, porosity, phospholipids
PS138_15-1	1	9	33	C. Bienhold (AWI/MPI)	MiBio/Biogeo	Chlorophyll, Enzyme activity
PS138_15-1	1	10	–	NA	NA	failed
PS138_15-1	1	11	29	F. Bonk, P. Martínez Arbizu (DZMB)	Meiofauna	4% Formaldehyde for morphological analysis
PS138_15-1	1	12	28	C. Bienhold (AWI/MPI)	MiBio/Biogeo	Chlorophyll, Enzyme activity
PS138_16-1		none	–	NA	NA	no samples
PS138_28-1	1	1	15	M. Bergmann (AWI, not on board)	Microplastic	smudged down, no loss of water
PS138_28-1	1	2	28	K. Vane (AWI)	Foraminifera, otoliths	
PS138_28-1	1	3	29	K. Vane (AWI)	Foraminifera, otoliths	
PS138_28-1	1	4	23	C. Bienhold (AWI/MPI)	MiBio/Biogeo (backup)	smudged down a bit, no loss of water, backup sample, stored at -20°
PS138_28-1	1	5	–	NA	NA	over board, failed
PS138_28-1	1	6	30	F. Wenzhöfer (AWI/ MPI)		
PS138_28-1	1	7	29	C. Uhlir (DZMB)	Macrofauna (-20°C)	
PS138_28-1	1	8	–	NA	NA	failed
PS138_28-1	1	9	30	F. Bonk, P. Martínez Arbizu (DZMB)	Meiofauna (EtOH)	stored at -20° for genetic analysis
PS138_28-1	1	10	30	F. Bonk, P. Martínez Arbizu (DZMB)	Meiofauna (EtOH)	stored at -20° for genetic analysis

Station	Ice station	Core Number	Core length [cm]	Distributed to	Methods	Comments
PS138_28-1	1	11	30	F. Bonk, P. Martínez Arbizu (DZMB)	Meiofauna (EtOH)	stored at -20° for genetic analysis
PS138_28-1	1	12	30	K. Vane (AWI)	Foraminifera, otoliths	
PS138_35-1	2	1	27	C. Bienhold (AWI/MPI)	MiBio/Biogeo	DNA, RNA, AODC/FISH, TOC, Chlorophyll, Enzyme activity, porosity, phospholipids
PS138_35-1	2	2	15	F. Bonk, P. Martínez Arbizu (DZMB)	Meiofauna	4% Formaldehyde for morphological analysis
PS138_35-1	2	3	32	C. Bienhold (AWI/MPI)	MiBio/Biogeo	DNA, RNA, AODC/FISH, TOC, Chlorophyll, Enzyme activity, porosity, phospholipids
PS138_35-1	2	4	28	C. Bienhold (AWI/MPI)	MiBio/Biogeo	DNA, RNA, AODC/FISH, TOC, Chlorophyll, Enzyme activity, porosity, phospholipids
PS138_35-1	2	5	27	C. Bienhold (AWI/MPI)	MiBio/Biogeo	Chlorophyll, Enzyme activity
PS138_35-1	2	6	29	C. Bienhold (AWI/MPI)	MiBio/Biogeo	Chlorophyll, Enzyme activity
PS138_35-1	2	7	28	F. Bonk, P. Martínez Arbizu (DZMB)	Meiofauna	4% Formaldehyde for morphological analysis
PS138_35-1	2	8	31	F. Bonk, P. Martínez Arbizu (DZMB)	Meiofauna	4% Formaldehyde for morphological analysis
PS138_35-1	2	9	31	F. Wenzhöfer, F. Janssen (AWI/MPI)	Microprofiling	
PS138_35-1	2	10	30	C. Bienhold (AWI/MPI)	Porewater	pore water (DIC, alkalinity, nutrients, iron, sulfate/ sulfide)
PS138_35-1	2	11	29	C. Bienhold (AWI/MPI)	Porewater	pore water (DIC, alkalinity, nutrients, iron, sulfate/ sulfide)
PS138_35-1	2	12	22	F. Wenzhöfer, F. Janssen (MPI)	Microprofiling	

Station	Ice station	Core Number	Core length [cm]	Distributed to	Methods	Comments
PS138_36-1	2	1	30	F. Bonk, P. Martinez Arbizu (DZMB)	Meiofauna (EtOH)	stored at -20° for genetic analysis
PS138_36-1	2	2	25	M. Bergmann (AWI, not on board)	Microplastic	
PS138_36-1	2	3	31	F. Wenzhöfer	biogeochemistry	
PS138_36-1	2	4	29	F. Bonk, P. Martinez Arbizu (DZMB)	Meiofauna (EtOH)	stored at -20° for genetic analysis
PS138_36-1	2	5	27	F. Wenzhöfer, F. Janssen (AWI/MPI)	Microprofiling	
PS138_36-1	2	6	27	F. Wenzhöfer, F. Janssen (AWI/MPI)	Microprofiling	
PS138_36-1	2	7	29	F. Wenzhöfer, F. Janssen (AWI/MPI)	Microprofiling	
PS138_36-1	2	8	31	F. Bonk, P. Martinez Arbizu (DZMB)	Meiofauna	extra sample, 4% Formaldehyde for morphological analysis
PS138_36-1	2	9	30	F. Bonk, P. Martinez Arbizu (DZMB)	Meiofauna (EtOH)	stored at -20° for genetic analysis
PS138_36-1	2	10	31	K. Vane (AWI)	Foraminifera, otoliths	
PS138_36-1	2	11	30	K. Vane (AWI)	Foraminifera, otoliths	
PS138_36-1	2	12	29	K. Vane (AWI)	Foraminifera, otoliths	
PS138_59-1	3	1	–	NA	NA	failed
PS138_59-1	3	2	–	NA	NA	failed
PS138_59-1	3	3	24	F. Bonk, P. Martinez Arbizu (DZMB)	Meiofauna	4% Formaldehyde for morphological analysis

Station	Ice station	Core Number	Core length [cm]	Distributed to	Methods	Comments
PS138_59-1	3	4	25	F. Bonk, P. Martínez Arbizu (DZMB)	Meiofauna	4% Formaldehyde for morphological analysis
PS138_59-1	3	5	23	C. Bienhold (AWI/MPI)	MiBio/Biogeo	DNA, RNA, AODC/FISH, TOC, Chlorophyll, Enzyme activity, porosity, phospholipids
PS138_59-1	3	6	22	C. Bienhold (AWI/MPI)	MiBio/Biogeo	DNA, RNA, AODC/FISH, TOC, Chlorophyll, Enzyme activity, porosity, phospholipids
PS138_59-1	3	7	–	NA	NA	failed
PS138_59-1	3	8	16	C. Bienhold (AWI/MPI)	MiBio/Biogeo	DNA, RNA, AODC/FISH, TOC, Chlorophyll, Enzyme activity, porosity, phospholipids
PS138_59-1	3	9	28	C. Bienhold (AWI/MPI)	MiBio/Biogeo	Chlorophyll, Enzyme activity
PS138_59-1	3	10	27	C. Bienhold (AWI/MPI)	Porewater	pore water (DIC, alkalinity, nutrients, iron, sulfate/ sulfide)
PS138_59-1	3	11	32	C. Bienhold (AWI/MPI)	Porewater	pore water (DIC, alkalinity, nutrients, iron, sulfate/ sulfide)
PS138_59-1	3	12	25	C. Bienhold (AWI/MPI)	MiBio/Biogeo	Chlorophyll, Enzyme activity
PS138_60-1	3	1	–	NA	NA	failed
PS138_60-1	3	2	–	NA	NA	failed
PS138_60-1	3	3	23	M. Bergmann (AWI, not on board)	Microplastic	
PS138_60-1	3	4	24	F. Bonk, P. Martínez Arbizu (DZMB)	Meiofauna	4% Formaldehyde for morphological analysis
PS138_60-1	3	5	23	F. Wenzhöfer, F. Janssen (AWI/MPI)	Microprofiling	K. Vane gets some of the samples after microprofiling
PS138_60-1	3	6	31	F. Wenzhöfer, F. Janssen (AWI/MPI)	Microprofiling	K. Vane gets some of the samples after microprofiling

Station	Ice station	Core Number	Core length [cm]	Distributed to	Methods	Comments
PS138_60-1	3	7	27	F. Wenzhöfer, F. Janssen (AWI/MPI)	Microprofiling	K. Vane gets some of the samples after microprofiling
PS138_60-1	3	8	–	NA	NA	failed
PS138_60-1	3	9	22	F. Wenzhöfer, F. Janssen (AWI/MPI)	Microprofiling	passed on to C. Uhlir (DZMB, sediment grain analyses)
PS138_60-1	3	10	31	F. Bonk, P. Martínez Arbizu (DZMB)	Meiofauna (EtOH)	stored at -20° for genetic analysis
PS138_60-1	3	11	–	NA	NA	failed
PS138_60-1	3	12	29	F. Bonk, P. Martínez Arbizu (DZMB)	Meiofauna (EtOH)	stored at -20° for genetic analysis
PS138_76-1	4	1	29	C. Bienhold (AWI/MPI)	MiBio/Biogeo	DNA, RNA, AODC/FISH, TOC, Chlorophyll, Enzyme activity, porosity, phospholipids
PS138_76-1	4	2	–	NA	NA	failed
PS138_76-1	4	3	–	NA	NA	failed
PS138_76-1	4	4	30	C. Bienhold (AWI/MPI)	Porewater	pore water (DIC, alkalinity, nutrients, iron, sulfate/ sulfide)
PS138_76-1	4	5	29	C. Bienhold (AWI/MPI)	Porewater	pore water (DIC, alkalinity, nutrients, iron, sulfate/ sulfide)
PS138_76-1	4	6	20	C. Bienhold (AWI/MPI)	MiBio/Biogeo	DNA, RNA, AODC/FISH, TOC, Chlorophyll, Enzyme activity, porosity, phospholipids
PS138_76-1	4	7	30	C. Bienhold (AWI/MPI)	MiBio/Biogeo	DNA, RNA, AODC/FISH, TOC, Chlorophyll, Enzyme activity, porosity, phospholipids
PS138_76-1	4	8	32	C. Bienhold (AWI/MPI)	MiBio/Biogeo	Chlorophyll, Enzyme activity
PS138_76-1	4	9	30	F. Wenzhöfer, F. Janssen (AWI/MPI)	Microprofiling	
PS138_76-1	4	10	29	F. Wenzhöfer, F. Janssen (AWI/MPI)	Microprofiling	

Station	Ice station	Core Number	Core length [cm]	Distributed to	Methods	Comments
PS138_76-1	4	11	32	F. Wenzhöfer, F. Janssen (AWI/MPI)	Microprofiling	passed on to C. Uhlir (DZMB, sediment grain analyses)
PS138_76-1	4	12	20	C. Bienhold (AWI/MPI)	MiBio/Biogeo	Chlorophyll, Enzyme activity
PS138_77-1	4	1	32	F. Wenzhöfer, F. Janssen (AWI/MPI)	Microprofiling	
PS138_77-1	4	2	–	NA	NA	failed
PS138_77-1	4	3	33	F. Wenzhöfer, F. Janssen (AWI/MPI)	Microprofiling	
PS138_77-1	4	4	26	F. Bonk, P. Martínez Arbizu (DZMB)	Meiofauna (EtOH)	stored at -20° for genetic analysis
PS138_77-1	4	5	20	F. Bonk, P. Martínez Arbizu (DZMB)	Meiofauna (EtOH)	stored at -20° for genetic analysis
PS138_77-1	4	6	19	F. Bonk, P. Martínez Arbizu (DZMB)	Meiofauna (EtOH)	stored at -20° for genetic analysis
PS138_77-1	4	7	26	M. Bergmann (AWI, not on board)	Microplastic	
PS138_77-1	4	8	–	NA	NA	failed
PS138_77-1	4	9	33	K. Vane (AWI)	Foraminifera, otoliths	
PS138_77-1	4	10	29	F. Bonk, P. Martínez Arbizu (DZMB)	Meiofauna	4% Formaldehyde for morphological analysis
PS138_77-1	4	11	30	F. Bonk, P. Martínez Arbizu (DZMB)	Meiofauna	4% Formaldehyde for morphological analysis
PS138_77-1	4	12	33	F. Bonk, P. Martínez Arbizu (DZMB)	Meiofauna	4% Formaldehyde for morphological analysis
PS138_98-1	5	1	29	F. Bonk, P. Martínez Arbizu (DZMB)	Meiofauna	4% Formaldehyde for morphological analysis

Station	Ice station	Core Number	Core length [cm]	Distributed to	Methods	Comments
PS138_98-1	5	2	28	F. Bonk, P. Martínez Arbizu (DZMB)	Meiofauna	4% Formaldehyde for morphological analysis
PS138_98-1	5	3	31	F. Bonk, P. Martínez Arbizu (DZMB)	Meiofauna	4% Formaldehyde for morphological analysis
PS138_98-1	5	4	27	F. Wenzhöfer, F. Janssen (AWI/MPI)	Microprofiling	
PS138_98-1	5	5	25	C. Bienhold (AWI/MPI)	MiBio/Biogeo	DNA, RNA, AODC/FISH, TOC, Chlorophyll, Enzyme activity, porosity, phospholipids
PS138_98-1	5	6	22	C. Bienhold (AWI/MPI)	MiBio/Biogeo	DNA, RNA, AODC/FISH, TOC, Chlorophyll, Enzyme activity, porosity, phospholipids
PS138_98-1	5	7	24	F. Wenzhöfer, F. Janssen (AWI/MPI)	Microprofiling	algae on top
PS138_98-1	5	8	28	C. Bienhold (AWI/MPI)	MiBio/Biogeo	DNA, RNA, AODC/FISH, TOC, Chlorophyll, Enzyme activity, porosity, phospholipids
PS138_98-1	5	9	29	C. Bienhold (AWI/MPI)	MiBio/Biogeo	Chlorophyll, Enzyme activity
PS138_98-1	5	10	27	C. Bienhold (AWI/MPI)	MiBio/Biogeo	Chlorophyll, Enzyme activity
PS138_98-1	5	11	26	C. Bienhold (AWI/MPI)	Porewater	pore water (DIC, alkalinity, nutrients, iron, sulfate/ sulfide)
PS138_98-1	5	12	29	C. Bienhold (AWI/MPI)	Porewater	pore water (DIC, alkalinity, nutrients, iron, sulfate/ sulfide)
PS138_99-1	5	1	26	C. Bienhold (AWI/MPI)	Marmic lab course	0-2 cm (~150 ml), + 150 ml filtered seawater. Stored at 0°C
PS138_99-1	5	2	28	C. Bienhold (AWI/MPI)	Marmic lab course	0-2 cm (~150 ml), + 150 ml filtered seawater. Stored at 0°C

Station	Ice station	Core Number	Core length [cm]	Distributed to	Methods	Comments
PS138_99-1	5	3	28	F. Bonk, P. Martínez Arbizu (DZMB)	Meiofauna (EtOH)	stored at -20° for genetic analysis
PS138_99-1	5	4	25	F. Bonk, P. Martínez Arbizu (DZMB)	Meiofauna (EtOH)	stored at -20° for genetic analysis
PS138_99-1	5	5	22	F. Bonk, P. Martínez Arbizu (DZMB)	Meiofauna (EtOH)	stored at -20° for genetic analysis
PS138_99-1	5	6	–	NA	NA	emptied on deck, failed
PS138_99-1	5	7	24	C. Bienhold (AWI/MPI)	Marmic lab course	0-2 cm (~150 ml), + 150 ml filtered seawater. Stored at 0°C
PS138_99-1	5	8	28	C. Bienhold (AWI/MPI)	Marmic lab course	0-2 cm (~150 ml), + 150 ml filtered seawater. Stored at 0°C
PS138_99-1	5	9	27	F. Wenzhöfer, F. Janssen (AWI/MPI)	Microprofiling	passed on to C. Uhlir (DZMB, sediment grain analyses)
PS138_99-1	5	10	28	F. Wenzhöfer, F. Janssen (AWI/MPI)	Microprofiling	algae on top
PS138_99-1	5	11	28	M. Bergmann (AWI, not on board)	Microplastic	
PS138_99-1	5	12	27	F. Wenzhöfer, F. Janssen (AWI/MPI)	Microprofiling	
PS138_130-1	6	1	27	C. Bienhold (AWI/MPI)	MiBio/Biogeo	DNA, RNA, AODC/FISH, TOC, Chlorophyll, Enzyme activity, porosity, phospholipids
PS138_130-1	6	2	27	C. Bienhold (AWI/MPI)	MiBio/Biogeo	DNA, RNA, AODC/FISH, TOC, Chlorophyll, Enzyme activity, porosity, phospholipids
PS138_130-1	6	3	30	C. Bienhold (AWI/MPI)	MiBio/Biogeo	DNA, RNA, AODC/FISH, TOC, Chlorophyll, Enzyme activity, porosity, phospholipids

Station	Ice station	Core Number	Core length [cm]	Distributed to	Methods	Comments
PS138_130-1	6	4	26	C. Bienhold (AWI/MPI)	MiBio/Biogeo	Chlorophyll, Enzyme activity
PS138_130-1	6	5	25	C. Bienhold (AWI/MPI)	MiBio/Biogeo	Chlorophyll, Enzyme activity
PS138_130-1	6	6	–	NA	NA	emptied on deck, failed
PS138_130-1	6	7	28	C. Bienhold (AWI/MPI)	Porewater	pore water (DIC, alkalinity, nutrients, iron, sulfate/ sulfide)
PS138_130-1	6	8	25	C. Bienhold (AWI/MPI)	Porewater	pore water (DIC, alkalinity, nutrients, iron, sulfate/ sulfide)
PS138_130-1	6	9	16	F. Bonk, P. Martínez Arbizu (DZMB)	Meiofauna	slightly smudged down, no loss of water, 4% Formaldehyde for morphological analysis
PS138_130-1	6	10	29	F. Bonk, P. Martínez Arbizu (DZMB)	Meiofauna	4% Formaldehyde for morphological analysis
PS138_130-1	6	11	27	F. Wenzhöfer, F. Janssen (AWI/MPI)	Microprofiling	
PS138_130-1	6	12	30	F. Wenzhöfer, F. Janssen (AWI/MPI)	Microprofiling	
PS138_131-1	6	1	28	M. Bergmann (AWI, not on board)	Microplastic	
PS138_131-1	6	2	26	F. Bonk, P. Martínez Arbizu (DZMB)	Meiofauna (EtOH)	stored at -20° for genetic analysis
PS138_131-1	6	3	30	F. Bonk, P. Martínez Arbizu (DZMB)	Meiofauna (EtOH)	stored at -20° for genetic analysis
PS138_131-1	6	4	29	C. Bienhold (AWI/MPI)	Marmic lab course	With a piece of Kolga (pushed down). 0-2 cm (~150 ml), + 150 ml filtered seawater. Stored at 0°C
PS138_131-1	6	5	30	F. Bonk, P. Martínez Arbizu (DZMB)	Meiofauna (EtOH)	stored at -20° for genetic analysis
PS138_131-1	6	6	–	NA	NA	emptied on deck, failed
PS138_131-1	6	7	27	F. Bonk, P. Martínez Arbizu (DZMB)	Meiofauna	4% Formaldehyde for morphological analysis

Station	Ice station	Core Number	Core length [cm]	Distributed to	Methods	Comments
PS138_131-1	6	8	31	F. Wenzhöfer, F. Janssen (AWI/MPI)	Microprofiling	passed on to C. Uhlir (DZMB, sediment grain analyses)
PS138_131-1	6	9	30	F. Wenzhöfer, F. Janssen (AWI/MPI)	Microprofiling	
PS138_131-1	6	10	27	C. Bienhold (AWI/MPI)	Marmic lab course	0-2 cm (~150 ml), + 150 ml filtered seawater. Stored at 0°C
PS138_131-1	6	11	26	C. Bienhold (AWI/MPI)	Marmic lab course	0-2 cm (~150 ml), + 150 ml filtered seawater. Stored at 0°C
PS138_131-1	6	12	19	C. Bienhold (AWI/MPI)	Marmic lab course	slightly smudged down. 0-2 cm (~150 ml), + 150 ml filtered seawater. Stored at 0°C
PS138_156-1	7	1	30	C. Bienhold (AWI/MPI)	MiBio/Biogeo	DNA, RNA, AODC/FISH, TOC, Chlorophyll, Enzyme activity, porosity, phospholipids
PS138_156-1	7	2	26	C. Bienhold (AWI/MPI)	Porewater	pore water (DIC, alkalinity, nutrients, iron, sulfate/ sulfide)
PS138_156-1	7	3	28	C. Bienhold (AWI/MPI)	MiBio/Biogeo	DNA, RNA, AODC/FISH, TOC, Chlorophyll, Enzyme activity, porosity, phospholipids
PS138_156-1	7	4	24	C. Bienhold (AWI/MPI)	MiBio/Biogeo	DNA, RNA, AODC/FISH, TOC, Chlorophyll, Enzyme activity, porosity, phospholipids
PS138_156-1	7	5	27	C. Bienhold (AWI/MPI)	Porewater	pore water (DIC, alkalinity, nutrients, iron, sulfate/ sulfide)
PS138_156-1	7	6	14	F. Bonk, P. Martínez Arbizu (DZMB)	Meiofauna	4% Formaldehyde for morphological analysis
PS138_156-1	7	7	31	C. Bienhold (AWI/MPI)	MiBio/Biogeo	Chlorophyll, Enzyme activity
PS138_156-1	7	8	34	C. Bienhold (AWI/MPI)	MiBio/Biogeo	Chlorophyll, Enzyme activity
PS138_156-1	7	9	32	F. Wenzhöfer, F. Janssen (AWI/MPI)	Microprofiling	

Station	Ice station	Core Number	Core length [cm]	Distributed to	Methods	Comments
PS138_156-1	7	10	28	F. Bonk, P. Martinez Arbizu (DZMB)	Meiofauna	4% Formaldehyde for morphological analysis
PS138_156-1	7	11	26	F. Wenzhöfer, F. Janssen (AWI/MPI)	Microprofiling	
PS138_156-1	7	12	25	F. Bonk, P. Martinez Arbizu (DZMB)	Meiofauna	4% Formaldehyde for morphological analysis
PS138_157-1	7	1	32	F. Wenzhöfer, F. Janssen (AWI/MPI)	Microprofiling	passed on to C. Bienhold, stored at -20°
PS138_157-1	7	2	27	F. Wenzhöfer, F. Janssen (AWI/MPI)	Microprofiling	passed on to C. Uhlir (DZMB, sediment grain analyses)
PS138_157-1	7	3	–	NA	NA	failed
PS138_157-1	7	4	25	C. Bienhold (AWI/MPI)	MiBio/Biogeo (backup)	backup sample, stored at -20°
PS138_157-1	7	5	26	C. Bienhold (AWI/MPI)	MiBio/Biogeo (backup)	backup sample, stored at -20°
PS138_157-1	7	6	23	C. Bienhold (AWI/MPI)	MiBio/Biogeo (backup)	backup sample, stored at -20°
PS138_157-1	7	7	29	M. Bergmann (AWI, not on board)	Microplastic	
PS138_157-1	7	8	33	C. Bienhold (AWI/MPI)	MiBio/Biogeo	
PS138_157-1	7	9	–	NA	NA	failed
PS138_157-1	7	10	27	F. Bonk, P. Martinez Arbizu (DZMB)	Meiofauna (EtOH)	stored at -20° for genetic analysis
PS138_157-1	7	11	25	F. Bonk, P. Martinez Arbizu (DZMB)	Meiofauna (EtOH)	stored at -20° for genetic analysis
PS138_157-1	7	12	32	F. Bonk, P. Martinez Arbizu (DZMB)	Meiofauna (EtOH)	stored at -20° for genetic analysis

Station	Ice station	Core Number	Core length [cm]	Distributed to	Methods	Comments
PS138_161-1	7	1	33	F. Bonk, P. Martínez Arbizu (DZMB)	Meiofauna	just two layers (0-1 cm & 1-5 cm), 4% Formaldehyde for morphological analysis
PS138_161-1	7	2	35	F. Bonk, P. Martínez Arbizu (DZMB)	Meiofauna (EtOH)	just one layer (0-3 cm), stored at -20° for genetic analysis
PS138_161-1	7	3	–	NA	NA	failed
PS138_161-1	7	4	27	F. Bonk, P. Martínez Arbizu (DZMB)	Meiofauna (EtOH)	just two layers (0-1 cm & 1-5 cm), stored at -20° for genetic analysis
PS138_161-1	7	5	19	F. Bonk, P. Martínez Arbizu (DZMB)	Meiofauna (EtOH)	just two layers (0-1 cm & 1-5 cm), stored at -20° for genetic analysis
PS138_161-1	7	6	17	F. Bonk, P. Martínez Arbizu (DZMB)	Meiofauna	just two layers (0-1 cm & 1-5 cm), 4% Formaldehyde for morphological analysis
PS138_161-1	7	7	29	F. Bonk, P. Martínez Arbizu (DZMB)	Meiofauna (EtOH)	just two layers (0-1 cm & 1-5 cm), stored at -20° for genetic analysis
PS138_161-1	7	8	30	F. Bonk, P. Martínez Arbizu (DZMB)	Meiofauna (EtOH)	just two layers (0-1 cm & 1-5 cm), stored at -20° for genetic analysis
PS138_161-1	7	9	–	NA	NA	failed
PS138_161-1	7	10	–	NA	NA	failed
PS138_161-1	7	11	30	F. Bonk, P. Martínez Arbizu (DZMB)	Meiofauna	just two layers (0-1 cm & 1-5 cm), 4% Formaldehyde for morphological analysis
PS138_161-1	7	12	34	F. Bonk, P. Martínez Arbizu (DZMB)	Meiofauna	just two layers (0-1 cm & 1-5 cm), 4% Formaldehyde for morphological analysis
PS138_181-1	8	1	30	F. Bonk, P. Martínez Arbizu (DZMB)	Meiofauna	4% Formaldehyde for morphological analysis
PS138_181-1	8	2	–	NA	NA	failed
PS138_181-1	8	3	–	NA	NA	failed
PS138_181-1	8	4	24	F. Wenzhöfer, F. Janssen (AWI/MPI)	Microprofiling	maybe some white spots/patch; microsensor profiles

Station	Ice station	Core Number	Core length [cm]	Distributed to	Methods	Comments
PS138_181-1	8	5	–	NA	NA	failed
PS138_181-1	8	6	28	F. Bonk, P. Martínez Arbizu (DZMB)	Meiofauna	4% Formaldehyde for morphological analysis
PS138_181-1	8	7	–	NA	NA	failed
PS138_181-1	8	8	32	F. Bonk, P. Martínez Arbizu (DZMB)	Meiofauna	slightly shaken/disturbed, but released and closed, 4% Formaldehyde for morphological analysis
PS138_181-1	8	9	–	NA	NA	failed
PS138_181-1	8	10	–	NA	NA	failed
PS138_181-1	8	11	–	NA	NA	failed
PS138_181-1	8	12	30	C. Bienhold (AWI/MPI)	Porewater	pore water (DIC, alkalinity, nutrients, iron, sulfate/ sulfide)
PS138_182-1	8	1	23	F. Wenzhöfer, F. Janssen (AWI/MPI)	Microprofiling	maybe some white spots/patch; microsensor profiles
PS138_182-1	8	2	22	C. Bienhold (AWI/MPI)	Porewater	pore water (DIC, alkalinity, nutrients, iron, sulfate/ sulfide)
PS138_182-1	8	3	32	C. Bienhold (AWI/MPI)	MiBio/Biogeo	DNA, RNA, AODC/FISH, TOC, Chlorophyll, Enzyme activity, porosity, phospholipids
PS138_182-1	8	4	25	C. Bienhold (AWI/MPI)	MiBio/Biogeo	DNA, RNA, AODC/FISH, TOC, Chlorophyll, Enzyme activity, porosity, phospholipids
PS138_182-1	8	5	22	F. Bonk, P. Martínez Arbizu (DZMB)	Meiofauna (EtOH)	stored at -20° for genetic analysis
PS138_182-1	8	6	20	F. Wenzhöfer, F. Janssen (AWI/MPI)	Microprofiling	maybe some white spots/patch; microsensor profiles
PS138_182-1	8	7	–	NA	NA	failed

Station	Ice station	Core Number	Core length [cm]	Distributed to	Methods	Comments
PS138_182-1	8	8	33	C. Bienhold (AWI/MPI)	MiBio/Biogeo	DNA, RNA, AODC/FISH, TOC, Chlorophyll, Enzyme activity, porosity, phospholipids
PS138_182-1	8	9	31	C. Bienhold (AWI/MPI)	MiBio/Biogeo	Chlorophyll, Enzyme activity
PS138_182-1	8	10	–	NA	NA	failed
PS138_182-1	8	11	–	NA	NA	failed
PS138_182-1	8	12	30	C. Bienhold (AWI/MPI)	MiBio/Biogeo	Chlorophyll, Enzyme activity
PS138_208-1	9	1	26	C. Bienhold (AWI/MPI)	MiBio/Biogeo	DNA, RNA, AODC/FISH, TOC, Chlorophyll, Enzyme activity, porosity, phospholipids
PS138_208-1	9	2	22	C. Bienhold (AWI/MPI)	MiBio/Biogeo	DNA, RNA, AODC/FISH, TOC, Chlorophyll, Enzyme activity, porosity, phospholipids
PS138_208-1	9	3	34	C. Bienhold (AWI/MPI)	MiBio/Biogeo	DNA, RNA, AODC/FISH, TOC, Chlorophyll, Enzyme activity, porosity, phospholipids
PS138_208-1	9	4	28	C. Bienhold (AWI/MPI)	Porewater	pore water (DIC, alkalinity, nutrients, iron, sulfate/ sulfide)
PS138_208-1	9	5	22	C. Bienhold (AWI/MPI)	MiBio/Biogeo	Chlorophyll, Enzyme activity
PS138_208-1	9	6	25	C. Bienhold (AWI/MPI)	MiBio/Biogeo	Chlorophyll, Enzyme activity
PS138_208-1	9	7	31	F. Bonk, P. Martínez Arbizu (DZMB)	Meiofauna	4% Formaldehyde for morphological analysis
PS138_208-1	9	8	36	F. Bonk, P. Martínez Arbizu (DZMB)	Meiofauna	4% Formaldehyde for morphological analysis
PS138_208-1	9	9	35	F. Bonk, P. Martínez Arbizu (DZMB)	Meiofauna	4% Formaldehyde for morphological analysis
PS138_208-1	9	10	30	F. Wenzhöfer, F. Janssen (AWI/MPI)	Microprofiling	

Station	Ice station	Core Number	Core length [cm]	Distributed to	Methods	Comments
PS138_208-1	9	11	30	C. Bienhold (AWI/MPI)	Porewater	pore water (DIC, alkalinity, nutrients, iron, sulfate/ sulfide)
PS138_208-1	9	12	34	F. Wenzhöfer, F. Janssen (AWI/MPI)	Microprofiling	
PS138_209-1	9	1	31	M. Bergmann (AWI, not on board)	Microplastic	
PS138_209-1	9	2	21	K. Vane (AWI)	Foraminifera, otoliths	
PS138_209-1	9	3	33	F. Wenzhöfer (AWI/ MPI)	live sediment	
PS138_209-1	9	4	25	F. Bonk, P. Martínez Arbizu (DZMB)	Meiofauna (EtOH)	stored at -20° for genetic analysis
PS138_209-1	9	5	18	K. Vane (AWI)	Foraminifera, otoliths	
PS138_209-1	9	6	27	K. Vane (AWI)	Foraminifera, otoliths	
PS138_209-1	9	7	30	F. Bonk, P. Martínez Arbizu (DZMB)	Meiofauna (EtOH)	stored at -20° for genetic analysis
PS138_209-1	9	8	30	F. Wenzhöfer, F. Janssen (AWI/MPI)	Microprofiling	
PS138_209-1	9	9	33	F. Wenzhöfer (AWI/ MPI)	live sediment	
PS138_209-1	9	10	–	NA	NA	failed
PS138_209-1	9	11	24	F. Bonk, P. Martínez Arbizu (DZMB)	Meiofauna (EtOH)	stored at -20° for genetic analysis
PS138_209-1	9	12	34	F. Wenzhöfer (AWI/ MPI)	live sediment	

Die **Berichte zur Polar- und Meeresforschung** (ISSN 1866-3192) werden beginnend mit dem Band 569 (2008) als Open-Access-Publikation herausgegeben. Ein Verzeichnis aller Bände einschließlich der Druckausgaben (ISSN 1618-3193, Band 377-568, von 2000 bis 2008) sowie der früheren **Berichte zur Polarforschung** (ISSN 0176-5027, Band 1–376, von 1981 bis 2000) befindet sich im electronic Publication Information Center **(ePIC)** des Alfred-Wegener-Instituts, Helmholtz-Zentrum für Polar- und Meeresforschung (AWI); see https://epic.awi.de. Durch Auswahl "Reports on Polar- and Marine Research" (via "browse"/"type") wird eine Liste der Publikationen, sortiert nach Bandnummer, innerhalb der absteigenden chronologischen Reihenfolge der Jahrgänge mit Verweis auf das jeweilige pdf-Symbol zum Herunterladen angezeigt.

The **Reports on Polar and Marine Research** (ISSN 1866-3192) are available as open access publications since 2008. A table of all volumes including the printed issues (ISSN 1618-3193, Vol. 377-568, from 2000 until 2008), as well as the earlier **Reports on Polar Research** (ISSN 0176-5027, Vol. 1–376, from 1981 until 2000) is provided by the electronic Publication Information Center **(ePIC)** of the Alfred Wegener Institute, Helmholtz Centre for Polar and Marine Research (AWI); see URL https://epic.awi.de. To generate a list of all Reports, use the URL http://epic.awi.de and select "browse"/"type" to browse "Reports on Polar and Marine Research". A chronological list in declining order will be presented, and pdf-icons displayed for downloading.

Zuletzt erschienene Ausgaben:

Recently published issues:

788 (2024) The Expedition PS138 of the Research Vessel POLARSTERN to the Arctic Ocean in 2024 edited by Antje Boetius and Christina Bienhold with contributions of the participants

786 (2024) The MOSES Sternfahrt Expeditions of the Research Vessels ALBIS, LITTORINA, LUDWIG PRANDTL and MYA II to the Elbe River, Elbe Estuary and German Bight in 2023 edited by Ingeborg Bussmann, Martin Krauss, Holger Brix, Norbert Kamjunke, Björn Raupers and Tina Sanders with contributions of the participants

785 (2024) The Expeditions PS139/1 and PS139/2 of the Research Vessel POLARSTERN to the Atlantic Ocean in 2023, edited by Simon Dreutter and Claudia Hanfland with contributions of the participants

784 (2024) Expeditions to Antarctica: ANT-Land 2022/23 NEUMAYER STATION III, Kohnen Station, Flight Operations and Field Campaigns. Edited by Julia Regnery, Thomas Matz, Peter Köhler and Christine Wesche with contributions of the participants

783 (2024) Mit Wilhelm Filchner in das Weddellmeer – Paul Björvigs Tagebuch von der deutschen Antarktischen Expedition 1911 – 1912. Aus dem Norwegischen übersetzt von Volkert Gazert und herausgegeben von Cornelia Lüdecke

782 (2024) Arctic Land Expeditions in Permafrost Research The MOMENT project: Expedition to the Arctic Station, Qeqertarsuaq, Disko Island and Ilulissat, West Greenland in 2022 edited by Julia Boike, Simone M. Stuenzi, Jannika Gottuk, Niko Bornemann, Brian Groenke

781 (2023) The Expedition PS137 of the Research Vessel POLARSTERN to the Arctic Ocean in 2023 edited by Vera Schlindwein with contributions of the participants

780 (2023) The Expedition PS136 of the Research Vessel POLARSTERN to the Fram Strait in 2023, edited by Thomas Soltwedel with contributions of the participants

779 (2023) The Expedition PS135/1 and PS135/2 of the Research Vessel POLARSTERN to the Atlantic Ocean in 2023, edited by Yvonne Schulze Tenberge and Björn Fiedler with contributions of the participants

ALFRED-WEGENER-INSTITUT
HELMHOLTZ-ZENTRUM FÜR POLAR-
UND MEERESFORSCHUNG

BREMERHAVEN

Am Handelshafen 12
27570 Bremerhaven
Telefon 0471 4831-0
Telefax 0471 4831-1149
www.awi.de

HELMHOLTZ